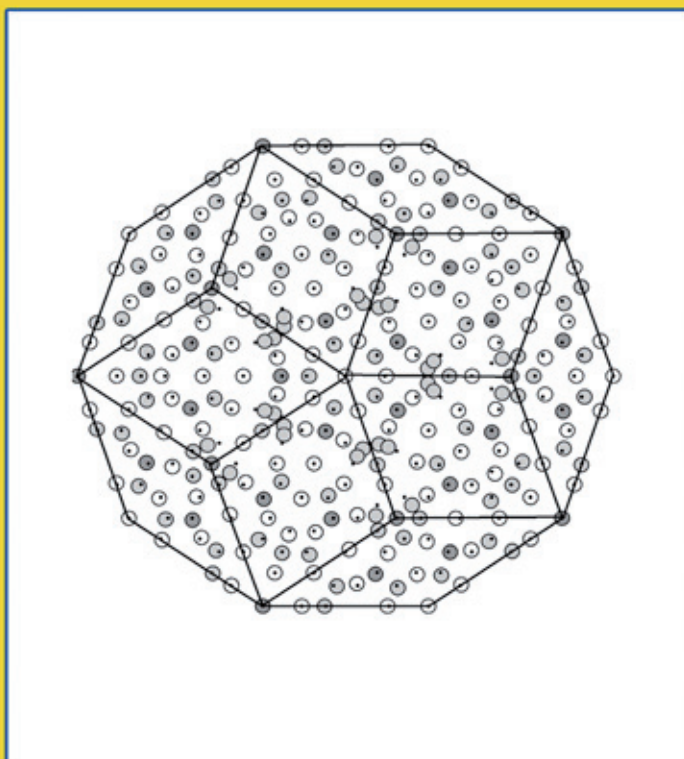


# SYNCHROTRON RADIATION IN NATURAL SCIENCE

**Bulletin of the Polish Synchrotron Radiation Society**  
**Volume 8, Number 1-2, September 2009**



**Includes: Programme and Abstracts of the of the 8th National Meeting  
of Synchrotron Radiation Users (KSUPS-8),  
(Podlesice, Poland, 24-26 September, 2009)**



**Organised by: August Chełkowski Institute of Physics, University of Silesia, Katowice  
and Polish Synchrotron Radiation Society**

**Sponsored by: Ministry of Science and Higher Education**

# SYNCHROTRON RADIATION IN NATURAL SCIENCE

Bulletin of the Polish Synchrotron Radiation Society

**Address:** al. Lotników 32/46, 02-668 Warsaw, Poland, phone/fax (0) 228436034, e-mail: bulletin@synchrotron.org.pl

## Editor

Wojciech Paszkowicz (Editor)  
Institute of Physics  
Polish Academy of Sciences  
al. Lotników 32/46  
02-668 Warsaw  
e-mail: paszk@ifpan.edu.pl

## Editorial Board

Andrzej Burian  
Institute of Physics  
Silesian University  
ul. Uniwersytecka 4  
40-007 Katowice  
e-mail: burian@us.edu.pl

Edward A. Görlich  
Institute of Physics  
Jagellonian University  
ul. Reymonta 4  
30-059 Kraków  
e-mail: ufgoerli@cyf-kr.edu.pl

Maciej Kozak  
Faculty of Physics  
A. Mickiewicz University  
ul. Umultowska 85  
61-614 Poznań  
e-mail: mkozak@amu.edu.pl

Wojciech Kwiatek  
Institute of Nuclear Physics  
Polish Academy of Sciences  
ul. Radzikowskiego 152  
31-342 Cracow  
e-mail: wojciech.kwiatek@ifj.edu.pl

Anna Wolska  
Institute of Physics  
Polish Academy of Sciences  
al. Lotników 32/46  
02-668 Warsaw  
e-mail: wolska@ifpan.edu.pl

Krystyna Jabłońska  
Institute of Physics  
Polish Academy of Sciences  
al. Lotników 32/46  
02-668 Warsaw  
e-mail: jablo@ifpan.edu.pl

Bronisław A. Orłowski  
Institute of Physics  
Polish Academy of Sciences  
al. Lotników 32/46  
02-668 Warsaw  
e-mail: orbro@ifpan.edu.pl

Danuta Żymierska  
Institute of Physics  
Polish Academy of Sciences  
al. Lotników 32/46  
02-668 Warsaw  
e-mail: zymier@ifpan.edu.pl

Bogdan J. Kowalski  
Institute of Physics  
Polish Academy of Sciences  
al. Lotników 32/46  
02-668 Warsaw, Poland  
e-mail: kowab@ifpan.edu.pl

Paweł Piszcza  
Faculty of Chemistry  
A. Mickiewicz University  
ul. Grunwaldzka 6  
60-780 Poznań  
e-mail: pawel@amu.edu.pl

---

**Note for contributors:** Contributions in English (preferred) or in Polish should be sent to the Editor. The topics include: synchrotron and alternative radiation sources, beamline instrumentation, experimental and theoretical results connected with application of various methods and approaches (x-ray scattering, x-ray diffraction, x-ray absorption, fluorescence and photoelectron spectroscopies, magnetic dichroism, etc.) in connection with application of synchrotron radiation in physics, chemistry, crystallography, materials science and life sciences.

---

Figure on the cover page: A projection of the refined structure of a Ni-rich decagonal Al-Ni-Co quasicrystal along the periodic axis, by P. Kuczera, B. Kozakowski, J. Wolny, and R. Strzalka, p. 57, this issue.

SYNCHROTRON RADIATION IN NATURAL SCIENCE is published and distributed by the Polish Synchrotron Radiation Society (PSRS). Typesetting and cover design by W. Paszkowicz. Technical assistance: J. Libera.

Detailed information on PSRS is given on cover page 3.

**Acknowledgements:** This issue of the journal was sponsored by Ministry of Science and Higher Education.

ISSN 1644-7190

Volume 8, No. 1-2, 2009, © Polish Synchrotron Radiation Society

## EDITORIAL

In this issue of *Synchrotron Radiation in Natural Science* the readers will find the abstracts of the KSUPS-8 (*8th National Symposium of Synchrotron Users*). The abstracts are preceded by a description of the Polish FEL project and memories of the early work at synchrotrons in mid 1980s. Brief information on the Polish synchrotron project is also included (pp. 41-42); more details have been given in previous issues. Both mentioned projects, of synchrotron and FEL, are at different stages of processing. The way to acceptance of the projects of this kind is typically long and meets many obstacles, as illustrated *e.g.* by Olof Hallonsten's [1] for the cases of MAXlab, ESRF and Stanford laboratories. Many more or less obvious factors account in the decision and choice of machine location and parameters. The cost of the machine is not so high (being comparable with the cost of a stadium or 10 km of a highway). Another important factor is a creation, in advance, of a lobby of a convincing power being able to reach the decision makers with the message about the mission of natural science for both, the society and for the technology. Understanding that modern light sources became a basic scientists' tool, and that their lack enhances the brain drain, a natural process causing that young people who learn the modern material characterisation techniques do not find job in their native countries, is a key point during the decision process. Moreover, it is worth noting that at the turn of the century, intense light sources started their work in relatively small countries such as Sweden, Switzerland and Singapore—the success of these scientific centres is well known and will, certainly, encourage other countries to follow the same way.

Thanks to the special programs of European Commission so called I3 (Integrated Infrastructure Initiative) scientists across Europe benefit from easier access to Europe's best synchrotron and free electron laser facilities. The main objective of this program is the support of the transnational open access to the synchrotrons and FELs facilities, for users from the European area. Under the 6<sup>th</sup> Framework Programme (FP6) the Integrating Activity on Synchrotron and Free Electron Laser Science (IA-SFS) project was active. The duration of the project was 5 years: from March 1<sup>st</sup>, 2004 to February 28<sup>th</sup>, 2009, and the total EU support was at the level of 27 million euro. Starting from March 2009,

the ELISA project is supported by the European Community - Research Infrastructure Action under the FP7 Programme [2]. It is the follow-up of a previous I3 [3]. The duration of the project is 30 months: March 1<sup>st</sup>, 2009 - August 31<sup>st</sup>, 2011, but the funds are only 10 million €, *i.e.* they are three times smaller than those got within the FP6 programme. Moreover, there is a discussion for further reduction and releasing the funding responsibility completely to national funding agencies. A special action should be taken to convince authorities from Brussels that this is not a right way and such politics can stress on the level of science in Europe and ruin the many years' efforts to build the international users community. In this aspect the users' voice should be heard. The synchrotron facilities have sent a letter to the users asking for filling a questionnaire to express their concern about need for European Commission support (see p. 99). This letter has been sent to 22000 e-mail addresses of the users but only 1100 answers were obtained through the webpage. The more actions are needed. At p. 100 you will find a Manifest prepared by an *ad-hoc* committee for a European Synchrotron User Organization (ESUO) describing the present situation with the proposition to perform activities which are very important for our future access to national facilities.

We are pleased to inform the readers that Prof. Krystyna Jablonska was elected by the ELISA Council as one of user delegates in the Council (the remaining ones are: Maria Arménia Carrondo, Keijo Hämäläinen, Ullrich Pietsch and Marc Vrakking). The user delegates will represent the users in the ELISA Council with mission of supporting the transnational open access of users to the synchrotrons and FELs facilities; developing innovative instrumentation and techniques, enhancing the communication between the consortium members and strengthening the links to the general public.

## References

- [1] O. Hallonsten, *Small science on big machines*, PhD thesis , <http://www.lu.se/o.o.i.s?id=12683&postid=1419054>, (Lund Univ. 2009).
- [2] <http://www.elettra.eu/ELISA/>.
- [3] <http://www.elettra.trieste.it/I3/>.

## CONTENTS

	<b>Editorial</b>	I
	Synchrotron Light News	1
<b>Regular contributions</b>		
G. Wrochna, J. Jagielski, J. Krzywiński, R. Nietubyć, J. Pełka, E. Pławski, J. Sekutowicz, R. Sobierajski, J. Szewiński	On the POLFEL free electron laser project	3
W. Kwiątek	It all started out innocently enough...	8
M. Stankiewicz	My first encounter with synchrotron. 34 years ago	15
<b>KSUPS-8</b>		
<b>8. Krajowe Sympozjum Użytkowników Promieniowania Synchrotronowego</b>		
<i>KSUPS-8 - 8th National Symposium of Synchrotron Users</i>		
Programme of 8 <sup>th</sup> National Symposium of Synchrotron Users		
A. Burian, J. Szade	Zaproszenie na 8. Krajowe Sympozjum Użytkowników Promieniowania Synchrotronowego	22
<i>Welcome to 8<sup>th</sup> National Symposium of Synchrotron Users</i>		
<b>KSUPS-8: invited lectures and oral presentations</b>		
T. Durakiewicz	Synchrotron quest for band renormalization in correlated f-electron systems	L01      23
W.M. Kwiątek, M. Podgórczyk, C. Paluszkiewicz, M. Gajda, Z. Stachura, M. Lekka, J. Lekki, M. Piccinini, D. Grolimund	Novel microscopy methods of medical imaging	L02      24
L. Chow, A. Misiuk, C.W. Pao, D.C. Ling, W.F. Pong, J. Bak-Misiuk	Synchrotron radiation study of Mn implanted silicon	O01      25
A. Wierzbicka, D. Lübbert, J.Z. Domagała, Z.R. Żytkiewicz	Rocking curve imaging studies of laterally overgrown GaAs and GaSb epitaxial layers	O02      26 ext
K. Wieteska, W. Wierzchowski, A. Malinowska, S. Turczyński, M. Lefeld-Sosnowska, D. Pawlak, T. Łukasiewicz, W. Graeff	X-ray topographic investigations of domain structure in Czochralski grown $\text{Pr}_x\text{La}_{1-x}\text{AlO}_3$ crystals	O03      28
G. Wrochna, J. Jagielski, J. Krzywiński, R. Nietubyć, J. Pełka, E. Pławski, J. Sekutowicz, R. Sobierajski, J. Szewiński	POLFEL – the high average power free electron laser	L03      29
J.B. Pełka, G. Wrochna, R. Nietubyć, K.R. Tybor	Applications of free electron lasers in biology and medicine	O04      30
R. Sobierajski, M. Jurek, D. Klänger, A.R. Khorsand, E. Louis, S. Bruijn, R. van de Kruis, E.D. van Hattum, K. Sokolowski-Tinten, U. Shymanovich, S. Toleikis, H. Wabnitz, K. Tiedtke, N. Stojanovic, L. Juha, J. Chalupsky, J. Cihelka, V. Hajkova, E.M. Gullikson, F. Bijkerk	Interaction of multilayer optics with intense femtosecond XUV pulses	O05      31

P. Zajdel, I. Kruk, P.-Y. Hsieh, W. van Beek, M.A. Green	Local and long range orders in transition metal oxides and selenides and metal organic frameworks studied using combined techniques (XRD and <i>in-situ</i> Raman)	L04	32
M. Sikora	Study of magnetism with XMCD and XES	L05	33
K. Lawniczak-Jablonska, A. Wolska, M.T. Klepka, J. Sadowski, A. Barcz, A. Hallen, D. Arvanitis	Charakteryzacja nano-wydzieleń w matrycach na bazie GaSb <i>Characterisation of nanoinclusions in GaSb-based matrices</i>	L06 ext	34
M. Kozak	Small angle scattering of synchrotron radiation studies of biomembranes	L07	36
S. Krzywda, W. Białek, A. Szczepaniak, M. Jaskólski	Atomic-resolution structure of cyanobacterial cytochrome c6 with an unusual sequence insertion	L08	37
H. Drozdowski, A. Romaniuk, Z. Błaszczać	Short-range ordering in <i>ortho</i> -chloroanisole at 293 K by x-ray diffraction	O06	38
K. Mazur, W. Wierzchowski, K. Wieteska, W. Hofman, K. Kościewicz, W. Strupiński, W. Graeff	X-ray reflectometric investigation of surface roughness of SiC substrate wafers and its influence on the structural perfection of the deposited SiC epitaxial layers	O07	39
R. Przeniosło	Badania struktury tlenków metali przejściowych metodą dyfrakcji neutronów i promieniowania synchrotronowego  <i>Studies of structure of transition metal oxides with the methods of neutron diffraction and synchrotron radiation</i>	L09	40
E.A. Görlich, K. Królas, M. Mlynarczyk, M.J. Stankiewicz, K. Tomala	Informacja na temat rozwiązań technicznych i stanu przygotowań do budowy synchrotronu w Polsce  <i>Information on technical solutions and preparations to synchrotron construction in Poland</i>		41
J. Szade, B. Orłowski, B. Kowalski, E.A. Görlich, K. Tomala, P. Starowicz	Pierwsza linia na polskim synchrotronie – spektroskopie miękkiego promieniowania rentgenowskiego  <i>First beamline at the Polish synchrotron: Spectroscopies of soft X-rays</i>		42

#### KSUPS-8: poster presentations

M. Kowalik, R. Zalecki, A. Kołodziejczyk	Electronic states of colossal magnetoresistive manganites $\text{La}_{0.67}\text{Pb}_{0.33}\text{Mn}_{1-x}\text{Fe}_x\text{O}_3$ from photoemission spectroscopy	P01	43
A. Malinowska, E. Wierzbicka, M. Lefeld-Sosnowska, K. Wieteska, W. Wierzchowski, T. Łukasiewicz, M. Świrkowicz, W. Graeff	Defect structure formed at different stages of growth process in erbium, calcium and holmium doped $\text{YVO}_4$ crystals	P02	44
M. Szczerbowska-Boruchowska, M. Lankosz, A. Smykla, D. Adamek	Synchrotron radiation as a tool of biochemical analysis in brain cancers	P03	45
J. Wolny, M. Duda, B. Kozakowski	Complex structure of $\text{Mg}_2\text{Al}_3$ $\beta$ and $\beta'$ phases	P04	46
E. Dynowska, W. Szuszkiewicz, C. Ziereis, J. Geurts, S. Müller, C. Ronning, J. Domagala, P. Romanowski, W. Caliebe	Structural studies of heavily transition metal implanted $\text{ZnO}$	P05	47
H. Grigoriew, L. Wiegert, A. Boczkowska	Dynamic SAXS correlation as method of structural research	P06	48
M.T. Klepka, K. Lawniczak-Jablonska, A. Wolska	Badania absorpcyjne zmodyfikowanych chemicznie chitozanów z żelazem  <i>Absorption studies of chemically modified Fecontaining chitosans</i>	P07	49

A. Wolska, K. Lawniczak-Jablonska, M.T. Klepka, A. Barcz, A. Hallen, D. Arvanitis	Lokalne otoczenie jonów manganu implantowanych w kryształach GaSb <i>Local environment of manganese ions implanted into GaSb crystals</i>	P08 ext	50
A. Wolska, K. Lawniczak-Jablonska, M.T. Klepka, J. Sadowski	Wytrącenia MnSb w matrycy GaSb wytwarzane przy pomocy metody MBE <i>MnSb precipitates in GaSb matrix, produced using the MBE methhod</i>	P09 ext	52
J. Bak-Misiuk, P. Romanowski, E. Dynowska, J.Z. Domagala, J. Sadowski, T. Wojciechowski, R. Jakielo, W. Wierzchowski, K. Wieteska, W. Caliebe, W. Graeff	Defect structure of GaMnSb grown on GaAs substrate	P10	54
A. Misiuk, W. Wierzchowski, K. Wieteska, J. Bak-Misiuk, B. Surma, A. Wnuk, C.A. Londos, Deren Yang, W. Graeff	Defect structure of Czochralski grown nitrogen doped silicon annealed under enhanced pressure	P11	55
D. Klinger, R. Sobierajski, M. Jurek, J. Krzywinski, J.B. Pelka, D. Źymierska, J. Chalupský, L. Juha, V. Hájková, J. Cihelka, T. Burian, L. Vyšín, H. Wabnitz, K. Tiedtke, S. Toleikis, T. Tschenetscher, R. London, S. HauRiege, K. Sokolowski- Tinten, N. Stojanovic, J. Hajdu, A.R. Khorsand, A.J. Gleeson	Modification of the surface morphology by ultra short pulses of XUV free electron laser	P12	56
P. Kuczera, B. Kozakowski, J. Wolny, R. Strzałka	Structure refinement of decagonal quasicrystal	P13	57
J. Nowak, R. Chatas, J. Lekki, A. Kuczumow	Microspectrometric study of internal structure of dentin-enamel boundary (DEJ) in molar teeth	P14	58
W. Nowicki, J. Darul, P. Piszora, T. Trots	Structural properties of $(\text{Mn}_{1-x}\text{Fe}_x)_2\text{O}_3$ solid solutions	P15	59
A. Pietnoczka, R. Bacewicz, M. Pękała, V. Drozd, W. Zalewski, J. Antonowicz	Local structure of Mn in $(\text{La}_{1-x}\text{Ho}_x)_{2/3}\text{Ca}_{1/3}\text{MnO}_3$ using X-ray absorption fine structure	P16	60
P. Piszora, J. Darul, W. Nowicki, C. Lathe	Diffraction HP/HT study of $\text{LiMn}_2\text{O}_4$	P17	61
P. Romanowski, J. Bak-Misiuk, E. Dynowska, J. Sadowski, T. Wojciechowski, A. Barcz, R. Jakielo, W. Caliebe	Structural properties of high-temperature-grown GaMnSb / GaSb	P18	62
P. Seremak-Peczkis, W. Zajączkowski, J. Przewoźnik, Cz. Kapusta, M. Sikora, D.A. Zająć, P. Pasierb, M. Bućko, M. Rękas	XAFS study and crystallographic structure of Ti and Y doped $\text{BaCeO}_{3-\delta}$ protonic conductors	P19	63
J. Stępień, J. Śliwińska, J. Przewoźnik, K. Schneider, Cz. Kapusta, D. Zajac, K. Michałów, D. Pomykalska, M. Bućko, M. Rękas	XAFS study of $\text{ZrO}_2$ -based SOFC materials	P20	64
T. Balcer, W. Wierzchowski	The simulation of Bragg-case section images of dislocations and inclusions in aspect of identification of defects in SiC crystals	P21	65
W. Tabiś, J. Kusz, N.-T.H. Kim-Ngan, Z. Tarnawski, F. Zontone, Z. Kąkol, A. Kozłowski, T. Kołodziej	Kinetics of the Verwey transition in magnetite	P22	66
M.S. Walczak, K. Lawniczak-Jablonska, A. Wolska, M. Sikora, A. Sienkiewicz, L. Suárez, A. Kosar, M.J. Bellemare, D.S. Bohle	Changes of iron state and local iron environment of malarial pigment's substitute in presence of chloroquine	P23	67

E. Werner-Malento, R. Minikayev, C. Lathe, H. Dąbkowska, W. Paszkowicz	High-pressure diffraction study of selected synthetic garnets	P24	68
J.B. Pełka, R. Sobierajski, M. Jurek, J. Krzywiński, D. Żymierska, D. Klinger, S. Hau Riege, H. Chapman, R. London, L. Juha, J. Chalupsky, J. Cihelka, U. Jastrow, K. Tiedtke, S. Toleikis, H. Wabnitz, W. Caliebe, K. Sokolowski- Tinten, N. Stojanovic, C. Riekel, R. Davies, M. Burghammer, W. Paszkowicz, A. Wawro	Damage of solids induced by single pulses of XUVFLASH	P25	69
L. Hawelek, A. Brodka, J.C. Dore, V. Honkimäki, T. Kyotani, A. Burian	Alignment test of N-doped carbon nanotubes using high- energy X-ray diffraction	P26	70
K. Lawniczak-Jablonska, M.T. Klepka, A. Wolska, S. Filipek, R. Sato	Okręsanie lokalnego otoczenia wokół wybranych atomów w nowych wodorkach faz Laves	P27	71
R. Minikayev, W. Paszkowicz, E. Werner-Malento, C. Lathe, H. Dąbkowska	Determination of local atomic order around selected atoms in new Laves-phase hydrides		
W. Paszkowicz, A. Wolska, M.T. Klepka, S. abd el All, F.M. Ezz-Eldin	Equation of state of zircon-type TbVO <sub>4</sub>	P28	72
W. Paszkowicz, P. Piszora, W. Łasocha, I. Margioliaki, M. Brunelli, A. Fitch	A combined X-ray diffraction and absorption study of Li <sub>2</sub> Si <sub>2</sub> O <sub>5</sub> doped with vanadium	P29	73
M.A. Pietrzyk, B.J. Kowalski, B.A. Orlowski, W. Knoff, T. Story, W. Dobrowolski, V.E. Slyntko, E.I. Slyntko, R.L. Johnson	Lattice parameter of polycrystalline diamond in the low- temperature range	P30	74
M. Dampc, B. Mielewska, M.R.F. Siggel- King, G.C. King, B. Sivaraman, S. Ptasińska, N. Mason, M. Zubek	A comparison of the valence band structure of bulk and epitaxial GeTe-based diluted magnetic semiconductors	P31	75
P.W. Wachulak, A. Bartnik, C.S. Menoni, J.J. Rocca, H. Fiedorowicz, M.C. Marconi	Threshold photoelectron spectra of isoxazole over the photon energy range 9-30 eV	P32	77
H. Drozdowski, K. Nowakowski	Nanometer patterning and holographic imaging using table-top EUV laser	P33	78
H. Drozdowski, K. Nowakowski	The determination of molecular structure of 2-methylcyclohexanone	P34	79
Z. Pietralik, M. Chrabaśczecka, M. Kozak	Study of the structure and of the internal ordering degree in liquid cyclohexylamine C <sub>6</sub> H <sub>11</sub> -NH <sub>2</sub>	P35	80
M. Kulik, A.P. Kobzey, A. Misiuk, W. Wierzchowski, K. Wieteska, J. Bak-Misiuk, A. Wnuk, B. Surma	Interactions of cationic gemini surfactants with DMPC	P36	81
R. Minikayev, E. Dynowska, P. Dziawa, E. Kamińska, A. Szczerbakow, D. Trots, W. Szuszkiewicz	Composition and structure of Czochralski silicon implanted with H <sub>2</sub> <sup>+</sup> and Mn <sup>+</sup> and annealed under enhanced hydrostatic pressure	P37	82
R. Nietubyć, W. Caliebe, E. Dynowska, K. Nowakowska-Langier, J. Pełka, P. Romanowski	High-temperature studies of Pb <sub>1-x</sub> Cd <sub>x</sub> Te solid solution: structure stability and CdTe solubility limit	P38	83
B. Sikora, A. Baranowska-Korczyc, W. Zaleszczyk, A. Nowicka, K. Fronc, W. Knoff, K. Gas, W. Paszkowicz, W. Szuszkiewicz, K. Świątek, Ł. Kłopotowski, K. Sobczak, P. Dłużewski, G. Karczewski, T. Wojtowicz, I. Fijałkowska, D. Elbaum	XRD studies of Nb/sapphire(001) thin films deposited with the ultra-high-vacuum cathodic ARC technique	P39	86
	Colloidal ZnO and ZnO/MgO core/shell nanocrystals – synthesis and properties	P40	87

A. Baranowska-Korczyc, B. Sikora, W. Zaleszczyk, A. Nowicka, K. Fronc, W. Knoff, K. Gas, W. Paszkowicz, R. Minikayev, W. Szuszkiewicz, K. Świątek, Ł. Kłopotowski, K. Sobczak, P. Dłużewski, G. Karczewski, T. Wojtowicz, J. Bujak, D. Elbaum	ZnO nanofibers prepared by electrospinning—characterization and doping	P41 ext	88
M. Kozak, M. Taube	Solution structure of RAR1-GST-TAG fusion protein	P42	90
<b>Chronicle</b>			
K. Jablonska	Membership of Poland in ESRF		91
	Information on ISSRNS 2010		92
M. Lefeld-Sosnowska	Wspomnienie. Prof. Jerzy Gronkowski (1949 – 2009)		94
	<i>Memories. Prof. Jerzy Gronkowski (1949 – 2009)</i>		
D. Zymierska	Z życia PTPS		96
	<i>News from PSRS</i>		
G. Margaritondo, F.C. Adams, O. Dutuit, A.E. Russell	The future of European transnational access for synchrotrons and FELs		99
U. Pietsch, M.A. Carrondo, K. Hämäläinen, K. Lawniczak-Jablonska	Manifesto: European Synchrotron User Organisation (ESUO)		100
	Authors' index		101

## SYNCHROTRON LIGHT NEWS

### NEWS

**Result of elections (September 2008).** The Polish Synchrotron Radiation Society (PSRS) President, Prof. Krystyna Jablonska, was reelected for the term 2008–2011. See page 96 for information on the new Council.

**The Bulletin: New Editorial Board (September 2008).** The new editorial board of the Bulletin is, as before, based on the elected Council of the PSRS. All members of previous Editorial Board are acknowledged for their collaboration and efforts to help in editing.

**MAX-IV project presented in Warsaw (September 2008).** On Sept. 25<sup>th</sup> 2008, Prof. Nils Mårtensson, the Director of MAXlab (Lund, Sweden), and coworkers, Prof. Ulf Karlsson and Prof. Åke Kvick, visited the Institute of Physics PAS. During a special half-day seminar (*cf.* Fig. 1), the visitors have presented the project of MAX-IV synchrotron, the fourth ring to be built in MAXlab, and the role of MAXlab in nanoscience and materials science (the MAX-IV project was accepted for financing in May 2009).



Figure 1. Director of MAXlab Prof. Nils Mårtensson (left), and Director of Institute of Physics PAS, Prof. Jacek Kossut (right), during the seminar.

Photo: W. Paszkowicz

**Workshop on Polish Synchrotron project (February 2009).** On 23.02.2009, an intensive one-day workshop took place at the Institute of Physics of the Jagellonian University. The experts in accelerator physics from BESSY, ELETTRA and MAXLab shared their expertise and opinions with the Polish synchrotron team. The meeting was instrumental for taking key decisions on the technical solutions adopted for the Polish project. The scale of the project was set at the circumference of about 95 m and the maximum electron beam energy of 1.5 GeV.

**The future of BM14 beamline (May 2009).** In May 2009, European Synchrotron Radiation Facility invited

its members and associate members for expressions of interest to take over the ownership and operation of the CRG beamline BM14. During The ESRF Science Advisory Committee meeting on 28-29 May 2009, also the proposal prepared by the group of Polish crystallographers and researchers working with X-ray Absorption Spectroscopy was presented by Maciej Kozak. At the present stage we are waiting for the official decision and offer from ESRF, and having got it we can apply for appropriate financial resources.

**'Polish Synchrotron' Consortium meeting (May 2009).** On 26.05.2009, successive meeting of the Consortium took place in Collegium Maius, Kraków. The Consortium *Polski Synchrotron* (*Polish Synchrotron*) was formed in April 2008 by thirty three leading universities and research institutes of Poland (presently, the number grew to 36 members) to actively support the initiative of building a synchrotron light source in Poland and to collaborate at the realisation of the project. The meeting (See Fig. 2) was devoted to a discussion on proposed solutions for the machine design and the beamline priorities after the scale of the project was defined.

**Financing of ESRF membership renewed (July 2009).** Financing of membership of Poland in ESRF continues. The funds have been obtained for the period mid-2009 – mid 2011 (see page 91). The membership means also that the scientific, doctoral, administrative and technical positions at ESRF are available for Polish citizens (<http://www.esrf.eu/Jobs>)

**First X-rays from the PETRA III source (July 2009).** In July 2009, our colleagues at DESY generated the first X-ray beam at the new synchrotron radiation source PETRA III. This is an important step towards making available for experiments the most brilliant X-ray source (of storage ring type) in the world. Congratulations! Read more at [http://petra3.desy.de/news/petra\\_iii\\_in\\_general/first\\_beam/index\\_eng.html](http://petra3.desy.de/news/petra_iii_in_general/first_beam/index_eng.html).

**Polish synchrotron project in progress.** The preliminary contract, specifying the frames of the Polish synchrotron project, was signed on November 28, 2008 between the Jagellonian University (coordinator of the project) and the Ministry of Science and Higher Education. The necessary documentation will be prepared by the end of 2009 to define prerequisites for detailed project. The first light from the Polish Synchrotron Light Source may be expected mid-2014.

**Reduction of funds from EU for support of experiments at large facilities.** This reduction may cause, in particular, a considerable weakening of international collaboration in the field of experimental studies. A *Manifesto* signed by an international committee points out the possible consequences of this reduction (see p. 100).



Figure 2. Representatives of the Consortium members participating in the Workshop.

---

#### FUTURE CONFERENCES & WORKSHOPS

**E-XFEL Workshop (October 2009).** The European XFEL-MID workshop, is organised on 28-29.10.2009, in Grenoble (France).

**4th Workshop on High Resolution Diffraction at PETRA III (November 2009).** The Workshop to be held on 5-6.11.2009 at DESY, Hamburg (Germany), will be connected with the planned start of P08 beamline (HighRes) at PETRA III, optimised for high  $q$ -resolution experiments at photons of energies from 5 up to 29 keV. <https://indico.desy.de/conferenceDisplay.py?confId=229601/09/2009>.

**Biology and Medical Applications (February 2010).** The meetings of Biology and Synchrotron Radiation (BSR) and Medical Applications of Synchrotron Radiation (MASR) will take place on 15-18.02.2010, Melbourne (Australia).

**Tenth ISSRNS Meeting (June 2010).** The 10<sup>th</sup> International School and Symposium on Synchrotron Radiation in Natural Sciences (ISSRNS 2010) will be held in Szklarska Poręba (south-western Poland), 6-12.06.2010.

**Free Electron Laser Meeting (August 2010).** 32<sup>nd</sup> International Free Electron Laser Conference will be organised on 23-27.08.2010 in Malmö (Sweden).

**Synchrotron Radiation Instrumentation Meeting (September 2010).** The Sixteenth Pan-American Synchrotron Radiation Instrumentation (SRI) Conference, is planned for 21-24.09.2010, Argonne, IL (USA)

---

#### USER MEETINGS

**SLS User Meeting (October 2009).** Joint Users' Meeting at PSI ([JUM@P'09](http://JUM@P'09)), will be held on 12-13.10.2009. This is a meeting of the users of three facilities: the Swiss Light Source (SLS), the Swiss Spallation Neutron Source (SINQ) and the Swiss Muon Source (**SμS**) (see <http://user.web.psi.ch/jump09/html/index.shtml>).

**MAXlab User Meeting (November 2009).** MAX-lab 22<sup>nd</sup> Annual User Meeting, will be held on 2-4.11.2009, in Lund (Sweden).

**BESSY-II User Meeting (November 2009).** First Joint BER II and BESSY II Users Meeting, takes place on 12-13.11.2009 in Berlin-Adlershof (Germany).

**HASYLAB User Meeting (January 2010).** HASYLAB Users' Meeting is organised on 29.01.2010 in Hamburg (Germany).

---

**More news at:** <http://www.lightsources.org/cms/>.

## ON THE POLFEL FREE ELECTRON LASER PROJECT

**G. Wrochna<sup>1</sup>, J. Jagielski<sup>1</sup>, J. Krzywiński<sup>2</sup>, R. Nietubyć<sup>1</sup>, J. Pełka<sup>3</sup>, E. Pławski<sup>1</sup>,  
J. Sekutowicz<sup>4</sup>, R. Sobierajski<sup>3</sup>, and J. Szewiński<sup>1</sup>**

<sup>1</sup> *The Andrzej Soltan Institute for Nuclear Studies PL-05500 Świerk, Poland*

<sup>2</sup> *SLAC National Accelerator Laboratory, 2575 Sand Hill Road, Menlo Park, CA94025, USA*

<sup>3</sup> *Institute of Physics PAS, Aleja Lotników 32/46, PL-00668 Warsaw, Poland*

<sup>4</sup> *Deutsches Elektronen-Synchrotron, Notkestrasse 85, D-22667 Hamburg, Germany*

*Keywords:* free electron laser, linear accelerator, vacuum ultraviolet (VUV) source.

\*) e-mail:[wrochna@ipj.gov.pl](mailto:wrochna@ipj.gov.pl)

The fabulous properties of the coherent radiation generated with the free electron lasers (FEL) gained broader perspective on the experimental capabilities in physics, chemistry, biology and medicine. They raise from the nanometer-ranged wavelength, femtosecond-ranged pulse duration and brightness in the range of  $10^{29}$  photons/(s·mrad<sup>2</sup>·mm<sup>2</sup>·0.1% bandwidth) accompanied by up to megahertz repetition frequency. Such a light source extends experimental capabilities in spectroscopy, photon counting, imagining, photo-induced material processing and warm dense plasma creation.

We propose to settle a high average power VUV FEL facility POLFEL at the Andrzej Soltan Institute for Nuclear Studies in Świerk. POLFEL is planned as a node of the EuroFEL network of complementary facilities, recommended by ESFRI. The great weight of the synchrotron radiation studies in modern science and technology makes us recognize the next, fourth generation light source facility as an instrument which will effectively improve the impact of research being run in Poland. Presented concept benefits from the long and wide experience of Polish scientists and engineers involved in the FEL activities world wide.

Here we present an overview of the general layout of the planned facility, paying a special attention to its novel solutions. The ground breaking feature of POLFEL is a continuous wave (cw) or near-cw operation. It will be achieved with a linear superconducting (sc) accelerator fed with a low emittance sc-electron injector furnished with the thin film sc lead photocathode. There are three outstanding characteristics of the VUV radiation emitted by FEL, which are often named as its fundamental advantages: femtosecond pulse duration, huge peak brilliance and high average intensity. As the first two of them are adequately accounted in the existing facilities or those being in the advanced phase of construction: FLASH, FERMI and LCLS, we turn our efforts towards the last of mentioned parameters – the average power.

The principal goal, which dictates that approach, is to enable experiments requiring maximization of the time integrated number of interacting photons. They are experiments dealing with diluted samples and/or processes occurring with a low probability [1-3]. For

those experiments, the significant improvement of experimental capabilities can be achieved when the recent progress in reduction of detectors readout time [4] goes together with the higher repetition rate of the light source.

POLFEL will operate basing on the SASE (Self-Amplified Spontaneous Emission) principle [5] and will generate the light as displayed in Table 1.

Table 1. Parameters of POLFEL light.

wavelength	7.5 – 230 nm
pulse duration	< 100 fs
pulse energy	> 10 μJ
peak power	> 0.1 GW
repetition rate	$10^5$ Hz
average power	>0.05 W

The experiments, which benefit from high integrated flux are, e.g., spectroscopy of highly charged ions and cold molecular ions, produced with low concentration in the ion traps [1, 2]; spectroscopy of low Z elements [3], and studies of low populated mass selected clusters [6].

High integrated photon flux is greatly appreciated by the photon-induced materials processing applications. They are lithography, pulsed laser deposition, micromachining and photochemistry [7, 8]. The significance of that parameter stems from the time and costs reduction achievable when a larger area is irradiated. To achieve a high duty factor, significant technical improvements are required in the accelerator construction. One of the main limitations precluding the emission of a large number of photons per second is the millisecond duration of the radio frequency (rf) pulse [9, 10]. In the existing and up to now proposed facilities, based on the sc linacs, this disadvantage results from the normal conducting electron injectors, which can operate only in the low duty factor pulse mode when they generate low emittance highly populated beams [11]. Some improvement was made when the sc high purity niobium injector cavities furnished with Cs<sub>2</sub>Te photocathode was implemented, however their performance is poor due to the technically challenging

integration of the non-superconducting cathode into the sc environment. We propose a fully sc injector, based on the lead photocathode located in the 1.6-cell niobium accelerating structure. The lead film, having one micrometer in thickness, has been chosen due to the superconducting Pb properties below its critical temperature of 7.32 K and high, as compared to other superconducting materials (e.g. Nb) quantum efficiency.

The UHV cathodic arc – based technology of the Pb film deposition onto the back wall of cavity has been proposed and is being currently implemented and optimized [14]. A number of TESLA type injectors were furnished with Pb thin film photocathode (Fig. 1). The quantum efficiency and resonant rf performance tests have been performed at TJNAF, their results have been found promising [15]. However, as a price for the longer lasting stable performance, the quantum efficiency of lead is roughly ten times lower than that for Cs<sub>2</sub>Te. This can be partially compensated with stronger pulse of the laser irradiating the photocathode.

Adopting the superconducting injector enables rf pulses lasting hundreds of milliseconds and longer up to continuous wave operation. In such a case, the time structure of FEL source is determined by the beat of the triggering laser. That enables the repetition rate up to 100 kHz, which ramps the average power at the fundamental wavelength up to tens of milliwatts i.e. few times higher than the designed topical average power of FLASH.

The accelerator capability to operate with a high repetition rate gives an opportunity to freely shape the time structure of the photon beam. In case of slow data acquisition, the possibility of launching next pulse immediately after the readout is completed, without waiting for the next rf period, yields additional enhancement in number of photons being used in an experiment.

Results of the performed preliminary evaluation of the linac (Fig. 2) performance are given in Table 2. It illustrates two adverse approaches to the operation of linear accelerator. The first is oriented towards maximal acceleration gradient, in cost of rf pulse duration, while the other reaches the maximal time integrated electron current through the undulator, in cost of electron energy. For the emitted photons, that alternative corresponds to the

choice of a short wavelength or a high flux. Typical, klystron based accelerators operate in one of those two manners. In our implementation both choices will be possible due to inductive output tubes (IOT) used to generate the rf power. Table 2 shows results for the linac consisted of 3, 5 and 7 cryomodules, each containing eight 9-cell TESLA sc structures. The increase of acceleration gradient bears the rise of power dissipation in the cavity wall. As this leads to increase of the cryogenic load it must be compensated with shortening the RF pulse duration, which at the highest energy gain of 225 MeV/cryomodule will be still ~100 ms long, i.e., two orders of magnitude longer than pulse of FLASH and planned for the European XFEL.



Figure 1. Superconducting electron guns. Upper picture shows lead photocathode spots deposited onto back wall of resonant cavities. The lower picture shows 0.5 and 1.6 – cell acceleration structures.

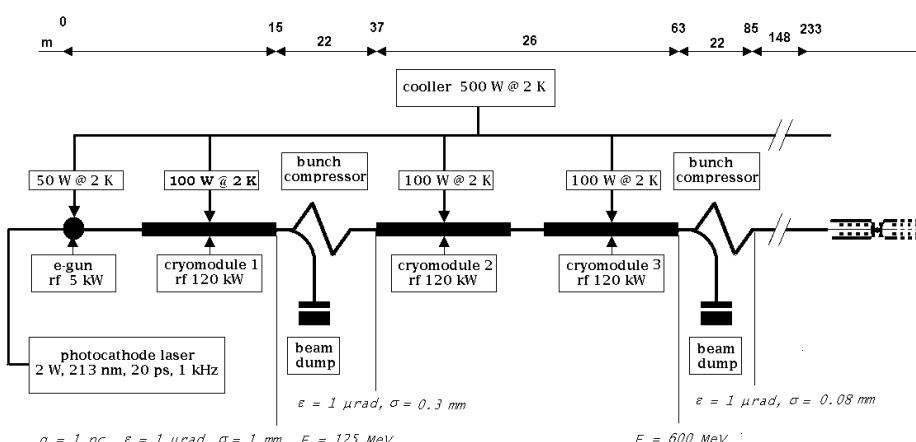


Figure 2. Conceptual drawing of POLFEL linac.

Figure 2. Conceptual drawing of POLFEL linac.

Table. 2. Polfel characteristics for 3, 5 and 7 cryomodules assuming resonance quality  $Q_0=2 \cdot 10^{10}$ , bunch charge 1 nC, max.e. beam current 0.1 mA and undulator period 40 mm. K=0.9.

accelerating gradient [MV/m]	9	12	15	18	21	24	27
electron energy increase per cryomodule [GeV]	0.175	0.100	0.125	0.150	0.175	0.200	0.225
electron energy [GeV]	3 cryomodules"	0.35	0.42	0.50	0.57	0.65	0.72
	5 cryomodules"	0.50	0.62	0.75	0.87	1.00	1.12
	7 cryomodules"	0.65	0.82	1.00	1.17	1.35	1.52
fundamental wavelength	3 cryomodules	79	53	39	30	23	19
$\lambda[\text{nm}]$	5 cryomodules	39	25	17	12	9.6	7.6
	7 cryomodules	23	14	9.6	7.0	5.3	4.1
dynamic losses per 9-cell structure at 2K [W]	4.3	7.7	12	17.2	23.5	30.6	38.8
total losses per 9-cell structure at 2K [W]	5.6	8.7	12.7	17.8	23.9	31.0	39.1
duty factor	1.00	0.72	0.49	0.35	0.26	0.19	0.15
repetition rate [MHz]	0.1	0.072	0.049	0.035	0.026	0.019	0.015
max. e-beam peak power [kW]	28	33	38	43	48	53	58
average electron beam power at the dump.[kW]	28	23	18	15	12	11	9

The cryogenic system will enable the accelerator operation in the temperature of 2 K.

In order to achieve the highest available performance of the machine, including long pulses and cw, high repetition rate and high gradients, an effective control system has to be used. To control the field in the cavities, a digital feedback system based on digital signal processing will be used. The analog part of the system must assure low-noise field detection and precise synchronization on the length of hundreds meters. The digital electronics must perform effective real time signal processing based on field programmable gate array (FPGA) devices and digital signal processors (DSP). The whole installation must be integrated with high bandwidth communication infrastructure (like Gigabit Ethernet) to provide on-line real time control and data acquisition. The ability of remote management helps in effective operation and also facilitates the maintenance of the machine. To have a highly automated and distributed installation, made of many small intelligent nodes, the usage of embedded systems will be preferred over the usage of industrial computers, which requires cooling, hard disks, and space in the rack.

As the statistics shows, that many large experimental systems fail due to a failure in power suppliers, an effort is being done in order to provide a robust installation. Particularly ATCA and uTCA standards are considered for electronics panels while the VME is considered as a backup solution.

A 20 m long, single track of APPLE II – type (Advanced, Planar Polarised Light Emitter) [16, 17] permanent magnet undulators will be installed behind the accelerator. It assures the tunability across various orientation of linear and elliptical polarization and wavelength tuning without changing the linac parameters. The whole system will be divided onto 10 sections. Each section will contain about 50 periods of

magnetic structure, each period includes four magnets. The system will operate in the K range from 1.0 up to 3.0. Figure 3 and Table 3 show the peak brightness values in photons/s mrad<sup>2</sup> mm<sup>2</sup> 0.1 BW (denoted as p. b. units) and average power achievable for the electron bunch charge 1 nC/bunch, energy 600 MeV and emittance  $8 \cdot 10^{-10}$  m-rad. Presented data base on the rough assumptions on the injector performance and assume the accelerating modules performance similar to that of FLASH machine. Improved data on POLFEL characteristic will be presented soon after the full start – to end simulation of electron beam propagation.

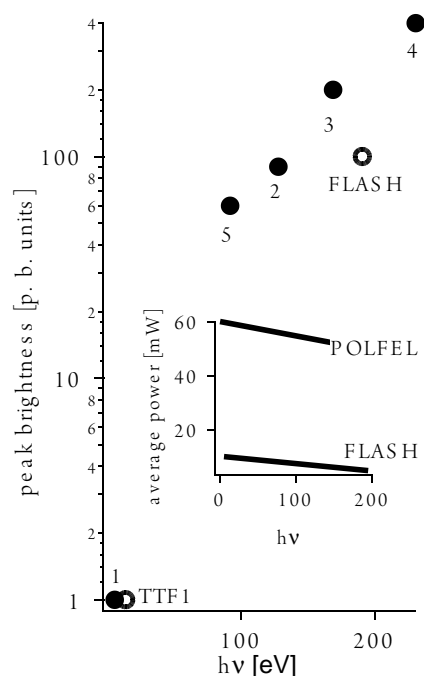


Figure 3 Estimated peak brightness and average

power of POLFEL.

machine parameters				photon energy and wavelength	peak brightness [p. b. units]
1	$q=10^{-9}$ C $\varepsilon l=10^{-9}$ m·rad $L=10 \times 2$ m $\lambda_u=0.04$ m	$\sigma=1 \cdot 10^{-4}$ m	$E_e=0.35$ GeV; $K=2.1$	5.28 eV, 234 nm	$1 \cdot 10^{28}$
2			$E_e=1.00$ GeV; $K=0.9$	128 eV, 9.5 nm	$9 \cdot 10^{29}$
3		$\sigma=5 \cdot 10^{-5}$ m	$E_e=1.00$ GeV; $K=0.9$	169 eV, 7.4 nm	$2 \cdot 10^{30}$
4			$E_e=1.25$ GeV; $K=0.7$	231 eV, 5.36 nm	$4 \cdot 10^{30}$
5		$\sigma=1 \cdot 10^{-4}$ m	$E_e=0.90$ GeV; $K=1.1$	91.8 eV, 13.5 nm	$6 \cdot 10^{29}$
TTF 1	$q=2.7 - 3.3 \cdot 10^{-9}$ C $\varepsilon=18.8 \pm 6.3 \cdot 10^{-9}$ m·rad $\sigma=4 \cdot 10^{-3}$ m $L=13.5$ m $\lambda_u=0.0273$ m		$E_e=0.98$ GeV; $K=1.23$	11.8 – 13.5 eV; 105 - 95 nm	$10^{28}$
FLASH	$q=0.5 - 1.0 \cdot 10^{-9}$ C $\varepsilon=1.5 \cdot 10^{-9}$ m·rad $\sigma=8 \cdot 10^{-4}$ m $L=27.3$ m $\lambda_u=0.0273$ m		$E_e=0.98$ GeV; $K=1.23$	191 eV; 6.5 nm	$10^{29} - 10^{30}$

Table 3. Estimated POLFEL parameters compared to TTF first lasing and FLASH lasing at 6.5 nm.  $K = K_x = K_y$ .

Start-to-end simulations will show the electron and photon beams parameters resulting from accelerator, undulators and beamline arrangements. The calculations will start from the photocathode emission and resulted in electron distribution determined from an energy density of UV laser pulse. Next, the electron bunch dynamics calculations will provide in turn: the injector emittance and bunch shapes at consecutive stages of accelerating and compression [18, 19]. The SASE beam parameters will be calculated, based on beams shape at the undulator entrance and its further evolution in the magnetic structure of the undulator [20]. Finally a wave front propagation through the optical path will be simulated and photon beam in the geometric place of experimental station will be revealed. Performed calculations allow the further refinement and optimization of the technical design refinement.

Two optical paths transferring the beam to two experimental end stations will be installed in the first stage of POLFEL operation. They represent the two branches of scientific programme: basic science and technology. The light will be switched between them with the mirror installed behind the common photo diagnostics section. The first branch, will be 25 m long and will be equipped with plane grating monochromator and will provide the micro-focused beam with energy resolution  $\Delta E/E$  in the range of  $10^{-5}$ . That branch will be dedicated to the fundamental studies of light interaction with matter. Second beamline will be oriented towards the maximization of photon flux. It is dedicated for materials processing and thus contain extended preparation antechamber. We plan to install eventually 6 beamlines guiding the light to dedicated experimental stations. Auxiliary, plasma sources and synchronized

solid state lasers will be installed. They will be hosted in the experimental hall together with appropriate workshop, laboratory and IT infrastructure.

We propose the FEL facility of distinguished average power and thus complementary to existing and planned light sources of this kind. With this project we facilitate new experiments and provide a technological novelty to the FEL physics and technology. The SASE light generation principle has been chosen as already well established approach, which brings us smoothly to the light generation and makes us concentrate on its further development, namely emission by external modulation and terahertz radiation generation.

## References

- [1] S.W. Epp, J.R. Crespo López-Urrutia, G. Brenner, V. Mäckel, P.H. Mokler, R. Treusch, M. Kuhlmann, M.V. Yurkov, J. Feldhaus, J.R. Schneider, M. Wellhöfer, M. Martins, W. Wurth, J. Ullrich, "Soft X-ray laser spectroscopy on trapped highly charged ions at FLASH", *Phys. Rev. Lett.* **98** (2007) 183001.
- [2] H. B. Pedersen, S. Altevogt, B. Jordon-Thaden, O. Heber, M.L. Rappaport, D. Schwalm, J. Ullrich, D. Zajfman, R. Treusch, N. Guerassimova, M. Martins, J.-T. Hoeft, M. Wellhöfer, A. Wolf, "Crossed beam photodissociation imaging of HeH<sup>+</sup> with Vacuum Ultraviolet Free-Electron Laser Pulses", *Phys. Rev. Lett.* **98** (2007) 223202.
- [3] Y.H. Jiang, A. Rudenko, M. Kurka, K.U. Kühnle, Th. Ergler, L. Foucar, M. Schöffler, S. Schössler, T. Havermeier, M. Smolarski, K. Cole, R. Dörner, S. Düsterer, R. Treusch, M. Gensch, C.D. Schröter, R. Moshammer, J. Ullrich, "Few-photon multiple ionization of N<sub>2</sub> by extreme ultraviolet free-electron laser radiation", *Phys. Rev. Lett.* **102** (2009) 123002.

- [4] R. Hartmann, W. Buttler, H. Gorke, S. Herrmann, P. Holl, N. Meidinger, H. Soltau, L. Strüder, "A high-speed pnCCD detector system for optical applications", *Nucl. Instr. & Meth. A* **568** (2006) 118–123.
- [5] V. Ayvazyan, N. Baboi, I. Bohnet, R. Brinkmann, M. Castellano, P. Castro, L. Catani, S. Choroba, Cianchi, M. Dohlus, H.T. Edwards, B. Faatz, A.A. Fateev, J. Feldhaus, K. Flöttmann, A. Gamp, T. Garvey, H. Genz, Ch. Gerth, V. Gretchko, B. Grigoryan, U. Hahn, C. Hessler, K. Honkavaara, M. Hüning, R. Ischebeck, M. Jablonka, T. Kamps, M. Körfer, M. Krassilnikov, J. Krzywinski, M. Liepe, A. Liero, T. Limberg, H. Loos, M. Luong, C. Magne, J. Menzel, P. Michelato, M. Minty, U.-C. Müller, D. Nölle, A. Novokhatski, C. Pagani, F. Peters, J. Pflüger, P. Piot, L. Plucinski, K. Rehlich, I. Reyzl, A. Richter, J. Rossbach, E.L. Saldin, W. Sandner, H. Schlarb, G. Schmidt, P. Schmüser, J.R. Schneider, A. Schneidmiller, H.-J. Schreiber, S. Schreiber, D. Sertore, S. Setzer, S. Simrock, R. Sobierajski, M.V. Yurkov, K. Zapfe, "Generation of GW radiation pulses from a VUV free-electron laser operating in the femtosecond regime", *Phys. Rev. Lett.* **88** (2002) 104802.
- [6] V. Senz, T. Fischer, P. Oelßner, J. Tiggesbäumker, J. Stanzel, C. Bostedt, H. Thomas, M. Schöffler, L. Foucar, M. Martins, J. Neville, M. Neeb, Th. Möller, W. Wurth, E. Rühl, R. Dörner, H. Schmidt-Böcking, W. Eberhardt, G. Ganteför, R. Treusch, P. Radcliffe, K.-H. Meiwes-Broer, "Core-Hole Screening as a Probe for a metal-to-nonmetal transition in lead clusters", *Phys. Rev. Lett.* **102** (2009) 138303.
- [7] Laser processing Consortium Proposal "*High Power Ultraviolet and infrared free electron laser for industrial processing*" (1994).
- [8] H.F. Dylla, S. Benson, J. Bisognano, C.L. Bohn, L. Cardman, D. Engwall, J. Fugitt, K. Jordan, D. Kehne, Z. Li, H. Liu, L. Merminga, G.R. Neil, D. Neuffer, M. Shinn, C. Sinclair, M. Wiseman, K.J. Brillson, D.P. Henkel, H. Helvajian, M.J. Kelly, "A high-average-power FEL for industrial applications", *Proc. of the Particle Accelerator Conference*, 1995, vol. 1, pp. 102–104.
- [9] W. Wuensch, "High gradient breakdown in normal conducting RF cavities", *Proc. of European Particle Accelerator Conference EPAC 2002*, Paris, France, pp. 124–138.
- [10] H. Bluem, T. Schultheiss, R. Rimmer, L.M. Young, "Normal conducting CW RF gun design for high performance electron beam", *Proc. of European Particle Accelerator Conference*, EPAC 2008 Genoa, pp. 223–225.
- [11] D. Janssen, H. Büttig, P. Evtushenko, M. Freitag, F. Gabriel, B. Hartmann, U. Lehnert, P. Michel, K. Möller, T. Quast, B. Reppe, A. Schamlott, Ch. Schneider, R. Schurig, J. Teicher, S. Konstantinov, S. Kruchkov, A. Kudryavtsev, O. Myskin, V. Petrov, A. Tribendis, V. Volkov, W. Sandner, I. Will, A. Matheisen, W. Moeller, M. Pekeler, P. v. Stein, Ch. Haberstroh, "First operation of superconducting RF-gun", *Nucl. Instr. & Meth. A* **507** (2003) 314–317.
- [12] J. Sekutowicz, J. Iversen, D. Klinke, D. Kostin, W. Moller, A. Muhs, P. Kneisel, J. Smedley, T. Rao, P. Strzyzewski, Z. Li, K. Ko, L. Xiao, R. Lefferts, A. Lipski, M. Ferrario, "Status of Nb-Pb superconducting RF-GUN cavities", *Proc. of Particle Accelerator Conference*, 2007, pp. 962–964.
- [13] M. Ferrario, W.D. Moeller, J.B. Rosenzweig, J. Sekutowicz, G. Travish, "Optimization and beam dynamics of a superconducting radio-frequency gun", *Nucl. Instr. & Meth. A* **557** (2006) 98–102.
- [14] P. Strzyzewski, M.J. Sadowski, R. Nietubyć, K. Rogacki, T. Paryjczak, J. Rogowski, "Fabrication of thin metallic films by arc discharges under ultra-high vacuum conditions", *Mater. Sci.-Poland* **26** (2008) 213–218.
- [15] J. Sekutowicz, A. Muhs, P. Kneisel, R. Nietubyć "Cryogenic test of the Nb-Pb SRF Photoinjector Cavities" submitted to the *Proc. of Particle Accelerator Conference*, PAC 2009, Vancouver.
- [16] E. Allaria, B. Diviacco, G. de Ninno, "Estimation of undulator requirements for coherent harmonics generation", *Proceedings of European Particle Accelerator Conference*, EPAC 2008 Genoa, pp. 67–69.
- [17] D. La Civita, B. Diviacco, C. Knapic, M. Musardo, D. Zangrando, L. Bregant, C. Poloni, "Development of the mechanical structure for FERMI@Elettra APPLE II undulators", *Proceedings of Particle Accelerator Conference*, 2007, pp. 980–982.
- [18] S. Thorin, M. Brandin, S. Werin, K. Goldammer, and J. Bahrdt, "Start-to-end simulations for a seeded harmonic generation free electron laser", *Phys. Rev. ST Accel. Beams* **10** (2007) 110701.
- [19] K. Flöttmann, *ASTRA User Manual* www.desy.de/~mpyflo/Astra\_documentation (DESY, Hamburg 2000)
- [20] S. Reiche, *PhD Thesis*, Hamburg University 1999.

## IT ALL STARTED OUT INNOCENTLY ENOUGH...

**Wojciech M. Kwiatek**

*The Henryk Niewodniczański Institute of Nuclear Physics, Polish Academy of Sciences  
ul. Radzikowskiego 152, 31-342 Kraków, Poland*

*Keywords:* *Synchrotron radiation, NSLS, X26, SRIXE*

*E-mail:* *wojciech.kwiatek@ift.edu.pl*

*to my wife Anna and all the friends from the former Division of Applied Science at Brookhaven National Laboratory*

On 27<sup>th</sup> of November, 1984, together with my wife Ania, I set off on what was originally planned for just one year but proved the most exciting and eventful, triple longer journey of my life, both literally and figuratively: so started my scientific research adventure with matter disclosing its secrets when illuminated by energetic and unusually intense photon beams. Our destination, New York, was by no means easy for us to reach at that time: American answer to the martial law in Poland (1981 – 1983) included Polish aircraft being banned from landing at U.S. airports. A detour via Montreal happily ended at La Guardia Airport in New York. In the arrival hall we soon spotted a gentleman wearing the BNL (Brookhaven National Laboratory) badge on his uniform. If it were not for this badge we would have never guessed that the word *Kwiatek* he uttered with an American accent was supposed to be my surname. He opened the door of a BNL Buick. "What a boat of a car", I thought, being used to the view of vehicles moving on Polish roads in mid-eighties. Another two hour drive down the Long Island Expressway (L.I.E or I-495) and we called at the door of our fully equipped apartment with keys and ID cards in our hands. Tired after a long journey, we reclined in comfy armchairs and listened to the happy silence of our new home. Impressed by what we had just experienced we realized: America – a dreamland for generation of Poles was welcoming us so warmly. Was it for real? Or maybe a daydream?

Next day I went to the Laboratory to see my new boss, Dr. Keith Jones. Rather short gentleman dressed in a navy-blue sweater was engaged in a telephone conversation with somebody. After a while he replaced the handset, noticed me, greeted me warmly and invited me to his office. Little could I understand of the words he spoke to me for my ear was not at all tuned to the American pronunciation of English. I could at most nod from time to time. Fortunately, a friend of mine, Marian Cholewa, accompanied me and helped me out of deep water a couple of times. Somehow I managed to survive until 5 p.m. and rushed home. Half an hour walk towards the *Apartment Area* could not change the mood of dismay brought on by my first day at BNL. I rang the doorbell of our Apt. 41G.

Ania was almost done unpacking our four suitcases. "Let's pack up! We are going back right away! I can't make a single word out of what they are talking to me!". My dear Ania, she really knew how to pour oil on troubled waters. She was right: I felt better and better with each coming day. The laws of physics, fortunately, do not depend on the particular language you speak. I worked with the proton beam from a 3.5-MeV Van de Graaff (Figs.1 & 2) accelerator and took to it like a duck to water. I needed no help. I knew what to do. Soon I met Mati Meron, a chap who spoke Polish, and our secretary, Lore Barbier, a lady of German origin, every so often refreshing my, once quite good, command of her mother tongue. No longer did I feel adrift.



Figure 1. At the back there is VdG accelerator. On the left – PIXE line, on the right – microbeam line.

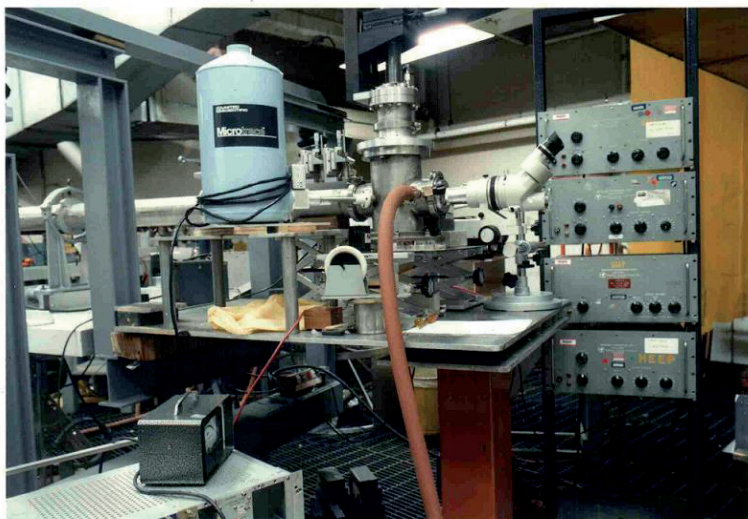


Figure 2. Microbeam experimental chamber with optical microscope clearly visible.

After a time I figured out that our group, named Division of Applied Science, was involved in building a beamline at Brookhaven's National Synchrotron Light Source (NSLS), whose X-ray ring had been just commissioned (1984). I realized that the X26A beamline under construction meant a unique chance for my scientific development. My Kosciuszko Foundation Scholarship would last another half a year and, despite a placement at a highly reputed research centre plus some further experience gained with the proton microbeam, I might be coming back home with few scientific achievements. A proton beam of 20 – 50 µm in diameter was proudly called *a microbeam* (now proton microbeams of cross section below 1 µm are commonly used for experiments). A manually operated manipulator allowed the sample to be positioned in X, Y, Z directions with a theoretical precision down to 5 µm. Collecting a 2-D scan took ages! Hardly anybody would now believe we really felt like doing all this by hand. Mind you, today my students would not even imagine their work without a fully-automatic sample positioning system; and the use of millimetre graphing paper to carry out spectrum energy calibration is for them like moving back to an ancient era. We are talking about the progress we have been witnessing over the period of twenty-five years!

I was lucky. In November 1985, during one of our weekly group meetings, Brant Johnson turned to Keith with an idea that I could join their team and participate in the construction of X26 at NSLS. Keith immediately approved and I eagerly took up the challenge, although it was absolutely obvious for me that a more-or-less experienced researcher on proton microbeams would have to turn into a newbie, fixing nuts and bolts. I did not object, though. Quite the contrary: I was proud to participate in this pioneering project of building a new instrument. Our group with Keith, Barry Gordon, Brant Johnson, Mark Rivers, Albert Hanson and Mati Meron were the great minds to listen to and learn from.

Computer networks, now considered a bloodstream of modern scientific work, information interchange, processing and storage, already at that time were of

tremendous help to researchers. I was happy to master *DECnet*, then a ten-years-old network protocol developed by DEC company and widely used to build architectures of PDP, VAX and like machines.

February 1986 approached fast. Our group, plus Professor Joe Smith from Chicago University, the boss of Mark Rivers and Steve Sutton, gathered at the X26C beamline to celebrate the first opening of the beam shutter. "Slits are open. Look at the wall" — announced Mark Rivers with the sonorous voice of a herald. The wall of the experimental cabin, called *hutch* among the X-ray community, was lined with lead plates. A sheet of fluorescent paper, fixed to the lead lining, now lit up, illuminated by X-ray beam (Fig. 3). Not for nothing was NSLS named a Light Source.

With Champagne in plastic cups we looked at glowing luminescent paper illuminated with synchrotron radiation, and into the glowing future of our research. A new era began for the group (Fig. 4) and a new stage in my own research career, marked by a love affair with synchrotron radiation.

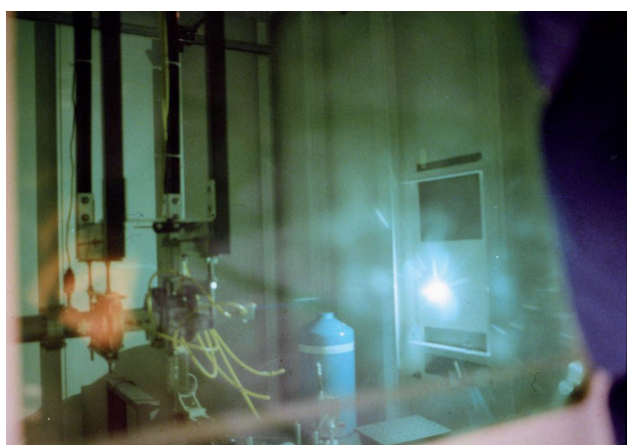


Figure 3. Glowing luminescent paper illuminated with synchrotron radiation.



Figure 4. At the X26C. Standing left to right: Albert L. Hanson, Keith W. Jones and Hu Bej-lai (both not visible behind Albert Hanson), George Schidlovsky, Józef Kajfusz, Joel Smith, Wojciech M. Kwiatek, Mati Meron, Steve Sutton, Mark Rivers, Brant Johnson, Per Spanne, Joel Pounds, Barry Gordon.

Joel Pounds, a toxicologist, joined our group, with the desire to apply the quickly developing synchrotron radiation techniques to biological problems. I liked the idea, as it agreed with my interest in interdisciplinary research. I had just completed a series of PIXE (Proton Induced X-ray Emission) measurements of trace elements in the hair of patients suffering from colon cancer and decided to write my first research proposal concerning SRIXE (Synchrotron Radiation Induced X-ray Emission) studies of cancer tissues. Everybody in our group was writing some proposals, for we had a new instrument: X26C (Fig. 5). In fact, Brant and Mati worked on the development of two X-ray instruments: "our" X26C and another one, X26A, dedicated to atomic spectroscopy (Fig. 6). The X-ray beam had to pass through the Brant's chamber before it entered X26C area. After years the hutches were separated, and the old X26C now became X26A.

Although my proposal was never submitted to NIH (National Institutes of Health), I received invaluable experience in writing research proposals. Now you cannot even dream of successful scientific activity without an ability to apply for funds. Moreover, Joel Pounds took interest in it and offered participation in his project. Soon Greg Long, his Ph.D. student, arrived and became my collaborator. Greg's work consisted in setting up a model experiment on the influence of a particular diet administered to rats on the elemental composition of various organs in these rodents [1]. My job, as a physicist, was to arrange and optimise the experimental setup on X26C for micro-SRIXE measurements.

Together with Albert Hanson and other group members, we embarked on this task. We studied the dependence of the MDL parameter (Minimum Detectable Limit) upon the position of the Si(Li) detector. We found that the signal-to-noise ratio (S/R) decreased whenever we departed from the plane of electron polarization in the storage ring. Similar

worsening of S/R was observed when we changed detector orientation with respect to the direction perpendicular to the beam. All the effects we observed provided an experimental proof to theoretical calculations of the beam polarization components and of the Klein-Nishina distribution of scattered beam. The sample takes its optimum position in focal plane. The task to determine the latter proved most difficult, though. Until now, no better way exists than to achieve a sharp image of the sample surface, as viewed through an optical microscope arranged perpendicular to this surface. Consequently, the sample positioned at the intersection of three straight lines: the symmetry axis of the X-ray beam, optical axis of the microscope, and the symmetry axis of the Si(Li) detector, provided optimum quality spectra of X-ray characteristic radiation [2].

Results which I obtained during our work were fundamental for my Ph.D. thesis which I defended in Poland after completion of my three years stay at the BNL.



Figure 5. General view of the X26 line from the port (at the back) towards the hutch. The space, then quite empty, now is jam-packed with equipment.

Experiment control post of X26C (Fig. 7) was located next to the hutch, along the beam direction. Mark Rivers (Fig. 8) was responsible for all its software. This included remote manipulation of the instrument components, such as step motors, data acquisition and analysis. The system relied on VAX computers, and data analysis programs were written in IDL (Interface Description Language). DECnet made it possible for Mark to carry out remotely a vast part of software development work.

Engaged in fascinating work as it was, I saw the days go by very fast. One Saturday Ania and I were leaving for a dinner party in Passaic, New Jersey. My key just

grated in the door lock when the phone rang. We were pretty short of time and I did not feel like opening the door but phone kept ringing insistently. A few more steps towards the car, and the ringtone seemed even louder. And what if something important happened? — I thought and returned home. It was Keith calling. Angry as hell at Keith I suspected bad news. Why on earth would he call Saturday afternoon? Sure it was not an invitation for dinner as at that time we still were not as close friends as we are now. My intuition did not fail me. *"Hi Wjiech, I have a good news for you. In two hours you will have beam time at X26C. I presume you are happy to come"* — I heard.



Figure 6. Setup for atomic physics experiments. Mark Rivers sitting at the back of the photo.



Figure 7. George Schidlovsky (left) and me at the measurements of lead concentration in bone tissue.



Figure 8. Mark Rivers, busy as usual, at the control post of X26C.

Many a reader of this tale may think: "sounds familiar", recalling similar stories from the beginning of their own research careers, of being proposed in no uncertain terms to do something interesting, yet at odds with young family life. With my Ph.D. thesis in mind I realized how important it was to catch every minute of the beamtime that was getting more and more difficult to obtain. Yet I took my courage in both hands and decided to tell Keith the truth. "*Keith, it is fantastic to have beam time tonight but I am just about to leave for New Jersey for dinner with Ania.*" — I replied. — "*We are invited by Polish Teachers' Association*". Keith knew that Ania taught at St. Isidore's Polish Supplementary School in Riverhead, New York. "*So, could I have it tomorrow morning?*" Silence hung in the air and after a while I heard: "*O.K. You go with Ania and I will stay here with your samples until midnight.*"

We set off. On our way to New Jersey we agreed with Ania that we should be leaving by 10 p.m. in order to call at the Light Source around midnight. What a good time we had that night! Ania was greeted by the President of Polish Supplementary School Council of America, Mr. Jan Woźniak, Ms. Helena Ziółkowski, Editor-in-Chief of Polish teachers' journal "*Głos Nauczyciela*" and the headmaster of Polish Supplementary School, Ms. Feliksa Sawicka. I stayed in the background as a mere accompanying person. However, Mrs. Diana Niewiarowski appeared out of the blue. She was a member of the Kościuszko Foundation Council. Ania and I were introduced to Dede (Diana's nick name). As soon as she learned that I was a grant holder of the Kościuszko Foundation, she invited us to the Athletic Club in New York, for the Debutante Branch and to the Debutante Ball to be held at the Waldorf-Astoria hotel in Manhattan. Was it all worth bargaining with Keith over returning to the beamline?

As it had been agreed, we left around 10 p.m. I took Ania home and called at our lab just before midnight, still in my evening suit. Keith was sitting in front of a

computer monitor, supervising measurements for me, so glad to see I kept my word.

Days passed by, almost unnoticed, as I was more and more committed to my work. Well, hours do not strike for a happy man at a source of synchrotron radiation. Together with Greg we sought the best solutions for the target preparation. The biological part of his experiment was almost completed and the time came to start measurements of elemental composition of the tissues under study (Fig. 9). The first results taught me a lesson on how complex data analysis would be. With biological material in beam, one had to consider a handful of factors that might possibly affect the spectra. To start with, the particular substrate underlying the sample, left its footprint on the results. Next, the spectra appeared dependent upon sample thickness, an effect easy to foresee but difficult to account for. Unlike most solid state samples, a biological specimen is often non-uniform, hence a need to identify precisely the area illuminated by X-ray beam. Despite the use of an optical microscope, such identification proved very difficult. It took some time until we learned how to dye a sister specimen and then to orient the tissue with respect to the microbeam. So far, only being able to vary the diaphragms (slits size), we had been working with a "white" beam [3].

The need for a monochromator and a beam focusing optics became evident. The use of diaphragms meant an obvious waste of photons and did not allow to decrease the MDL parameter. Efforts to obtain the necessary funds started forthwith. I also enjoyed studying the field of physics I was not very familiar with so far, that the foundation of X-ray optics.. Future use of the X-26A beam line was based on the use of an ellipsoidal 8:1 platinum-coated mirror machined from an aluminum block.

With this equipment installed our measurements gained tremendously in quality. We were able to

determine even small concentrations of elements we were interested in [4]. With the use of visualisation software that Mark wrote, spatial distributions of concentrations under study could be easily seen (Fig. 10). I looked at my work with satisfaction: not only was it extremely interesting but also had practical applications.

In the meantime Per Spanne was setting up tomography experiments. He placed a sample on the path of an intense, well collimated beam, an intensity monitoring detector right behind the sample (Fig. 11). The intensity of the incoming X-rays was measured by means of an ionisation chamber. In this way absorption of radiation by the sample could be determined accurately. The sample orientation with respect to the beam could then be varied and, by measuring the absorption coefficient as a function of sample orientation, a cross section of the inner structure of the sample could be reconstructed.

Per did this measurements in one plane but already it was apparent that the imaging capabilities of synchrotron beams would reach far beyond that achievement. Nowadays high resolution 3-D X-ray imaging is a routine measurement. Per illustrated his experiments by reconstructing a cross section of a pencil (Fig. 12).



Figure 9. Sample of rat *cerebellum* tissue we analysed.

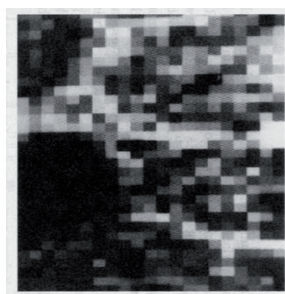


Figure 10. Iron distribution in a selected area of tissue section shown in Fig. 9. The brighter the pixel the higher Fe concentration.

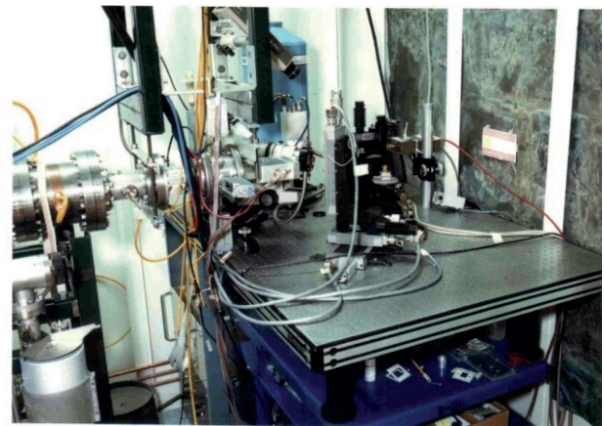


Figure 11. One of the first experimental set-ups for X-ray tomography.

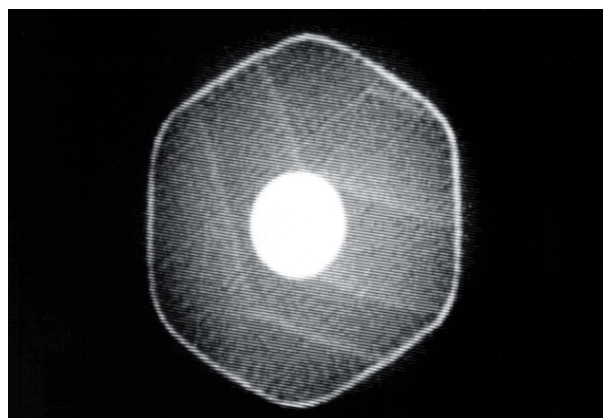


Figure 12. Tomography image of a cross section of an office pencil.

One day in January 1987 I was busy doing measurements. Suddenly an announcement was broadcast: following a decision of the Lab Director, the working day would end at noon, due to an approaching snowstorm. Were they joking? — I thought. Only a few moments ago I walked from our building 901A to NSLS in full sunlight, under clear skies, without a trace of snow anywhere. Suddenly Al turned up. I hardly recognised him. He wore a hat covered with a thick layer of snow. I looked at him, amazed by the accuracy of the weather forecast. That very day Ania visited our friends at their place near the end of the Island. I rang them up only to learn that she had left an hour earlier. I was worried in earnest: how was she going to make it through such a blizzard, a driving license holder for half a year only. Another two hours of waiting and I could tell her at the doorstep how proud I was of her. There were many vehicles abandoned on L.I.E., with only one lane open for traffic. A couple of days later, with that snowstorm and my wife's courage still in mind, I was again busy measuring on a Light Source. Suddenly the telephone rang. I answered with usual: "X26. Wojtek is speaking". The voice on the other side said: "Good morning Mr. Kwiatek. This is Dr. Halfen. I'm so glad to tell you: your

wife is pregnant". I was speechless for a good while with teardrops of happiness around my eyes. Dr. Abraham Halfen was Ania's gynaecologist. Everything had changed since then. We were awaiting the joy of our life. Neither of us wanted to know the baby's gender in advance, although we were offered such information a couple of times during medical examination. There was something of a miraculous mystery in this uncertainty. On September 22, 1987 our daughter Joanna (Joasia) was born. Today she is a student at Jagiellonian University, exploring the mysteries of biophysics. She already took part in a few experiments on synchrotron beams in Frascati and Hamburg. It looks like Dr. Halfen's phone call came at right time in a right place. I am very proud of Joasia and sure Ania would also be... Or, rather, she IS.

Until the end of my stay at Brookhaven I was occupied not only with newborn Joasia but also with collecting results for the Ph.D. thesis. The days, one by one, were "growing tense" with more and more new ideas, measurements, possible interpretations. Together with my Ph.D. supervisor, professor A.Z. Hrynkiewicz, we agreed as to the main contents of the thesis. It would discuss optimum experimental conditions for experiments on the elemental composition of biological tissues. The thesis entitled "Trace element analysis using synchrotron radiation" was completed in English, while still at BNL. I am deeply thankful to Al Hanson, with whom we made friends, for the revision of this work.

My stay at the BNL was originally planned for one year. I owe it to Dr. Keith W. Jones, who believed in me

and who recognized my capabilities, that I spent there three most fascinating years of my life.

All three of us returned to Poland on November 27, 1987 with my Ph.D. thesis ready to submit. The adventure that began with an innocent group meeting at the BNL lasts until now. The adventure with synchrotron radiation.

**Acknowledgements:** Financial support from the Kosciuszko Foundation for the Scholarship of 1984–1985 is highly appreciated as well as funding through the US Department of Energy and National Institutes of Health grants during the extension of my stay at the BNL (1985–1987).

## References

- [1] J.G. Pounds, G.J. Long, W.M. Kwiatak, K.R. Reuhl, A.L. Hanson, B.M. Gordon, K.W. Jones, "Application of synchrotron radiation-induced x-ray fluorescence to trace element toxicology", *Toxicologist* **6**, 1 (1986) 208.
- [2] A.L. Hanson, W.M. Kwiatak, K.W. Jones, "The use of a SiTek position sensitive detector for synchrotron radiation beam monitoring and alignment", *Nucl. Instrum. Meth. Phys. Res. A* **260** (1987) 529-533.
- [3] A.L. Hanson, K.W. Jones, B.M. Gordon, J.G. Pounds, W.M. Kwiatak, G.J. Long, M.L. Rivers, S.R. Sutton, "Trace element measurements using white synchrotron radiation", *Nucl. Instrum. Meth. Phys. Res. B* **24/25** (1987) 400-404.
- [4] W.M. Kwiatak, G.L. Long, K.R. Reuhl, A.L. Hanson, K.W. Jones, J.G. Pounds, "Distribution of Fe, Cu, Zn, and Hg in the mouse cerebellum", *Toxicologist* **7**, 1 (1987) 302a.

## MY FIRST ENOUNTER WITH SYNCHROTRON. 34 YEARS AGO

**Marek Stankiewicz**

*Institute of Physics, Jagiellonian University, ul. Reymonta 4, 30-059 Kraków, Poland*

*Keywords:* synchrotron, vacuum, ionization, coincidence

### Synchrotron radiation?

It was already 34 years ago when I got aware of its existence for the first time!

It was the beginning of 1985. In my pigeon hole, at the Jagiellonian University Institute of Physics there was a letter from my good colleague, Leszek Frasiński, a former assistant in the Department of Atomic Optics in the Institute. Then, he had been working for the last few years for the Atomic and Molecular Spectroscopy Group at University of Reading (UK). In the letter he very strongly persuaded me to apply for a post doc position in Reading. It was all about participating in a very interesting, in his opinion, research project regarding molecular spectroscopy using synchrotron radiation. The head of the group was Prof. Keith Codling, which had pioneered synchrotron radiation based research, fully appreciating its research potential from the very beginning [1]

I must admit that those days my knowledge of the subject was none. Synchrotron radiation? Synchrotron means accelerator. What it has got to do with molecular spectroscopy was boggling my mind. Is it about collisions? Electron- molecule? For sure this can not be the case!

Nowadays, the first reaction would be to type *synchrotron radiation* into a web search engine. One immediately gets hundred thousands hits! However, that time, hard to believe, there was no internet! It was up to many hours in library, browsing through abstracts. There was not so many of them though. This was followed by telephone calls to Reading (via operator, after many hours of waiting) and conversations with Leszek. Some requested literature arrived by mail (not email!). After few weeks came the decision time.

I decided to go for it. I was convinced: this must be a very exciting project full of many challenges in diverse fields. Already advanced talks with University of Stirling about a post doc position connected with some conventional high resolution optical spectroscopy had to be abandoned.

Going abroad those days meant loads of formalities, young readers are not aware of. It had to start, of course with the passport application, submitting all variety of forms in Jagiellonian University SB (Secret Police) office. Will they accept the application or will they not?

After few weeks of apprehensive waiting – yes, passport was ready for collection! Now time for a trip to Warsaw to visit UK embassy and for an interview with a UK immigration officer in order apply for visa (hopefully

a multi-entry one) and work permit. After queuing long hours from early dawn eventually came a rather unpleasant and comprehensive grilling. Questions about membership to any political parties or organization, financial status, properties, personal situation, children, parents etc. Rather revolting experience, not far away from interrogations by Polish SB. Apparently nothing suspicious emerged and I was judged as an individual who was not threatening the security of the United Kingdom of Great Britain and Northern Ireland. After few weeks I was able to collect all the required stamps and documents. Eventually, at the beginning of September 1985 I was ready for take off to commence my duties at University in Reading. One more thing to do – go and buy from a bank 10 USD with a special, very generous exchange rate—a special allowance for Polish citizens going abroad those days!

On the 1<sup>st</sup> of October 1985 I took a seat on a Polish Airlines LOT flight from Kraków to Heathrow. From there I took a bus to Reading, only 60 km (40 miles I should rather say!) west from Heathrow. There I was, looking forward to the new chapter in my career. Next day, a morning meeting was planned at J.J. Thomson (1906 Nobel Prize in Physics for discovery of electron) Physical Laboratory. All members of the Atomic and Molecular Spectroscopy Group were present: Keith Codling, Leszek Frasiński, Kevin Randall and Paul Hatherly.

The title of our project was: “Coincidence studies of molecular ions fragmentation using synchrotron radiation”. A sharp start was needed, timing was very tight. In the first four months we had to design and construct the devoted experimental setup (entire experimental station) and design from scratch a data acquisition system together with developing the relevant software. We needed to divide the work. I was eager to be in charge of the latter task. Electronics had been always my hobby and in the eighties PC computers joined the game. Leszek, Kevin and Paul took on the design and construction of the experimental setup: vacuum chamber, time of flight analyzers, micro channel detectors. This was definitely a big challenge time – for all of us. Many aspects of the tasks were new areas for all of us, including Keith.

Accordingly with the assignment, next day I unpacked a brand new IBM AT PC computer with EGA (Enhanced Graphics Adapter—16 colours, 640×350 pixels) graphics card and corresponding colour monitor. I remember its serial number: 0011. Other parameters of the machine: CPU clock: 8 MHz, hard disk capacity:

20 MB, RAM memory: 624 kB. For the first time in my life I switched on a PC. Armoured with a Fortran compiler and Basic interpreter.

It was a thrill indeed! Those days, in Poland, the IT technology was represented mostly in the shape of Sir Sinclair's ZX Spectrums (8 bit processor, few kB of RAM). Sporadically one was able to see a Neptun – Polish clone of Commodore PET (another 8 bit machine). These small machines, developed for the consumer market were used in Polish research environment for computational purposes and also some relatively efficient data acquisition systems were designed utilising these 'machines', painfully interfacing them with hardware. IBM PC XT's in 'advanced' configuration with 10 MB hard disk equipped with DOS or CP/M operating system were just coming to Poland and were subjects of great admiration.

My AT was supposed to be the heart of the data acquisition system of our experiment. The task was to communicate with a CAMAC crate equipped with Autonomous Logic and Arithmetic Unit, memory, a time to digital converter and numerous auxiliary and interfacing modules.

The goal was to have the acquired coincidences displayed in real time as a false colour map. The first big problem came rather fast: tests revealed that it took minutes to display such a  $256 \times 256$  map (65536 individual pixels) using the purchased Fortran graphics library. For me that meant programming the graphics card in assembler, if I was lucky. If not it meant using the machine code. Which was going to be the case anyway to communicate with the CAMAC controller. Some good fun was ahead! The colleagues could not complain about lack of work either. The experimental setup was quite complicated, equipped with rotatable double time-of-flight analyzers. Everything needed to be built from scratch and experience was needed in designing the detector setups and high vacuum hardware and instrumentation. Our technician was also giving all his best to manage to machine all the bits and pieces in time.

Those days, in Kraków vacuum chambers were built mostly of glass. This meant outgassing the Apiezon greased glass valves and continuous fight with small leaks. Diffusion pumps were used with all the associated problems (presence of hydrocarbons, oil burning etc.). Vacuum conditioning lasted for days and weeks. The glass blowing technician was the person to be in very good relation with!

There we had to produce a high vacuum chamber, free of hydrocarbons to be able to connect it to the synchrotron source termination. Forget glass, Apiezon, diffusion pumps etc. New vacuum culture had to be applied: stainless steel chamber and fittings, turbo molecular pumps, KF and CF fittings and flanges.  $10^{-7}$  torr vacuum achievable in few hours. All new technology - quite a step forward.

That autumn and even the Christmas period was a very busy time for all of us; hard work. In January we were almost ready. Came the last time for tests and modifications. The acquisition system eventually seemed

to be working: collecting and displaying in real time the data from a home built multi-coincidence simulating generator. However, something was wrong: there were very annoying intermittent problems. The communication between the CAMAC controller and the PC sporadically got lost. This certainly was not good and made me frustrated. However, as sometimes happens, after few days of furious tests the problem got resolved by sheer accident. It was just a 5 m long, multi wire ribbon cable connecting the PC with CAMAC, which was causing problems. But it was not as trivial as its contacts. It was just when it was nicely arranged in a tidy roll when apparently some crosstalk between the signals was scrambling the communication. An interesting lesson of applied electronics: keep the cables untidy!

Vacuum chamber was also ready, the two time of flight analyzers and the detectors tested. Our experimental session was planned in few weeks time at Daresbury Laboratory Synchrotron Radiation Source – the *second generation* UK synchrotron radiation facility – e.g. designed and built solely as a source of synchrotron radiation, mostly from bending magnets.

Eventually the time has come. We hired a van and after filling it up with all the equipment we took off to Daresbury. Daresbury is a small village (few houses, a church and of course a pub) in the north of England, near Manchester and Liverpool. On my way there I learned that it is known not only because of the synchrotron facility there but because the author of "Alice's Adventures in Wonderland", Lewis Carroll was born there. However his true name was Charles Lutwidge Dodgson and his principal job was lecturing mathematics at Christ Church College in Oxford in the second half of the XIX century. Apparently the place was special and we were going to a wonderland!

The team appeared to be relaxed, however the prospect of using such a unique source of radiation and working in the large scale facility environment increased my adrenaline level for sure. Above all, I am a researcher and an experimentalist hence I bound to be excited!

We drove very carefully. Such a fragile load needed special care. We did not want the detectors to crack from the vibration. Or any connections got loose inside the vacuum chamber. Eventually we arrived to Daresbury in the evening. It took us some hours to unload and wheel the equipment to the beamline (no. 3.11 – Seya monochromator). When we finished it was time to go straight to bed in a small hostel for the users run by Daresbury Laboratory. Next day morning we were welcomed with typical English breakfast with toasts, fried eggs, sausages and baked beans. It made a perfect introduction into our first session at Daresbury. So it has started. Next month we spent on conquering our experiment, getting known all the control subtleties of our beamline and the monochromator, learning the storage ring refilling procedures; working 20 hours per day. The synchrotron crew had also their share of problems and challenges to provide a stable operation in a single bunch mode, which was required for our experiment in order to ionize oxygen molecules by a

everything one day everything was ready, the equipment was fine tuned, stable single bunch stored in the ring – and we started the real measurement! We were acquiring coincidences between photons, electrons and ions! We were watching, point after point, how our dreamt of colour map of coincidences between the exciting light pulse, photoelectron and photoion in the time of flight (momentum) domain was built up in real time.

Everything was going as we planned – emerging map illustrated energy levels in molecular oxygen – in colour (Fig.1)! A wonderland indeed!

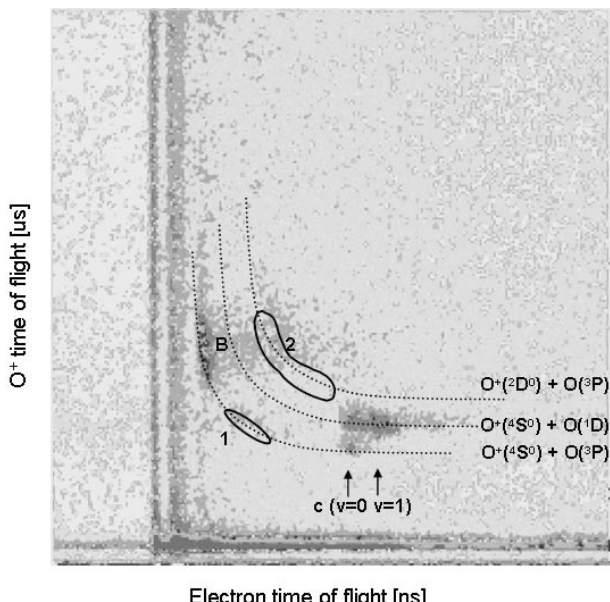


Figure 1. Electron-ion coincidences in ionization of  $O_2$  at 486 Å (25.5 eV). Coincidence features: B, predissociation of the  $B^2\Sigma_g^-$  state to  $O^+(4S^0) + O(^3P)$ ; c,  $v = 0$  and  $v = 1$ , predissociation of the  $c^4\Sigma_u^-$  state to the limits  $O^+(4S^0) + O(^3P)$  and  $O^+(4S^0) + O(^1D)$ ; 1, repulsive state to the limit  $O^+(4S^0) + O(^3P)$ ; 2, repulsive state III  $^2\Pi_u$  to the limit  $O^+(2D^0) + O(^3P)$ . The horizontal line is due to cross-talk; the vertical lines are due to false coincidences. Taken from Ref. [2].

Of course, that day we had to celebrate this success in the nearby, very popular (ask any of the Daresbury Laboratory users!) "Ring'o'Bells" pub with "a pint or two" of a decent English ale.

This is how my adventure with synchrotron radiation based research has started. Since then, for the last 34 years, my research activities have been focused closely on investigation of molecular processes excited by synchrotron radiation.

The Daresbury Synchrotron Radiation Source ceased its operation last year. UK research community has now a new, advanced *third generation* synchrotron source – "Diamond" available.

Nowadays I commute from Kraków mostly to *MAX-lab* in Lund and to *Sincrotrone Elettra* in Trieste, where I have met a very friendly environment. Keith Codling has

retired. Leszek Frasiński holds professorship at Imperial College in London, Paul Hatherly works for Open University in Milton Keynes (England-Buckinghamshire) and the last place where I localized Kevin Randall was Advanced Light Source in Berkeley (California, USA). We are all still around synchrotrons. I am sure that we all remember the period of our first project at Daresbury as a very special one.

From that time the spectrum of synchrotron radiation users has immensely broadened. Nowadays physicists are just one of many groups representing diverse fields of research done at synchrotron radiation facilities. Investigations are carried out, amongst others, in such fields as medicine, biology, chemistry, material science, archaeology etc. Much has changed in the field of electronics, IT technology, and vacuum generation. There has been a big progress in synchrotron design and associated instrumentation, focused on optimizing the radiation output. There are many companies providing synchrotron specific instrumentation which spun off from relevant research projects. Many new synchrotron radiation facilities have been built all around the world. Availability of these unique sources of radiation allows thousands of researchers from different fields for performing experiments otherwise impossible. New, *fourth generation* sources – *Free Electron Lasers* are the latest challenge in the field. Some such facilities are already operating (e.g. *FLASH*, *TESLA* in Europe) another being constructed (*FERMI*), opening new horizons in science.

I am writing these memories when there are strong initiatives to build in Poland a synchrotron radiation source and a free electron laser. I wish that one day in the nearest future at least one of these initiatives is going to be successful. I am convinced that this would be a great day. I am sure about the immense benefits which these projects could bring to the Polish research and education community.

**Acknowledgements:** I would like to thank Prof. Wojciech Paszkowicz for inviting me to write these memories. I mostly appreciate his initiative.

**References:** I have decided to refer only to two publications. Anyone interested in whichever aspect of synchrotron radiation is strongly encouraged to visit <http://www.lightsources.org/cms/> where there is a copious amount of information available.

- [1] R.P. Madden, K. Codling,, "New autoionizing atomic energy levels in He, Ne, and Ar", *Phys. Rev. Lett.* **10**, (1963) 516–518.
- [2] J. Frasinski, M. Stankiewicz, K. Randall, P. Hatherly, K. Codling, "Dissociative photoionisation of molecules probed by triple coincidence; double time of flight techniques", *J. Phys. B: Atom. Mol. Opt. Phys.* **19** (1986) L819–L824..

Marek Stankiewicz  
Instytut Fizyki UJ  
Kraków, August 2009

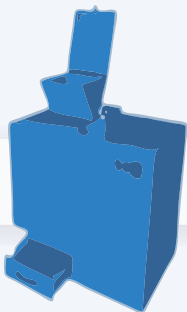
# TESTCHEM

Produkcja urządzeń laboratoryjnych



## Młynki

Laboratoryjne i specjalnego przeznaczenia.



## Kruszarki

Do laboratorium i dla przemysłu.



## Układy chłodzenia

Do dyfraktometrów, spektrometrów i innych urządzeń.

## Prasy

Do przygotowywania próbek spektrometrycznych.



## Nippon Instruments Co.

Analizatory rtęci w ciałach stałych, cieczach i gazach.



## Rigaku

Spektrometry rentgeno-fluorescencyjne. Dyfraktometry rentgenowskie.



# **8. Krajowe Sympozjum Użytkowników Promieniowania Synchrotronowego Podlesice, 24-26 września 2009**

*KSUPS-8: 8<sup>th</sup> National Symposium of Synchrotron Users*



*organizowane przez*

*Instytut Fizyki im. Augusta Cieślowskiego, Uniwersytet Śląski w Katowicach,  
Polskie Towarzystwo Promieniowania Synchrotronowego*

## **KOMITET PROGRAMOWY**

Krystyna Lawniczak-Jabłońska (IF PAN, Warszawa)  
Andrzej Burian (UŚ, Katowice)  
Danuta Żymierska (IF PAN, Warszawa)  
Wojciech Paszkowicz (IF PAN, Warszawa)  
Anna Wolska (IF PAN, Warszawa)  
Edward A. Görlich (UJ, Kraków)  
Bogdan Kowalski (IF PAN, Warszawa)  
Bronisław Orłowski (IF PAN, Warszawa)  
Paweł Piszora (UAM, Poznań)

## **KOMITET ORGANIZACYJNY**

Alicja Ratuszna, Uniwersytet Śląski w Katowicach  
Andrzej Burian, Uniwersytet Śląski w Katowicach  
Jacek Szade, Uniwersytet Śląski w Katowicach  
Andrzej Ślebarski, Uniwersytet Śląski w Katowicach  
Aleksander Bródka, Uniwersytet Śląski w Katowicach  
Katarzyna Grzybowska, Uniwersytet Śląski w Katowicach  
Łukasz Hawełek, Uniwersytet Śląski w Katowicach

## **SPONSORZY**



## 8. Krajowe Sympozjum Użytkowników Promieniowania Synchrotronowego Podlesice, 24-26 września 2009 r.

### Program

<b>Czwartek 24.09.2009</b>		
10.00-13.00	Przyjazd i rejestracja	
13.00-15.00	obiad	
15.00-15.15	Otwarcie 8 KSUPS	
15.15-16.30	L-01	<b>Tomasz Durakiewicz</b> (Los Alamos National Laboratory) <i>Poszukiwanie renormalizacji pasmowej w skorelowanych układach f-elektronowych przy użyciu promieniowania synchrotronowego</i>
16.30-17.15	L-02	<b>Wojciech Kwiatek</b> (Instytut Fizyki Jądrowej PAN) <i>Nowe mikroskopowe metody obrazowania medycznego</i>
17.15-17.30	O-01	<b>Lee Chow</b> (University of Central Florida) <i>Synchrotron radiation study of Mn implanted silicon (Synchrotronowe badania krzemu implantowanego manganem)</i>
17.30-17.45	O-02	<b>Aleksandra Wierzbicka</b> (Instytut Fizyki PAN) <i>Badanie lateralnych warstw epitaksjalnych GaAs i GaSb przy pomocy techniki 'Rocking Curve Imaging'</i>
17.45-18.00	O-03	<b>Wojciech Wierzchowski</b> (Instytut Technologii Materiałów Elektronicznych) <i>Rentgenowskie badania topograficzne struktury domenowej w kryształach <math>Pr_xLa_{1-x}AlO_3</math> wyhodowanych metodą Czochralskiego</i>
18.00-19.00	kolacja	
<b>Piątek 25.09.2009</b>		
19.00	Sesja posterowa	
8.00-9.00	śniadanie	
9.00-9.45	L-03	<b>Grzegorz Wrochna</b> (Instytut Problemów Jądrowych im. Andrzeja Sołtana) <i>POLFEL – laser na swobodnych elektronach o wysokiej mocy średniej</i>
9.45-10.00	O-04	<b>Jerzy Pełka</b> (Instytut Fizyki PAN) <i>Zastosowania laserów na swobodnych elektronach w biologii i medycynie</i>
10.00-10.15	O-05	<b>Ryszard Sobierański</b> (Instytut Fizyki PAN) <i>Oddziaływanie wielowarstwowych układów optycznych z silnymi femtosekundowymi impulsami w zakresie XUW</i>
10.15-11.00	L-04	<b>Paweł Zajdel</b> (Uniwersytet Śląski) <i>Uporządkowanie bliskiego i dalekiego zasięgu w selenkach i tlenkach metali przejściowych na podstawie badań dyfrakcyjnych i ramanowskich</i>
11.00-11.30	przerwa kawowa	
11.30-12.15	L-05	<b>Marcin Sikora</b> (Akademia Górnictwo-Hutnicza) <i>Badania magnetyzmu metodami XMCD i XES</i>

12.15-13.00	L-06	<b>Krystyna Ławniczak-Jabłońska</b> (Instytut Fizyki PAN) <i>Charakteryzacja nanowytrąceń magnetycznych w matrycach na bazie GaSb</i>
13.00-14.30		obiad
14.30-15.15	L-07	<b>Maciej Kozak</b> (Uniwersytet Adama Mickiewicza) <i>Wykorzystanie rozpraszania promieniowania synchrotronowego w badaniach błon biologicznych</i>
15.15-16.00	L-08	<b>Szymon Krzywda</b> (Uniwersytet Adama Mickiewicza) <i>Struktura o atomowej rozdzielcości cytochromu c6 cyjanobakterii o niezwykłej sekwencji wtrąceń</i>
16.00-16.15	O-06	<b>Henryk Drozdowski</b> (Uniwersytet Adama Mickiewicza) <i>Uporządkowanie krótkozasięgowe w orto-chloroanizolu w 293 K – rentgenowskie badania dyfrakcyjne</i>
16.15-16.30	O-07	<b>Krystyna Mazur</b> (Instytut Technologii Materiałów Elektronicznych) <i>Rentgenowskie badania reflektometryczne chropowatości powierzchni kryształów podłożowych SiC i jej wpływ na stopień doskonałości strukturalnej osadzonych epitaksjalnych warstw SiC</i>
16.30-16.45		przerwa kawowa
16.45-17.30	L-09	<b>Radosław Przeniosło</b> (Uniwersytet Warszawski) <i>Badania struktury tlenków metali przejściowych metodą dyfrakcji neutronów i promieni X</i>
17.30-17.45		Wystąpienie przedstawiciela firmy <b>PREVAC</b>
17.45-18.00		Wystąpienie przedstawiciela firmy <b>TESTCHEM</b>
18.00-19.00		Zebranie PTPS
19.00		kolacja konferencyjna
<b>Sobota 26.09.2009</b>		
8.00-9.00		śniadanie
9.00-9.30	L-10	<b>Edward Goerlich</b> (Uniwersytet Jagielloński) <i>Informacja na temat rozwiązań technicznych i stanu przygotowania do realizacji budowy synchrotronu w Polsce</i>
9.30-9.50	L-11	<b>Jacek Szade</b> (Uniwersytet Śląski) <i>Pierwsza linia eksperimentalna na polskim synchrotronie: spektroskopie miękkiego promieniowania rentgenowskiego</i>
10.00-13.00 (z przerwą kawową 11.00-11.30)	Centrum Promieniowania Synchrotronowego	<i>Plenarna (powszechna) dyskusja dotycząca aspektów merytorycznych i organizacyjnych proponowanych linii eksperimentalnych przy polskim synchrotronie [prowadzenie <b>Edward A. Görlich i Krzysztof Tomala</b> (Uniwersytet Jagielloński)]</i>
13.00-14.00		obiad

**Witamy w Podlesicach**  
**na 8. Krajowym Sympozjum Użytkowników Promieniowania Synchrotronowego**

Ósme Krajowe Sympozjum Użytkowników Promieniowania Synchrotronowego (8 KSUPS) odbywa się w dniach 24-26 września 2009 roku w Podlesicach, w gminie Kroczyce u stóp Góry Zborów, w jednym z najbardziej malowniczych rejonów Wyżyny Krakowsko-Częstochowskiej. Jest to kolejne, odbywające się co dwa lata z inicjatywy Polskiego Towarzystwa Promieniowania Synchrotronowego, spotkanie pracowników naukowych, doktorantów i studentów, reprezentujących krajowe uczelnie oraz instytuty naukowo-badawcze. W tym roku jego organizatorami są Instytut Fizyki Uniwersytetu Śląskiego i Polskie Towarzystwo Promieniowania Synchrotronowego.

Podobnie jak w przypadku poprzednich spotkań, liczba uczestników przekracza sześćdziesiąt osób. Cieszy nas bardzo liczna, bo ponad dwudziestoosobowa reprezentacja doktorantów i studentów, stanowiąca bezpośrednio zaplecze naukowo-badawcze dla przyszłych użytkowników krajowego źródła promieniowania synchrotronowego. Tematyka dziewięciu wykładów, które zostaną wygłoszone podczas sympozjum obejmuje zagadnienia związane z badaniem struktury elektronowej w skorelowanych układach *f*-elektronowych, zastosowania metod spektroskopowych i kołowego dichroizmu magnetycznego do badań właściwości magnetycznych, dyfrakcją promieniowania rentgenowskiego, rozpraszaniem ramanowskim, krystalografią białek i strukturą błon biologicznych oraz mikroskopowymi metodami obrazowania medycznego. Jeden z wykładów będzie dotyczył polskiego źródła laserowego na swobodnych elektronach. Przedpołudniowa część sympozjum w dniu 26 września zostanie poświęcona bardzo ważnemu problemowi, a mianowicie budowie polskiego źródła promieniowania synchrotronowego w Krakowie. Ponadto wygłoszonych zostanie siedem referatów oraz przedstawionych prawie czterdzieści prezentacji plakatowych z prawie wszystkich dziedzin zastosowań promieniowania synchrotronowego.

Mamy nadzieję, że 8 Krajowe Sympozjum Użytkowników Promieniowania Synchrotronowego będzie owocnym przeglądem osiągnięć coraz liczniejszej polskiej społeczności naukowej, wykorzystującej w swoich badaniach to jedno z najnowocześniejszych narzędzi badawczych, bez którego trudno sobie dziś wyobrazić postęp w wielu dziedzinach nauki, szczególnie interdyscyplinarnych. Chcielibyśmy również, aby przyczyniło się do zdobycia nowej wiedzy i doświadczeń przez młodych pracowników naukowych, doktorantów i studentów w ich kontaktach z bardziej zaawansowanymi użytkownikami promieniowania synchrotronowego. Ponadto powinno być ono okazją do dalszej konsolidacji środowiska w celu skonstruowania jak najlepszego krajowego źródła i linii pomiarowych oraz skutecznego jego użytkowania w przyszłości.

W imieniu Komitetów Programowego i Organizacyjnego serdecznie dziękujemy wszystkim uczestnikom za liczny udział w Sympozjum, wykładowcom za trud przygotowania wystąpień, referującym i autorom plakatów za prezentację uzyskanych wyników. Życzymy owocnych obrad i dyskusji jak również miłego pobytu w Podlesicach.

*Andrzej Burian i Jacek Szade*

# SYNCHROTRON QUEST FOR BAND RENORMALIZATION IN CORRELATED *F*-ELECTRON SYSTEMS

T. Durakiewicz<sup>1</sup>

<sup>1</sup>*Los Alamos National Laboratory, MPA-10 Group, Los Alamos, NM87545, USA*

*Keywords:* correlated electrons, 4*f*, 5*f*, photoemission

*e-mail:* tomasz@lanl.gov

Numerous low energy scales are observed in heavy fermion materials. Information about some of the scales is imprinted in the electron self-energy which can be measured by angle-resolved photoemission (ARPES). The successful line of attack in *d*-electron materials over the last decade was based on using high energy- and momentum-resolution photoemission techniques to extract the self energy information from measured spectra and applying many-body theoretical approaches to find a link between self-energy and interactions: electron-electron correlations, coupling to bosons, magnetic fluctuations.

In 2008, we discovered a small energy scale in USb<sub>2</sub>, via the observation of a kink in *f*-electron dispersion [1, 2]. The kink structure was observed for the first time in any *f*-electron system. The kink energy scale of 21 meV and the ultra-small intrinsic peak width of 3 meV were seen. Our finding extended the context of quasiparticle band renormalization from *d* to *f*-electrons, hence creating a link between high temperature superconductors and heavy fermions and actinide based compounds. A new model of point-like Fermi surface renormalization was proposed to explain the spectroscopic properties of the kink.

In late 2008 we have found numerous kinks in the band crossing the Fermi level along the G-M direction in CeIrIn<sub>5</sub>. We have clearly identified two energy scales, one leading to a kink at around 270 meV below Fermi level that is related to the lower, incoherent part of the 4*f* 5/2 spin-orbit split, and another one at 7 meV below Fermi level. The 7 meV renormalization may be related to a maximum in phonon density of states observed by

inelastic neutron scattering experiments. The spin-fluctuation energy scale of the order of 1 meV expected to exist in this material is difficult if not impossible to find with ARPES, due to the fundamental resolution limitations. The third scale appears to be located around 20-25 meV above the Fermi level, and corresponds very well to the size of hybridization gap predicted by DMFT [3].

Our preliminary results look very promising, and we plan to (i) expand the suite of *f*-electron materials where kink structures can be characterized and (ii) link the temperature evolution of self-energy with onset of coherence in *f*-electron materials.

## References

- [1] T. Durakiewicz, P.S. Riseborough, C.G. Olson, J.J. Joyce, P.M. Oppeneer, S. Elgazzar, E.D. Bauer, J.L. Sarrao, E. Guziewicz, D.P. Moore, M.T. Butterfield, K.S. Graham, "Observation of a kink in the dispersion of f-electrons", *Europhys. Lett.* **84** (2008) 37003.
- [2] X. Yang, P.S. Riseborough, T. Durakiewicz, C.G. Olson, J.J. Joyce, E.D. Bauer, J.L. Sarrao, D.P. Moore, K.S. Graham, S. Elgazzar, P.M. Oppeneer, E. Guziewicz, M.T. Butterfield, "Unusual quasiparticle renormalizations from angle resolved photoemission on USb<sub>2</sub>", *Philos. Mag.* **89** (2009) 1893–1911.
- [3] J.H. Shim, K. Haule, G. Kotliar, "Modeling the localized-to-itinerant electronic transition in the heavy fermion system CeIrIn<sub>5</sub>" *Science* **318** (2007) 1615-1617.

## NOVEL MICROSCOPY METHODS OF MEDICAL IMAGING

**W.M. Kwiatek<sup>1\*</sup>, M. Podgórczyk<sup>1</sup>, C. Paluszakiewicz<sup>2</sup>, M. Gajda<sup>3</sup>, Z. Stachura<sup>1</sup>,  
M. Lekka<sup>1</sup>, J. Lekki<sup>1</sup>, M. Piccinini<sup>4</sup>, and D. Grolimund<sup>5</sup>**

<sup>1</sup> Institute of Nuclear Physics PAN, ul.Radzikowskiego 152, 31-342 Kraków, Poland

<sup>2</sup> AGH University of Science and Technology, Al. Mickiewicza 30, 30-059 Kraków, Poland

<sup>3</sup> Chair of Histology Collegium Medicum, Jagiellonian University, ul. Kopernika 7, 30-059 Kraków, Poland

<sup>4</sup> INFN - Laboratori Nazionali di Frascati, Via E. Fermi 40, I-00044 Frascati, Italy

<sup>5</sup> Swiss Light Source, Paul Scherrer Institut, 5232 Villingen PSI, Switzerland

*Keywords:* synchrotron radiation, medical imaging, SR-XRF, SR-FTIR, XANES

\*) e-mail: Wojciech.Kwiatek@ifj.edu.pl

Nowdays, the proper diagnosis requires medical imaging at scales ranging from single molecules through cells, tissues, organs, and up to whole body. Traditionally used optical microscopy and some other commonly used techniques quite often become insufficient for accurate diagnostics. Combining different imaging techniques may deliver complementary information from a sample, providing a combination of analytical performance that could enhance the accuracy of diagnosis and thus the quality of prognosis and possibly the speed of it.

Imaging technologies in different scientific areas have been rapidly developing in last decades, requiring higher and higher level of skills and knowledge. This puts medical specialists in a situation of continuous challenge to stay at the cutting edge of the technology already available to help patients timely and efficiently. Such a situation is obviously connected with synchrotron radiation based techniques.

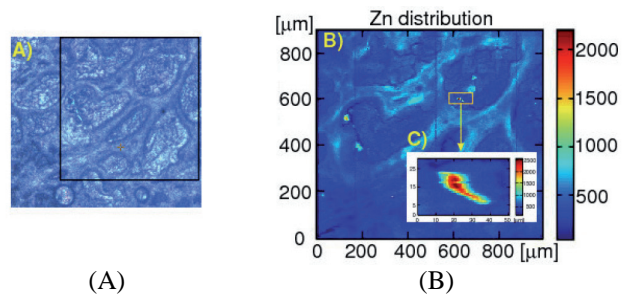
SR-XRF (Synchrotron Radiation-X-ray Fluorescence), XANES (Xray Absorption Near Edge Structure), SR-FTIR (Synchrotron Radiation – Fourier Transform InfraRed), micro-spectroscopy techniques as well as phase contrast microscopy, computer tomography, or a family of scanning probe microscopes (STM, NSOM, AFM...), give new opportunities of medical imaging.

Figure 1 presents the application of SR-XRF Zn distribution within tissue section [1] while Figure 2 shows an example of SR-FTIR image of the prostate cancerous tissue. A closer look at the results permitted to distinguish between the healthy, cancerous and hyperplastic parts of the tissue.

The examples of some other applications will be presented and discussed in terms of complementarities and opportunities.

**Acknowledgements:** This work was supported by the European Community Research Infrastructure Action under the FP6 "Structuring the European Research Area" Programme,

contract No. RII-CT-2004-506008, project No. II-04-079EC and EU Integrated Infrastructure Initiative Hadron Physics Project, contract No. RII3-CT-2004-506078, Tari Programs No. 48, 67, and 85. Also, support from Ministry of Science and Higher Education is appreciated, Grant No. NN301464734.



(A)

(B)

Figure 1. (A) Histological view of prostate tissue section, (B) Zn Distribution over the marked section, (C) High resolution 2D scan of Zn distribution over the “hot spot” [1].

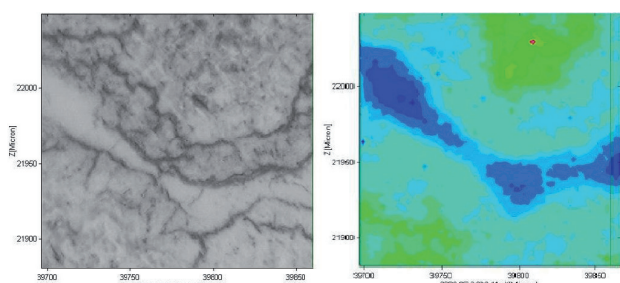


Figure 2. Histological view of prostate cancerous tissue (left), 2D distribution of  $\text{CH}_2/\text{CH}_3$  intensity ratio (right).

### References

- [1] M. Podgórczyk, W.M. Kwiatek, D. Grolimund, C. Borca, "Technical aspects of Zn microanalysis of human prostate cancer tissues and cells", *Radiat. Phys. Chem.* **78** (2009) S53-S57.

# SYNCHROTRON RADIATION STUDY OF Mn IMPLANTED SILICON

**L. Chow<sup>1\*</sup>, A. Misiuk<sup>2</sup>, C.W. Pao<sup>3</sup>, D.C. Ling<sup>3</sup>, W.F. Pong<sup>3</sup>, and J. Bak-Misiuk<sup>4</sup>**

<sup>1</sup>Dept. of Physics, University of Central Florida, Orlando, FL 32816 USA

<sup>2</sup>Institute of Electron Technology, al. Lotników 46, 02-668 Warsaw, Poland

<sup>3</sup>Dept. of Physics, Tamkang University, Tamsui, Taiwan, 25137, R.O.C.

<sup>4</sup>Institute of Physics, PAS, al. Lotników 32/46, 02-668 Warsaw, Poland

*Keywords:* diluted magnetic semiconductor, spintronic materials, X-ray absorption spectroscopy

\*) e-mail: chow@mail.ucf.edu

Diluted magnetic semiconductors (DMSs) based on III-V and II-VI compounds have been extensively studied for the last fifteen years [1]. However, for practical purpose, silicon-based DMS materials are much more desirable due to their compatibility with existing silicon technology. Recently, Bolduc *et al.* [2] reported room temperature ferromagnetism in Mn ion implanted silicon samples. This finding has generated a lot of new excitements in the DMS community.

Here we present the first synchrotron so called XMCD measurement on the MnSi system to clarify our understanding of the observed room temperature ferromagnetism in the Mn-implanted silicon. In addition, x-ray absorption spectroscopy of Mn  $L_{3,2}$ -edge, Mn  $K$ -edge, and magnetization measurements were also performed on the Mn-implanted silicon. Details of our findings are presented below.

Figure 1 displays the normalized Mn  $L_{3,2}$ -edge XANES spectra [3] for the as-implanted and annealed samples. These spectra are compared with the Mn  $L_{3,2}$ -edge XANES spectra of the reference Mn foil and of three different manganese oxides.

The normalized Mn  $L_{3,2}$ -edge XANES and XMCD (denoted as  $I_+$  -  $I_-$ ) spectra for the as-implanted sample and the samples annealed at 300°C, 700°C, and 1000°C

are presented in Figure 2. The general line shapes of  $I_+$  and  $I_-$  are similar for the all samples. And it shows a barely vanishing XMCD intensity for the samples investigated, indicating that the average magnetic moment of Mn ions in silicon is almost zero.

**Acknowledgements:** DCL and WFP would like to thank the National Science Council of Taiwan for financial support under the grants Nos. NSC 96-2212-M-032-008-MY3 and NSC96-2212-M-032-012-MY3. LC would like to acknowledge a grant from US Agreicultural Department.

## References

- [1] S.A. Wolf, D.D. Awschalom, R.A. Buhrman, J.M. Daughton, S. Von Molnar, M.L. Roukes, A.Y. Chtchelkanova, D.M. Treger, "Spintronics", *Science* **294** (2001) 1488.
- [2] M. Bolduc, C. Awo-Affouda, A. Stollenwerk, M.B. Huang, F.G. Ramos, G. Agnello, V.P. LaBella, "Above room temperature ferromagnetism in Mn-ion implanted Si", *Phys. Rev. B* **71** (2005) 033302.
- [3] A. Wolska, K. Lawniczak-Jablonska, S. Kret, P. Dluzewski, A. Szczepanska, M. Klepka, M.S. Walczak, Y. Lefrais, M.J. Hych, A. Misiuk, "Atomic order in magnetic Mn inclusions in Si Crystals: XAS and TEM studies", *J. Non-crystalline Solids* **354** (2009) 418.

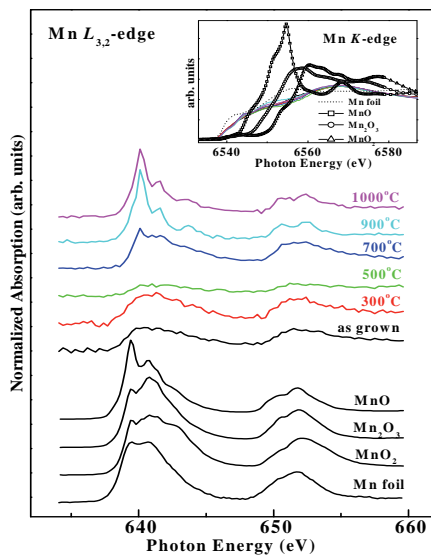


Figure 1 (left). XANES spectra of Mn-implanted silicon sample, as-implanted and annealed. For comparison, XANES spectra of manganese oxide and Mn metal are also shown. In the insert the Mn K X-ray absorption near edge spectra are shown.

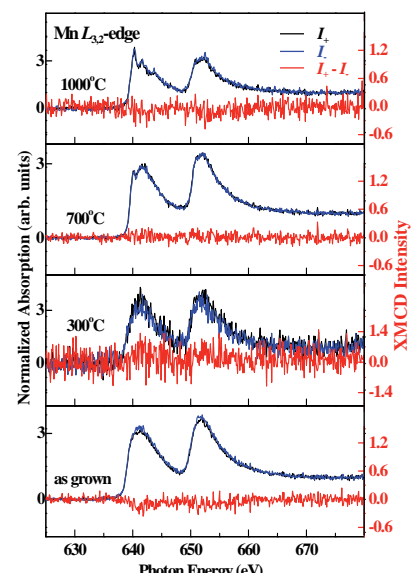


Figure 2 (right). Normalized Mn  $L_{3,2}$ -edge XANES and XMCD spectra for as-implanted sample and samples annealed at 300°C, 700°C, and 1000°C.

## ROCKING CURVE IMAGING STUDIES OF LATERALLY OVERGROWN GaAs AND GaSb EPITAXIAL LAYERS

**A. Wierzbicka<sup>1\*</sup>, D. Lübbert<sup>2</sup>, J.Z. Domagała<sup>1</sup>, and Z.R. Żytkiewicz<sup>1</sup>**

<sup>1</sup>*Institute of Physics, Polish Academy of Sciences, Al. Lotników 32/46, 02-668 Warszawa, Poland*

<sup>2</sup>*Humboldt-Universität, Newtonstr. 15, 12489 Berlin, Germany*

*Keywords:* III-V semiconductors, X-ray diffraction, digital synchrotron topography, epitaxial lateral overgrowth

\*) e-mail: [czyzak@ifpan.edu.pl](mailto:czyzak@ifpan.edu.pl)

The development of modern electronics requires fast techniques that allow precise analysis of the structural quality of crystalline materials starting from bare wafers up to complicated semiconductor structures. The aim of this work was to apply synchrotron radiation based technique of Rocking Curve Imaging (RCI) for detection and visualization of crystalline lattice microdefects in laterally overgrown epitaxial (ELO) layers. Since ELO layers consist of parallel monocrystalline layers regularly arranged on a template (see Fig. 1) they are perfectly suitable to demonstrate the potential of the RCI technique.

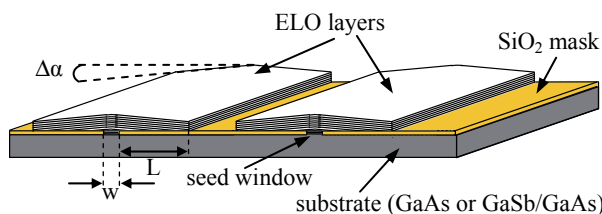


Figure 1. Schematic drawing of ELO structure.  $L$  and  $w$  denote widths of the ELO wing and of the seeding line, respectively.  $\Delta\alpha$  is the maximal tilt angle of the ELO lattice planes.

Briefly, RCI is a technique which combines the features of X-ray imaging (very high spatial resolution) and X-ray diffractometry (very high angular resolution). The method is realized as follows (see Fig. 2): a wide, homogeneous and monochromatic synchrotron X-ray beam illuminates large parts of the sample. A precise goniometer allows rotating the sample close to the Bragg position with very small angular step around the axis perpendicular to the diffraction plane. Next, for each angular position series of local diffraction images are acquired by using very fast detector (Frelon camera -  $2048 \times 2048$  pixels, pixel size equals to  $1.4 \mu\text{m}$ ). Finally, all digital images collected are used to create RCI maps of the sample that later on are visualized and analyzed with dedicated software [1].

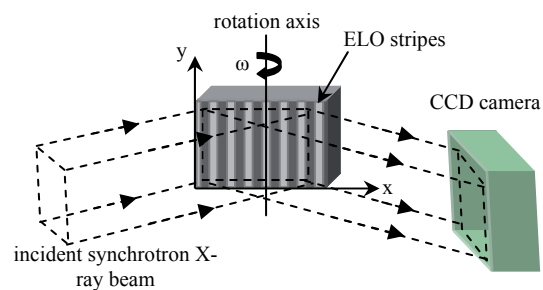


Figure 2. Schematic drawing of RCI setup. A wide beam of monochromatic X-rays is diffracted on ELO sample. Diffraction plane is oriented horizontally, perpendicular to ELO stripes.

First we focus on the RCI analysis of a single GaAs ELO stripe grown by liquid phase epitaxy on  $\text{SiO}_2$ -masked GaAs substrate. Details of the growth procedure can be found elsewhere [2]. Figure 3a shows the spatial distribution of Bragg peak position over a wide area of the sample. Signals coming from the substrate, from ELO wings and from the material grown vertically over the window in the mask are easily distinguishable.

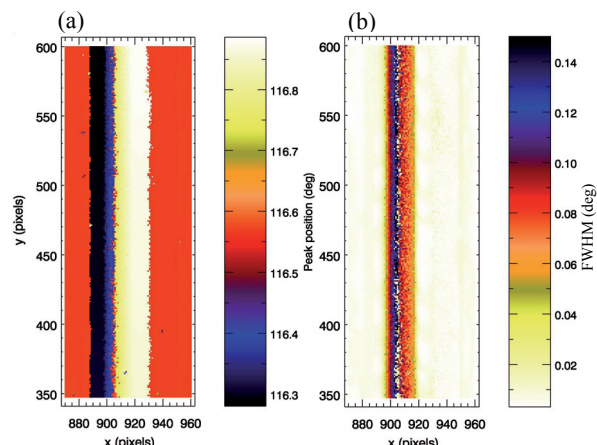


Figure 3. Spatial distribution of Bragg peak position (a) and map of local rocking curve FWHM values (b) in GaAs/GaAs single ELO stripe. Pixel size is  $1.4 \mu\text{m}$ .

Figure 3b shows the spatial distribution of the full width at half maximum (FWHM) of the rocking curve. As seen, FWHM is largest in the central part of the layer. Note that the Bragg angle position changes continuously across the ELO stripe. This is even better visible in Figure 4 that shows a cross-section at the position  $y = 539$  of the map in Figure 3a. Such distribution of Bragg peak position clearly indicates tilting of ELO wings towards the mask – a phenomenon commonly observed in many ELO systems [2]. As can be seen, the maximum wing tilt angle, denoted as  $\Delta\alpha$  in Figure 1, equals  $\sim 0.3^\circ$ . Figure 4 shows that the fastest changes of the Bragg angle take place in the central part of the layer. Thus, the crystal lattice there must be strongly strained, which explains enhanced values of FWHM in that part of the layer (compare Figure 3b). Note also that RCI maps show that homoepitaxial GaAs/GaAs ELO layers are uniform along the ELO stripe. This is not necessarily the case in heteroepitaxial ELO layers where lattice and thermal expansion mismatches lead to strongly stressed epilayers.

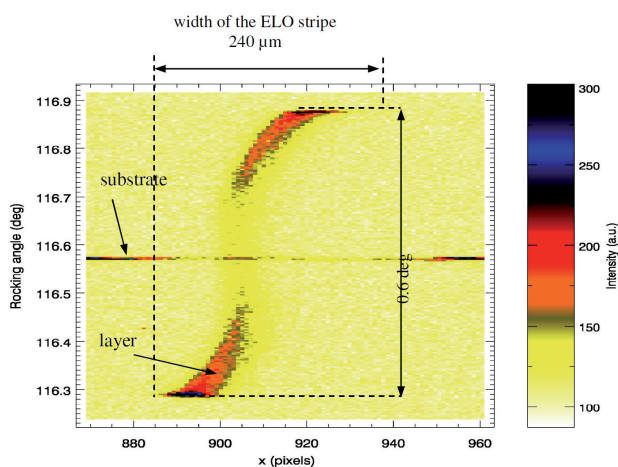


Figure 4. x- $\omega$ -map of the GaAs/GaAs single ELO stripe.

As an example Figure 5 shows a map of local diffraction intensity in a GaSb ELO stripe grown on a GaAs substrate coated by a planar GaSb buffer and  $\text{SiO}_2$  mask. Local mosaicity in the wing area is clearly visible. Due to high spatial resolution of the RCI technique individual grains (microblocks) are visualized, so their sizes and relative misorientation can be readily determined.

Finally, results of RCI analysis of GaAs/GaAs and GaSb/GaAs ELO structures are compared with those obtained for the same samples by laboratory technique of spatially resolved X-ray diffraction (SRXRD) [3]. Due to

more intense synchrotron X-ray beam and application of modern detectors, the spatial resolution of RCI is much higher, which makes this technique preferable for the detection of strongly localized strain fields in textured heteroepitaxial structures. On the other hand, analyzer crystals can be easily used in laboratory SRXRD technique allowing precise separation of overlapping signals in homoepitaxial ELO layers [4, 5].

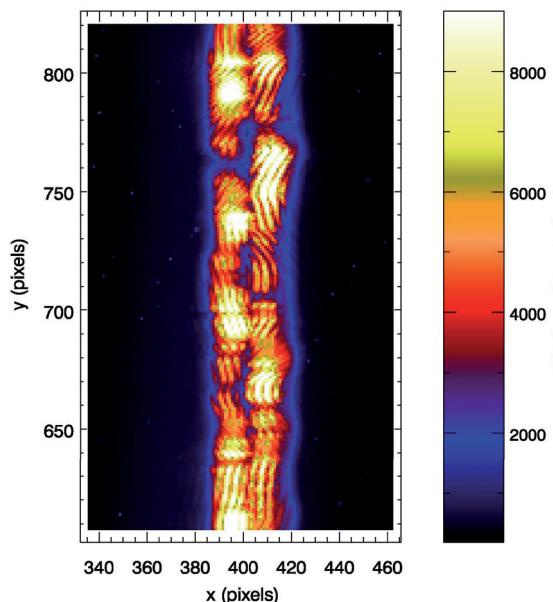


Figure 5. Spatial distribution of local diffraction intensity for GaSb/GaAs ELO layer. Pixel size is  $1.4 \mu\text{m}$ . Microblock structure of the layer is visible.

**Acknowledgements:** This work was supported by special project ESRF/MA/623/2009 from the Polish Ministry of Science and High Education.

## References

- [1] D. Lübbert, T. Baumbach, "Visrock: a program for digital topography and X-ray microdiffraction imaging", *J. Appl. Cryst.* **40** (2007) 595–597.
- [2] Z.R. Zytkiewicz, "Laterally overgrown structures as substrates for lattice mismatched epitaxy", *Thin Solid Films* **412** (2002) 64–75.
- [3] J.Z. Domagala, A. Czyzak, Z.R. Zytkiewicz, "Imaging of strain in laterally overgrown GaAs layers by spatially resolved x-ray diffraction", *Appl. Phys. Lett.* **90** (2007) 241904.
- [4] A. Czyzak, J.Z. Domagala, G. Maciejewski, Z.R. Zytkiewicz, "X-ray diffraction micro-imaging of strain in laterally overgrown GaAs layers. Part I: analysis of a single GaAs stripe", *Appl. Phys. A* **91** (2008) 601–608.
- [5] A. Czyzak, J.Z. Domagala, Z.R. Zytkiewicz, "X-ray diffraction micro-imaging of strain in laterally overgrown GaAs layers. Part II: analysis of multi-stripe and fully overgrown layers", *Appl. Phys. A* **91** (2008) 609–614.

## X-RAY TOPOGRAPHIC INVESTIGATIONS OF DOMAIN STRUCTURE IN CZOCHRALSKI GROWN $\text{Pr}_x\text{La}_{1-x}\text{AlO}_3$ CRYSTALS

**K. Wieteska<sup>1</sup>, W. Wierzchowski<sup>2\*</sup>, A. Malinowska<sup>2</sup>, S. Turczyński<sup>2</sup>, M. Lefeld-Sosnowska<sup>3</sup>,  
D. Pawlak<sup>2</sup>, T. Łukasiewicz<sup>2</sup>, and W. Graeff<sup>4</sup>**

<sup>1</sup>*Institute of Atomic Energy POLATOM, 05-400 Otwock-Świerk, Poland*

<sup>2</sup>*Institute of Electronic Materials Technology, ul. Wólczyńska 133, 01-919 Warsaw, Poland*

<sup>3</sup>*Institute of Experimental Physics, University of Warsaw, ul. Hoża 69, 00-681 Warsaw, Poland*

<sup>4</sup>*HASYLAB at DESY, Notkestr. 85, 22-603 Hamburg, Germany*

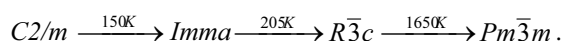
*Keywords:*  $\text{Pr}_x\text{La}_{1-x}\text{AlO}_3$  crystals, domain structure, crystallographic defects, X-ray diffraction topography

\*) e-mail: wierzc\_w@itme.edu.pl

Praseodymium lanthanum aluminium perovskite is interesting in view of the complicated phase transitions, some of them ascribed to ion lattice coupling. One of the aspects of the interest is connected with the preparation of crystals with self-organized domain structure with possible application in light guiding [1]. The open problem in the technology of these crystals is the characterization including examination of the regularity and crystallographic features of the domain structure, and the presence of common crystallographic defects, as dislocations and inclusions.

In the present paper we attempted to apply the X-ray diffraction topographic techniques exploring both synchrotron and conventional X-ray sources to a number of samples cut out from Czochralski-grown  $\text{Pr}_x\text{La}_{1-x}\text{AlO}_3$  crystals with different ratio of praseodymium and lanthanum. The investigated crystals included both the cases, when praseodymium replaced part of lanthanum atoms, or was introduced as a dopant.

It is well known, that  $\text{PrAlO}_3$  similarly as  $\text{LaAlO}_3$  is a rhombohedrally distorted perovskite (space group  $R\bar{3}c$ , tilt system  $\bar{a}\bar{a}\bar{a}$ ) [2, 3]. The phase transition of  $\text{PrAlO}_3$  can be described as



The majority of the investigated samples contained extended domain structure, expected to be a result of twinning with  $\{100\}$  invariant twin planes. The domains are visible using the optical microscopy equipped with polarizers, or with Nomarski phase contrast, but some fine details of the domains were previously studied with the FM method [1]. The width of the particular domains was in the range from tens to hundreds of micrometers.

The synchrotron X-ray topographic experiments were performed using white synchrotron beam mainly in back reflection geometry and only to some selected sample the transmission X-ray topography was applied. The conventional X-ray Lang topographs were taken for a number of samples selected from parts of the crystals with relatively low concentration of defects.

The synchrotron white beam topographs usually reproduced the domains as series of mutually displaced stripes corresponding to different orientation of

the crystal inside the domains. The density of domains was different in the samples cut out from various crystals with different composition, but generally it was most numerous in the case of crystals with highest concentration of praseodymium. In this case, the synchrotron topographs usually revealed sets of domains corresponding to more than one system of twinning. It is also probable that in the case of most dense domain structure the stripes revealed by the topographs correspond rather to some sets of domains than single domains. The representative topograph of a sample with such a dense domain structure is shown in Fig. 1.

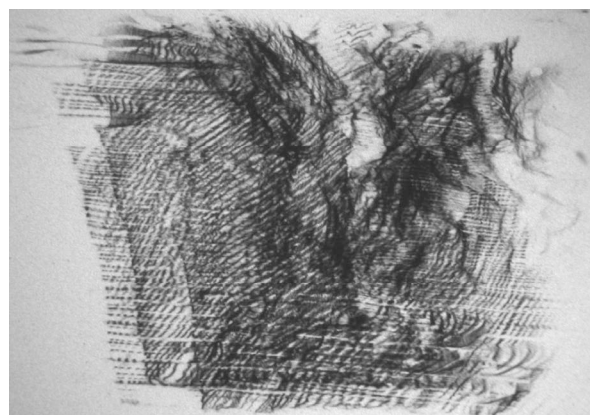


Figure 1. The representative white beam back-reflection projection topograph of the sample cut out from  $\text{Pr}_{0.75}\text{La}_{0.25}\text{AlO}_3$  crystal with extended domain structure.

The samples with low concentration of praseodymium contained large single crystal regions, where it was possible to reveal the individual dislocations and the segregation fringes.

### References

- [1] D.A. Pawlak, T. Lukasiewicz, M. Carpenter, M. Malinowski, R. Diduszko, J. Kisielewski, *J. Cryst. Growth* **282** (2005) 260.
- [2] A.M. Glazer, *Acta Crystallogr. B* **28** (1972) 3384.
- [3] A.M. Glazer, *Acta Crystallogr. A* **31** (1975) 765.

## POLFEL – THE HIGH AVERAGE POWER FREE ELECTRON LASER

**G. Wrochna<sup>1</sup>, J. Jasielski<sup>1</sup>, J. Krzywiński<sup>2</sup>, R. Nietubyć<sup>1</sup>, J. Pełka<sup>3</sup>, E. Pławski<sup>1</sup>,  
J. Sekutowicz<sup>4</sup>, R. Sobierajski<sup>3</sup>, and J. Szewiński<sup>1</sup>**

<sup>1</sup>*The Andrzej Soltan Institute for Nuclear Studies PL-05500 Świerk, Poland*

<sup>2</sup>*SLAC National Accelerator Laboratory, 2575 Sand Hill Road, Menlo Park, CA94025, USA*

<sup>3</sup>*Institute of Physics PAS, Al. Lotników 32/46, PL-00668 Warsaw, Poland*

<sup>4</sup>*Deutsches Elektronen-Synchrotron, Notkestrasse 85, D-22667 Hamburg, Germany*

*Keywords:* free electron laser, linear accelerator, vacuum ultraviolet (VUV) source.

\*) e-mail:[wrochna@ipj.gov.pl](mailto:wrochna@ipj.gov.pl)

A high average power VUV range free electron laser POLFEL is planned at The Andrzej Soltan Institute for Nuclear Studies in Świerk. The project is to satisfy the demands for the intense coherent VUV light beam declared by numerous conventional laser laboratories as well as synchrotron radiation users. We recognize it as an important step in the growth of the experimental capabilities in natural sciences and material engineering as well as a development of the FEL physics and technology.

The forthcoming paper will overview the general layout of the planned facility, paying a special attention to its novel solutions. The ground breaking feature of POLFEL is a continuous wave (cw) or near-cw operation. It will be achieved with a linear superconducting (sc) accelerator fed with a low emittance sc-electron injector furnished with the thin film sc lead photocathode. In the article, we will present the

results of the electron beam dynamics start-to-end simulation, a concept of variable polarization undulator, layouts of the diagnostics, timing and synchronization systems and general design of a two-fold branched beamline containing high energy resolution and high energy density experimental stations.

We will describe a number of experiments constituting a preliminary approach to the scientific programme of the proposed FEL facility. The all presented experimental techniques, base on the work being hitherto conducted in numerous laser and synchrotron laboratories. They will extensively benefit from the new features brought by the proposed FEL source.

A brief overview of the POLFEL concept is presented in the paper published in the current issue.

## APPLICATIONS OF FREE ELECTRON LASERS IN BIOLOGY AND MEDICINE

**J.B. Pelka<sup>1\*</sup>, G. Wrochna<sup>2</sup>, R. Nietubyć<sup>2</sup>, and K.R. Tybor<sup>3</sup>**

<sup>1</sup>*Institute of Physics, Polish Academy of Sciences, Warsaw, Poland*

<sup>2</sup>*The Andrzej Soltan Institute for Nuclear Studies, Świerk, Poland*

<sup>3</sup>*Medical University of Łódź, Department of Neurosurgery, Łódź, Poland*

*Keywords:* free electron laser; coherent diffraction imaging, ultrafast spectroscopy, radiation damage, tissue ablation, ultrafast dynamics, laser surgery

\*) e-mail: pelkay@ifpan.edu.pl

Synchrotron radiation (SR), both from storage rings and from free electron lasers (FEL), has been extensively applied in biology and in medicine for more than thirty years, opening up new opportunities to study life forms on different levels, from biomolecules and subcellular structures up to whole organisms [1, 2]. Intense synchrotron beams turned out to be invaluable in soft tissue probing with superior sensitivity, capable to detect even small tissue variations.

In recent few years, a rapidly growing interest in application of FEL beams is observed in many areas of science and technology. It is due to the fact that FELs show specific advantages to classical SR synchrotron sources, strongly enhancing probing of soft matter structure and dynamics of processes with very high spatial and temporal resolution. They were also successfully tested as precise tissue ablation tools in surgery and oncology being superior to regularly used classical laser sources.

FELs utilize a relativistic electron beam as a lasing medium. As a result, a monochromatic radiation is generated in ultrafast pulses, of duration down to the fs range, with a unique combination of tunability, coherence, polarization, and high power that can exceed more than 1 GW in a single pulse. Some FEL types can deliver radiation in the spectral regions of short wavelengths, ranging from vacuum ultraviolet (VUV-FEL) to X-ray regions (X-FEL), unattainable with other types of lasers. Spectral brightness of the new X-FEL sources, to be operational in the next few years, will be up to 9 orders of magnitude higher, as compared to the most intense 3GLS sources and will reach a value of  $10^{29}$

photons/s · mrad<sup>2</sup> · mm<sup>2</sup> · 0.1% BW, emitted in ultrafast pulses of only 10-20 fs [3].

The aim of this report is to draw a spectrum of biomedical applications at FEL sources operating with a wide ranges of wavelegths, from Terahertz up to soft X-rays, that are currently available at various FEL machines. It will be shown, basing on examples of particular applications, the importance of the new sources to study ultrafast dynamics of life processes, imaging soft tissue and proteins with unprecedented spatial resolution, as well as search of new medical techniques for surgery and therapy, which can be further transferred to common clinical tools with conventional intense lasers. Possible biomedical applications at the Polish Free Electron Laser (POLFEL), proposed to be built at the Andrzej Soltan Institute for Nuclear Studies in Świerk near Warsaw will be metioned as well.

**Acknowledgements:** This work has been partially supported by the Ministry of Science and Higher Education of Poland, SPB nr. DESY/68/2007.

### References

- [1] G. Margaritondo, Y. Hwu, J.H. Je, "Synchrotron light in medical and materials science radiology", *Rivista del Nuovo Cimento* **27** (2004) 1–40.
- [2] J.B. Pelka, *Acta Phys. Polon.* "Synchrotron radiation in biology and medicine", **114** (2008) 309–330.
- [3] N. Patel, "Shorter, brighter, better", *Nature* **415** (2002) 110–111.

## INTERACTION OF MULTILAYER OPTICS WITH INTENSE FEMTOSECOND XUV PULSES

**R. Sobierajski**<sup>1,2\*</sup>, **M. Jurek**<sup>1</sup>, **D. Klinger**<sup>1</sup>, **A.R. Khorsand**<sup>2</sup>, **E. Louis**<sup>2</sup>, **S. Bruijn**<sup>2</sup>,  
**R. van de Kruijjs**<sup>2</sup>, **E.D. van Hattum**<sup>2</sup>, **K. Sokolowski-Tinten**<sup>3</sup>, **U. Shymanovich**<sup>3</sup>, **S. Toleikis**<sup>4</sup>,  
**H. Wabnitz**<sup>4</sup>, **K. Tiedtke**<sup>4</sup>, **N. Stojanovic**<sup>4</sup>, **L. Juha**<sup>5</sup>, **J. Chalupsky**<sup>5</sup>, **J. Cihelka**<sup>5</sup>,  
**V. Hajkova**<sup>5</sup>, **E.M. Gullikson**<sup>6</sup>, and **F. Bijkerk**<sup>2#</sup>

<sup>1</sup> Institute of Physics Polish Academy of Sciences, Al. Lotników 32/46, PL 02-668 Warszawa, Poland

<sup>2</sup> FOM-Institute for Plasma Physics Rijnhuizen, Edisonbaan 14, NL-3430 BE Nieuwegein, The Netherlands,

<sup>3</sup> Institut fuer Experimentelle Physik, Universitaet Duisburg-Essen, Lotharstr. 1, 47048 Duisburg, Germany

<sup>4</sup> HASYLAB/DESY, Notkestrasse 85, D-22603 Hamburg, Germany

<sup>5</sup> Institute of Physics AS CR, Na Slovance 2, 182 21 Prague 8, Czech Republic

<sup>6</sup> Center for X-Ray Optics, Lawrence Berkeley National Laboratory Berkeley, CA 94720 USA

<sup>#</sup> also at MESA+ Institute for Nanotechnology, University of Twente, The Netherlands

*Keywords:* XUV, FEL, damage, multilayer optics

\*) e-mail: sobieraj@ifpan.edu.pl

Multilayer coated optics are used for control of XUV and soft X-ray radiation in many fields of science and technology, and has experienced a considerable boost of technology due to the application in advanced photolithography. A new field is the application in experiments at short wavelength Free Electron Lasers. This includes the x-ray sources – LCLS (USA), XFEL (Europe) & SPRING8 (Japan) and the XUV source – FLASH (Germany), ELETTRA (Italy). Multilayer coated optics are most promising candidates for optical schemes at such sources, fulfilling extreme requirements in terms of figure and roughness errors, wavefront preservation, and stability. It enables deflection angles much larger than those reasonably achieved with monolayer mirrors. In addition, due to its good wavelength selectivity, it can be used as a narrow band filter.

The photon flux from short wavelength Free Electron Lasers is extremely high. In the case of FLASH, operating in the XUV regime the ~10 fs long pulses can have energy of up to 50 µJ, corresponding to  $10^{11}$  W/cm<sup>2</sup> for a 4 mm beam spot on the optics. This is at least 10 orders of magnitude higher than in the case of lithography. Damage or even destruction of the optics can be expected. Moreover, for some application the mirrors have to be placed in the focused beam. In this case the intensity on the optics is even higher and can reach  $10^{14}$  W/cm<sup>2</sup>. Under such conditions the optical properties of the reflecting elements would be changed already during the pulse and the mirror would not work. These two effects, permanent damage of the coatings and change of the optical properties of materials under high intensity XUV irradiation, can limit the performance of the multilayer optics.

We have carried out research on the flux resistivity of a standard MoSi multilayer for a wavelength range in the soft X-ray / XUV part of the spectrum by means of exposures at FLASH. Samples were irradiated at different intensity levels with single shots.

Morphological and structural surface changes were measured with phase-contrast microscopy, atomic force microscopy and scanning transmission electron microscopy. The dynamics of damage were studied by means of time resolved microscopy. The damage mechanisms was determined as an ultrafast silicides formation induced by enhanced diffusion in a melted Si layer.

The other operating regime where multilayers can be used is when the coating reflects only during the pulse (and is possibly damaged shortly after): the range of single shot optics. However, under irradiation with ultrashort intense pulses the mirror reflectivity can decrease even within the timeframe of the fs pulse due to the change of the layers' optical properties – namely the real and imaginary part of the refractive index. The responsible physical process is a strong electron gas excitation during the pulse [1] which depends on the structure of the multilayer and materials used. The phenomenon was studied by means of angular resolved reflectivity measurements at different intensities.

The results will be used as input for the further development of multilayer coatings for the short wavelength FEL optics.

**Acknowledgements:** The authors wish to thank the staff of FLASH at DESY, Hamburg, Germany for supplying the beam time at FLASH. This work has been partially supported by the Foundation for Fundamental Research on Matter (Stichting voor Fundamentele Onderzoek der Materie, FOM), the Nederlandse Organisatie voor Wetenschappelijk Onderzoek (NWO) for funding this research and the Ministry of Science and Higher Education of Poland, SPB nr. DESY/68/2007.

### References

- [1] S. Hau-Riege *et al.*, "Subnanometer-scale measurements of the interaction of ultrafast soft x-ray free-electron-laser pulses with matter", *Phys. Rev. Lett.* 98 (2007) 145502.

# LOCAL AND LONG RANGE ORDERS IN TRANSITION METAL OXIDES AND SELENIDES AND METAL ORGANIC FRAMEWORKS STUDIED USING COMBINED TECHNIQUES (XRD AND IN-SITU RAMAN)

**P. Zajdel<sup>1\*</sup>, I. Kruk<sup>2,3</sup>, P-Y. Hsieh<sup>2,5</sup>, W. van Beek<sup>4</sup>, and M.A. Green<sup>2,5</sup>**

<sup>1</sup> Institute of Physics, University of Silesia, ul. Uniwersytecka 4, 40-007 Katowice, Poland

<sup>2</sup> NIST Center for Neutron Research, 100 Bureau Drive, Gaithersburg MD-20899, USA

<sup>3</sup> Department of Chemistry, University College of London, 20 Gordon Str, WC1H 0AJ London, UK

<sup>4</sup> Swiss-Norwegian Beamline, ESRF, Grenoble Cedex F-38043, France

<sup>5</sup> Materials Science & Engineering, University of Maryland, College Park MD-20742-6033, USA

*Keywords:* transition metal, x-ray diffraction, Raman spectroscopy

\*) e-mail: pawel.zajdel@us.edu.pl

Constant development of synchrotron radiation sources opens up new avenues in investigation of local and long range structure of materials. On one side, it improves already existing techniques like powder diffraction (XRD) by increasing their angular and time resolutions. On the other hand, the increased signal to noise ratio allows to extract new useful information from the same data, like the Pair Distribution Function (PDF) encoded in the background of XRD.

Unfortunately, the long time needed for such „one-shot” experiments makes them unusable for regular use. The solution to this problem is the use of combined techniques to obtain the equivalent information in a shorter time, while maintaining the correlation between the studied properties and the external stimulus like the temperature or pressure.

While the XRD remains the method of choice for the long range structure, the local properties can be obtained using different techniques with Extended X-Ray Absorption Fine Structure (EXAFS) being the prominent example. However, when light elements (C, N, O, H) are involved, Raman spectroscopy is more advantageous.

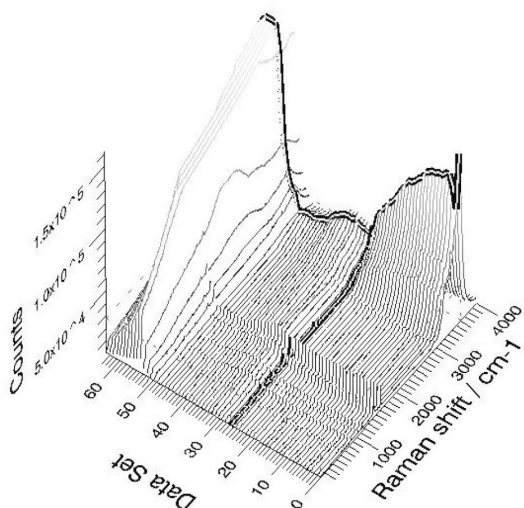


Figure 1. Evolution of Raman signal on heating up of holmium based MOF. The dark strips mark point where the first solvent molecule is lost. The sudden increase of signal at dataset 60 is due to decomposition of the compound.

The presentation will include results obtained for 3 classes of materials: seleno-spinels ( $ZnCr_2Se_4$ ), transition metal (TM) oxides and metal-organic frameworks (MOF). In particular, MOFs recently fueled rapid development of these combined techniques due to their possible applications as a storage material for use in the hydrogen based economy.

Research was conducted at the ESRF beamline BM1 (Swiss-Norwegian Beamline) [1] and consisted of simultaneous measurements of XRD and Raman spectra in the temperature range from 90 K to 700 K as well as under the gas pressure up to 20 bar.

For the chalcogenides and oxides we have searched for the signature of local deformations happening at temperatures higher than the critical temperature of the long range structural transition. In the case of oxides the distortions were expected to appear due to Jahn-Teller effect, for selenides due to possible magnetostriction.

For the metal-organic materials the research aimed at finding the correlation between structural properties of the host framework and the amount of the guest species adsorbed inside it as function of the temperature and pressure.

In the first part the as-synthesized MOF was heated up in order to empty up the structure from the solvents used during the synthesis (Fig. 1). Here, Raman spectroscopy was used to monitor the disappearance of the signal from guest molecule and host-guest interactions. Such approach is much superior than the usual two step, „off-line” technique, when material is desolvated separately at high temperature, then transferred to different place where the XRD study is made at (usually) different temperature.

In the next step, while different gases were introduced to the empty system, the Raman spectra was used to monitor the interactions between host and the adsorbed gas while XRD patterns are used to verify the position of adsorption sites.

Additionally the time resolution of the order of minutes allowed to identify new intermediate phases and check the phase integrity upon cooling.

## References

- [1] E.Boccaleri *et al.*, *J. Appl. Crystallogr.* **40**. (2007) 684.

## STUDY OF MAGNETISM WITH XMCD AND XES

M. Sikora \*

Faculty of Physics and Applied Computer Science, AGH University of Science and Technology,  
Av. Mickiewicza 30, 30-059 Kraków, Poland

*Keywords:* Magnetic moments, X-ray magnetic circular dichroism, X-ray emission spectroscopy

\*) e-mail: marcins@agh.edu.pl

X-ray absorption and emission spectroscopy techniques give an element and symmetry sensitive insight into the electronic structure of condensed matter. Using intensive hard X-rays produced by modern synchrotron sources bulk and surface properties of solid and liquid phases may be studied *in-situ* in a demanding sample environments, *e.g.* extreme temperatures, high pressure, high magnetic field, etc.

In this contribution the experimental and theoretical aspects of X-ray Magnetic Circular Dichroism (XMCD) and high resolution  $K\beta$  X-ray emission spectroscopy (XES) in the element selective investigation of magnetic moments will be presented and illustrated with examples of spotlight publications found in literature accompanied with a specific application example for each of the techniques to be discussed in details.

The first example will focus on the evolution of spin and orbital moment of rhenium in  $\text{Ca}_2\text{FeReO}_6$  double perovskite upon application of strong magnetic field. Using an energy dispersive XMCD setup combined with a pulsed magnetic field installation, magnetic moment of Re was observed in a wide temperature (10–250 K) and magnetic field (up to 30 T) range, Fig. 1. The results reveal a spatial separation between two phases characterised by the different magnetostructural coupling and the distinct transport properties. A strong external magnetic field controls the relative abundance of the phases, thus having a strong influence on the average structural and electronic properties and being responsible for colossal magnetoresistance phenomena observed in this compound.

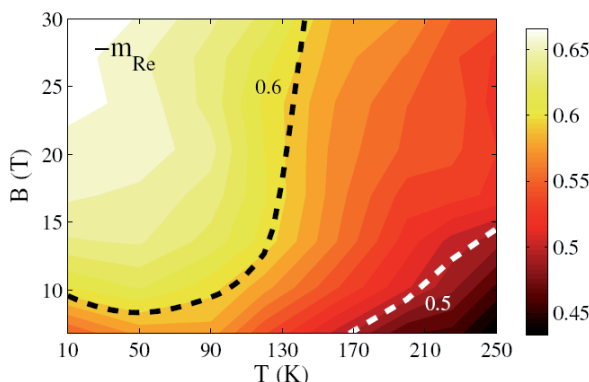


Figure 1. Low temperature, high field magnetisation dependence of the rhodium magnetic moment in  $\text{Ca}_2\text{FeReO}_6$  double perovskite as derived from the Re  $L_{2,3}$ -edge XMCD spectra acquired using pulsed magnetic field generation.

In the second example the application of X-ray emission and absorption spectroscopy to study the electronic and magnetic properties of  $\text{LaMn}_{1-x}\text{Co}_x\text{O}_3$  solid solution will be shown. Combined analysis of the  $K$ -edge absorption edges and  $K\beta$  emission lines is applied to determine the average charge and spin of the transition metal ions. Quantitative analysis of the spectral shape reveal electron transfer from Mn to Co site with a tendency to creation of  $\text{Co}^{2+}/\text{Mn}^{4+}$  ordered phase. Comparison of the charge and spin evolution revealed that  $\text{Mn}^{3+/4+}$  and  $\text{Co}^{2+}$  ions are in their high spin configurations. The  $\text{Co}^{3+}$  ions are at room temperature in their low spin configuration up to  $x \leq 0.6$ , while at higher doping level an increase of the average  $\text{Co}^{3+}$  spin state is observed, which plausibly explains the magnetization anomalies observed in the bulk magnetization measurements.

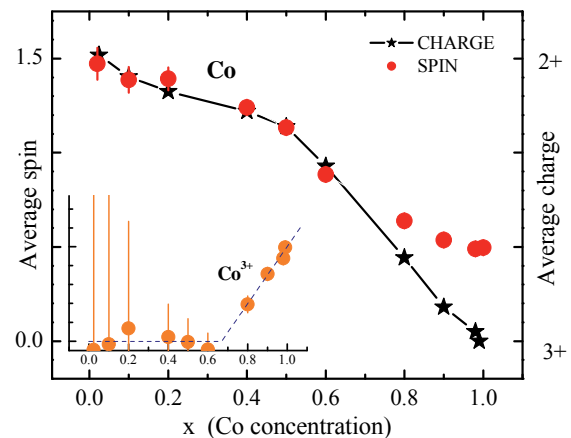


Figure 2. Comparison of the average Co charge and spin evolution in  $\text{LaMn}_{1-x}\text{Co}_x\text{O}_3$  perovskite series as derived from the  $K$ -edge energy shift (stars) and shape of the  $K\beta$  emission spectra (circles), respectively. Inset shows evolution of the average  $\text{Co}^{3+}$  spin state.

**Acknowledgements:** The authors are indebted to P. Glatzel, P. van der Linden, O. Mathon, S. Pascarelli, T.-C. Weng, Z. Jirak, K. Knizek, V. Prochazka, J.M. DeTeresa, R. Ibarra, J. Michalik, D. Zajac and Cz. Kapusta for support and valuable discussions. European Synchrotron Radiation Facility, Grenoble, is acknowledged for providing beamtime. This work was partly supported from the AGH UST project 11.11.220.01 "Basic and applied research in nuclear and solid state physics".

## CHARAKTERYZACJA NANO-WYDZIELEŃ W MATRYCACH NA BAZIE GaSb

**K. Lawniczak-Jablonska<sup>1\*</sup>, A. Wolska<sup>1</sup>, M.T. Klepka<sup>1</sup>, J. Sadowski<sup>1,2</sup>,  
A. Barcz<sup>1</sup>, A. Hallen<sup>3</sup>, and D. Arvanitis<sup>4</sup>**

<sup>1</sup>*Institute of Physics PAS, al. Lotników 32/46, 02-668 Warsaw, Poland*

<sup>2</sup>*Lund University, MAX-Lab, Lund SE-221 00, Sweden*

<sup>3</sup>*Royal Inst. of Technology, Dept. of Microelectronics and Applied Physics, Box 226, SE 164 40 Kista, Sweden*

<sup>4</sup>*Department of Physics and Materials Science, Uppsala University, Box 530, 75121 Uppsala, Sweden*

*Slowa kluczowe:* MnSb, GaSb, nano-inclusions, spintronics

\*) e-mail: jablo@ifpan.edu.pl

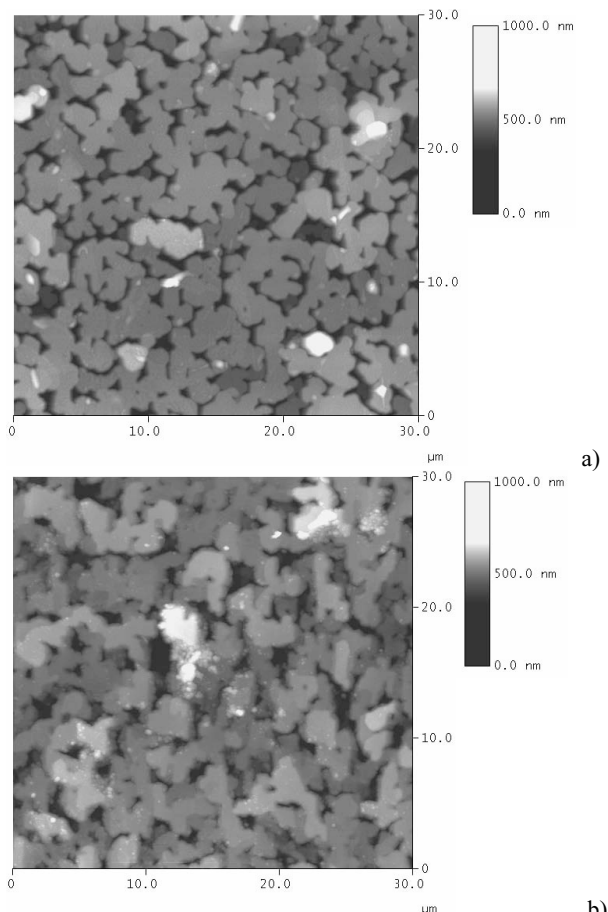
Heterostruktury składające się z metalicznych ferromagnetycznych warstw nałożonych na materiał półprzewodnikowy są potencjalnie użyteczne dla zastosowań spintronycznych. Wśród nich te, wytworzone przez wprowadzenie ferromagnetycznych wtrąceń do matrycy półprzewodnikowej wydają się być bardzo obiecujące. Wymaga to przygotowania systemu w taki sposób, żeby małe ferromagnetyczne nanocząstki były zanurzone w sieci materiału półprzewodnikowego. Taki złożony materiał może być rozważany jako półprzewodnik wypełniony nanomagnesami dostarczającymi wbudowanego pola magnetycznego.

Przeprowadzono wiele badań wydzieleń MnAs w matrycy GaAs, natomiast stosunkowo mało doniesień literaturowych dotyczy badań wydzieleń MnSb. Materiał ten wydaje się interesujący, ponieważ jego temperatura Curie jest wyższa niż temperatura pokojowa, co otwiera nowe możliwości jego wykorzystania.

Jako materiał referencyjny zbadano komercyjny proszek MnSb oraz warstwy MnSb wyhodowane metodą MBE na podłożach GaAs(111)B oraz GaAs(100). Okazało się, że warstwy te są niejednorodne i wykazują tendencje do wzrostu domenowego o kierunku zależnym od struktury podłoża. Stwierdzono również ślady innych faz. Topografia wzrostu tych warstw jest również różna (Rys. 1), co jest zgodne z doniesieniami literaturowymi [1-3]. Również materiał proszkowy wykazywał obecność fazy MnSb o dużym stopniu zdefektowania. Wydaje się, że materiał ten wykazuje naturalną tendencję do segregacji powinien więc być dobrym kandydatem do wytworzenia nano-wydzieleń pod warunkiem opracowania odpowiedniej technologii.

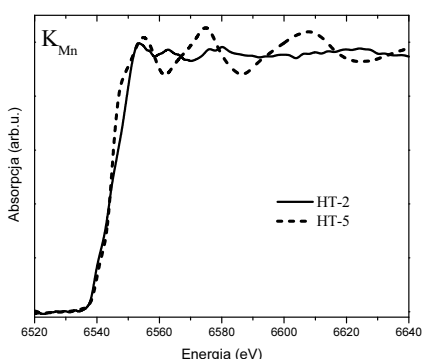
Zostaną zaprezentowane wyniki prób wytworzenia ferromagnetycznych nano-wydzieleń MnSb za pomocą różnych technologii. Mn był wprowadzany do matrycy GaSb zarówno w procesie MBE, jak i poprzez implantację. Stosowano różne warunki wzrostu oraz różne dawki i sposoby poimplantacyjnego wygrzewania. Na tak przygotowanych próbkach przeprowadzono pomiary absorpcji rentgenowskiej, pomiary rozkładu pierwiastków w funkcji głębokości oraz pomiary

dyfrakcyjne, mikroskopowe i magnetyczne w celu pełnej charakteryzacji utworzonych wydzieleń.

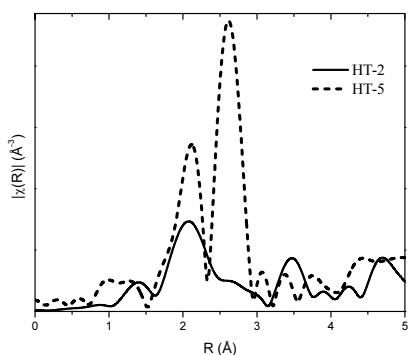


Rysunek 1. Obrazy AFM topografii powierzchni dla próbki a) MnSb na GaAs(111)B i b) dla MnSb na GaAs(100).

Stwierdzono, że bardzo trudno jest wytworzyć wydzielenia MnSb za pomocą implantacji, ponieważ Mn znacznie łatwiej łączy się z tlenem niż antymonem. Ponadto w procesie wygrzewania antymon łatwo ulatnia się z próbki i w efekcie tworzą się wydzielenia  $Ga_xMn_y$ .



Rysunek 2. XANES na krawędzi K manganu.



Rysunek 3. Transformata Fouriera oscylacji EXAFS na krawędzi K manganu.

W przypadku wydzielień hodowanych metodą MBE stwierdzono silną zależność od temperatury wzrostu, koncentracji Mn oraz od kierunku i rodzaju podłoża. Struktury z wydzieleniami MnSb udało się wyhodować jedynie na podłożach GaSb(100) oraz GaAs(111)B. Dla obydwu podłoży w procesach prowadzonych w temperaturze powyżej 450°C znacząca część atomów manganu lokowała się w sieci GaAs lub GaSb (próbka HT-2, Rys. 2 i 3). Dopiero dla temperatury 450°C udało się wytworzyć wydzielenia MnSb o strukturze heksagonalnej (próbka HT-5, Rys. 2). Zmiany w

sposobie wiązania atomów manganu są widoczne zarówno w strukturze XANES (Rys. 2), jak i w rozkładzie atomów wokół Mn uzyskanym z analizy EXAFS (Rys. 3).

Zaobserwowano również zależność od koncentracji Mn dla obydwu rodzajów podłoża. Wynika z niej, że w próbkach o wyższej zawartości manganu wykształciła się struktura MnSb. Natomiast tam, gdzie zawartość manganu jest bliska 1% tylko część atomów lokuje się w wytrącenach MnSb, zaś reszta podstawa się w miejsce antymonu w strukturze GaSb. Wielkość nano-wydzielen zależy od zawartości Mn oraz szybkości wzrostu struktury, natomiast kierunek wzrostu i topologia struktury zależą od rodzaju podłoża.

Absorpcja rentgenowska jako technika selektywna ze względu na rodzaj pierwiastka okazała się idealnym narzędziem do określenia sposobu wbudowania się atomów Mn wprowadzanych do matrycy GaSb za pomocą różnych technologii. Wykazano, że widma absorpcyjne mogą być wskaźnikiem utworzenia się wydzielień w matrycach półprzewodnikowych.

**Podziękowania:** Autorzy wyrażają podziękowanie za finansowanie uzyskane dzięki grantowi Ministerstwa Nauki i Edukacji N202-052-32/1189 oraz DESY/HASYLAB i Unii Europejskiej w ramach projektu RII3-CT-2004-506008 (IA-SFS).

## Literatura

- [1] H. Akinaga, K. Tanaka, K. Ando, T. Katayama, "Fabrication and magneto-optical properties of epitaxial ferromagnetic  $Mn_{1-x}Sb$  thin films grown on GaAs and sapphire", *J. Cryst. Growth* **150** (1995) 1144–1149.
- [2] S.X. Liu, S.M. Bedair, N.A. El-Masry, "Mn-prelayer effects on the epitaxial growth of MnSb on (11) B GaAs by pulsed laser deposition", *Mat. Lett.* **42** (2000) 121–129.
- [3] A.F. Panchula, C. Kaiser, A. Kellock, S.S. Parkin, "Spin polarization and magnetotransport of Mn–Sb alloys in magnetic tunnel junctions", *Appl. Phys. Lett.* **83** (2003) 1812–1814.

# SMALL ANGLE SCATTERING OF SYNCHROTRON RADIATION STUDIES OF BIOMEMBRANES

**M. Kozak**

*Department of Macromolecular Physics, Faculty of Physics A. Mickiewicz University,  
ul. Umultowska 85, 61-614 Poznań, Poland*

*Keywords: phospholipids, surfactants, small angle X-ray scattering*

\*) e-mail: mkozak@amu.edu.pl

Cell membranes consists of lipids, proteins and carbohydrates. Phospholipids are the main group of cell membranes lipids. The occurrence of a hydrophilic and a hydrophobic part in the phospholipide molecule determined their ability to self-organization in such solvents as water. Fully hydrated phospholipids exhibit tendency to aggregation and formation of different structural phases. Typical for phospholipids lamellar phases (lamellar gel phase, rippled phase, liquid crystalline phase) are formed by stacks of bilayers and water. The cubic phases are formed by spherical micelles organized in cubic lattice or bicontinuous 3D-network of finite phospholipids rods. The hexagonal phase is composed of hexagonally packed long rods formed by molecules of phospholipids [1].

In mixtures of phospholipids with short-chain phospholipids or surfactants the discoidal (bicellar) phase can be formed [2].

The most intense study concentrates not just on the structure and interactions in the lipid/water systems but also on more complex systems including additional components such as surfactants, polyelectrolytes, peptides or liquid crystals [3].

Small angle X-ray and neutron scattering techniques are one of the most effective methods for structural analysis of lipids and their mixtures. These methods permit determination of such structural parameters as the radius of gyration, intramolecular distance distribution function ( $p(r)$ ), phospholipid double layer thickness or diameters of the tubes in the hexagonal phase. The SAXS method also permit getting the information on the orientation and symmetry of the scattering molecules.

The lecture gives analysis of performance of selected and the most popular applications of the small angle scattering of synchrotron radiation in structural biology of biomembranes. The presentation will be illustrated on the several examples: discoidal (bicellar) phases formed

by phospholipids [4] and mixtures of phospholipids and cationic surfactants [5], cubic phases observed for mixtures of phospholipids and zwitterionic surfactants [6] and structures formed in phospholipid/gemini surfactant systems.

**Acknowledgements:** The research was supported in part by research grant (No. N N202 248935) from the Ministry of Science and Higher Education (Poland). The data collection was supported by EC - EMBL Hamburg Outstation, contract number: RII3-CT-2004-506008. The data collection in MaxLab were supported by the EC - Research Infrastructure Action under the FP6 "Structuring the European Research Area" Programme (through the Integrated Infrastructure Initiative "Integrating Activity on Synchrotron and Free Electron Laser Science").

## References

- [1] R. Koynova, M. Caffrey, "Phases and phase transitions of the phosphatidylcholines", *BBA-Rev Biomembranes* **1376** (1998) 91-145.
- [2] J. Katsaras, T.A. Harroun, J. Pencer, M.P. Nieh, "«Bicellar» lipid mixtures as used in biochemical and biophysical studies", *Naturwiss.* **92** (2005) 355-366.
- [3] J. Katsaras, T. Gutberlet, (Ed.). *Lipid bilayers – structure and interactions* (Springer-Verlag, Berlin-Heidelberg, 2001).
- [4] M. Kozak, M. Kempka, K. Szpotkowski, S. Jurga, "NMR in soft materials: A study of DMPC/DHPC bicellar system", *J. Non-Cryst. Solids* **353** (2007) 4246-4251.
- [5] M. Kozak, L. Domka, S. Jurga, "The effect of selected surfactants on the structure of a bicellar system (DMPC/DHPC) studied by SAXS", *J. Mol. Struct.* **846** (2007) 108-111.
- [6] M. Kozak, K. Szpotkowski, A. Kozak, R. Zieliński, D. Wieczorek, M.J. Gajda, L. Domka. "The FTIR and SAXS studies of influence of a morpholine derivatives on the DMPC-based biological membrane systems", *Radiat. Phys. Chem.* (2009), doi:10.1016/j.radphyschem.2009.03.090.

# ATOMIC-RESOLUTION STRUCTURE OF CYANOBACTERIAL CYTOCHROME C6 WITH AN UNUSUAL SEQUENCE INSERTION

**S. Krzywda<sup>1\*</sup>, W. Bialek<sup>2</sup>, A. Szczepaniak<sup>2</sup>, and M. Jaskolski<sup>1</sup>**

<sup>1</sup>*Faculty of Chemistry, Adam Mickiewicz University, Poznań, Poland*

<sup>2</sup>*Faculty of Biotechnology, University of Wrocław, Poland*

*Keywords:* *high-resolution structure, cytochrome, photosynthesis*

\*) e-mail: szymon@amu.edu.pl

During photosynthesis, electron transfer between two membrane-bound complexes, cytochrome  $b_{6f}$  and photosystem I can be accomplished by the copper-containing protein, plastocyanin, or the heme protein, cytochrome  $c_6$  [1]. Cytochromes  $c_6$  are water-soluble, low-spin heme-containing proteins involved in the high-potential (340–390 mV) electron transport chain. They are characterized by low molecular mass, 80–90 amino acid residues in the mature protein, and have a covalently bound heme group.

Cytochrome  $c_6$  from the mesophilic cyanobacterium *Synechococcus* sp. PCC 7002 is unique among all known cytochromes  $c_6$  due to the presence of an unusual seven-residue insertion, K<sub>44</sub>DGSKSL<sub>50</sub>. Furthermore, the present protein is unusual because of its very high content (36%) of the smallest residues (glycine and alanine) [2].

The crystallization experiments used the hanging-drop vapor-diffusion method. Red crystals (Fig. 1) suitable for X-ray analysis were obtained from 10 mM sodium Hepes, pH 6.2, and 2.2 M ammonium sulfate over a period of one week.

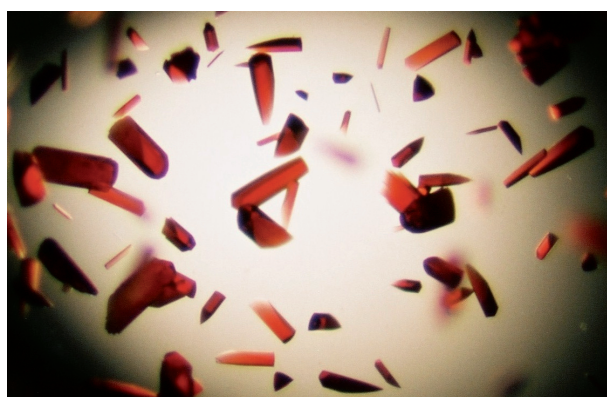


Figure 1. Crystals of reduced cytochrome  $c_6$  from *Synechococcus* sp. PCC 7002.

The structure of the reduced form of cytochrome  $c_6$  has been determined at 1.2 Å and refined to an  $R$  factor of 0.107. It reveals that the overall fold of the protein is similar to that of other class I  $c$ -type cytochromes despite

the presence of the specific insertion. The insertion is located within the most variable region of cytochrome  $c_6$  sequence, *i.e.* between helices II and III. The first six residues (K<sub>44</sub>DGSKSL<sub>50</sub>) form a loop, whereas the last residue, Leu<sub>50</sub>, extends the N-terminal beginning of helix III. Several specific non-covalent interactions are found inside the insertion as well as between the insertion and the rest of the protein. Energetically significant cation...π interactions have been detected between Tyr<sub>43</sub>, Tyr<sub>56</sub>, Phe<sub>68</sub> and, respectively, Lys<sub>37</sub>, Lys<sub>48</sub> and Arg<sub>71</sub> (Fig. 2).

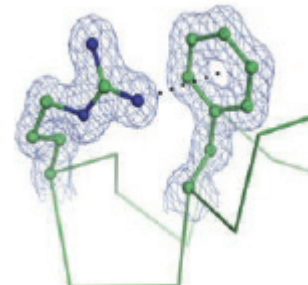


Figure 2. N-H...π interaction between the only Arg and Phe68 ( $2F_0 - F_c$  electron density map contoured at  $1.2\sigma$ ).

The crystal structure contains three copies of the  $c_6$  molecule per asymmetric unit and is characterized by unusually high packing density, with solvent occupying barely 17.58% of the crystal volume.

**Acknowledgements:** Some of the calculations were carried out in the Poznan Metropolitan Supercomputing and Networking Center. This work was funded in part by grants number N N204 245635 and N N303 3856 33 from the Ministry of Science and Higher Education.

## References

- [1] W.A. Cramer, P.N. Furbacher, A. Szczepaniak, G.S. Tae, *Electron transport between photosystem II and photosystem I* (Academic Press, San Diego 1991).
- [2] W. Bialek, M. Nelson, K. Tamiola, T. Kallas, A. Szczepaniak, "Deeply branching  $c_6$ -like cytochromes of cyanobacteria", *Biochemistry* **47** (2008) 5515–5522.

## SHORT-RANGE ORDERING IN *ORTHO*-CHLOROANISOLE AT 293 K BY X-RAY DIFFRACTION

**H. Drozdowski<sup>\*</sup>, A. Romaniuk, and Z. Błaszczałk**

*Faculty of Physics, Adam Mickiewicz University ul. Umultowska 85, PL 61-614 Poznań, Poland*

*Keywords:* short-range ordering, X-ray scattering in molecular liquids

\*) e-mail: riemann@amu.edu.pl

Structural analysis of liquid *o*-chloroanisole C<sub>7</sub>H<sub>7</sub>ClO by X-ray monochromatic radiation scattering method was elaborated. The X-ray measurements were made at 273 K for the scattering angle range  $\Theta$  varying from 3° to 60°. The compounds to be studied of 99% purity were purchased from Koch-Light Laboratories (England).

The short-range arrangement is characterized by the values of the distances between the nearest molecules determined by the so-called radii of coordination spheres and a number of molecules in subsequent coordination spheres around one molecule chosen as central [1].

From the known interatomic distances and valence angles, and assuming the van der Waals atomic radii determined by X-ray methods for crystalline organic compounds, one can construct the *o*-chloroanisole molecule (Fig. 1) and hence perform an analysis of the mutual dispositions of molecules in the liquid.

From the shape of the intensity scattered in liquid *o*-chloroanisole (Fig. 2), most probable intermolecular distances in liquid *o*-chloroanisole can be assigned to the maxima of the distribution function.

The angular distribution of the intensity of scattered X-ray (Fig. 2) is characterized by two general maxima which are responsible for intermolecular interaction. The calculated mean, most often occurring, smallest mutual distances between molecules of liquid *o*-chloroanisole are:  $r_1 = 6.66 \text{ \AA}$ ,  $r_2 = 7.15 \text{ \AA}$ ,  $r_3 = 8.23 \text{ \AA}$ . Local, most probable manners of packing and mutual orientation of molecules within the space of the first coordination sphere are discussed.

X-ray structural analysis was applied to determine the packing coefficient [2] of *o*-chloroanisole molecules.

Because of the permanent dipole moment of the molecule, *o*-chloroanisole  $\mu = 2.85 \text{ D}$ , the neighbouring molecules are arranged so that their dipolar moments are antiparallel. In liquid *o*-chloroanisole only in the antiparallel conformation the distance between the centres of the chlorine groups is Cl–Cl' =  $7.15 \pm 0.15 \text{ \AA}$ .

These results can be interpreted in terms of a simple model of local arrangement of molecules, which probably can be valid for a larger class of molecular liquids, i.e. polar monosubstituted derivatives of anisole.

Computer techniques [3] were used to minimise the effects of experimental errors, uncertainties in the scattering factors, and termination errors.

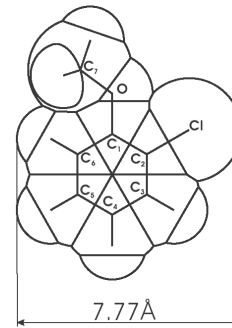


Figure 1. A model of the *o*-chloroanisole molecule structure ( $d = 1.123 \text{ g/cm}^3$ ), with van der Waals radii taken into account.

The packing coefficient of molecules in liquid *o*-chloroanisole is  $k = 60\%$ .

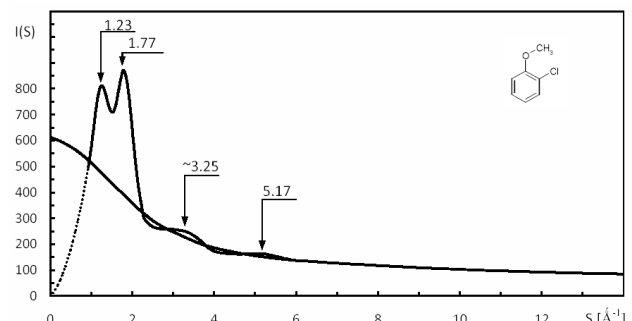


Figure 2. Normalized, experimental curve of angular distribution of X-ray scattered intensity in liquid *o*-chloroanisole.

### References

- [1] H. Drozdowski, "Local structure and molecular correlations in liquid 1-methylnaphthalene at 293 K", *Chem. Phys. Letters* **351** (2002) 53–60.
- [2] H. Drozdowski, "The packing coefficient of liquid 2-phenylnaphthalene molecules at 396 K", *Phys. Chem. Liq.* **40** (2002) 421–434.
- [3] A. Renninger, R. Kaplow, *Computer Programs for Radial Distribution Analysis of X-rays* (Massachusetts Institute of Technology Cambridge, MA, 1987).

# X-RAY REFLECTOMETRIC INVESTIGATION OF SURFACE ROUGHNES OF SiC SUBSTRATE WAFERS AND ITS INFLUENCE ON THE STRUCTURAL PERFECTION OF THE DEPOSITED SiC EPITAXIAL LAYERS

**K. Mazur<sup>1\*</sup>, W. Wierzchowski<sup>1</sup>, K. Wieteska<sup>2</sup>, W. Hofman<sup>1</sup>,  
K. Kościewicz<sup>1</sup>, W. Strupiński<sup>1</sup>, and W. Graeff<sup>3</sup>**

<sup>1</sup> Institute of Electronic Materials Technology, Wólczyńska 133, 01-919 Warsaw, Poland

<sup>2</sup> Institute of Atomic Energy POLATOM, 05-400 Otwock-Świerk, Poland

<sup>3</sup> HASYLAB at DESY, Notkestr. 85, 22-603 Hamburg, Germany

*Keywords:* SiC crystals, epitaxial layers, roughnes, crystallographic defects, reflectometry,  
X-ray diffraction topography

\*) e-mail: Krystyna.Mazur@itme.edu.pl

The technology of modern high temperature electronic materials often includes the epitaxial deposition of SiC layers on the SiC substrates. The essential for the application is achieving high perfection of the deposited layers, especially elimination of the micro-pipes and basal plane dislocations. The last ones are very dangerous in the high-voltage devices in view of possible migration associated by the formation of the large stacking faults.

Obtaining of highly perfect epitaxial layers is even more conditioned by the appropriate finishing of the surface, than by the concentration of the defects in the substrate crystal, although obviously the last factor cannot be to any extent neglected. It should be also noted that the important influence on the epitaxial growth is also affected by the high temperature etching in the mixture of hydrogen and gaseous propane.

In the present case the important tool of controlling the state of the surface was the specular X-ray reflectometric method supported by fitting of the theoretical reflectometric curves. The perfection of the epitaxial layers and the substrate wafers was also controlled by synchrotron X-ray diffraction topography realized both in the white and monochromatic beam at HASYLAB.

The present X-ray reflectometric investigations were performed for a number of samples both of 4H and 6H polytypes prepared at ITME using various finishing regimes. The investigations confirmed a very good quality of the surface finishing with the processes actually developed at ITME providing in case of 4H wafers the surface roughness  $\sigma = 0.55 \pm 0.07$  nm, improved after the high temperature initial etching to  $\sigma = 0.22 \pm 0.005$  nm. These values were better than in case of substrate wafers offered by many commercial producers. A relatively good structural quality was confirmed in the case of 4H epitaxial wafers deposited on the wafers prepared from the best ITME crystals with the 8° off-cut.

The synchrotron topographic investigation indicated on the other hand many cases when the not perfect surface finishing lead to the formation of defects and strains in the deposited epitaxial layers. That concerns especially to the phenomenon of step bunging. Also in many other cases we observed a characteristic „grain like” contrast and broadening of the reflection curves of the epitaxial layers deposited on the layers with the irregular surface relief.

# BADANIA STRUKTURY TLENKÓW METALI PRZEJŚCIOWYCH METODĄ DYFRAKCJI NEUTRONÓW I PROMIENIOWANIA SYNCHROTRONOWEGO

Radosław Przeniosło

*Instytut Fizyki Doświadczalnej, Wydział Fizyki Uniwersytetu Warszawskiego*

*Słowa kluczowe: dyfrakcja neutronowa, metal przejściowy, perowskit*

Dyfrakcja neutronów i promieniowanie synchrotronowego to dwie komplementarne techniki badania struktury krystalicznej materiałów. Zalety oraz ograniczenia obydwu tych technik zostaną opisane na przykładzie badań związków tlenowych o strukturze odkształconego perowskitu:  $\text{NdFeO}_3$  [1, 2] oraz  $\text{CaCu}_x\text{Mn}_{7-x}\text{O}_{12}$  [3, 4]. Materiały te wykazują silną anizotropię rozszerzalności termicznej która jest związana z magnetycznymi przejściami fazowymi. Wnioski wynikające z badań dyfrakcji neutronów oraz promieniowania synchrotronowego stanowią ważną informację na temat sprzężenia magnetycznych, ładunkowych i spinowych stopni swobody w związkach tlenowych metali przejściowych.

## References

- [1] W. Sławiński, R. Przeniosło, I. Sosnowska, M. Brunelli, M. Bieringer, "Anomalous thermal expansion in polycrystalline  $\text{NdFeO}_3$  studied by SR and X-ray diffraction", *Nucl. Instrum. Meth. B* **254** (2007) 149-152.
- [2] W. Sławiński, R. Przeniosło, I. Sosnowska, E. Suard, "Spin reorientation and structural changes in  $\text{NdFeO}_3$ ", *J. Phys.: Condens. Matt.* **17** (2005) 4605-4614.
- [3] W. Sławiński, R. Przeniosło, I. Sosnowska, M. Bieringer, I. Margioliaki, "Thermal lattice parameters variation of  $\text{CaCu}_x\text{Mn}_{7-x}\text{O}_{12}$  compounds with trigonal crystal structure", *Acta Phys. Polon. A* **113** (2008) 1225-1230.
- [4] W. Sławiński, R. Przeniosło, I. Sosnowska, M. Bieringer, I. Margioliaki, A.N. Fitch, E. Suard, "Charge ordering in  $\text{CaCu}_x\text{Mn}_{7-x}\text{O}_{12}$  ( $x = 0.0$  and  $0.1$ )", *J. Phys. Condens. Matter* **20** (2008) 104239 1-7.

# INFORMACJA NA TEMAT ROZWIĄZAŃ TECHNICZNYCH I STANU PRZYGOTOWAŃ DO BUDOWY SYNCHROTRONU W POLSCE

E.A. Görlich, K. Królas, M. Mlynarczyk, M.J. Stankiewicz, i K. Tomala

*Instytut Fizyki, Uniwersytet Jagielloński, ul. Reymonta 4, 30-059 Kraków*

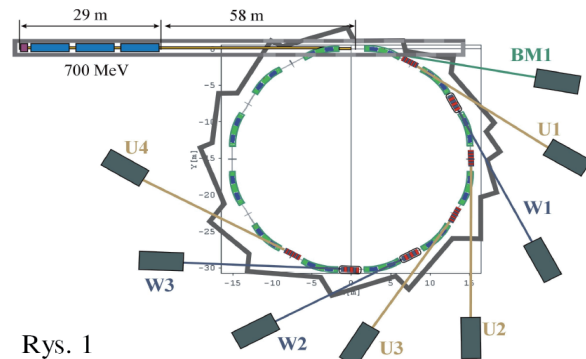
*Słowa kluczowe: synchrotron, linia pomiarowa*

Ogólne ramy merytoryczne i finansowe projektu klu-  
czowego „Narodowe Centrum Promieniowania Elektro-  
magnetycznego dla Celów Badawczych” zostały określone w umowie wstępnej zawartej w dniu 28 XI 2008 r. pomiędzy Uniwersytetem Jagiellońskim a Ministerstwem Nauki i Szkolnictwa Wyższego. Szerokie konsultacje z wybitnymi ekspertami pozwoliły na sprecyzowanie optymalnych (z punktu widzenia przyszłych możliwości badawczych, oczekiwanych przez środowisko naukowe), a jednocześnie realistycznych budżetowo, rozwiązań technicznych. Konstrukcja i rozwiązania techniczne oparte są o koncepcję stworzoną przez zespół prof. Mikaela Eriks-  
sona (MAXLab) dla planowanego w Lund nowego synchrotronu MAXV. Pierścień akumulujący o obwodzie 96 m będzie magazynował elektrony, których źródło sta-  
nowić będzie akcelerator liniowy, pracujący w systemie jednokrotnego zwracania wiązki, dostarczający elektrony o energii 700 MeV (Rys. 1). Następnie będą mogły one podlegać dalszemu przyspieszeniu w zakresie 0.7 - 1.5 GeV już w samym ringu. Projekt budowlany prze-  
widuje miejsce w tunelu akceleratora liniowego na za-  
montowanie w przyszłości dalszych modułów przyspieszania, co pozwoli na uzyskanie pełnej maksymalnej energii wstrzykiwanych elektronów (1.5 GeV) i pracę w systemie *top-up*, czyli quasi-ciągłego podtrzymywania prądu w pierścieniu.

Dzięki magnesom odchyłającym i *insertion devices* (undulatorom i wigglерom) dostępne stanie się promieniowanie elektromagnetyczne o dużej intensywności w zakresie od podczerwieni do twardego promieniowania rentgenowskiego, nawet o energii fotonów do 20 keV. Ten ostatni obszar fal krótkich zostanie otwarty w przyszłości dzięki zastosowaniu wigglérów (także nadprzewodzących). Z drugiej strony, przy odpowiednich warunkach pracy, synchrotron pozwoli również stworzyć intensywne źródło promieniowania terahercowego ( $30 \text{ THz} > v > 0.2 \text{ THz}$ ,  $10 \mu\text{m} < \lambda < 1500 \mu\text{m}$ ) otwierając dostęp do bardzo interesujących i aktualnych obszarów badań np. w dziedzinie nauk biologicznych i fizycznych.

Przyjęto strategię skierowania możliwie dużych nakładów, w ramach dostępnych środków finansowych, na budowę systemu akceleracji i pierścienia akumulującego elektronów, ponieważ to determinuje jakość i wszechstronność narzędzia badawczego, tak jak tego oczekuje społeczność naukowa, a późniejsze, daleko idące zmiany w tej części byłyby w praktyce niemożliwe lub ekonomicznie nieuzasadnione.

Dlatego też, w pierwszym etapie, objętym tą pre-  
umową, projekt przewiduje konstrukcję jednej linii eksperimentalnej (U1), której założenia omawia referat prof. J. Szade. Linia ta będzie stwarzała możliwości



Rys. 1

badawcze w zakresie różnych spektroskopii miękkiego promieniowania rentgenowskiego.

Równolegle planowane jest prowadzenie prac nad stworzeniem dalszych kilku linii doświadczalnych, których uruchomienie mogłoby sukcesywnie następować w krótkim czasie po uruchomieniu synchrotronu. Sobotnie sesje (26 IX 2009) poświęcone będą w głównej mierze otwartej dyskusji nad poniższymi lub dalszymi propozycjami linii eksperymentalnych, zarówno w aspekcie merytorycznym jak i w odniesieniu do praktycznej strony organizacyjnej ich finansowania i realizacji. Proponowane linie<sup>1</sup>:

U2 – Mikroskopia i mikrotomografia miękkiego promieniowania rentgenowskiego,

U4 – Linia absorpcyjna dla materiałów magnetycznych,

U3 – Linia niskich energii (NIR, Vis, UV, miękkie promieniowanie X),

BM1 – Spektroskopia bliskiej i dalekiej podczerwieni, mikroskopia,

W1 – Dyfrakcja promieniowania rentgenowskiego,

W2 – Krystalografia makromolekuł,

W3 – Linia do badań materiałowych.

Obecnie przygotowano dwa zasadnicze dokumenty stanowiące, w świetle umowy wstępnej, podstawę do wystąpienia z wnioskiem o finansowanie projektu, tj. „Program funkcjonalno-użytkowy z koncepcją technologiczną” i „Studium wykonalności”. Można oczekiwać, że do podpisania umowy dojdzie jeszcze w tym roku, a wtedy realistyczny harmonogram przewiduje uzyskanie pierwszych wyników doświadczalnych na początku drugiego półrocza 2014 roku. Dotrzymanie bardzo ciasnych ram czasowych będzie możliwe dzięki ścisłej współpracy z ośrodkiem w Lund przy wykorzystaniu pomocy innych centrów synchrotronowych, np. w zakresie szkolenia kadry.

<sup>1</sup> Więcej informacji dostępnych jest na stronie <http://synchrotron.pl> pod zakładką ‘Beamlines’.

# PIERWSZA LINIA NA POLSKIM SYNCHROTRONIE – SPEKTROSKOPIE MIĘKKIEGO PROMIENIOWANIA RENTGENOWSKIEGO

**J. Szade<sup>1</sup>, B. Orłowski<sup>2</sup>, B. Kowalski<sup>2</sup>, E.A. Görlich<sup>3</sup>, K. Tomala<sup>3</sup> i P. Starowicz<sup>3</sup>**

<sup>1</sup> Instytut Fizyki im. A. Chełkowskiego, Uniwersytet Śląski, ul. Uniwersytecka 4, 40-007 Katowice

<sup>2</sup> Instytut Fizyki PAN, Al. Lotników 32/46; 02-668 Warszawa

<sup>3</sup> Instytut Fizyki, Uniwersytet Jagielloński, ul. Reymonta 4, 30-059 Kraków

*Słowa kluczowe:* synchrotron, linie eksperymentalne

Zgodnie z decyzjami finansowymi w pierwszym etapie budowy polskiego synchrotronu w Krakowie zostanie oddana do użytku jedna linia eksperymentalna. Ma to być linia poświęcona spektroskopiom miękkiego promieniowania rentgenowskiego, głównie spektroskopii fotoelektronów.

Planujemy, żeby źródłem promieniowania był onulator umożliwiający zmianę polaryzacji promieniowania i zapewniający uzyskanie zakresu energii **50-1500 eV**. Monochromator powinien zapewnić rozdzielcość energetyczną **E/ΔE~10<sup>4</sup>**.

Linie o podobnych do planowanych u nas parametrach można znaleźć na prawie wszystkich światowych synchrotronach trzeciej generacji. Polski synchrotron będzie prawdopodobnie budowany w oparciu o nowe koncepcje rozwijane w ośrodku Max-Lab w Lund w Szwecji. Pierwsza linia na polskim synchrotronie będzie zbliżona pod względem parametrów i technik badawczych do linii I311 i I511 pracujących obecnie przy pierścieniu akumulacyjnym MAX II.

Podstawowymi technikami badawczymi będą spektroskopia fotoelektronów i spektroskopia absorpcyjna. Konstrukcja linii powinna umożliwić poszerzenie w przyszłości możliwości badawczych o takie techniki jak spektromikroskopia i spektroskopia emisyjna.

**Stacja pomiarowa powinna umożliwić badania przy użyciu takich metod jak:**

- **Rezonansowa spektroskopia fotoelektronów**  
- typu Fano pozwalająca na określenie wkładu stanów elektronowych pochodzących od różnych pierwiastków (np. 4f metali ziem rzadkich) do pasma walencyjnego oraz badanie reakcji chemicznych na powierzchni.
- **Spinowo rozdzielcza spektroskopia fotoelektronów**  
- pozwalająca na powiązanie polaryzacji spinowej z konkretnymi stanami elektronowymi, konieczny będzie dodatkowy detektor (np. Motta) przy spektrometrze fotoelektronów.
- **Absorpcja promieniowania rentgenowskiego (XAS)**  
- badanie krawędzi absorpcji ziem rzadkich, metali przejściowych, tlenu, krzemu i innych pierwiastków

w zakresie miękkiego promieniowania X, pomiar w trybach TEY (Total Electron Yield) and TFY (Total Fluorescence Yield).

Dzięki możliwości zmiany polaryzacji promieniowania można będzie wykonywać badania dichroizmu magnetycznego w absorpcji i fotoemisji przy zachowaniu warunków bezpieczeństwa dla analizatora fotoelektronów ograniczających wartość pola magnetycznego wewnętrz komory pomiarowej.

Manipulator powinien umożliwiać pomiary w szerokim zakresie temperatur, co najmniej 20-1000 K. Dzięki sześciu osiom obrotu będzie częściowo możliwe zastosowanie rozdzielczej katowo spektroskopii fotoelektronów (ARPES) przy zastosowaniu odpowiednich soczewek analizatora i modułu pracy. Stosunkowo wysoka wartość dolnej energii granicznej stawia wysokie wymagania dla analizatora fotoelektronów, ale szybki rozwój w tej dziedzinie powinien umożliwić przynajmniej częściowo pomiary w trybie ARPES. Pomiary takie pozwalają na badanie struktury pasmowej. Możliwe będzie też badanie dyfrakcji fotoelektronów – źródła informacji o strukturze krystalicznej powierzchni.

Przewidujemy instalację odpowiednich komór preparacyjnych, gdzie znajdą się działo jonowe, łupacz kryształów oraz komórki efuzyjne do naparowania cienkich warstw.

Stacja pomiarowa pierwszej linii eksperymentalnej ma mieć charakter raczej uniwersalny ze spektroskopią fotoelektronów jako techniką dominującą. Pozwoli to na prowadzenie badań w wielu rozwijanych już dziś w Polsce dziedzinach, takich jak:

- Fizyka silnie skorelowanych elektronów,
- Fizykochemia powierzchni, zjawiska katalizy, badania reakcji na powierzchni,
- Nowe materiały - cienkie warstwy, heterostruktury, materiały dla spintroniki,
- Magnetyzm powierzchni,
- Biomateriały,
- Mineralogia i geologia.

# ELECTRONIC STATES OF COLLOSOAL MAGNETORESISTIVE MANGANITES $\text{La}_{0.67}\text{Pb}_{0.33}\text{Mn}_{1-x}\text{Fe}_x\text{O}_3$ FROM PHOTOEMISSION SPECTROSCOPY

**M. Kowalik<sup>1,2\*</sup>, R. Zalecki<sup>1</sup>, and A. Kołodziejczyk<sup>1</sup>**

<sup>1</sup> Faculty of Physics and Applied Computer Science, AGH University of Science and Technology,  
Al. Mickiewicza 30, PL 30-059, Kraków, Poland

<sup>2</sup> Department of Physics, Rzeszów University of Technology,  
Al. Powstańców Warszawy 6, PL 35-959 Rzeszów, Poland

*Keywords:* manganites, photoemission, electronic states

\*) e-mail: mkowalik@prz.edu.pl

The electron photoemission spectra of the valence bands and the core level states of manganese perovskite  $\text{La}_{0.67}\text{Pb}_{0.33}(\text{Mn}_{1-x}\text{Fe}_x)\text{O}_3$  with  $x = 0, 0.01, 0.03, 0.06, 0.1$  and  $0.15$  were measured by the Ultraviolet and the X-ray Photoemission Spectroscopy (UPS/XPS) below and above the metal-insulator transition. X-ray diffraction showed that the compounds were phase pure. The magnetic and resistance measurements exhibited the large colossal magnetoresistance behaviour around the metal – insulator transitions. The common feature of the UPS spectra was the two-peak structure at about  $-4.0$  and  $-6$  eV below the upper edge of the valence band (Fig. 1). The same was observed in Refs. [1, 2].

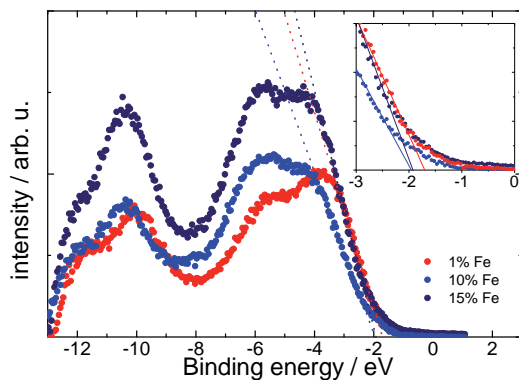


Figure 1. UPS spectra of  $\text{La}_{0.66}\text{Pb}_{0.33}\text{Mn}_{1-x}\text{Fe}_x\text{O}_3$  for  $x = 0.01, 0.1, 0.15$  at room temperature.

The insulating energy gaps were estimated at room temperature to be about  $1.7 \pm 2.0$  eV and were composition dependent. Total energy scan and low binding energy spectra of X-ray (XPS- Al, Mg  $K_\alpha$ ) as well as the Mn  $2p$ - and  $3s$ - core-level spectra were also measured and analyzed (Fig. 2). Comparison of the spectra with the band structure calculations and with the high-resolution spectra measured at synchrotron radiation for Ca- and Ce- substituted manganites [3, 4] revealed the strong hybridization of the Mn  $3d$  and of the O  $2p$  states between  $-3$  and  $-7$  eV and no oxygen states between  $0$  and  $-2$  eV where the Mn-  $3d$  states play predominant role. Reasons for this behaviour were

discussed taking into account our previous analysis of UPS/XPS spectra of other manganese perovskites [1, 2].

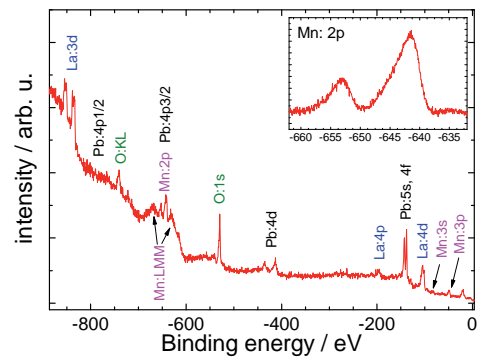


Figure 2. The total X-ray (Mg,  $K_\alpha$ ) spectra of  $\text{La}_{0.66}\text{Pb}_{0.33}\text{MnO}_3$  with the core-level and Auger lines indicated at room temperature. Inset: the Mn  $2p$  core-level spectrum taken with Al- $K_\alpha$  without background.

**Acknowledgements:** The samples were prepared within the collaboration with Professor Gritzner group from the Kepler University in Linz, Austria. This was supported by the Faculty of Physics and Applied Computer Science, AGH University of Science and Technology, Cracow, Poland.

## References

- [1] R. Zalecki, A. Kołodziejczyk, C. Kapusta, K. Krop, "Electronic states of  $\text{La}_{1-x}\text{Ca}_x\text{MnO}_3$  from photoelectron spectroscopy", *J. Alloys Compds.* **328** (2001) 175–180.
- [2] R. Zalecki, A. Kołodziejczyk, C. Kapusta, G. Zaręba, J. Fink-Finowicki, M. Baran, R. Szymczak, H. Szymczak, "Photoemission band structure of  $\text{La}_{0.7}(\text{Ca}, \text{Ce})_{0.3}\text{MnO}_3$  thin films and a  $\text{La}_{0.9}\text{Ca}_{0.1}\text{CoO}_3$  crystal", *J. Alloys Compds.* **442** (2007) 296–298.
- [3] D.N. McIlroy, C. Waldorf, J. Zhang, J.W. Choi, F. Foong, S.H. Liou, P.A. Dowben, "Comparison of the temperature-dependent electronic structure of the perovskites  $\text{La}_{0.65}\text{A}_{0.35}\text{MnO}_3$  ( $\text{A}=\text{Ca}, \text{Ba}$ )", *Phys. Rev. B* **54** (1996) 17438.
- [4] S.W. Han, J.-S. Kang, K.H. Kim, J.D. Lee, J.H. Kim, S.C. Wi, C. Mitra, P. Raychaudhuri, S. Wirth, K.J. Kim, B.S. Kim, J.I. Jeong, S.K. Kwon, B.I. Min, "Photoemission and x-ray absorption spectroscopy study of electron-doped colossal magnetoresistive manganite  $\text{La}_{0.7}\text{Ce}_{0.3}\text{MnO}_3$  films", *Phys. Rev. B* **69** (2004) 104406.

# DEFECT STRUCTURE FORMED AT DIFFERENT STAGES OF GROWTH PROCESS IN ERBIUM, CALCIUM AND HOLMIUM DOPED $\text{YVO}_4$ CRYSTALS

**A. Malinowska<sup>1\*</sup>, E. Wierzbicka<sup>1</sup>, M. Lefeld-Sosnowska<sup>2</sup>, K. Wieteska<sup>3</sup>, W. Wierzchowski<sup>1</sup>  
T. Łukasiewicz<sup>1</sup>, M. Świerkowicz<sup>1</sup>, and W. Graeff<sup>4</sup>**

<sup>1</sup>*Institute of Electronic Materials Technology, ul. Wólczyńska 133, 01-919 Warsaw, Poland*

<sup>2</sup>*Institute of Experimental Physics, University of Warsaw, ul. Hoża 69, 00-681 Warsaw, Poland*

<sup>3</sup>*Institute of Atomic Energy POLATOM, 05-400 Otwock-Świerk, Poland*

<sup>4</sup>*HASYLAB at DESY, Notkestr. 85, 22-603 Hamburg, Germany*

*Keywords:*  $\text{YVO}_4$  crystals, crystallographic defects, X-ray diffraction topography

\*) e-mail: malinows@if.pw.edu.pl

Yttrium orthovanadate ( $\text{YVO}_4$ ) is one of the most important laser host materials due to high quantum efficiency and low excitation level when doped with rare earth ions. It is especially useful in micro-laser systems pumped with semiconductor laser diodes. In these applications the crystals should be highly doped with the rare earth elements as erbium or holmium.  $\text{YVO}_4$  is of zircon tetragonal structure with space group  $I4_1/amd$  and lattice parameter  $a = b = 0.712 \text{ nm}$  and  $c = 0.629 \text{ nm}$ . The crystallographic structure enables efficient introduction of the required ions. Some recent results concerning growth of  $\text{YVO}_4$  are described in Refs. [1-3].

The investigated samples were cut out from different regions of a number of Czochralski grown  $\text{YVO}_4$  crystals, doped with erbium, holmium and calcium. The concentrations of the introduced dopants were 0.5 at. %, 5 at. %, and 0.4 at. %, respectively. Some samples were cut out from the regions of the spiral growth, which is one of the most important problems in technology of the crystals. The X-ray topographic methods exploring both conventional and synchrotron X-ray sources were used as the principal methods of characterization. The conventional X-ray Lang topographs were obtained both in transmission and back reflection geometry. The synchrotron investigations were performed in white X-ray beam and included taking the topographs through a fine mesh with a wire spacing of 0.7 mm, enabling precise evaluation of the lattice deformation.

Despite very large concentrations of the dopants the topographs obtained with all used methods did not reveal any segregation fringes. That proves a high homogeneity of chemical composition, corresponding to the

segregation coefficient close to the unity. The main defects revealed in the topographs were the numerous subgrain boundaries, which density and character were different in various regions of the crystals. In the examined crystals we observed much lower density ( $< 10^4 \text{ cm}^{-2}$ ) of weak point-like contrasts (most probably attributed to dislocation outcrops), than in the case of formerly investigated undoped  $\text{YVO}_4$  crystal [4].

The values and directions of lattice misorientation connected with the subgrain boundaries were most precisely revealed by the synchrotron back-reflection projection topographs exposed through a mesh, and to some extend by the synchrotron section topographs, and by the Lang conventional topographs as well. The evaluated misorientation values were in the range of 0.1-0.7°.

## References

- [1] S. Wu, G. Wang, J. Xie, X. Wu, G. Li, "Growth of large birefringent  $\text{YVO}_4$  crystal", *J. Cryst. Growth* **249** (2003) 176–178.
- [2] H. Zhang, Y. Yu, Y. Cheng, J. Liu, H. Li, W. Ge, X. Cheng, X. Xu, J. Wang, M. Jiang, "Growth of  $\text{YbVO}_4$  stoichiometric crystal", *J. Cryst. Growth* **283** (2005) 438–443.
- [3] Y. Yu, Y. Cheng, H. Zhang, J. Wang, X. Cheng, H. Xia, "Growth and thermal properties of  $\text{YbVO}_4$  single crystal", *Mater. Lett.* **60** (2006) 1014–1018.
- [4] K. Wieteska, W. Wierzchowski, E. Wierzbicka, A. Malinowska, M. Lefeld-Sosnowska, T. Łukasiewicz, W. Graeff, "X-Ray topographic studies of defect structure in  $\text{YVO}_4$  crystals", *Acta Phys. Polon. A* **114** (2008) 455–461.

# SYNCHROTRON RADIATION AS A TOOL OF BIOCHEMICAL ANALYSIS IN BRAIN CANCERS

**M. Szczerbowska-Boruchowska<sup>1\*</sup>, M. Lankosz<sup>1</sup>, A. Smykla<sup>1</sup>, and D. Adamek<sup>2</sup>**

<sup>1</sup> Faculty of Physics and Applied Komputer Science, AGH University of Science and Technology,  
Al. Mickiewicza 30, 30-059 Krakow, Poland

<sup>2</sup> Institute of Neurology, Medical College, Jagiellonian University  
Botaniczna Str. 3, 31-503 Krakow, Poland

*Keywords:* trace elements, oxidation states of elements, biomolecules, brain cancers

\*) e-mail:[boruchowska@novell.ftj.agh.edu.pl](mailto:boruchowska@novell.ftj.agh.edu.pl)

The recent development of synchrotron radiation based microprobe beamlines has enabled spatially resolved XRF (X-ray fluorescence), XANES (X-ray absorption near edge structure spectroscopy) and FTIRM (Fourier transform infrared microspectroscopy) at cellular and subcellular level. Synchrotron radiation XRF (SR-XRF) microprobe analysis as a multielemental analytical method was applied to simultaneous imaging of chemical elements in human brain tumors. Micro-XANES technique which gives information primarily about geometry and oxidation state was used to determine the chemical state of Fe and S in brain gliomas. FTIRM that provides direct information on the molecular composition of the tissue was applied to determine organic composition of brain cancers. The SR-XRF and Fe XANES measurements were performed at the bending magnet beamline L at HASYLAB. Micro-imaging of sulfur oxidation states using XANES measurements was carried out on beamline ID21 at ESRF. FTIRM measurements were performed on SMIS beamline at the synchrotron SOLEIL.

The SR-XRF research allowed detection of P, S, Cl, K, Ca, Fe, Cu, Zn, Br and Rb in human brain tumors. The topographic analysis enabled to determine two-dimensional distribution of elements in characteristic tissue structures in case of cancerous tissues. The Fe XANES analysis in selected points of the tissue showed

that all the XANES spectra obtained for the brain glioma samples are situated between the spectra measured for reference materials containing Fe in the second and third oxidation state (Fig. 1). However, taking into account inhomogeneity of the tissue structure the knowledge based on the results from random points seems to be insufficient. Therefore, the micro-imaging of iron oxidation states were performed. The mapping of different chemical form of iron allowed finding areas where bivalent or trivalent iron compounds were dominant.

The results of S XANES analysis showed that cancer cells accumulate sulfur mainly as sulfide ( $S^{2-}$ ) form. The preliminary results indicated also higher accumulation of this form of sulfur in glioma of IV grade of malignancy in comparison with the samples of II grade neoplasms. The presence of sulfate ( $S^{+6}$ ) species was revealed in histological structures outside the cancer cells. The sulfite ( $S^{+4}$ ) form of sulfur was not detected in the scanned areas of tissue.

In the FTIRM the tissue areas were mapped to generate two-dimensional images of the main biological molecules of interest. Integrated intensities of selected bands were extracted after raster scanning of the sample. The obtained IR maps were compared with the microscopic view of the slices prepared previously for histopathological examination. It allowed determining biochemical composition of the structures of different types of cancerous tissue. The preliminary studies showed differences in biomolecular composition between the studied cases of brain tumors. It will be used in the future (when statistically reliable number of samples will be investigated) to identify biological molecules typical for various types of brain cancers.

**Acknowledgements:** The authors are indebted to Dr. P. Dumas (SOLEIL), Dr. J. Susini (ESRF) and Dr. K. Rickers-Apple (HASYLAB) for their assistance. Support of the Ministry of Science and High Education, Warsaw, Poland and the following grants Ministry of Science and High Education, Warsaw, Poland; Grant Number: 155/ESR/2006/03, DESY/304/2006 as well as European Community; Grant Number: RII3-CT-2004-506008 (IA-SFS) are acknowledged.

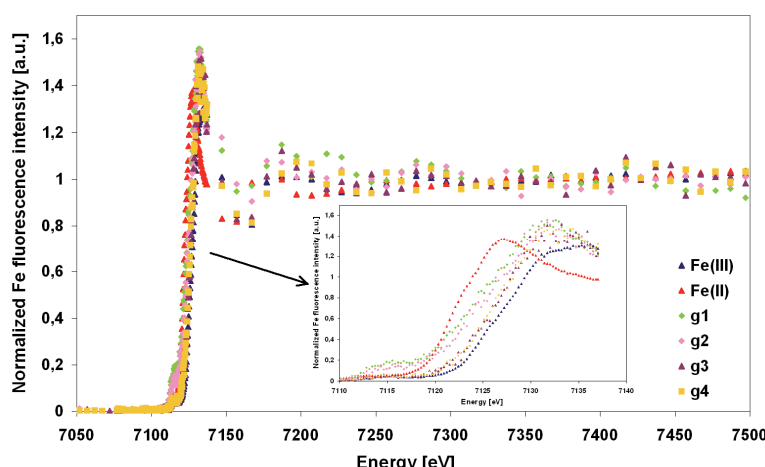


Figure 1. The Fe XANES spectra different cases of glioma tissues (g1-g4) and reference materials.

## COMPLEX STRUCTURE OF $Mg_2Al_3$ $\beta$ AND $\beta'$ PHASES

**J. Wolny<sup>1\*</sup>, M. Duda<sup>1</sup>, and B. Kozakowski<sup>1</sup>**

<sup>1</sup>*Faculty of Physics and Computer Science, AGH University of Science and Technology,  
al. Mickiewicza 30, 30-059 Kraków, Poland*

*Keywords:*  $Mg_2Al_3$ , Samson phase, hexagonal layers

\*) e-mail: wolny@novell.ftj.agh.edu.pl

The Samson phase structure is one of the most complex intermetallic structures. The first description of the  $\beta$ - $Mg_2Al_3$  structure was provided by Samson [1] in 60'. Because of its complexity and potential new technical applications, during the last few years the Samson structure aroused considerable interest among crystallographers. A good example of that interest is a review publication, written by 36 authors from 15 leading European laboratories [2].

Its cubic elementary cell ( $Fd\bar{3}m$ , no. 227 space group) contains 1168 atoms which are distributed over 1832 atomic positions. About 75% of atoms (879 to be exact) form the framework of the structure (skeleton atoms). The framework is made up of Samson's positions which are occupied by atoms with SOF equal to 1. The remaining 289 (25%) atoms partially occupy 953 positions with the average occupation probability of 30%. They form clusters arranged in an elementary cell in a tetrahedral lattice. Their structure has been described in detail in [2 and the following references] and in [3]. The lattice constant of the Samson structure is gigantic:  $a = 2.8242(1)$  nm. At a temperature of 214°C, the structure undergoes a phase transformation to the rhombohedral  $\beta'$ - $Mg_2Al_3$  (space group  $R\bar{3}m$ , no. 160, which is a subgroup of the  $Fd\bar{3}m$  group - index 4) with  $a = 1.9968(1)$  nm,  $c = 4.89114(8)$  nm. It should be pointed out that the constant  $c$  of a rhombohedral structure is practically equal to the length of the diagonal of the cubic structure  $a_{cubic}\sqrt{3} = 4.89166$  nm  $\approx c_{rhomb}$ . The near equivalence in length between the  $c$  axis of the rhombohedral  $\beta'$ - $Mg_2Al_3$  structure and the diagonal of the cubic  $\beta$ - $Mg_2Al_3$  is a consequence of lattice transformation connecting the hR cell of the  $\beta'$ -phase to the F cell of the  $\beta$ -phase.

Comparison of two different types of  $Mg_2Al_3$  structure – cubic  $\beta$  and rhombohedral  $\beta'$  ones – leads to the conclusion that all skeleton atoms of a Samson structure don't change their position during the phase transformation. The skeleton atoms of a Samson phase lie within hexagonal layers [4]. These layers form three structural domains shifted with respect to each other by 1/3 of the length of the main diagonal of the cubic unit structure.

Besides within a hexagonal layer the length of every shift vector is a multiple of about 1/7 of the distances

characteristic for hexagonal structures. Once the shift vectors were found, one could describe the structure as a modulated one.

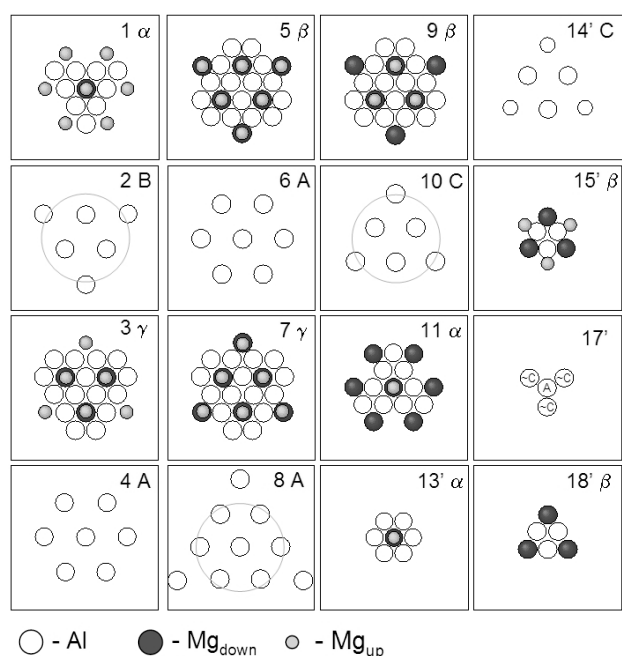


Figure 1. Eighteen layers forming a structural domain. Positions of Al and Mg atoms within the consecutive hexagonal layers for a structural domain of the Samson structure. Aluminium atoms take the hexagonal positions A, B, C. Magnesium atoms occupy positions which are shifted with respect to the Al layers.

### References

- [1] S. Samson, "The crystal structure of the phase  $\beta$ - $Mg_2Al_3$ ", *Acta Crystallogr.* **19** (1965) 401–413.
- [2] M. Feuerbacher *et al.*, "The Samson phase,  $\beta$ - $Mg_2Al_3$  revisited", *Z. Kristallogr.* **222** (2007) 259–288.
- [3] W. Sikora *et al.*, "Symmetry analysis in the investigation of clusters in complex metallic alloys", *J. Phys.: Conf. Ser.* **104** (2008) 012023.
- [4] J. Wolny, B. Kozakowski, M. Duda, J. Kusz, "Stacking of hexagonal layers in the structure of  $\beta$ - $Mg_2Al_3$ ", *Philos. Mag. Lett.* **88** (2008) 501–507.

## STRUCTURAL STUDIES OF HEAVILY TRANSITION METAL IMPLANTED ZnO

**E. Dynowska<sup>1</sup>, W. Szuszkiewicz<sup>1</sup>, C. Ziereis<sup>2</sup>, J. Geurts<sup>2</sup>, S. Müller<sup>3</sup>, C. Ronning<sup>4</sup>,  
J. Domagala<sup>1</sup>, P. Romanowski<sup>1</sup>, and W. Caliebe<sup>5</sup>**

<sup>1</sup>*Institute of Physics, Polish Academy of Sciences, al. Lotników 32/46, 02-668 Warszawa, Poland*

<sup>2</sup>*Physikalischs Institut, Universität Würzburg, am Hubland, 97074 Würzburg, Germany*

<sup>3</sup>*II. Physikalischs Institut, Universität Göttingen, Friedrich-Hund-Platz 1, 37077 Göttingen, Germany*

<sup>4</sup>*Institut für Festkörperphysik, Universität Jena, Max-Wien-Platz 1, 07743 Jena, Germany*

<sup>5</sup>*Hasylab at DESY, Notkestr. 85, D-22603 Hamburg, Germany*

*Keywords:* diffraction, ZnO, implantation

The study of ZnO alloyed with transition metals (TM) has been stimulated by theoretical predictions of room temperature ferromagnetism for these compounds [1, 2]. One of the methods for the incorporation of TM into ZnO is ion implantation connected with proper thermal treatment. The magnetic properties of ZnO:TM compounds depend on their crystal structure after such procedure.

In this work we report the results of structural characterization of ZnO crystals implanted with 16 at.% of Mn, Co, Fe and Ni ions and annealed at 900°C in air. The X-ray structural characterization was performed using synchrotron radiation at the W1.1 beamline at DESY-Hasylab. The monochromatic X-ray beam of wavelength  $\lambda = 1.54056 \text{ \AA}$  was used. Two modes of measurement were applied: symmetrical  $\omega$ - $2\theta$  scan and coplanar  $2\theta$  scan in the glancing incidence geometry.

Fig. 1 shows the X-ray  $\omega$ - $2\theta$  patterns for Mn- and Co-implanted and annealed ZnO samples, respectively. The interpretation of these patterns leads to different results for these two samples. The main effect of annealing of Mn-implanted ZnO sample is the creation of monocrystalline inclusion of  $\text{ZnMn}_2\text{O}_4$  tetragonal phase ( $a = 5.7204 \text{ \AA}$  and  $c = 9.2450 \text{ \AA}$ ) - the (101) lattice planes of this phase are parallel to the (0001) lattice planes of ZnO matrix. Moreover, the left-side asymmetry of 0001 peaks of ZnO matrix (Fig. 1a) indicates the presence of the solid solution  $\text{Zn}_{1-x}\text{Mn}_x\text{O}$  phase with very low quantity of Mn corresponding to  $x \approx 0.005$ .

In the pattern presented in Fig. 1b the very strong peaks originating mainly from the bulk ZnO and several much weaker ones are visible. The detailed analysis of the peaks originated from ZnO exhibits the right-side asymmetry of these peaks that confirms a creation of the solid solution  $\text{Zn}_{1-x}\text{Co}_x\text{O}$  with estimated composition  $x \approx 0.075$ . The weak peaks visible in the pattern are probably caused by a trace inclusions of some single crystalline phases with crystallographic orientation closely connected with (0001) planes of ZnO. Only three weak reflections have been identified up to now: two of them as belonging to the elemental Zn and one can be attributed to the  $\text{ZnCo}_2\text{O}_4$  or  $\text{Co}_3\text{O}_4$  phases – these phases have very similar crystal structure.

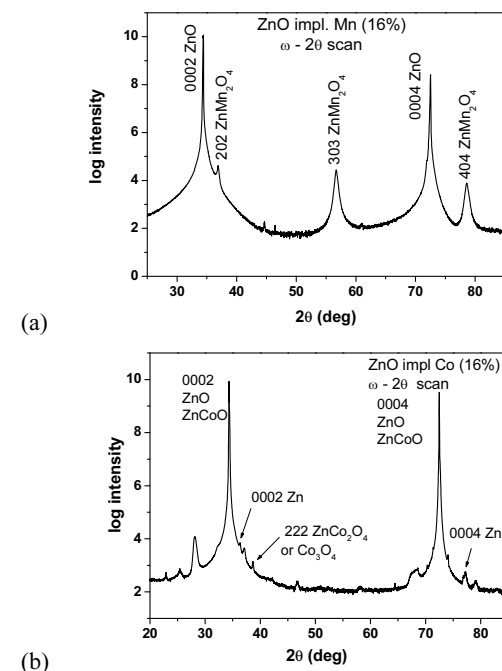


Figure 1. The X-ray  $\omega$ - $2\theta$  diffraction patterns of ZnO:Mn (a) and ZnO:Co (b) samples after annealing.

Concluding, we can state that in the case of ZnO:Mn majority of Mn incorporated by implantation into bulk sample of ZnO after annealing has been located in  $\text{ZnMn}_2\text{O}_4$  spinel phase, while in ZnO:Co majority of Co have been built into ZnO matrix creating the ternary compound  $\text{Zn}_{0.925}\text{Co}_{0.075}\text{O}$ .

**Acknowledgements:** This work was partially supported by the European Community - Research Infrastructure Action under the FP6 "Structuring the European Research Area" Programme (through the Integrated Infrastructure Initiative "Integrating Activity on Synchrotron and Free Electron Laser Science", Contract RII3-CT-2004-506008).

### References

- [1] T. Dietl, H. Ohno, F. Matsukura, J. Cibert, D. Ferrand, "Zener model description of ferromagnetism in zinc-blende magnetic semiconductors", *Science* **287** (2000) 1019.
- [2] K. Sato, H. Katayama-Yoshida, "Stabilization of ferromagnetic states by electron doping in Fe-, Co- or Ni-doped ZnO", *Jpn. J. Appl. Phys.* **40** (2001) L334.

## DYNAMIC SAXS CORRELATION AS METHOD OF STRUCTURAL RESEARCH

**H. Grigoriew<sup>1\*</sup>, L. Wiegert<sup>2</sup>, and A. Boczkowska<sup>3</sup>**

<sup>1</sup> Institute of Nuclear Chemistry and Technology, 03-195 Warsaw, Poland

<sup>2</sup> ESRF, Grenoble 38043 Cedex, France

<sup>3</sup> Faculty of Materials Science, Warsaw University of Technology, 02-507 Warsaw, Poland

*Keywords:* XPCS method, structural dynamics, magnetic field

\*) e-mail: hgrgori@ichtj.waw.pl

Composite-type material consisted of polyurethane gel, and carbonyl iron (CI) of 7  $\mu\text{m}$  size spheres. The gel constituents were: MDI/OAE+DCDA with molar ratio 70/30. The material was processed with 11.5 vol.% of CI under magnetic field, during 24 h at 25°C.

SEM images of the composite showed short chains of CI formed inside the material.

- XPCS (X-ray Photon Correlation Spectroscopy) measurements were performed on the Troika beamline (ID10A) of the ESRF in SAXS configuration. The measurements depending on time ( $t$ ) and angle ( $q$ ), using X-beam wavelength of 1.745 Å, and detector type CCD were used. The sample was placed between electromagnet poles with magnetic lines direction perpendicular to the X-beam and parallel to the sample surface and CI chains inside it. Measurements were performed for: 0, 300 and 600 mT. It occurred that correlation of scattered intensity took place in the time range: from  $5 \times 10^2$  to  $100 \times 10^2$  sec.

- *Correlation curves,  $g_2(t)$ :* The correlation function  $g_2(t) = \langle I(t_0+t)I(t_0) \rangle / \langle I(t_0) \rangle^2$  was obtained from  $I(t, q)$  CCD measurements using masks to get them in directions: parallel (par), isotropic (iso) and perpendicular (per) to the magnetic field lines.

- The reference curves at 0 mT are of extremely slow dynamics behavior with correlation reached for about  $10^4$  sec and of weak differentiation between the measurement directions. For 300 mT, the correlation is faster ( $\sim 1.2 \times 10^3$  sec) with the dependence on different directions. For 600 mT the correlation is the fastest, of less than  $10^3$  sec.

- *Correlation rates,  $\Gamma(q)$ .* The correlation rates,  $\Gamma(q)$ , were found by fitting exponential function:  $y = a e^{-2T_x}$  to the subsequent  $g_2(t)$  curves, in their region of correlation behavior. Fig. 1 shows  $\Gamma(q)$  curves for subsequent magnetic field value, with sets of three curves for each directions (par, iso and per). When magnetic field increases, from 0 through 300 to 600 mT, correlation rate also increases. It occurred that the magnetic field essentially influences the correlation rate, up to ten times (Fig. 1). Besides, within each set the highest curve is for direction parallel to the magnetic field (par), the lowest one for direction perpendicular (per) and the middle one is for isotropic (without mask) measurement. The straight-line shape of all  $\Gamma(q)$  curves are of no significant deviations. The

correlation process is thus not due to structural reorganization on measured length scale.

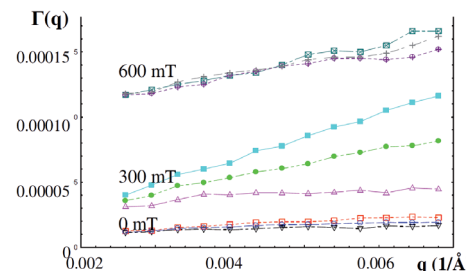


Figure 1. Correlation rates  $\Gamma(q)$  for different magnetic field values. At each three curve set: bottom – perpendicular, middle – isotropic, top – parallel to the field lines.

In the case of linear  $\Gamma(q)$  shape, the dependence it on diffusion coefficient is:  $\Gamma(q) = D \times q$ . The  $D$  [Å/sec] values were found from slope of straight lines fitted to  $\Gamma(q)$  (Table 1).

- For the reference curves for 0 mT the very moderate values of the  $\Gamma(q)$  and  $D$  as well as no differentiation from direction seem to be an evidence of very strong structure.

- For the middle value of the field (300 mT), the same parameters are strongly dependent on the magnetic field direction and are of much bigger values (Fig. 1 and Table 1). Here dependence on the material dynamics from direction of the outer magnetic field is very clear, with strongly privileged parallel direction (par).

- But for the magnetic field of 600 mT, despite the highest correlation rate, the dependence on magnetic field direction became weak, as well as  $D$  values (Fig. 1 and Table 1). Simultaneously, on the  $\Gamma(q)$  curves the bigger fluctuation around the fitted straight lines are observed. There probably mechanism of dynamics behavior altered.

Table 1. Diffusion coefficients,  $D$  [Å /sec].

	0 mT	300 mT	600 mT
Par	0.0027	0.0180	0.0119
iso	0.0018	0.0109	0.0096
per	0.0011	0.0029	0.0083

### Reference

- [1] J. Lal, D. Abernathy, L. Auvray, O. Diat, G. Gruebel, "Dynamics and correlations in magnetic colloidal systems studied by X-ray photon correlation spectroscopy", *Eur. Phys. J. E4* (2001) 263.

# BADANIA ABSORPCYJNE ZMODYFIKOWANYCH CHEMICZNIE CHITOZANÓW Z ŻELAZEM

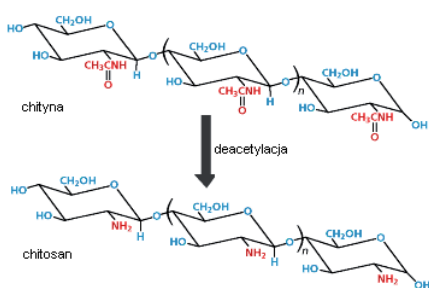
**M.T. Klepka<sup>1\*</sup>, K. Lawniczak-Jablonska<sup>1</sup>, and A. Wolska<sup>1</sup>**

<sup>1</sup>*Instytut Fizyki Polskiej Akademii Nauk, al. Lotników 32/46, 02-668 Warszawa*

*Slowa kluczowe:* chitozan, absorpcja, synchrotron

\*) e-mail: [mklepka@ifpan.edu.pl](mailto:mklepka@ifpan.edu.pl)

Kompleksy metal-chitozan zawierające metale przejściowe wzbudzają zainteresowanie wielu grup naukowych. Na intensywne badania tych materiałów mają wpływ ich nietuzinkowe właściwości. Chitozan jest produktem deacetyleacji chityny (Rys. 1), a ta jest jednym z głównych składników pancerzy skorupiaków morskich. Oba te materiały są liniowymi polimerami. Chitozan jest materiałem pochodzenia naturalnego, a więc jest nietoksyczny, biokompatybilny, bioaktywny oraz ulega łatwej biodegradacji. Szczególne zainteresowanie budzi jednak zdolność chitozanolu do związywania w swojej strukturze metali zarówno ciężkich jak i toksycznych [1]. Polimer ten dzięki swoim własnościom jest już wykorzystywany w wielu gałęziach przemysłu, a możliwości jego zastosowań ciągle się powiększają [2].



Rysunek 1. Deacetyleacja chityny.

Obecnie trwają badania nad zastosowaniem kompleksów żelazo-chitozan jako biotransporterów leków z kontrolowanym uwalnianiem substancji aktywnych. Możliwe jest to, gdyż chitozan po związaniu jonu metalu wykazuje właściwości magnetyczne [3]. Chitozan znajduje także inne zastosowania w biomedycynie dzięki takim cechom jak działanie bakteriobójcze, immunologiczne czy przeciwnowotworowe [4, 5]. W celu zwiększenia właściwości adsorpcyjnych chitozanolu stosuje się różnorodne modyfikacje chemiczne, jak sieciowanie łańcuchów polimeru czy przyłączanie grup aktywnych, jak np. -COOH.

Pomimo dużego zainteresowania tymi materiałami i wieloma doniesieniami literackimi o jego właściwościach i zastosowaniach, wciąż nie jest jasny

mechanizm związywania metali przez te polimery. Podstawową techniką stosowaną do określania pozycji atomów metalu w tych materiałach jest spektroskopia Mössbauera, nie pozwala ona jednak na określenie rodzaju sąsiadujących atomów, w przeciwieństwie do rentgenowskiej spektroskopii absorpcyjnej.

Zaprezentowane zostaną wyniki, uzyskane na podstawie badań absorpcji promieniowania rentgenowskiego, dla kilku kompleksów żelazo-chitozan poddanych różnym modyfikacjom chemicznym.

Pomiary absorpcyjne dla krawędzi K żelaza zostały przeprowadzone na synchrotronie DORIS III, stacja A1, HASYLAB, DESY. Przeprowadzono je wykorzystując metodę fluorescencyjną, korzystając z siedmioelementowego detektora krzemowego.

Rentgenowska spektroskopia absorpcyjna ze względu na wysoką czułość i selektywność pierwiastkową okazuje się być bardzo dobrym narzędziem do badań nieuporządkowanych strukturalnie układów.

**Podziękowania:** Autorzy składają podziękowanie za finansowanie uzyskane dzięki grantowi Ministerstwa Nauki i Edukacji N202-052-32/1189 oraz DESY/HASYLAB i Unii Europejskiej w ramach projektu RI3-CT-2004-506008 (IA-SFS).

## Literatura

- [1] N.V. Majeti, K. Ravi, "A review of chitin and chitosan applications", *React. Funct. Polym.* **46** (2000) 1–27.
- [2] M.F.A. Goosen, *Applications of chitin and chitosan* (CRC Press 1996).
- [3] M.T. Klepka, N. Nedelko, J.M. Greene, K. Lawniczak-Jablonska, I.N. Demchenko, A. Ślawska-Waniewska, C.A. Rodrigues, A. Debrassi, C. Bordini, "Local atomic structure and magnetic ordering of iron in Fe-chitosan complexes", *Biomacromolec.* **9** (2008) 1586–1594.
- [4] X. Wang, Y. Du, H. Liu, "Preparation, characterization and antimicrobial activity of chitosan-Zn complex", *Carbohydr. Polym.* **56** (2004) 21–26.
- [5] K. Kurita, "Chitin and chitosan: functional biopolymers from marine crustaceans", *Marine Biotechnol.* **8** (2006) 203–226.

## LOKALNE OTOCZENIE JONÓW MANGANU IMPLANTOWANYCH W KRYSZTAŁACH GaSb

**A. Wolska<sup>1\*</sup>, K. Lawniczak-Jablonska<sup>1</sup>, M.T. Klepka<sup>1</sup>, A. Barcz<sup>1</sup>,  
A. Hallen<sup>2</sup>, and D. Arvanitis<sup>3</sup>**

<sup>1</sup>*Institute of Physics PAS, al. Lotników 32/46, 02-668, Warsaw, Poland*

<sup>2</sup>*Royal Inst. of Technology, Dept. of Microelectronics and Applied Physics, Box 226, SE 164 40 Kista, Sweden*

<sup>3</sup>*Department of Physics and Materials Science, Uppsala University, Box 530, 75121 Uppsala, Sweden*

*Keywords:* MnSb, GaSb, implantation

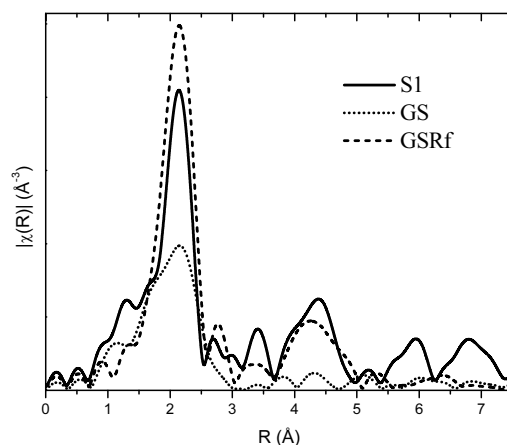
\*) e-mail: wolska@ifpan.edu.pl

Wśród materiałów ferromagnetycznych, które mogą znaleźć zastosowanie w urządzeniach wykorzystujących spin, najczęściej wymienia się związek GaMnAs. Intensywnie bada się zarówno jednorodny potrójny stop, jak i wytrącenia MnAs w matrycy GaAs. Co więcej, okazało się, że ferromagnetyczne nanowytrącenia MnAs można uzyskać nie tylko poprzez hodowlę metodą MBE, ale także poprzez implantację jonów Mn do kryształów GaAs [1-3]. Ma to istotne znaczenie praktyczne, gdyż implantacja jest metodą tańszą w masowej produkcji. Innym typem wytrąceń o potencjalnie interesujących właściwościach magnetycznych są wytrącenia MnSb. Objętościowy związek MnSb ma temperaturę Curie 587 K i magnetyzację nasycenia w temperaturze pokojowej 710 emu/cm<sup>3</sup>. Wykazano też, że warstwy Mn<sub>1-x</sub>Sb<sub>x</sub> hodowane na podłożu GaAs osiągają temperaturę Curie 620 K [4, 5]. Umiejętność otrzymywania ich poprzez implantację ułatwiałaby potencjalne zastosowania przemysłowe. Dlatego więc znalezienie optymalnych warunków do uzyskiwania wytrąceń o pożądanych właściwościach jest szczególnie istotne.

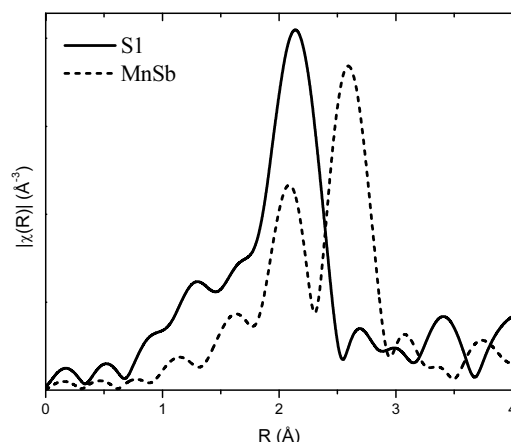
Próbki badane w prezentowanej pracy zostały przygotowane poprzez implantację kryształów GaSb jonami Mn. Energia jonów wynosiła 10 keV dla zestawu próbek oznaczonego S oraz 150 keV dla zestawu oznaczonego GS. Dawki jonów użyte dla zestawu S były następujące: 1×10<sup>16</sup> Mn/cm<sup>2</sup> (S1), 2×10<sup>16</sup> Mn/cm<sup>2</sup> (S2) oraz 3×10<sup>16</sup> Mn/cm<sup>2</sup> (S3). Dla zestawu GS dawka wynosiła 1.7×10<sup>17</sup> Mn/cm<sup>2</sup>. Pierwszy zestaw był następnie wygrzany w piecu próżniowym przez 10 min. w temperaturze 650°C. W przypadku zestawu drugiego jedna próbka pozostała niewygrzana (GS), kolejna była wygrzana w atmosferze argonu przez 5 min. w 350°C (GSRf), kolejne dwie zaś wygrzewano w parach antymonu w 400°C przez 48 h (GS4) oraz 600°C przez 2 h (GS6).

Pomiary absorpcji promieniowania synchrotronowego zostały przeprowadzone w laboratorium Hasylab na stacjach Cemo i E4. Wykonano pomiary widm EXAFS na krawędzi K manganu na próbkach schłodzonych do temperatury ciekłego azotu i przy użyciu detektora fluorescencyjnego. Dodatkowo metodą transmisyjną zmierzono widma komercyjnych proszków MnSb oraz MnO. Uzyskane dane były

analizowane przy pomocy programów Athena i Artemis wchodzących w skład pakietu IFEFFIT [6].

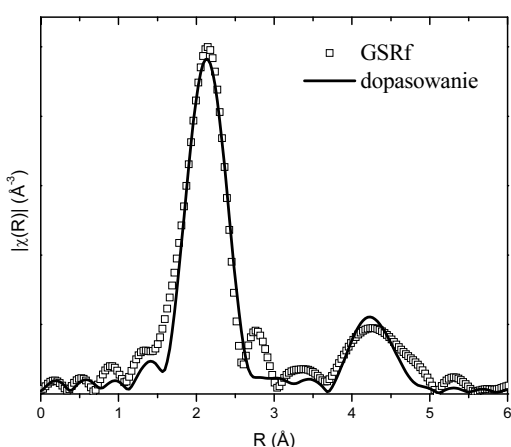


Rysunek 1. Porównanie transformat Fouriera oscylacji EXAFS dla wybranych implantowanych próbek.



Rysunek 2. Porównanie transformat fouriera dla próbki implantowanej (S1) oraz dla standardowego MnSb.

Rysunek 1 przedstawia porównanie transformaty fouriera oscylacji EXAFS dla wybranych próbek. Nie pokazano transformat dla próbek S2 i S3, gdyż są one podobne do S1. Pominieto też GS4 i GS6, gdyż zaobserwowano w nich głównie tlenek manganu. Tak jak się należało spodziewać, w próbce niewygrzewanej (GS) widoczna jest tylko pierwsza strefa koordynacyjna atomów wokół Mn. Jest ona niesymetryczna i dosyć szeroka, co sugeruje amorfizację otoczenia jonów Mn. W próbce GSRf pierwsza strefa staje się symetryczna, a dodatkowo wykształca się druga strefa, co oznacza, że wygrzewanie prowadzi do częściowej rekonstrukcji struktury. W przypadku próbki S1 widoczne są także dwie kolejne strefy co wskazuje na dobrze uporządkowaną strukturę.



Rysunek 3. Wynik dopasowania modelu teoretycznego do widma eksperymentalnego próbki implantowanej (GSRf).

W żadnej z badanych próbek nie wytworzyły się wytrącenia MnSb. Na Rys. 2 przedstawiono porównanie transformaty fouriera dla standardowej próbki MnSb oraz dla jednej z implantowanych próbek (S1). Jak widać, zarówno kształt jak i położenie pierwszej strefy różnią się w stosunku do MnSb. Również próby dopasowania widma eksperymentalnego przy użyciu modelu struktury MnSb nie przyniosły pozytywnych rezultatów. Po wielu próbach eksperymentalną strukturę rozkładu atomów wokół Mn udało się odtworzyć wykorzystując model GaSb (grupa przestrzenna  $F\text{-}43m$ ), gdzie centralny atom manganu był podstawiony pod atom antymonu. Model ten daje dobre dopasowanie pod warunkiem, że pominie się strefy zawierające antymon. Rysunek 3 przedstawia wynik takiego dopasowania

dla próbki GSRf. Pierwsza strefa składa się z 4, a druga z 12 atomów galu. Odległości stref znalezione z dopasowania wynoszą: 2.46 Å (w modelu 2.64 Å) i 4.62 Å (w modelu 5.07 Å). Różnią się one znacząco od odległości przewidzianych przez model. Wynika to stąd, że brak podsiedzi antymonowej powoduje skurczanie się podsiedzi galowej, przez co kolejne strefy znajdują się bliżej niż to wynika z modelu. Brak antymonu w obszarze implantowanym potwierdziły także pomiary SIMS. Natomiast, jak już wspomniano wcześniej, próby wygrzewania w atmosferze Sb (próbki GS4 i GS6) spowodowały utworzenie tlenku Mn.

Metody wykorzystane do utworzenia wydzielin MnSb w prezentowanych tu próbkach nie doprowadziły do powstania wytrąceń Mn o strukturze MnSb. Ponadto, wygrzewanie w próżni doprowadziło do odparowania atomów antymonu z części próbek, gdzie dotarły jony manganu, zaś podsiedź galowa skurczyła się zachowując przy tym strukturę, którą posiadała w krysztale GaSb. Wygrzewanie w atmosferze antymonu spowodowało utlenienie zaimplantowanych jonów Mn.

**Podziękowania:** Autorzy wyrażają podziękowanie za finansowanie uzyskane dzięki grantowi Ministerstwa Nauki i Edukacji N202-052-32/1189 oraz DESY/HASYLAB i Unię Europejską w ramach projektu RII3-CT-2004-506008 (IA-SFS).

#### Literatura

- [1] A. Serres, G. Benassayag, M. Respaud, C. Armand, J.C. Pesant, A. Mari, Z. Liliental-Weber, A. Claverie, "Structural and magnetic properties of MnAs nanoclusters formed by Mn ion implantation in GaAs", *Mat. Sci. Eng. B* **101** (2003) 119–123.
- [2] O.D.D. Couto, Jr M.J.S.P. Brasil, F. Likawa, G. Giles, C. Adriano, J.R.R. Bortoleto, M.A.A. Pudenzi, H.R. Gutierrez, I. Danilov, "Ferromagnetic nanoclusters formed by Mn implantation in GaAs", *Appl. Phys. Lett.* **86** (2005) 071906.
- [3] A. Chanda, H.L. Lenka, C. Jacob, "Study of high energy Mn<sup>+</sup> ion implantation in GaAs", *Appl. Phys. A* **94** (2009) 89–94.
- [4] A.F. Panchula, C. Kaiser, A. Kellock, S.S. Parkin, "Spin polarization and magnetotransport of Mn–Sb alloys in magnetic tunnel junctions", *Appl. Phys. Lett.* **83** (2003) 1812–1814.
- [5] H. Akinaga, K. Tanaka, K. Ando, T. Katayama, "Fabrication and magneto-optical properties of epitaxial ferromagnetic Mn<sub>1-x</sub>Sb thin films grown on GaAs and sapphire", *J. Cryst. Growth* **150** (1995) 1144–1149.
- [6] B. Ravel, M. Newville, "ATHENA, ARTEMIS, HEPHAESTUS: data analysis for X-ray absorption spectroscopy using IFEFFIT", *J. Synchrotron Rad.* **12** (2005) 537–541.

## WYTRĄCENIA MnSb W MATRYCY GaSb WYTWARZANE PRZY POMOCY METODY MBE

**A. Wolska<sup>1\*</sup>, K. Lawniczak-Jablonska<sup>1</sup>, M.T. Klepka<sup>1</sup> and J. Sadowski<sup>1,2</sup>**

<sup>1</sup>*Institute of Physics PAS, al. Lotników 32/46, 02-66, Warsaw, Poland*

<sup>2</sup>*Lund University, MAX-Lab, Lund SE-221 00, Sweden*

*Slowa kluczowe:* MnSb, GaSb, MBE

\*) e-mail: wolska@ifpan.edu.pl

Wśród materiałów, które mogą znaleźć zastosowanie w spintronice, duże zainteresowanie budzą te, które zawierają ferromagnetyczne wytrącenia w matrycy półprzewodnikowej. W celu uzyskania materiałów o pożądanych własnościach magnetycznych, rozsądnie jest zacząć od wytrąceń związku, którego temperatura Curie ( $T_C$ ) przekracza temperaturę pokojową. Warunek ten spełnia MnSb. Objętościowy MnSb ma  $T_C$  równą 587 K [1], zaś dla warstw  $Mn_{1-x}Sb_x$  hodowanych na podłożu GaAs  $T_C$  sięga 620 K [2].

Poszukiwanie sposobu formowania wytrąceń MnSb w matrycy GaSb podczas hodowli przy pomocy metody MBE wymagało przetestowania różnych typów podłoż, temperatur wzrostu i wygrzewania. Jako przykład przedstawione zostaną warstwy wyhodowane na trzech różnych podłożach: GaMnSbAs na GaAs(100), GaMnSb na GaAs(111)B oraz GaMnSb na GaSb(100).

W przypadku pierwszej próbki warstwa GaMnAs o grubości 700 Å zawierająca 6% Mn została naniesiona na podłoż GaAs(100). Następnie naniesiono na nią 1 ML Mn oraz amorficzny antymon. Tak przygotowaną próbke wygrzewano przez 1.5 h w temperaturze 200°C. Nadmiarowy antymon odparowano wygrzewając ją dodatkowo przez 10 min w temperaturze 400°C.

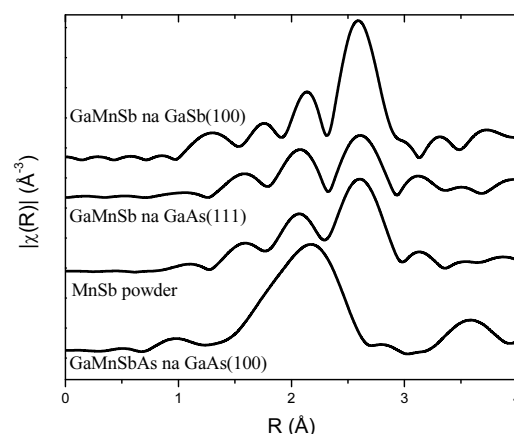
Próbkę drugą otrzymano nakładając najpierw bufor GaSb o grubości 0.12 μm na podłoż GaAs(111)B, a następnie warstwę GaMnSb o grubości 0.63 μm i zawartości mangana około 1%, w temperaturze 450°C.

Próbkę trzecią to warstwa GaMnSb o grubości 0.63 μm i zawartości Mn bliskiej 1% naniesiona na podłoż GaSb(100) w temperaturze 450°C.

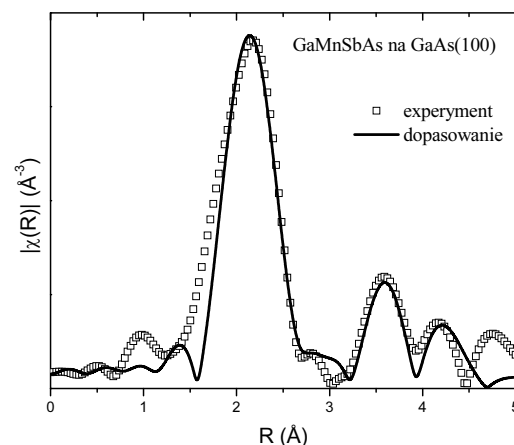
Pomiary widm EXAFS na krawędzi K Mn zostały wykonane w laboratorium Hasylab na stacjach Cemo i E4 przy użyciu 7-elementowego krzemowego detektora fluorescencyjnego. Próbki były schłodzone do temperatury ciekłego azotu. Dodatkowo metodą transmisyjną zmierzono widmo komercyjnego proszku MnSb. Uzyskane dane były analizowane przy pomocy programów Athena i Artemis wchodzących w skład pakietu IFEFFIT [3].

Rysunek 1 przedstawia porównanie transformat fouriera oscylacji EXAFS dla badanych próbek i proszku MnSb. Można zauważać, że tylko warstwa GaMnSbAs na GaAs(100) różni się zdecydowanie od standardowego MnSb. Najlepsze dopasowanie uzyskano w tym przypadku rozważając model, gdzie Mn lokuje się na

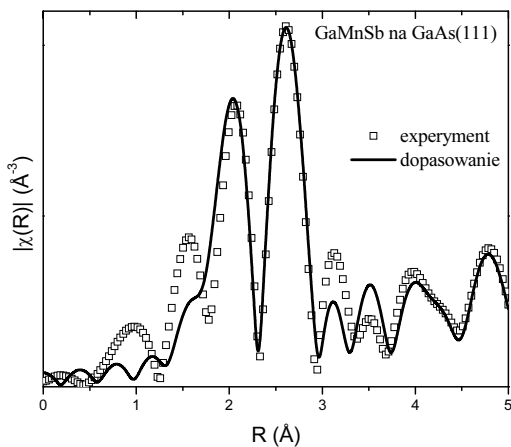
pozycjach podstawieniowych w związku GaAs (Rys. 2). W widmie EXAFS dominuje mangan z warstwy GaMnAs. Jeżeli nawet amorficzny antymon związał się z nanesioną warstwą Mn to jego wkład do obserwowanego sygnału jest bardzo niewielki.



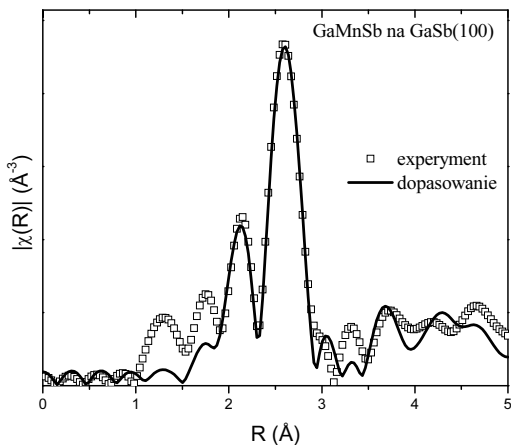
Rysunek 1. Porównanie transformat Fouriera oscylacji EXAFS dla prezentowanych próbek.



Rysunek 2. Wynik dopasowania modelu teoretycznego do widma eksperymentalnego warstwy GaMnSbAs na GaAs(100).



Rysunek 3. Wynik dopasowania modelu teoretycznego do widma eksperymentalnego warstwy GaMnSb na GaAs(111).



Rysunek 4. Wynik dopasowania modelu teoretycznego do widma eksperymentalnego warstwy GaMnSb na GaSb(100).

W przypadku warstwy GaMnSb na GaAs(111)B dopasowanie przy użyciu tylko modelu MnSb nie przyniosło pozytywnego wyniku. Po sprawdzeniu innych modeli, okazało się, że część atomów manganu podstawa się pod atomy antymonu w matrycy GaSb. Wykorzystując oba modele w dopasowaniu określono, że dla tej próbki około 50% atomów manganu lokuje się w wytrąceniach MnSb, zaś kolejne 50% lokuje się w matrycy GaSb podstawiając atomy antymonu (Rys. 3). Czyste wytrącenia MnSb zostały natomiast uzyskane w warstwie GaMnSb na GaSb(100). Rysunek 4 przedstawia dopasowanie przy użyciu tylko modelu MnSb.

W zależności od typu podłoża i procedury wzrostu, atomy manganu lokowały się w różny sposób w sieciach GaAs i GaSb. Wytrącenia MnSb udało się uzyskać w przypadku dwóch typów podłoża: GaAs(111)B oraz GaSb(100) i procesu prowadzonego w stosunkowo wysokiej temperaturze równej 450°C.

**Podziękowania:** Autorzy wyrażają podziękowanie za finansowanie uzyskane dzięki grantowi Ministerstwa Nauki i Edukacji N202-052-32/1189 oraz DESY/HASYLAB i Unię Europejską w ramach projektu RII3-CT-2004-506008 (IASFS).

#### Literatura

- [1] A.F. Panchula, C. Kaiser, A. Kellock, S.S. Parkin, "Spin polarization and magnetotransport of Mn–Sb alloys in magnetic tunnel junctions", *Appl. Phys. Lett.* **83** (2003) 1812–1814.
- [2] H. Akinaga, K. Tanaka, K. Ando, T. Katayama, "Fabrication and magneto-optical properties of epitaxial ferromagnetic  $Mn_{1-x}Sb$  thin films grown on GaAs and sapphire", *J. Cryst. Growth.* **150** (1995) 1144–1149.
- [3] B. Ravel, M. Newville, "ATHENA, ARTEMIS, HEPHAESTUS: data analysis for X-ray absorption spectroscopy using IFEFFIT", *J. Synchrotron Rad.* **12** (2005) 537–541.

## DEFECT STRUCTURE OF GaMnSb GROWN ON GaAs SUBSTRATE

**J. Bak-Misiuk<sup>1</sup>, P. Romanowski<sup>1</sup>, E. Dynowska<sup>1</sup>, J.Z. Domagala<sup>1</sup>, J. Sadowski<sup>1,2</sup>, T. Wojciechowski<sup>1</sup>, R. Jakiela<sup>1</sup>, W. Wierzchowski<sup>3</sup>, K. Wieteska<sup>4</sup>, W. Caliebe<sup>5</sup>, and W. Graeff<sup>5</sup>**

<sup>1</sup>*Institute of Physics, PAS, Al. Lotników 32/46, 02-668 Warsaw, Poland*

<sup>2</sup>*Lund University, MAX-Lab, Lund SE-22100, Sweden*

<sup>3</sup>*Institute of Electronic Materials Technology, 01-919 Warsaw, Poland*

<sup>4</sup>*Institute of Atomic Energy, 05-400 Otwock - Świerk, Poland*

<sup>5</sup>*HASYLAB at DESY, D-22603 Hamburg, Germany*

*Keywords:* X-ray diffraction, strain, GaMnSb

\*) e-mail: [bakmi@ifpan.edu.pl](mailto:bakmi@ifpan.edu.pl)

Ferromagnetic semiconductors have recently focused much interest since they hold out prospects for using electron spin in electronic devices. A possible way to yield such materials is producing of inclusions in a semiconductor matrix [1]. It has been shown that bulk MnSb has  $T_c$  of 587 K [2, 3], therefore it can be a good candidate to form nanoinclusions, ferromagnetic above room temperature.

We report the results concerning the defect structure and strain state of the  $\text{Ga}_{1-x}\text{Mn}_x\text{Sb}$  layer grown by MBE method on the GaAs(111) A substrates, with thin GaSb buffer layer, for various Mn concentration,  $x = 0.01, 0.06, 0.08$ . Secondary Ion Mass Spectroscopy (SIMS, Cameca SF) was applied to determine the concentration of elements in the layers. To prepare the multiphase material the temperature of substrate during layer growth was equal to 770 K. Microscopic nature of the MnSb phase was studied by scanning electron microscopy (SEM).

Structural characterization of the layers was carried out by X-ray diffraction method using standard laboratory source or synchrotron radiation at the DESY-Hasylab at the F1, E2 and W1.1 experimental stations. The lattice parameter and strain state of samples were studied applying the X-ray high-resolution diffractometer. The strain state of the layers was determined from the in-plane and out-of-plane lattice parameters and from reciprocal space mapping made for the symmetrical and asymmetrical reflections. Two modes of diffraction measurement were applied with synchrotron radiation: the symmetrical  $\omega$ - $2\theta$  and coplanar  $2\theta$  scans in the glancing incidence geometry. Such measurements allow to detect the lattice planes of the layers parallel to the crystallographic orientation of the substrate and to obtain information concerning polycrystalline inclusions.

The  $2\theta/\omega$  scan performed for  $\text{Ga}_{0.99}\text{Mn}_{0.01}\text{Sb}/\text{GaAs}$  is presented in Fig. 1. The main diffraction peaks, observed for the layers grown on (111) GaAs, were indexed as 111 GaMnSb. Three phases: MnSb,  $\text{Mn}_2\text{Sb}$  and  $\text{Mn}_2\text{O}_3$  were found also. For this sample no diffraction peaks originating from polycrystalline inclusions were also found.

SEM studies reveal the presence of isolated MnSb clusters with typical lateral dimension 200-600 nm.

White and monochromatic synchrotron topographs in the Bragg case geometry were made, but no misfit dislocations were detected.

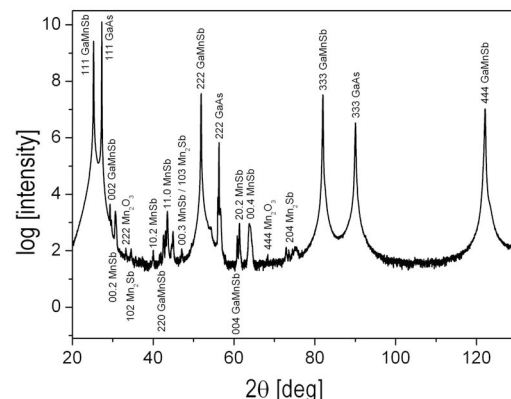


Figure 1.  $2\theta/\omega$  X-ray diffraction pattern of  $\text{Ga}_{0.99}\text{Mn}_{0.01}\text{Sb}$  grown on GaAs(111)A substrate.

**Acknowledgements:** This work was partially supported by national grant of Polish Ministry of Science and High Education, N202-052-32/1189.

### References

- [1] M. Moreno, B. Jenichen, V.M. Kaganer, W. Braun, L.A. Trampert, L. Daueritz, K. Ploog, "Micromechanics of MnAs nanocrystals embedded in GaAs", *Phys. Rev. B* **67** (2003) 235206-1.
- [2] A. Panchula, C. Kaiser, A. Kellock, S.S. Parkin, "Spin polarization and magnetotransport of Mn-Sb alloys in magnetic tunnel junction", *Appl. Phys. Lett.* **83** (2003) 1812.
- [3] H. Akinaga, K. Tanaka, K. Ando, T. Kontayama, "Fabrication and magneto-optical properties of epitaxial ferromagnetic  $\text{Mn}_{1-x}\text{Sb}$  thin films grown on GaAs and sapphire", *J. Cryst. Growth* **150** (1995) 1144.

# DEFECT STRUCTURE OF CZOCHRALSKI GROWN NITROGEN DOPED SILICON ANNEALED UNDER ENHANCED PRESSURE

**A. Misiuk<sup>1</sup>, W. Wierzchowski<sup>2</sup>, K. Wieteska<sup>3</sup>, J. Bak-Misiuk<sup>4</sup>, B. Surma<sup>2</sup>, A. Wnuk<sup>2</sup>, C.A. Londos<sup>5</sup>, Deren Yang<sup>6</sup>, and W. Graeff<sup>7</sup>**

<sup>1</sup>*Institute of Electron Technology, Al. Lotników 46, 02-668 Warsaw, Poland*

<sup>2</sup>*Institute of Electronic Materials Technology, 01-919 Warsaw, Poland*

<sup>3</sup>*Institute of Atomic Energy, 05-400 Otwock-Świerk, Poland*

<sup>4</sup>*Institute of Physics, PAS, Al. Lotników 32/46, 02-668 Warsaw, Poland*

<sup>5</sup>*University of Athens, Athens 15784, Greece*

<sup>6</sup>*State Key Laboratory of Silicon Materials, Hangzhou 310027, China*

<sup>7</sup>*HASYLAB at DESY, D-22603 Hamburg, Germany*

*Keywords:* silicon, defect structure, topography, diffraction

Microdefects and their distribution in oxygen-containing Czochralski grown silicon (Cz-Si) are strongly influenced by the presence of nitrogen [1]. Annealing of nitrogen-doped Cz-Si:N at high temperatures (HT) results, first of all, in precipitation of oxygen interstitials, O<sub>i</sub>'s, also dependent on hydrostatic pressure (HP) applied at processing [2].

The defect structure of Cz-Si:N samples with N concentration,  $c_N \leq 5 \times 10^{14} \text{ cm}^{-3}$ , was investigated in this work after processing 2 mm thick Cz-Si:N samples at HT  $\leq 1400 \text{ K}$  under HP  $\leq 1.1 \text{ GPa}$ . About 150  $\mu\text{m}$  thick near-surface layer was removed after processing from the Cz-Si:N surface by chemical polishing.

The defect structure of Cz-Si:N was investigated by synchrotron diffraction topography at the F1 and E2 experimental stations of the DORIS III synchrotron in HASYLAB (Germany). White and monochromatic ( $\lambda = 0.1115 \text{ nm}$ ) beam topographic methods in the Bragg geometry were used. Section topography (with the application of a fine 5  $\mu\text{m}$  slit and glancing angle of 5°) enabled indication of volume character of the defect distribution. High sensitivity to strains associated with small inclusions and dislocation loops was provided by monochromatic beam topography.

Also high resolution X-ray diffraction (recording the  $\omega$  and  $2\theta/\omega$  scans in the triple axis configuration of diffractometer), photoluminescence and IR absorption methods were used during our research.

Nitrogen admixture prevents formation of extended defects at processing done under  $10^5 \text{ Pa}$ . Such defects are created, however, in Cz-Si:N processed at first at 920 K under  $10^5 \text{ Pa}$  (to create nucleation centres for oxygen precipitation) and next at 1270 K / 1400 K under HP.

Annealing of nitrogen doped Czochralski grown silicon at 1230–1400 K under HP results in a creation of specific structure; numerous oxygen- and/or nitrogen-containing clusters are created. Investigation of the temperature–pressure effects in nitrogen-doped Cz-Si contributes in understanding the role of nitrogen in doped silicon considered for application in microelectronics.

## References

- [1] M. Kulkarni, "Defect dynamics in the presence of nitrogen in growing Czochralski silicon crystals", *J. Cryst. Growth* **310** (2008) 324.
- [2] A. Misiuk, B. Surma, Deren Yang, M. Pruszczyk, "Stress dependent structure of annealed nitrogen-doped Cz-Si", *Mater. Sci. Engn. B* **134** (2006) 218.

## MODIFICATION OF THE SURFACE MORPHOLOGY BY ULTRA SHORT PULSES OF XUV FREE ELECTRON LASER

**D. Klinger<sup>\*1</sup>, R. Sobierajski<sup>1,8</sup>, M. Jurek<sup>1</sup>, J. Krzywinski<sup>1,5</sup>, J.B. Pelka<sup>1</sup>, D. Żymierska<sup>1</sup>,  
J. Chalupský<sup>2,3</sup>, L. Juha<sup>2</sup>, V. Hájková<sup>2</sup>, J. Cihelka<sup>2</sup>, T. Burian<sup>2,3</sup>, L. Vyšín<sup>2,3</sup>, H. Wabnitz<sup>4</sup>,  
K. Tiedtke<sup>4</sup>, S. Toleikis<sup>4</sup>, T. Tschenetscher<sup>4</sup>, R. London<sup>5</sup>, S. Hau-Riege<sup>5</sup>,  
K. Sokolowski-Tinten<sup>6</sup>, N. Stojanovic<sup>6</sup>, J. Hajdu<sup>7</sup>, A.R. Khorsand<sup>8</sup>, and A.J. Gleeson<sup>9</sup>**

<sup>1</sup>*Institute of Physics, Polish Academy of Sciences, Al. Lotników 32/46, PL-02-668 Warsaw, Poland*

<sup>2</sup>*Institute of Physics, Czech Academy of Sciences, Na Slovance 2, 182 21 Prague 8, Czech Republic*

<sup>3</sup>*Czech Technical University in Prague, Brehova 7, 115 19 Praha 1, Czech Republic*

<sup>4</sup>*Deutsches Elektronen-Synchrotron DESY, Notkestrasse 85, D-22603 Hamburg, Germany*

<sup>5</sup>*Lawrence Livermore National Laboratory, 7000 East Avenue, CA 94550 Livermore, USA*

<sup>6</sup>*University of Duisburg-Essen, D-45117 Essen, Germany*

<sup>7</sup>*Uppsala University, SE-75124 Uppsala, Sweden*

<sup>8</sup>*FOM-Institute for Plasma Physics Rijnhuizen, P.O. Box 1207, 3430 BE Nieuwegein, The Netherlands*

<sup>9</sup>*CCRLC Daresbury Laboratory, Warrington, Cheshire, WA4 4AD, UK*

*Keywords: dielectrics, laser processing, XUV free electron laser, material modification,  
laser ablation, fused silica*

\*) e-mail: kling@ifpan.edu.pl

The investigations of the interaction of ultra short laser pulse with dielectric materials realised in the last decade have lead to better clarity of the interaction mechanism by studying the influence of the pulse duration [1-6] and the material [7-10] on the ablation threshold. The differences in the results demonstrate that many questions referred to ablation of dielectric materials by ultra short pulses remain open as before.

In this work we present a research of ablation in fused silica which is the most widely studied dielectric material. Structural modifications were induced with the intense XUV femtosecond pulses generated by the TESLA test facility free electron laser (TTF FEL) at DESY, Hamburg. The investigated samples were irradiated during a few following phases of the experiment with different wavelength (32 nm, 13.2 nm, and 7 nm) of the laser radiation. Effects of the laser ablation were studied by means of the interference-polarizing microscopy using the Nomarski reflection contrast. A size and shape as well as morphological forms occurring in the formed craters were analysed as a function of the irradiation fluency. Obtained results were compared with available literature data.

**Acknowledgements:** This work was supported in part by the Ministry of Science and Higher Education (Poland) under special research project No. DESY/68/2007.

### References

- [1] M. Lenzner, "Femtosecond laser-induced damage of dielectrics," *Int. J. Mod. Phys. B* **13** (1999) 1559–1578.
- [2] An-Chun Tien, S. Backus, H. Kapteyn, M. Murnane, G. Mourou, "Short-pulse laser damage in transparent materials as a function of pulse duration," *Phys. Rev. Lett.* **82** (1999) 3883–3886.
- [3] D. Du, X. Liu, G. Korn, J. Squier, G. Mourou, "Laser-induced breakdown by impact ionisation in SiO<sub>2</sub> with pulse widths from 7 ns to 150 fs," *Appl. Phys. Lett.* **64** (1994) 3071–3073.
- [4] B.C. Stuart, M.D. Feit, A.M. Rubenchik, B.W. Shore, M.D. Perry, "Laser-induced damage in dielectrics with nanosecond to subpicosecond pulses," *Phys. Rev. Lett.* **74** (1995) 2248–2251.
- [5] A. Rosenfeld, M. Lorenz, D. Ashkenasi, P. Rudolph, J. Kueger, W. Kautek, "Femtosecond- and nanosecond-pulse laser ablation of bariumalumoborosilicate glass," *Appl. Phys. A* **69** (1999) 759–761.
- [6] T.Q. Jia, Z.Z. Xu, R.X. Li, D.H. Feng, X.X. Li, C.F. Cheng, H.Y. Sun, N.S. Xu, H.Z. Wang, "Formation of nanogratings on the surface of a ZnSe crystal irradiated by femtosecond laser pulses," *Phys. Rev. B* **72** (2005) 1254291–1254294.
- [7] D. von der Linde, H. Schueler, "Breakdown threshold and plasma formation in femtosecond laser-solid interaction," *J. Opt. Soc. Am. B* **13** (1996) 216–222.
- [8] K. Sokolowski-Tinten, J. Bialkowski, M. Boing, A. Cavalleri, D. von der Linde, "Thermal and nonthermal melting of gallium arsenide after femtosecond laser excitation," *Phys. Rev. B* **58** (1998) 805–807.
- [9] I.H. Chowdhury, A.Q. Wu, X. Xu, A.M. Weiner, "Ultra-fast laser absorption and ablation dynamics in wide-band-gap dielectrics," *Appl. Phys. A* **81** (2005) 1627–1632.
- [10] K. Sokolowski-Tinten, J. Bialkowski, A. Cavalleri, D. von der Linde, A. Oparin, J. Mejer-ter-Vehn, S.I. Anisimov, "Transient states of matter during short pulse laser ablation," *Phys. Rev. Lett.* **81** (1998) 224–227.

# STRUCTURE REFINEMENT OF DECAGONAL QUASICRYSTAL

**P. Kuczera<sup>1</sup>, B. Kozakowski<sup>1</sup>, J. Wolny<sup>1\*</sup>, and R. Strzałka<sup>1</sup>**

<sup>1</sup>Faculty of Physics and Applied Computer Science, AGH-University of Science and Technology,  
al. Mickiewicza 30, 30-059 Kraków, Poland

*Keywords:* structure, decagonal quasicrystals

\*) e-mail: wolny@novell.ftj.agh.edu.pl

For the last several years, the structure of basic Ni-rich decagonal Al-Ni-Co quasicrystal has been thoroughly examined by many scientists [1-2]. Their work resulted in some outstanding structural descriptions of this quasicrystal. The majority of published papers focused however on a higher-dimensional approach i.e. the atomic surface modelling method. We present the results of a real space structure refinement of the basic Ni-rich decagonal phase based on a diffraction data set, without referring to the higher-dimensional properties of decagonal quasicrystals.

The structure factor, which was used for the modelling process, was calculated on the basis of a statistical method described briefly in Ref. [3]. Statistical approach allows a purely 3-dimensional, real space optimization of a quasicrystalline structure. The decagonal basic Ni-rich phase is known to consist of aperiodic planes stacked periodically along the quasi-tenfold axis (*c*-axis). There are two planes within one period of the *c* axis. We assumed, that the projection of these two planes along the *c*-axis results in Penrose tiling. The rhombuses of Penrose tiling are divided three times with obedience to the inflation rules. The idealized positions of atoms are the points of subsequent divisions. We also put several atoms in the positions of the fourth division to fulfil the density restriction. There are 71 atoms decorating our structure units. They are divided into groups according to the overlapping rules for kite-clusters [4]. A shift from ideal position, anisotropic Debye-Waller factor, occupation probability and concentration of TM atom are refined. For some groups however some parameters are fixed. We obtained *R*-factor at the level of 12% and *R<sub>w</sub>*-factor of 6%. The resulting structure has the chemical composition, point density and overall density values very close to the experimental ones. The optimization was performed on a set of averaged and corrected 2767 diffraction peaks taken by a four-circle diffractometer at beamline D3 HASYLAB [1].

**Acknowledgements:** The authors are grateful to Prof. Walter Steurer (ETH Zuerich) for the diffraction data set.

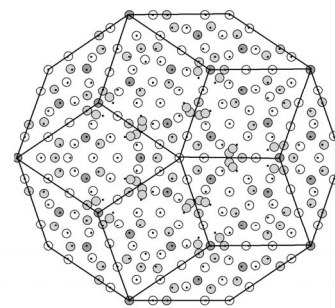


Figure 1. A projection of the refined structure along the periodic axis. Dark grey, light grey and white circles are TM, Al/TM, Al atoms respectively. Black dots indicate ideal Penrose tiling positions.

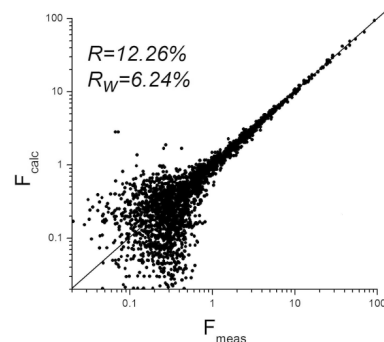


Figure 2. The  $F_{\text{meas}}/F_{\text{calc}}$  plot.

## References

- [1] A. Cervellino, T. Haibach, W. Steurer, "Structure solution of basic decagonal Al-Co-Ni phase by the atomic surface modelling method", *Acta Cryst. B* **58** (2002) 8–33.
- [2] H. Takakura, A. Yamamoto, A.P. Tai, "The structure of Decagonal Al<sub>72</sub>Ni<sub>20</sub>Co<sub>8</sub> quasicrystal", *Acta Cryst. A* **57** (2001) 576–585.
- [3] B. Kozakowski, J. Wolny, "Decorated quasicrystals and their diffraction patterns", *Phil. Mag.* **86** (2006) 549–555.
- [4] M. Duda, B. Kozakowski, J. Wolny, "Penrose structures described by different kite-clusters", *J. Non-Cryst. Solids* **353** (2007) 2500–2505.

## MICROSPECTROMETRIC STUDY OF INTERNAL STRUCTURE OF DENTIN-ENAMEL BOUNDARY (DEJ) IN MOLAR TEETH

**J. Nowak<sup>1\*</sup>, R. Chalas<sup>2</sup>, J. Lekki<sup>3</sup>, and A. Kuczumow<sup>1</sup>**

<sup>1</sup> Department of Chemistry, John Paul II Catholic University of Lublin,  
Al. Krasnicka 102, 20-718 Lublin, Poland

<sup>2</sup> Department of Conservative Dentistry, Medical University of Lublin,  
ul. Karmelicka 7, 20-081 Lublin, Poland

<sup>3</sup> Department of Nuclear Spectroscopy, Niewodniczanski Institute of Nuclear Physics,  
ul. Radzikowskiego 152, 31-342 Krakow, Poland

*Keywords:* microanalysis, phase junction; inorganic + organic components

\*) e-mail: nowakj@kul.lublin.pl

Dentin-enamel junction (DEJ) is unique interface of two natural phases: dentin and enamel in teeth. The studied matrix is generally composed of hydroxyapatite, although in uneven concentrations (up to 97% in enamel while up to 70 % in dentin) and of different structure (greater rod-like crystallites in enamel while ball-like smaller crystallites in dentin) with additions of different organic compounds with main contribution of collagen, essentially in dentin. Due to such composition, the recognition of the space distribution of components is difficult. Using the combination of microspectral methods (X-ray and PIXE) for the determination of inorganic components has to be supplemented with the application of Raman microscope for the recognition

of organic components and it is shown in Fig. 1. The latter method in advanced version permits to locate the area of crystal reorganization. The data are superimposed on the optical image to join the chemical results to the morphological details. Recent study is performed on the teeth of humans, African buffalo and extinct shark. For comparison, the PIXE and optical results for dog, sheep, horse are added.

Beyond the aim to recognize the DEJ structure as strictly as possible, the more far-reaching aim is to have the basis for the biomimetic reconstruction of the junction, also with the manufacturing of the smart dentistic fillings and implants.

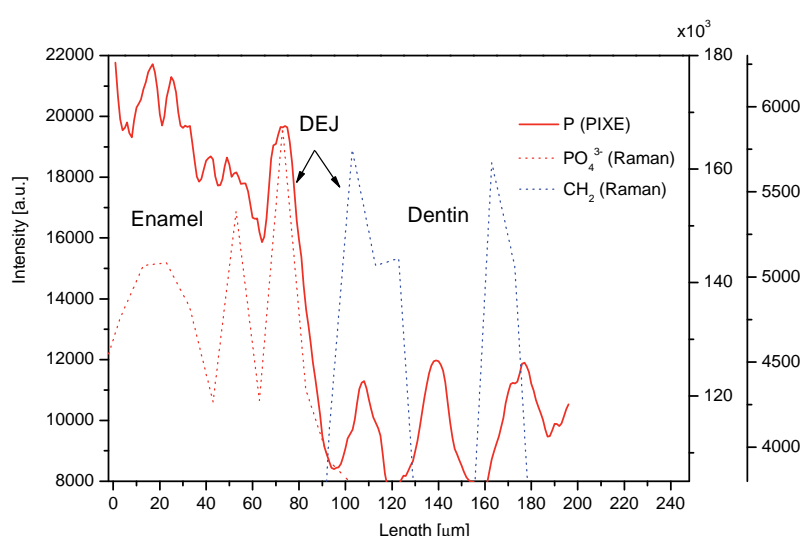


Figure 1. Visualization of DEJ with Raman microscopy (oscillation  $\nu_1$   $981\text{ cm}^{-1}$ ) for  $\text{PO}_4^{3-}$  and  $2900\text{ cm}^{-1}$  for  $\text{CH}_2$  and complementary partial visualization with PIXE –  $\text{PK}_{\alpha 1}$  signal.

# STRUCTURAL PROPERTIES OF $(\text{Mn}_{1-x}\text{Fe}_x)_2\text{O}_3$ SOLID SOLUTIONS

**W. Nowicki<sup>1\*</sup>, J. Darul<sup>1</sup>, P. Piszora<sup>1</sup>, and D. Trots<sup>2</sup>**

<sup>1</sup> Department of Materials Chemistry, Faculty of Chemistry, Adam Mickiewicz University, Grunwaldzka 6, PL-60780 Poznań, Poland

<sup>2</sup> Synchrotronstrahlungslabor HASYLAB at DESY, Notkestrasse 85, D-22603 Hamburg, Germany

*Keywords:* transition-metal oxides, preparation, crystal structure refinement

\*) e-mail: waldek@amu.edu.pl

Manganese-iron oxides with bixbyite structure are an active field of research, because there are technologically important materials with unusual physical properties [1, 2, 3]. Earlier studies showed that a solid state solution exists for the system  $(\text{Mn}_{1-x}\text{Fe}_x)_2\text{O}_3$  with  $0 \leq x \leq 0.6$  [4, 5].

The samples of composition  $(\text{Mn}_{1-x}\text{Fe}_x)_2\text{O}_3$  with the range of  $0.0 \leq x \leq 0.3$ , were synthesized by coprecipitation of amorphous manganese-iron-hydroxides from the mixed  $\text{Mn}^{2+}/\text{Fe}^{3+}$ -nitrate solutions of the mole ratio of  $n_{\text{Fe}} = \text{Fe}/(\text{Fe}+\text{Mn}) = 0.0, 0.1, 0.2$  and 0.3, with sodium hydroxide. Washed and dried at the room temperature, they were dehydrated for 2 h at 250°C, and then underwent the thermal treatment in air, successively at 400°C, 500°C and 600°C for 4 h. After heating, the preparations were cooled slowly to the room temperature, at a rate of about 20–30°C per hour, during 24 h.

The X-ray diffraction experiments were carried out at the Desy/Hasylab high-resolution powder diffractometer at the beamline B2, equipped with Image Plate OBI detector [6, 7]. The wavelength, determined by calibration using NIST standard, was  $\lambda = 0.49602 \text{ \AA}$ . Full patterns were collected at room temperature in the 2-theta range of 4.0° – 60.0°, with a step size of 0.004°. The structure refinements were performed using the FullProf program [8].

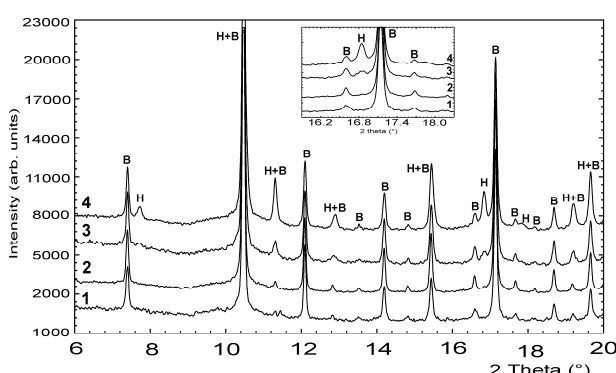


Figure 1. Experimental X-ray powder diffraction patterns of 1.  $\text{Mn}_2\text{O}_3$  ( $n_{\text{Fe}} = 0.0$ ), 2.  $\text{Mn}_{1.8}\text{Fe}_{0.2}\text{O}_3$  ( $n_{\text{Fe}} = 0.1$ ), 3.  $\text{Mn}_{1.6}\text{Fe}_{0.4}\text{O}_3$  ( $n_{\text{Fe}} = 0.2$ ) and 4.  $\text{Mn}_{1.4}\text{Fe}_{0.6}\text{O}_3$  ( $n_{\text{Fe}} = 0.3$ ) oxides, recorded at the room temperature, (B – bixbyite phase, H – hematite phase).

The preliminary studies have shown single crystalline phase with bixbyite structure only up to the first compound with the iron ions,  $\text{Mn}_{1.8}\text{Fe}_{0.2}\text{O}_3$  ( $n_{\text{Fe}} = 0.1$ ). Furthermore, at higher iron concentrations, second different phase of hematite-like structure was found. The X-ray diffraction patterns of these samples are shown in Fig. 1. An example of two-phase system fitting for the  $\text{Mn}_{1.6}\text{Fe}_{0.4}\text{O}_3$  ( $n_{\text{Fe}} = 0.2$ ) pattern is presented in Fig. 2.

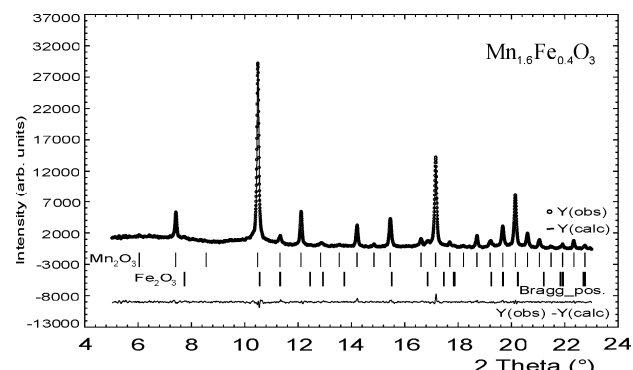


Figure 2. Rietveld refinement pattern of the  $\text{Mn}_{1.6}\text{Fe}_{0.4}\text{O}_3$  ( $n_{\text{Fe}} = 0.2$ ) oxide for the XRD data measured at room temperature.

**Acknowledgements:** The synchrotron measurements at HASYLAB were supported by the IA-SFS-Contract No. RII3-CT-2004-06008 of European Commission.

## References

- [1] M. Regulski, R. Przeniosło, I. Sosnowska, D. Hohlwein, R. Schneider, *J. Alloys Compds.* **362** (2004) 236–240.
- [2] S.N. de Medeiros, A. Luciano, L.F. Cótica, I.A. Santos, A. Paesano, Jr., J.B.M. da Cunha, *J. Magn. Magn. Mater.* **281** (2004) 227–233.
- [3] D. Saha, A. Das Sharama, A. Sen, H.S. Maiti, *Mater. Lett.* **55** (2002) 403–406.
- [4] S. Geller, *Acta Cryst.* **B27** (1971) 821–828.
- [5] R.W. Grant, S. Geller, J.A. Cafe, G.P. Espinosa, *Phys. Rev.* **175** (1968) 686–695.
- [6] M. Knapp, J. Joco, C. Baethz, H.H. Brecht, A. Berghaeuser, H. Ehrenberg, H. von Seggern, H. Fuess, *Nucl. Instr. Meth. Phys. Res. A* **521** (2004) 565–570.
- [7] M. Knapp, C. Baethz, H. Ehrenberg, H. Fuess, *J. Synchrotron Rad.* **11** (2004) 328–334.
- [8] J. Rodriguez-Carvajal, *Physica B* **192** (1993) 55–69.

## LOCAL STRUCTURE OF Mn IN $(La_{1-x}Ho_x)_{2/3}Ca_{1/3}MnO_3$ USING X-RAY ABSORPTION FINE STRUCTURE

**A. Pietnoczka<sup>1\*</sup>, R. Bacewicz<sup>1</sup>, M. Pękała<sup>2</sup>, V. Drozd<sup>3</sup>,  
W. Zalewski<sup>1</sup>, and J. Antonowicz<sup>1</sup>**

<sup>1</sup> Faculty of Physics, Warsaw University of Technology, ul. Koszykowa 75, 00-662 Warsaw, Poland

<sup>2</sup> Department of Chemistry, University of Warsaw, Al. Zwirki i Wigury 101, PL-02-089 Warsaw 22, Poland

<sup>3</sup> Center for Study Matter at Extreme Conditions, Florida International University, Miami, USA

*Keywords:* XAFS, local structure, manganite

\*) e-mail: pietnoczka@if.pw.edu.pl

Manganese perovskite-based oxides have attracted a renewed interest due to their unusual colossal magnetoresistance CMR. They exhibit a great variety of magnetic and transport properties that strongly depend on the stoichiometry and the structure of the materials.

The  $La_{1-x}Ca_xMnO_3$  is one of the most thoroughly studied manganites. The pure compounds like  $LaMnO_3$  and  $CaMnO_3$  are antiferromagnetic insulators. When  $LaMnO_3$  is doped with a divalent element such as  $Ca^{2+}$ , substituting for  $La^{3+}$ , holes are introduced in the filled Mn *d* orbitals, which leads to strong ferromagnetic coupling between Mn sites. Ca ions in  $La_{1-x}Ca_xMnO_3$  introduce crystal lattice distortion and mixed valence Mn ions ( $Mn^{3+}$  and  $Mn^{4+}$ ). Compounds in the doping range  $0.2 < x < 0.5$  show both ferromagnetic and metallic behavior, together with colossal magnetoresistance effect near the Curie temperature. The highest value of  $T_c = 270$  K has been obtained for  $La_{2/3}Ca_{1/3}MnO_3$  [1].

In this study we present results of the X-ray Absorption Fine Structure (XAFS) measurements in manganites  $(La_{1-x}Ho_x)_{2/3}Ca_{1/3}MnO_3$  in the doping range  $0.15 < x < 0.50$ . Substitution of La for Ho without varying the proportion of  $Mn^{3+}$  to  $Mn^{4+}$  changes the local lattice

distortion due to a difference in atomic size which alters the Curie temperature. This deformation influences the Mn-O-Mn angle, which is the parameter that determines the magnetic and transport properties in these compounds. Thus, the determination of the local atomic structure around Mn ions plays a crucial role in understanding of the Ho doping effect.

Manganese K-edge absorption has been measured by the transition method at HASYLAB synchrotron facility in Hamburg (E4 beamline). EXAFS data analysis provides information on the local structure around Mn (the bond lengths, the coordination numbers and Debye-Waller factor). The charge state of Mn is determined from the XANES data. Also an attempt to find the Mn-O-Mn angle is made. XAFS results are in good agreement with the magnetic characteristics of the studied materials.

### References

- [1] G. Subias, J. Garcia, J. Blasco, M. Conception Sanchez, M. Grazia Proietti, *J. Phys.: Condens. Matt.* **14** (2002) 5017–5033.

## DIFFRACTION HP/HT STUDY OF $\text{LiMn}_2\text{O}_4$

**P. Piszora<sup>1\*</sup>, J. Darul<sup>1</sup>, W. Nowicki<sup>1</sup>, and C. Lathe<sup>2</sup>**

<sup>1</sup> Department of Materials Chemistry, Faculty of Chemistry, Adam Mickiewicz University, Grunwaldzka 6, 60-780 Poznan, Poland

<sup>2</sup> GeoForschungsZentrum Potsdam, Telegrafenberg A17, D-14473 Potsdam, Germany

**Keywords:** lithium-manganese oxide, lithium-ion batteries, high pressure

\*) e-mail: pawel@amu.edu.pl

Rechargeable lithium batteries with lithium-manganese spinel as a cathode material are state-of-the-art power sources for consumer electronics and automotive applications [1]. Knowledge of the properties of the lithium-manganese oxides under the conditions of high temperatures and pressures is of fundamental concern to solid-state chemistry and is important for the battery materials manufacturing. The *in-situ* high-pressure experiment, performed on  $\text{LiMn}_2\text{O}_4$  with the energy-dispersive multi-anvil setup, have revealed cubic to tetragonal phase transition of  $\text{LiMn}_2\text{O}_4$  [2]. The effect of a hydrostatic pressure on the crystal structure of  $\text{LiMn}_2\text{O}_4$  has been studied by measuring the X-ray diffraction pattern along three isotherms at 350, 385 and 415 K [3], whereas pressure has been obtained with a diamond anvil cell in the range between 0 and 20 GPa. At the pressure of 1.8 GPa and at 350 K the cubic→orthorhombic phase transition, similar to that observed during cooling of  $\text{LiMn}_2\text{O}_4$ , has been reported, nevertheless the nature of this transition seemed to be not clear. Rietveld refinement of the X-ray diffraction pattern collected of the  $\text{LiMn}_2\text{O}_4$  sample mounted in a diamond-anvil cell revealed that the high-pressure polymorphs have tetragonal structures ( $F4_1/ddm$ ) [4]. However, it has been also observed by Paolone *et al.* [3] that at ~10 GPa and at 415 K,  $\text{LiMn}_2\text{O}_4$  transformed into a new phase,

which persisted also when the external pressure was released. The high-pressure high-temperature structure of lithium manganese oxide has been studied *ex-situ* by X-ray diffraction method after compression at 6 GPa and heating above 1373 K [5]. The new  $\text{CaFe}_2\text{O}_4$ -type ( $Pnma$ ) structure of the lithium-manganese oxide, stable at ambient condition, has been reported.

$\text{LiMn}_2\text{O}_4$  sample was obtained by the solid state reaction of  $\text{Mn}_2\text{O}_3$  with  $\text{Li}_2\text{CO}_3$  at 1073 K. The phase transitions in  $\text{LiMn}_2\text{O}_4$  were investigated at high pressure and high temperature (HP/HT) up to 4 GPa and 1500 K with *in-situ* X-ray diffraction measurements at the synchrotron beamline F2.1 (DESY/HASYLAB).

The cubic ( $Fd3m$ ) lithium-manganese spinel transforms to the tetragonal phase ( $F4_1/ddm$ ) at 3 GPa and 300 K. The tetragonal phase transforms again to a cubic HP/HT structure at about 4 GPa and at 648 K. Some new additional diffraction peaks were observed at about 4 GPa and in the temperature region of 748 – 773 K. Subsequently, at 873 K diffraction lines from the spinel-like phase vanished and some new intense diffraction lines of the HP/HT phase can be observed. Neither  $\text{CaFe}_2\text{O}_4$ -type nor orthorhombic structures, previously proposed as HP or HP/HT phase, were observed in the applied pressure and temperature range.

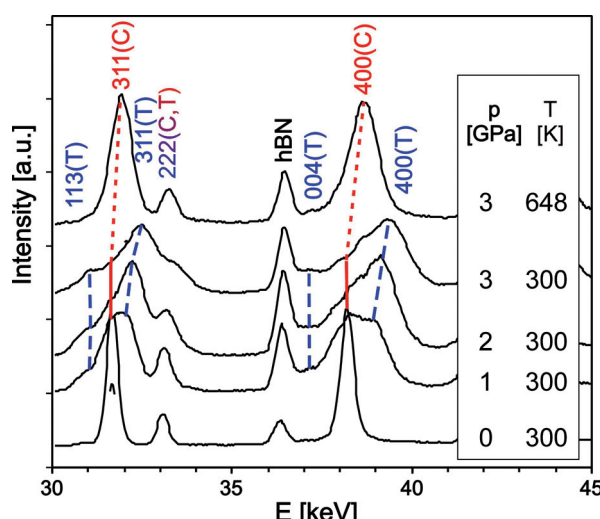


Figure 1. Section of the energy-dispersive X-ray diffraction pattern of  $\text{LiMn}_2\text{O}_4$  at varied pressure and temperature. C and T are for cubic ( $Fd3m$ ) phase and tetragonal phase with  $c/a > 1$  ( $F4_1/ddm$ ), respectively.

**Acknowledgements:** The authors are grateful for the support from the European Community - Research Infrastructure Action under the FP6 "Structuring the European Research Area" Programme (through the Integrated Infrastructure Initiative "Integrating Activity on Synchrotron and Free Electron Laser Science".) by DESY/HASYLAB (Contract RII3-CT-2004-506008).

### References

- [1] J.M. Tarascon, M. Armand, *Nature* **414** (2001) 359.
- [2] P. Piszora, Z. *Kistallogr. Suppl.* **26** (2007) 387.
- [3] A. Paolone, A. Sacchetti, P. Postorino, R. Cantelli, A. Congeduti, G. Rousse, C. Masquelier, *Solid State Ionics* **176** (2005) 635.
- [4] P. Piszora, W. Nowicki, J. Darul, *J. Mater. Chem.* **18** (2008) 2447.
- [5] K. Yamaura, Q. Huang, L. Zhang, K. Takada, Y. Baba, T. Nagai, Y. Matsui, K. Kosuda, E. Takayama-Muromachi, *J. Am. Chem. Soc.* **128** (2006) 9448.

## STRUCTURAL PROPERTIES OF HIGH-TEMPERATURE-GROWN GaMnSb / GaSb

**P. Romanowski<sup>1\*</sup>, J. Bak-Misiuk<sup>1</sup>, E. Dynowska<sup>1</sup>, J. Sadowski<sup>1,2</sup>,  
T. Wojciechowski<sup>1</sup>, A. Barcz<sup>1,3</sup>, R. Jakiel<sup>1</sup>, and W. Caliebe<sup>4</sup>**

<sup>1</sup> Institute of Physics, Polish Academy of Sciences, al. Lotników 32/46, PL-02668 Warsaw, Poland

<sup>2</sup> Lund University, MAX-lab, Ole Romers vag 1, SE-22363 Lund, Sweden

<sup>3</sup> Institute of Electron Technology, al. Lotników 32/46, PL-02668 Warsaw, Poland

<sup>4</sup> HASYLAB at DESY, Notkestr. 85, D-22603 Hamburg, Germany

*Keywords:* GaMnSb, X-rays, synchrotron, diffraction, XRD, SIMS, SEM, MBE

\*) e-mail: Przemyslaw.Romanowski@ifpan.edu.pl

GaMnSb is considered as one of the materials useful for spintronics. Especially much interest received the ferromagnetic ordering related to the MnSb inclusions produced during high-temperature growth of GaMnSb films [1, 2]. The aim of this work is to determine structural properties of this material, in dependence on different content of manganese.

To achieve the creation of ferromagnetic precipitates, investigated  $\text{Ga}_{1-x}\text{Mn}_x\text{Sb}$  layers were grown on GaSb(100) substrate, using the MBE technology. Epitaxial growth was performed at high temperature equal to 720 K. The thickness of  $\text{Ga}_{1-x}\text{Mn}_x\text{Sb}$  layers was equal to 0.63  $\mu\text{m}$ . Three types of samples were investigated: GaMnSb-1, GaMnSb-3 and GaMnSb-7, with different Mn concentration (1%, 3% and 7% respectively).

Strain state and lattice parameter of  $\text{Ga}_{1-x}\text{Mn}_x\text{Sb}$  layers were studied using high-resolution diffractometer in double- and triple-axis configuration. Reciprocal space maps (RCMs) for symmetrical 004 and asymmetrical 224 reflection, as well as the rocking curves and  $2\theta/\omega$  diffraction patterns were registered. Polycrystalline phase was investigated using monochromatic synchrotron X-ray beam at W1 station in HASYLAB-DESY at Hamburg, applying the glancing incidence diffraction method ( $2\theta$  scan). To examine the depth profiles of Ga, Sb and Mn elements, secondary ion mass spectrometry (SIMS) measurements were performed. Also scanning electron microscopy (SEM) was used for probing the sample surface.

**Acknowledgements:** This work was partially supported by national grant of Polish Ministry of Science and High Education N202-052-32/1189.

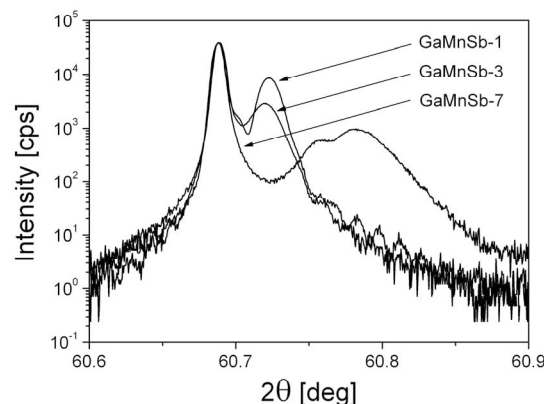


Figure 1.  $2\theta/\omega$  diffraction pattern of GaMnSb samples.

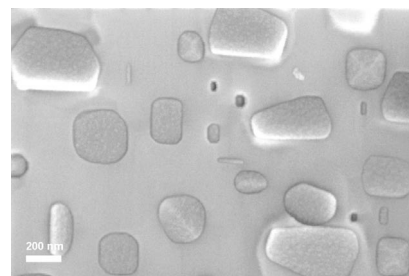


Figure 2. SEM image of GaMnSb-3 sample surface.

### References

- [1] K. Ganesan, H.L. Bhat, "Magnetic and magnetotransport properties of diluted magnetic semiconductor (Ga,Mn)Sb crystals", *J. Supercond. Novel Magn.* **21** (2008) 391–397.
- [2] W.L. Lim, T. Wojtowicz, X. Liu, M. Dobrowolska, J.K. Furdyna, "MBE growth and magnetotransport studies of ferromagnetic  $\text{Ga}_{1-x}\text{Mn}_x\text{Sb}$  semiconductor layers on hybrid ZnTe/GaAs substrates", *Physica E* **20** (2004) 346–349.

# XAFS STUDY AND CRYSTALLOGRAPHIC STRUCTURE OF Ti AND Y DOPED BaCeO<sub>3-δ</sub> PROTONIC CONDUCTORS

**P. Seremak-Peczkis**<sup>1\*</sup>, **W. Zajączkowski**<sup>1</sup>, **J. Przewoźnik**<sup>1</sup>, **Cz. Kapusta**<sup>1</sup>, **M. Sikora**<sup>1,2</sup>,  
**D.A. Zając**<sup>3</sup>, **P. Pasierb**<sup>4</sup>, **M. Bućko**<sup>4</sup>, and **M. Rękas**<sup>4</sup>

<sup>1</sup> AGH University of Science & Technology, Faculty of Physics & Applied Computer Science,  
Dept. of Solid State Physics, 30-059 Krakow, Poland

<sup>2</sup> European Synchrotron Radiation Facility, BP 220, 38043 Grenoble, France

<sup>3</sup> Hasylab at DESY, D22607 Hamburg, Germany

<sup>4</sup> AGH University of Science & Technology, Faculty of Materials Science & Ceramics, Krakow, Poland

*Keywords:* protonic conductors, barium cerate, synchrotron radiation, XAFS, XRD

\*) e-mail: seremak@agh.edu.pl

We report on the XAFS and XRD study of the titanium and yttrium doping influence on the evolution of the crystal structure of a new class of solid electrolytes, Ba(Ce<sub>1-x</sub>Ti<sub>x</sub>)<sub>(1-y)</sub>Y<sub>y</sub>O<sub>3-δ</sub> (0 ≤ x ≤ 0.3, 0 ≤ y ≤ 0.1) [1-3].

The compounds studied belong to the family of protonic conductive perovskites, which have potential applications in intermediate temperature fuel cells [4]. The undoped barium cerate is orthorhombic, while the increasing content of Ti dopant up to x = 0.2 leads to a tetragonal or even cubic structure. In the case of Y dopant an increase of ionic conductivity, which is desirable for applications, was observed. The long-term stability of barium cerate in atmospheres containing CO<sub>2</sub> can be improved by titanium addition, while the introduction of yttrium has the opposite effect.

In the present study the local ionic arrangement around the Ti, Y and Ce cations has been studied by means of X-ray absorption spectroscopy in the XANES (X-ray Absorption Near Edge Structure) region and in the EXAFS (Extended X-ray Absorption Fine Structure) region, and compared to the X-ray diffraction results.

The XANES spectra of BaCe<sub>1-x</sub>Ti<sub>x</sub>O<sub>3</sub> at the Ti K-edge show that up to x = 0.2 Ti occupies octahedral B sites in the perovskite structure with a gradual decrease of the symmetry of the environment of the Ti site. The doping at x = 0.3 corresponds to a symmetry of the Ti site possibly close to tetrahedral.

The XAFS spectra at the Ti K and Ce L<sub>2</sub> edges were collected in the transmission mode at ambient conditions at the X and A1 stations, while Y K-edge spectra were measured at room temperature (RT) and 10 K, using K<sub>α</sub> PFY (partial fluorescence yield) at the CEMO beamline of the HASYLAB/DESY synchrotron facility and at the ID26 beamline of the ESRF laboratory.

The cerium EXAFS spectra of the Ba<sub>1-y</sub>Ce<sub>1-x</sub>Y<sub>x</sub>O<sub>3</sub> series show that a larger amount of oxygen vacancies is created by Y doping than by Ba understoichiometry. The yttrium EXAFS reveals a possible location of some Y ions at the Ba sites. The dynamic Debye-Waller effect is

slightly stronger for the Ba stoichiometric sample than for the understoichiometric one.

The cerium EXAFS spectra were simulated for the first coordination shell in BaCeO<sub>3-δ</sub> (Fig. 1), using FEFF code.

The results are discussed and compared to the electrical transport properties of the materials.

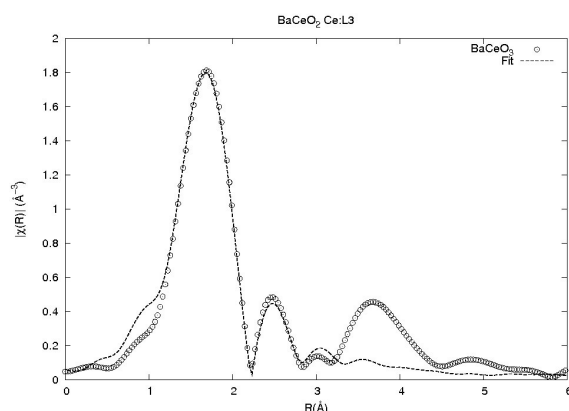


Figure 1. An example of the FEFF fit of the cerium first coordination shell in the *Pnma* structure.

**Acknowledgements:** This work was supported by the Polish Ministry of Science and Higher Education, Projects no. PBZ/MEiN/01/2006/57 and R15 019 02.

## References

- [1] P. Pasierb, E. Drożdż-Cieśla, M. Rękas, *J. Power Sources* **181** (2008) 17.
- [2] P. Pasierb, M. Wierzbicka, S. Komornicki, M. Rekas, *J. Power Sources* (2009) DOI:10.1016/j.jpowsour.2009.01.098.
- [3] P. Pasierb, E. Drożdż-Cieśla, R. Gajerski, S. Łabuś, S. Komornicki, M. Rękas, *J. Thermal Anal. Calorim.* (2009) DOI: 10.1007/s10973-008-9829-x.
- [4] H. Iwahara, T. Esaka, H. Uchida, N. Maeda, *Solid State Ionics* **34** (1981) 359.

## XAFS STUDY OF $\text{ZrO}_2$ -BASED SOFC MATERIALS

**J. Stepien<sup>1\*</sup>, J. Śliwińska<sup>1</sup>, J. Przewoźnik<sup>1</sup>, K. Schneider<sup>1</sup>, Cz. Kapusta<sup>1</sup>, D. Zajac<sup>2</sup>, K. Michałów<sup>3</sup>, D. Pomykalska<sup>3</sup>, M. Bućko<sup>3</sup>, and M. Rękas<sup>3</sup>**

<sup>1</sup> AGH University of Science and Technology, Faculty of Physics and Applied Computer Science,  
Dept. Solid State Phys., Al. Mickiewicza 30, 30-059 Krakow, Poland

<sup>2</sup> Hasylab at DESY, D22607 Hamburg, Germany

<sup>3</sup> AGH University of Science and Technology, Faculty of Material Science and Ceramics,  
Al. Mickiewicza 30, 30-059 Krakow, Poland

**Keywords:** stabilised zirconia solid solution, synchrotron radiation, XAFS, solid oxide fuel cell

\*) e-mail: jstepien@agh.edu.pl

A XAFS study of yttrium stabilized manganese doped zirconia solid solutions is presented. The materials are promising candidates for intermediate layers between electrolyte and cathode in solid oxide fuel cells. Presence of manganese in the zirconia solid solution is expected to bring about electronic conductivity owing to the formation of electron defects at manganese ions. In consequence, the resistance for charge transfer between electrolyte and cathode would be reduced.

Powder samples of  $\text{Mn}_x(\text{Y}_{0.08}\text{Zr}_{0.92})_{1-x}\text{O}_{2-\delta}$  ( $0 < x < 0.25$ ) used for XAFS study were prepared by co-precipitation-calcination method and then sintered for 2 h at  $1500^\circ\text{C}$ . The dependence of the lattice parameters on  $x$  follows the Vegard rule from zero to about 18 mol.% of manganese where the cubic zirconia structure of the solid solution is preserved.

The measurements have been carried out in Hasylab/DESY, Hamburg, in the XANES (X-ray Absorption Near Edge Structure) and EXAFS (Extended X-ray Absorption Fine Structure) ranges at the manganese and yttrium K edges at room temperature and at 10 K. The XANES spectra at the Mn K edge are presented in Fig. 1.

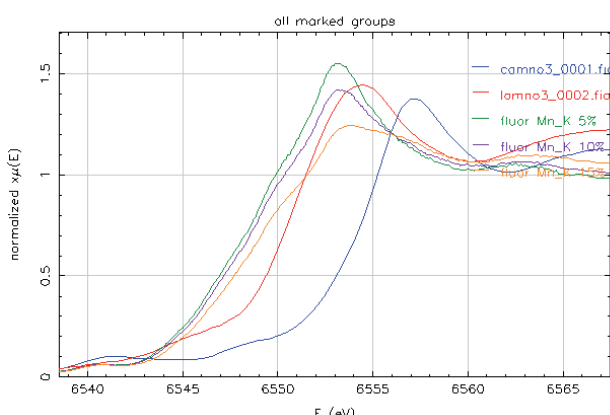


Figure 1. XANES spectra of Mn:K edge of yttrium stabilised zirconia oxide doped with 5, 10 and 15% of manganese.

The absorption edge energies of the samples studied derived from the spectra were compared to those of the reference samples. Assuming a linear dependence between the valence and the edge energy, the valences of Mn in the samples studied were obtained. They are collected in the table below and show that the Mn average oxidation degree is between +2 and +3. It increases with increasing manganese content.

Sample	Edge energy [eV]	Average oxidation
5% Mn	6547.0	$2.44 \pm 0.02$
10% Mn	6547.2	$2.47 \pm 0.02$
15% Mn	6547.7	$2.60 \pm 0.02$

Fourier transforms of EXAFS spectra obtained at the Y K edge are presented in Fig. 2. They show significant changes with Mn content in the second coordination shell ( $3.6 \text{ \AA}$ ) corresponding to metal ions, whereas only slight modifications in the first coordination shell ( $2.1 \text{ \AA}$ ) corresponding to oxygen neighbours is found.

**Acknowledgements:** This work was supported by the Polish Ministry of Science and Higher Education, Projects no. PBZ/MEiN/01/2006/57 and R15 019 02.

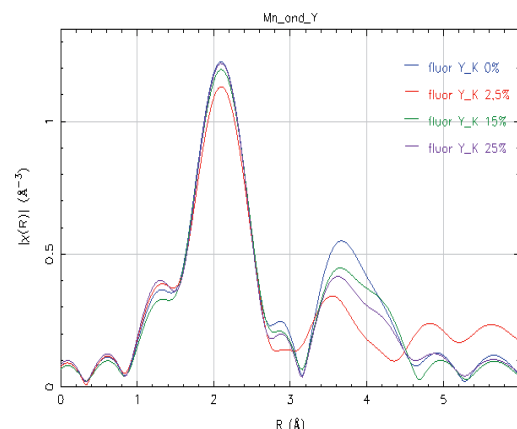


Figure 2. Fourier transforms of the EXAFS spectra obtained at the Y K edge at room temperature for the zirconia oxide doped with 2.5%, 15% and 25% Mn.

# THE SIMULATION OF BRAGG-CASE SECTION IMAGES OF DISLOCATIONS AND INCLUSIONS IN ASPECT OF IDENTIFICATION OF DEFECTS IN SiC CRYSTALS

**T. Balcer**<sup>1\*</sup> and **W. Wierzchowski**<sup>1</sup>

<sup>1</sup> Institute of Electronic Materials Technology, ul. Wolczynska 131, 01-919 Warsaw, Poland

*Keywords:* dislocation, rod-like inclusion, micro-pipes, numerical simulation, SiC

Bragg-case section topography is the important method of X-ray diffraction topography allowing to reveal fine details of strains defects thanks to appearing of the interference effects. It also provides the possibility of effective simulation of the images of topographical defects based on the numerical integration of the Takagi equations. The formation of contrast in the method seems to be equivalent to the diffraction of the spherical wave from a certain number of closely located excitation points.

In the present paper the conventional section topography supported by numerical simulation of defects is applied for studying of the images of dislocation and pipe-formed cavities in SiC bulk crystals. The important goal of the paper was also studying of the elements of the contrast of the dislocations to check the possibility of using simple approximations of extinction contrast, often dominating in the Bragg-case section images of dislocations.

The numerical analysis of the Bragg-case section images was performed for the case of screw dislocation perpendicular to the crystal surface in an arbitrary asymmetrical reflection. It is well known that this kind of dislocations is particularly important in the case of SiC, because it is relatively common and was also suggested by Dudley and coworkers [1] as the possible source of micro-pipes, where many single screw dislocations may join in forming one hollow-core super-screw dislocations with a large Burgers vector.

The present simulation became more realistic and better corresponding to the experimental dislocation images by adding many shifted spherical images, filling the area irradiated by the narrow beam, analogously at it was proposed by Epelboin and Soyer [2] in the case of transmission projection topography. The obtained

simulated images were compared with two adapted simplified models of extinction contrast described by Miltat and Bowen [3]. The results evidently indicated that the extinction contrast in the simulated images and topographs is very similar to the contours limiting the effective change of the diffracting conditions and differs substantially from the contours representing the condition of the wave-field decomposition.

For studying of the strain field of some pipe-formed cavities and rod like defects, we revealed a method of approximate evaluation of the strain field of rod like inclusion, integrating the contribution from a very large number of point like inclusions filling the assumed volume of inclusion. The model allowed taking into account the relaxation of strains on the free surface using the initial formulae given by Sen [4], and calculation of strains for differently inclined rods. The application of the model enabled obtaining realistic test simulation of topographic images of some solute trails in garnet, and some similarity to the Bragg-case section topographic images of some pipe formed inclusions in SiC.

## References

- [1] M. Dudley X.R. Huang, V.M. Vetter, "Contribution of x-ray topography and high-resolution diffraction to the study of defects in SiC", *J. Phys. D: Appl. Phys.* **36** (2003) A30–A36.
- [2] Y. Epelboin, A. Soyer, "Simulation of X-ray traverse topographs by means of a computer", *Acta Cryst. A* **41** (1985) 67–72.
- [3] J.E.A. Miltat, D.K. Bowen, "On the widths of dislocation images in X-ray topography under low-absorption conditions", *J. Appl. Cryst.* **8** (1975) 657–669.
- [4] R. Sen, *J. Quant. Mech.* **VIII** (4) (1949) 365.

## KINETICS OF THE VERWEY TRANSITION IN MAGNETITE

**W. Tabiś<sup>1\*</sup>, J. Kusz<sup>2</sup>, N.-T.H. Kim-Ngan<sup>3</sup>, Z. Tarnowski<sup>1</sup>, F. Zontone<sup>4</sup>,  
Z. Kąkol<sup>1</sup>, A. Kozłowski<sup>1</sup>, and T. Kołodziej<sup>1</sup>**

<sup>1</sup> AGH University of Science and Technology, Faculty of Physics and Applied Computer Science,  
Al. Mickiewicza 30, 30-059 Kraków, Poland

<sup>2</sup> Institute of Physics, University of Silesia, Uniwersytecka 4, 40- 007 Katowice, Poland

<sup>3</sup> Institut of Physics, Pedagogical University, Kraków, Poland

<sup>4</sup> European Synchrotron Radiation Facility, P.B. 200, F-38043 Grenoble, France

*Keywords:* magnetite, Verwey phase transition, diffraction

\*) e-mail: wtabis@agh.edu.pl

The Verwey phase transition in magnetite at 124 K is mainly known due to the drop of resistance by two orders of magnitude while heating above the Verwey temperature  $T_V$ . Following the concept of Verwey [1] and Anderson [2], it was believed that strongly correlated electrons, one from each of two iron located at octahedral B-sites, travelling relatively freely between iron B cations, are responsible for the good conductivity at  $T > T_V$ . The abrupt increase in resistivity below  $T_V$  was explained as due to the localization of those interacting electrons at particular positions. The low-temperature order is described by formula:  $\text{Fe}^{3+} [\text{Fe}^{(2.5+\delta)+} \text{Fe}^{(2.5-\delta)+}] \text{O}_4$  where the square brackets mark the octahedral positions. The disproportionation value of  $\delta_{12} = 0.12 \pm 0.025$  for one kind of Fe-atoms and  $\delta_{34} = 0.1 \pm 0.06$  for another is confirmed by a resonant x-ray diffraction (RXD) [3]. This electronic charge ordering is related to the change in the structure symmetry, from high  $T$  cubic ( $Fd\text{-}3m$ ) to monoclinic ( $Cc$ ) for  $T$  below  $T_V$ . The results of recent investigations, however, suggest that there is decoupling between charge ordering and the lattice distortion [4].

To investigate the kinetics of the transition in details, two kinds of experiments have been performed. First, simultaneous measurements of the resistivity and the magnetic susceptibility while temperature maintained constant, were performed at the AGH Univ. of Sci. and Tech. in Krakow. The results are shown in Fig. 1.

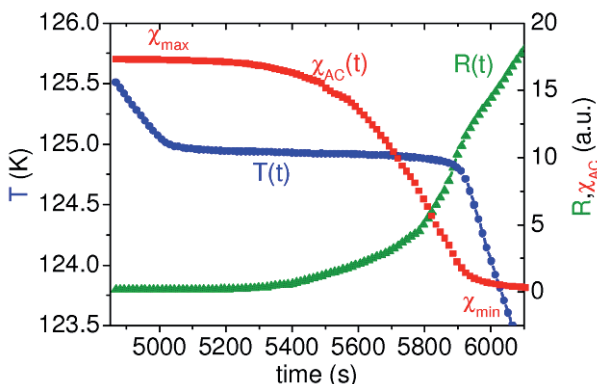


Figure 1. Temporal behavior of the resistivity  $R(t)$  and the magnetic AC susceptibility  $\chi_{\text{AC}}(t)$  measured simultaneously with the temperature  $T(t)$  at the Verwey transition during sample cooling.

The second experiment has been performed at ESRF in Grenoble, ID10 beam line. The aim was to work out the processes related to the lattice distortion. For that we observed simultaneously the  $(1\frac{1}{2}2)$  superstructure peak intensity (absent in high- $T$  cubic phase) and, for comparison with the previous experiment, the magnetic susceptibility. The results are shown in Fig. 2.

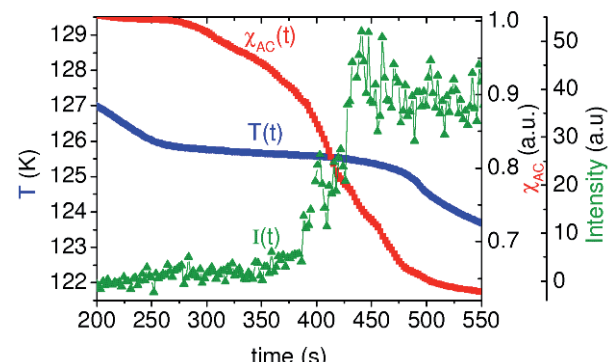


Figure 2. Temporal behavior of the integrated  $(1\frac{1}{2}2)$  superstructure peak intensity  $I(t)$  and the magnetic AC susceptibility  $\chi_{\text{AC}}(t)$  measured simultaneously with the temperature  $T(t)$  at the Verwey transition.

We have traced all the ongoing processes, trying to see their temporal dependences and the subtleties of the transition. We note here that, although AC susceptibility is a magnetic parameter, it reflects both the changing electronic system and the structure symmetry.

**Acknowledgements:** The project was supported by the Polish Ministry of Education and Science grant No 1P03 B01530.

### References

- [1] E.J. Verwey, "Electronic conduction of magnetite ( $\text{Fe}_3\text{O}_4$ ) and its transition point at low temperatures". *Nature (London)* **144** (1939) 327–328.
- [2] P.W. Anderson, "Ordering and antiferromagnetism in ferrites", *Phys. Rev.* **102** (1956) 1008–1013.
- [3] E. Nazarenko, *et al.*, "Resonant x-ray diffraction studies on the charge ordering in magnetite", *Phys. Rev. Lett.* **97** (2006) 056403–1–4.
- [4] J.E. Lorenzo, *et al.*, "Charge and orbital correlations at and above Verwey phase transition in magnetite", *Phys. Rev. Lett.* **101** (2008) 226401–1–4.

# CHANGES OF IRON STATE AND LOCAL IRON ENVIRONMENT OF MALARIAL PIGMENT'S SUBSTITUTE IN PRESENCE OF CHLOROQUINE

**M.S. Walczak<sup>1\*</sup>, K. Lawniczak-Jablonska<sup>1</sup>, A. Wolska<sup>1</sup>, M. Sikora<sup>2,3</sup>, A. Sienkiewicz<sup>4</sup>,  
L. Suárez<sup>5</sup>, A. Kosar<sup>5</sup>, M.J. Bellemare<sup>5</sup>, and D.S. Bohle<sup>5</sup>**

<sup>1</sup> Institute of Physics, PAS, Al. Lotników 32/46, 02-668 Warsaw, Poland

<sup>2</sup> Faculty of Physics and Applied Computer Science, AGH University of Science and Technology,  
Al. Mickiewicza 30, 30-059 Krakow, Poland

<sup>3</sup> European Synchrotron Radiation Facility, BP 220, 38043 Grenoble, France

<sup>4</sup> Institute of Physics of Condensed Matter, Ecole Polytechnique Fédérale de Lausanne,  
CH-1015 Lausanne, Switzerland

<sup>5</sup> Department of Chemistry, McGill University, 801 Sherbrooke Street West, Montreal, Canada

*Keywords:* hemozoin, hemozoin's substitute, chloroquine, EXAFS, XANES

\*) e-mail: mwalczak@ifpan.edu.pl

Malaria remains the world's most prevalent vector-borne disease, which causes serious health problem particularly in African and Asiatic countries [1]. The most severe form of malaria is caused by Plasmodium falciparum (Pf) parasite. The intraerythrocytic stage of Pf involves hemoglobin proteolysis and detoxification of heme molecules into an inert crystalline material, called malarial pigment, or hemozoin. The crystal structure of hemozoin has been solved by X-ray powder diffraction in the last years and its synthetic analogue,  $\beta$ -hematin was synthesized [2]. The ferriprotoporphyrin IX is believed to be a target for commonly used antimalarial drugs but their interactions are still not understood on molecular level.

In presented work we are especially interested in drug-induced perturbations of the structures of soluble  $\beta$ -hematin-like compound, iron(III) (meso-porphyrin-IX anhydride) called meso-hematin. Similarly to its insoluble parent compound,  $\beta$ -hematin, this compound is also built of dimers. The XAS measurements on frozen sample of meso-hematin in solution were performed at ESRF (station ID26). Pure acetic acid and acetic acid with water of volume ratio respectively 30:1 and 15:1 were used as solvents. The high resolution XANES and EXAFS spectra on iron K-edge enabled us to reveal the evolution of iron oxidation state and local environment of Fe atoms in investigated solutions upon chloroquine drug addition. The main difference revealed by EXAFS concerns the coordination number of the ligand oxygen, which is lower in the presence of chloroquine for both the water containing solutions. On the other hand the Fe-O distance is significantly shorter in solution with smaller H<sub>2</sub>O/acetic acid ratio and at the presence of drug. Analysis of the XANES revealed small changes in local iron geometry and its spin state, being close to  $S = 3/2$ , instead of  $S = 5/2$  observed in natural product of malaria parasite – microcrystalline hemozoin.

**Acknowledgements:** This work was supported by research grant N20205332/1197 and special project ESRF/73/2006 from the Ministry of Science and High Education.

## References

- [1] (a) L.H. Miller, D.I. Baruch, K. Marsch, O.K. Duombo, "The pathogenic basis of malaria", *Nature* **415** (2002) 673-679; (b) World Health Organization, *The World Malaria Report 2008*, <http://apps.who.int/malaria/wmr2008/>
- [2] S. Pagola, P.W. Stephens, D.S. Bohle, A.D. Kosar, S.K. Madsen, "The structure of malaria pigment beta-haematin", *Nature* **404** (2000) 307-310.

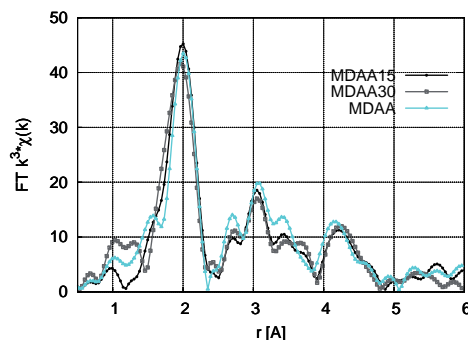


Figure 1. Comparison of Fourier transformed EXAFS oscillations of solved meso-hematin without (MDAA) and with (MDAA15, MDAA30) water addition.

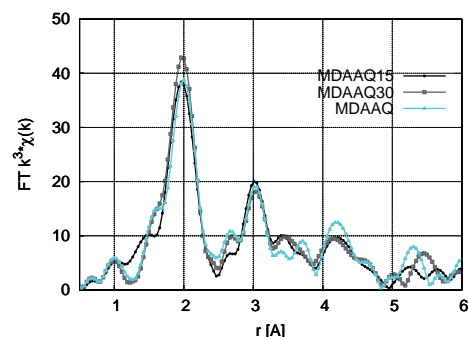


Figure 2. Comparison of Fourier transformed EXAFS oscillations of solved meso-hematin in chloroquine presence without (MDAAQ) and with (MDAAQ15, MDAAQ30) water addition.

## HIGH-PRESSURE DIFFRACTION STUDY OF SELECTED SYNTHETIC GARNETS

**E. Werner-Malento<sup>1\*</sup>, R. Minikayev<sup>1</sup>, C. Lathe<sup>2,3</sup>, H. Dąbkowska<sup>4</sup>, and W. Paszkowicz<sup>1</sup>**

<sup>1</sup> Institute of Physics, Polish Academy of Sciences, Al. Lotników 32/46, 02-668 Warsaw, Poland

<sup>2</sup> HASYLAB at DESY, Notkestrasse 85, D-22603 Hamburg, Germany

<sup>3</sup> GFZ German Research Centre for Geosciences, Dept. 5, Telegrafenberg, Potsdam, Brb D-14473, Germany

<sup>4</sup> Department of Physics, McMaster University, Hamilton, Ontario, L8S 4M1 Canada

*Keywords:* garnets, equation of state, EOS, high-pressure diffraction study

\*) e-mail: ewerner@ifpan.edu.pl

Crystals of synthetic garnets exhibit physical properties that may lead to various applications. These materials are characterized by high resistance for plastic flow even at high temperatures, by low thermal conductivity [1], and by Mohs hardness between 6.5 and 8.5. Garnets are applied in solid-state lasers [2]. Some of them (e.g.  $\text{Gd}_3\text{Ga}_5\text{O}_{12}$ , gadolinium gallium garnet – GGG) can be used for substrates for epitaxy of superconducting films [3]. Some doped oxide garnet materials can be used as optical pressure sensors [4, 5].

Mechanical properties of garnets are also of interest from the point of view of Earth science, because minerals of garnet structure are considered as one of major components of the deep interior of the Earth [6].

The general chemical formula for a garnet is  $\text{X}_3\text{Y}_2\text{Z}_3\text{O}_{12}$ , with divalent X, trivalent Y, and tetravalent Z cations (for example:  $\text{Ca}_3\text{Ga}_2\text{Ge}_3\text{O}_{12}$ ) or with trivalent cations.

At ambient conditions, garnets crystallize in *Ia3d* space group. In four-component's garnets ( $\text{X}_3\text{Y}_2\text{Z}_3\text{O}_{12}$ ), the Z atoms are bonded to four oxygens (tetrahedral), Y atoms – to six oxygens (octahedral), and X atoms – to eight oxygens (distorted cube). In three-component garnets ( $\text{X}_3\text{Y}_5\text{O}_{12}$ ) the five Y ions occupy two octahedral and three tetrahedral sites.

High-pressure diffraction study for selected garnets is presented in this work. The *in-situ* X-ray diffraction experiments were conducted using the energy-dispersive method at the F2.1 beamline equipped with a large-anvil diffraction press, MAX80. The pressures ranging to 8.7 GPa were calibrated using a NaCl equation of state. The lattice parameters of garnets were determined from Le Bail refinements performed with the Fullprof2k program.

Analysis of the data collected for one of the measured garnets,  $\text{Ca}_3\text{Ga}_2\text{Ge}_3\text{O}_{12}$  (calcium gallium germanium garnet, CGGG) shows that the garnet structure is conserved in the studied pressure range. The lattice parameter of the garnet structure decreases with the applied pressure from 12.202(1) Å at ambient pressure to 11.995(4) Å at 8.7 GPa. The resulting bulk modulus value for the CGGG is by about 15% lower than that for gadolinium gallium garnet [7].

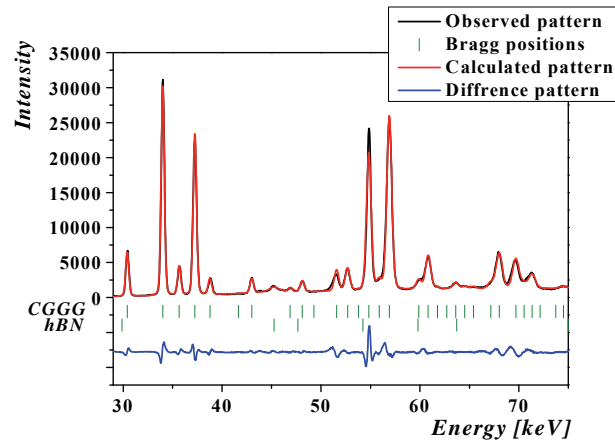


Figure 1. Le Bail refinement plot of the calcium gallium germanium garnet, sample after compression without pressure. The vertical bars refer to peak positions for CGGG and hBN.

### References

- [1] N.P. Padture, P.G. Klemens, "Low thermal conductivity in garnets", *J. Am. Ceram. Soc.* **80** (1996) 1018–1020.
- [2] J. Lu, K. Ueda, H. Yagi, T. Yanagitani, Y. Akiyama, A.A. Kaminskii, "Neodymium doped yttrium aluminum garnet ( $\text{Y}_3\text{Al}_5\text{O}_{12}$ ) nanocrystalline ceramics—a new generation of solid state laser and optical materials", *J. Alloys Compds.* **341** (2002) 220–225.
- [3] P. Mukhopadhyay, "High-Tc films on GGG substrates", *Supercond. Sci. Technol.* **7** (1993) 298–299.
- [4] J. Liu, Y.K. Vohra, "Sm:YAG optical pressure sensor to 180 GPa: Calibration and structural disorder", *Appl. Phys. Lett.* **64** (1994) 3386–3388.
- [5] S. Kobyakov, A. Kamiska, A. Suchocki, D. Galanciak, M. Malinowski, " $\text{Nd}^{3+}$ -doped yttrium aluminum garnet crystal as a near-infrared pressure sensor for diamond anvil cells", *Appl. Phys. Lett.* **88** (2006) 234102.
- [6] S. Karato, Z. Wang, B. Liu, K. Fujino, "Plastic deformation of garnets: systematics and implications for the rheology of the mantle transition zone", *Earth Planet. Sci. Lett.* **130** (1995) 13–30.
- [7] A. Durygin, V. Drozd, W. Paszkowicz, E. Werner-Malento, R. Buczko, A. Kaminska, S. Saxena, A. Suchocki, "Influence of pressure on lattice parameter of gadolinium gallium garnet crystals", *Appl. Phys. Lett.* (2009), accepted.

## DAMAGE OF SOLIDS INDUCED BY SINGLE PULSES OF XUV-FLASH

**J.B. Pełka<sup>1</sup>, R. Sobierajski<sup>1</sup>, M. Jurek<sup>1</sup>, J. Krzywiński<sup>1</sup>, D. Żymierska<sup>1</sup>, D. Klinger<sup>1</sup>, S. Hau Riege<sup>2</sup>, H. Chapman<sup>2</sup>, R. London<sup>2</sup>, L. Juha<sup>3</sup>, J. Chalupsky<sup>3</sup>, J. Cihelka<sup>3</sup>, U. Jastrow<sup>4</sup>, K. Tiedtke<sup>4</sup>, S. Toleikis<sup>4</sup>, H. Wabnitz<sup>4</sup>, W. Caliebe<sup>4</sup>, K. Sokolowski-Tinten<sup>5</sup>, N. Stojanovic<sup>5</sup>, C. Riek<sup>6</sup>, R. Davies<sup>6</sup>, M. Burghammer<sup>6</sup>, W. Paszkowicz<sup>1</sup>, and A. Wawro<sup>1</sup>**

<sup>1</sup> Institute of Physics, Polish Academy of Sciences, Al. Lotników 32/46, 02-668 Warsaw, Poland

<sup>2</sup> Lawrence Livermore National Laboratory, 7000 East Avenue, Livermore, CA 94555, USA

<sup>3</sup> Institute of Physics, Academy of Sciences of the Czech Republic, Na Slovance 2, 182 21 Prague, Czech Republic

<sup>4</sup> Deutsches Elektronen-Synchrotron DESY, Notkestrasse 85, D-226 3 Hamburg, Germany

<sup>5</sup> Institut für Experimentelle Physik, Universität Duisburg-Essen, Lotharstr. 1, 4748 Duisburg, Germany

<sup>6</sup> European Synchrotron Radiation Facility, 6 rue Jules Horowitz, BP 220, 38043 Grenoble, France

**Keywords:** XUV FEL, radiation damage, ablation, structure modifications, x-ray diffraction, pump and probes

\*) e-mail: pelkay@ifpan.edu.pl

The VUV- and XUV-FEL beam interaction with matter has been extensively investigated for the last few years with a special attention paid to the damage induced in solids. Most of this work was performed with the Free electron LASer in Hamburg (FLASH). This new type of the IV<sup>th</sup> generation SR source delivers intense pulses of coherent light in the wavelength range of 6 - 50 nm with the unique combination of quantum energy, extreme short pulse duration of only 25 fs and high power/pulse up to 5 GW. Application of the radiation opens up an access to study not yet explored phenomena, remaining unattainable with classical sources.

Interaction of XUV FLASH pulses with solids can change optical properties of the materials and induces complex damage processes leading to the formation of specific morphological structures with sizes on micrometric and nanometric scales [1, 2]. The absorbed pulse energy can also provoke phase transitions that change composition or crystalline state of the near-surface material [3]. Investigation of these phenomena is crucial for refinement of theoretical models, necessary to predict performance and lifetime of optical components for the new generation of FELs operating in the XUV and X-ray region.

In this work we put together some of our important experimental results, obtained with aid of various techniques, on the interaction of high intensity ( $10^{11}$  –  $10^{14}$  W/cm<sup>2</sup>) ultrashort pulses, delivered by FLASH, with solids. The one-color pump and probe technique made it possible to probe fluency-dependent variations in the optical constants of materials on the time scales of a single pulse duration.

The dynamics of ablation process was studied on the sample surface by the two-color pump and probe method with aid of an external optical laser. A detailed *ex-situ* characterization of irradiation-induced modifications on the solid surfaces was obtained by mixing the traditional microscopic methods with AFM. The x-ray microdiffraction with submicrometer beam was applied to probe the crystalline state with lateral resolution of only 250 nm.

By combining the results obtained with various experimental techniques, a more comprehensive picture of the processes in solids excited by an intense femtosecond XUV pulse was achieved.

**Acknowledgements:** This work has been partially supported by the Ministry of Science and Higher Education of Poland, SPB nr. DESY/68/2007, by the Czech Ministry of Education from the National Research Centers program (Projects LC510 and LC528) and program INGO (Grant LA08024) and by Academy of Sciences of the Czech Republic (Grants Z10100523, IAA400100701, and KAN300100702). Irradiation with FLASH has been performed within the framework of the *Peak-Brightness-Collaboration* [project II-20022049 EC]. Support from the PBC and the operators of the FLASH facility are gratefully acknowledged. The synchrotron measurements at HASYLAB, Hamburg were supported by the RIA FP6 Contract RII3-CT-2004-506008 of the European Community, The microdiffraction study has been done at the ID-13 beamline at ESRF, Grenoble.

### References

- [1] S.P. Hau-Riege, R.A. London, R.M. Bionta, M.A. McKernan, S.L. Baker, J. Krzywinski, R. Sobierajski, R. Nietubyc, J.B. Pełka, M. Jurek, L. Juha, J. Chalupský, J. Cihelka, V. Hájková, A. Velyhan, J. Krásá, "Damage threshold of inorganic solids under free-electron-laser irradiation at 32.5 nm wavelength", *Appl. Phys. Lett.* **90** (2007) 173128.
- [2] J. Krzywinski, R. Sobierajski, M. Jurek, R. Nietubyc, J. Pełka, L. Juha, M. Bittner, V. Létal, V. Vorlíček, A. Andrejczuk, J. Feldhaus, B. Keitel, E.L. Saldin, E.A. Schneidmiller, R. Treusch, M.V. Yurkov, "Conductors, semiconductors, and insulators irradiated with short-wavelength free-electron laser", *J. Appl. Phys.* **101** (2007) 043107.
- [3] J.B. Pełka, R. Sobierajski, D. Klinger, W. Paszkowicz, J. Krzywinski, M. Jurek, D. Żymierska, A. Wawro, A. Petrouček, L. Juha, V. Hájková, J. Cihelka, J. Chalupský, T. Burian, L. Vysin, S. Toleikis, K. Sokolowski-Tinten, N. Stojanovic, U. Zastrau, R. London, S. Hau-Riege, C. Riek, R. Davies, M. Burghammer, E. Dynowska, W. Szuszkiewicz, W. Caliebe, R. Nietubyc, "Damage in solids irradiated by a single shot of XUV free-electron laser: Irreversible changes investigated using X-ray microdiffraction, atomic force microscopy and Nomarski optical microscopy", *Rad. Phys. Chem.* **78**, (2009) S46-S52.

## ALIGNMENT TEST OF N-DOPED CARBON NANOTUBES USING HIGH-ENERGY X-RAY DIFFRACTION

**L. Hawelek<sup>1</sup>, A. Brodka<sup>1</sup>, J.C. Dore<sup>2</sup>, V. Honkimäki<sup>3</sup>, T. Kyotani<sup>4</sup>, and A. Burian<sup>1</sup>**

<sup>1</sup> *A. Chelkowski Institute of Physics, University of Silesia,  
ul. Uniwersytecka 4, 40-007 Katowice, Poland*

<sup>2</sup> *School of Physical Sciences, University of Kent, Canterbury, CT2 7NR, UK*

<sup>3</sup> *European Synchrotron Radiation Facility, BP 220, 38043 Grenoble, France*

<sup>4</sup> *Institute of Multidisciplinary Research and Advanced Material, Tohoku University,  
Katahira, Sendai 980-88577 Japan*

*Keywords:* *N-doped carbon nanotubes; X-ray diffraction*

Alignment test of multi-wall N-doped carbon nanotubes prepared by template pyrolytic carbon deposition method inside channels of an alumina membrane have been performed using high-energy X-ray diffraction on the ID15B beam-line at the European Synchrotron Radiation Facility (ESRF, Grenoble). The two-dimensional diffraction pattern of deposited carbon nanotubes, recorded directly within the alumina membrane using image plate detector, exhibits two non-continues arcs corresponding to the (002) graphitic reflection. Four values of angle between the axis of

carbon nanotubes within membrane channels and the incident beam were taken into consideration (0, 30, 45 and 60 degree). The anisotropic scattering distribution of two-dimensional pattern corresponds to the appropriate position of the carbon nanotubes, thus indicates their alignments. The one-dimensional intensity pattern for (002) anisotropic peaks over whole azimuthal angle was performed by circular slicing the two-dimensional pattern and the Full Width at Half Maximum (FWHM) parameter of anisotropy effect was determined by procedure of non-linear Gaussian curve fitting.

# OKREŚLANIE LOKALNEGO OTOCZENIA WOKÓŁ WYBRANYCH ATOMÓW W NOWYCH WODORKACH FAZ LAVESA

**K. Lawniczak-Jablonska<sup>1\*</sup>, M.T. Klepka<sup>1</sup>, A. Wolska<sup>1</sup>, S. Filipek<sup>2</sup>, and R. Sato<sup>2</sup>**

<sup>1</sup> Instytut Fizyki PAN, al. Lotników 32/46, 02-668 Warszawa, Polska

<sup>2</sup> Instytut Chemii Fizycznej PAN, ul. Kasprzaka 44/52, 01 224 Warszawa, Polska

*Słowa kluczowe:* fazy Laves'a, absorpcja rentgenowska, wiązanie chemiczne

\*) e-mail: jablo@ifpan.edu.pl

Absorpcja rentgenowska jest unikatową techniką, która pozwala wyznaczyć położenie atomów danego pierwiastka w sieci krystalicznej, określić jego wiązanie chemiczne oraz zmiany wprowadzone poprzez różnego rodzaju procedury (np. wygrzewanie, wprowadzenie wodoru, czy domieszkowanie). Technika ta jest więc doskonałym narzędziem do badania nowych materiałów. W niniejszej pracy zastosowano tą metodę do badania nowych wodorków faz Lavesa.

Fazy Lavesa są grupą międzymetalicznych związków, które poza bardzo interesującymi właściwościami fizycznymi i chemicznymi są uważane za ważne materiały w kontekście poszukiwania nośników wodoru dla energetyki wodorowej, w której wódór miałby zastąpić konwencjonalne źródła energii. Zainteresowanie nimi związane jest więc również z rozwojem energetyki wodorowej. Udało się ostatnio zsyntezować stosując technikę wysokich ciśnień szereg nowych wodorków faz Lavesa. Wodorki te są stabilne i mogą być przechowywane przez długi czas w warunkach normalnego ciśnienia i temperatury [1]. Pośród nowo zsyntezowanych materiałów najbardziej interesująca wydaje się grupa deuterków opisana wzorem chemicznym  $RMn_2D_6$  (gdzie  $R = Y$  lub  $Dy$  oraz pseudobinarne związki, w których Mn jest częściowo zastąpiony przez Fe lub Cr). Materiały takie udało się po raz pierwszy wytworzyć ze związków Lavesa. Ich właściwości fizyczne i chemiczne są intensywnie badane, ale położenie atomów Fe i Cr w sieci krystalicznej nie zostało do tej pory jednoznacznie wyznaczone [2].

Pomiary krawędzi absorpcji K Mn, Fe i Cr przeprowadzono w HASYLAB na stacji E4 w zakresie bliskim krawędzi (XANES z ang. X-ray Absorption Near Edge Structure) i dla rozciągniętej struktury (EXAFS z ang. Extended X-ray Absorption Fine Structure). W celu dokonania analizy tych widm przeprowadzono obliczenia widma XANES dla różnych położień atomów Mn, Fe i Cr w sieci krystalicznej tych związków korzystając z programu FEFF8.4. Widma teoretyczne zostały następnie porównane z widmami eksperymentalnymi. Pozwoliło to stwierdzić, który z modeli jest najbliższym rzeczywistemu

rozmięsczeniu atomów w sieci. Rozważono również możliwość występowania danego pierwiastka w więcej niż jednym położeniu w sieci.

Do analizy widm EXAFS zastosowano programy Artemis i Athena z pakietu IFEFIT. Związki podwójne były wykorzystane jako materiały referencyjne o znanej strukturze. Określono zmiany w wiązaniu chemicznym wprowadzone przez obecność wodoru lub deuteru w strukturze faz Lavesa oraz wpływ drugiego metalu przejściowego o dobrze zlokalizowanych stanach d (tutaj Fe lub Cr). Wyznaczono również położenie atomów Mn, Fe i Cr w sieci krystalicznej tych materiałów. Pozwoliło to zweryfikować istniejące modele teoretyczne oraz wnioski z neutronowych i rentgenowskich badań dyfrakcyjnych [3]. Po wyznaczeniu właściwego położenia metali przejściowych w sieci krystalicznej tych materiałów obliczono strukturę elektronową wokół każdego z metali i przedyskutowano ją w kontekście właściwości fizyko-chemicznych.

**Podziękowania:** Badania zostały dofinansowane jako wspólne badania sieci naukowej "Nowe Materiały - wytwarzanie i badania strukturalne" przez MNiSW oraz z programu Unii Europejskiej w ramach projektu RII3-CT-2004-506008 (IA-SFS).

## Literatura

- [1] V. Paul-Boncour, S.M. Filipek, M. Dorogova, F. Bourée, G. André, I. Marchuk, A. Percheron-Guégan, R.S. Liu, "Neutron diffraction study, magnetic properties and thermal stability of  $YMn_2D_6$  synthesized under high deuterium pressure", *J. Sol. State Chem.* **178** (2005) 356–362.
- [2] S.M. Filipek, H. Sugiura, V. Paul-Boncour, R. Wierzbicki, R.S. Liu, N. Bagkar, "Studies of Novel Deuterides  $RMn_2D_6$  ( $R$  – Rare Earth) compressed in DAC up to 30 GPa", *J. Phys.: Conf. Ser.* **121** (2008) 022001.
- [3] V. Paul-Boncour, S.M. Filipek, I. Marchuk, G. André, F. Bourée, G. Wiesinger, A. Percheron-Guégan, "Structural and magnetic properties of  $ErFe_2D_5$  studied by neutron diffraction and Mössbauer spectroscopy", *J. Phys.: Cond. Matt.* **15** (2003) 4349–4359.

## EQUATION OF STATE OF ZIRCON-TYPE $\text{TbVO}_4$

**R. Minikayev<sup>1</sup>, W. Paszkowicz<sup>1</sup>, E. Werner-Malento<sup>1</sup>, C. Lathe<sup>2,3</sup>, and H. Dąbkowska<sup>4</sup>**

<sup>1</sup>*Institute of Physics, Polish Academy of Sciences, Al. Lotników 32/46, 02-668 Warsaw, Poland*

<sup>2</sup>*HASYLAB at DESY, Notkestrasse 85, D-22603 Hamburg, Germany*

<sup>3</sup>*GFZ German Research Centre for Geosciences, Dept. 5, Telegrafenberge, Potsdam, Brb D-14473, Germany*

<sup>4</sup>*Department of Physics, McMaster University, Hamilton, Ontario, L8S 4M1 Canada*

*Keywords:* diffraction, equation of state, orthovanadate,  $\text{TbVO}_4$ , bulk modulus

\*) e-mail: minik@ifpan.edu.pl

$\text{RVO}_4$  ( $R = \text{Y, Sc, La} - \text{Lu}$ ) orthovanadates belong to a large class of  $AX\text{O}_4$  compounds that typically adopt the structures of zircon, scheelite, fergusonite, monazite, wolframite,  $\text{CrVO}_4$ ,  $\text{ZnSO}_4$  and rutile types [1-3]. Phase relationships in this class, observed as a function of pressure have been systematized by Fukunaga and Yamaoka [2] and Errandonea and Manjón [4] (for all possible  $AX\text{O}_4$  compounds), and by Kolitsch and Holtstam [3] for  $RX\text{O}_4$  compounds ( $X = \text{P, As, V}$ ). For  $\text{RVO}_4$ ,  $R = \text{Pr}$  to  $\text{Lu}$ , the most stable ambient pressure structure is of zircon type, space group  $I4_1/\text{amd}$ , this structure can be also obtained for  $R = \text{La}$  using special preparation methods. The zircon-type  $\text{RVO}_4$  orthovanadates exhibit physical properties that may lead to a number of applications. Known examples are the europium and neodymium doped  $\text{YVO}_4$  crystals used as phosphor and laser materials, respectively. Some of compounds of this family are considered as being suitable for optical waveguides and polarizers, they can be used for remote thermometry, as catalysts for oxidative dehydrogenation, and are candidates for advanced bio-imaging phosphors and as components of toughened ceramic composites.

A number of  $\text{RVO}_4$  oxides have been studied at high-pressure conditions using the *in-situ* or *ex situ* X-ray diffraction and other methods. They are known to undergo an irreversible phase transition to scheelite-type structure. In this work,  $\text{TbVO}_4$  is studied in the pressure range 0-7 GPa. The elastic properties of this oxide have been studied under pressure by an indirect technique,

only, using the Raman spectroscopic data by Chen *et al.* [4]. The crystal investigated in the present work was grown from  $\text{PbO}/\text{PbF}_2$  flux by the slow cooling method.

The *in-situ* X-ray diffraction experiments were conducted using the energy-dispersive method at the F2.1 beamline equipped with a large-anvil diffraction press,

MAX80. The pressure was calibrated using a NaCl equation of state. The lattice parameters of  $\text{TbVO}_4$  were determined from Le Bail refinements performed with the Fullprof program. The bulk modulus calculated by fitting the second order Birch-Murnaghan equation of state to the unit-cell-volume dependence of pressure. The bulk modulus value, lattice parameter and axial ratio dependence on pressure will be shown.

### References

- [1] O. Muller, R. Roy, "Phase transitions among the  $\text{ABX}_4$  compounds", *Z. Kristallogr.* **198** (1973) 237-253.
- [2] O. Fukunaga, S. Yamaoka, "Phase transformations in  $\text{ABO}_4$  type compounds under high pressure", *Phys. Chem. Miner.* **5** (1979) 167-177.
- [3] U. Kolitsch, D. Holtstam, "Crystal chemistry of REEXO<sub>4</sub> compounds ( $X = \text{P, As, V}$ ). II. Review of REEXO<sub>4</sub> compounds and their stability fields", *Eur. J. Mineral.* **16** (2004) 117-126.
- [4] D. Errandonea, F.J. Manjón, "Pressure effects on the structural and electronic properties of  $\text{ABX}_4$  scintillating crystals", *Prog. Mater. Sci.* **53** (2008) 711.

# A COMBINED X-RAY DIFFRACTION AND ABSORPTION STUDY OF $\text{Li}_2\text{Si}_2\text{O}_5$ DOPED WITH VANADIUM

**W. Paszkowicz<sup>1</sup>, A. Wolska<sup>1</sup>, M.T. Klepka<sup>1</sup>, S. abd el All<sup>1,2</sup>, and F.M. Ezz-Eldin<sup>2</sup>**

<sup>1</sup> Institute of Physics PAS, al. Lotników 32/46, Warszawa 02-668, Poland

<sup>2</sup> Center of Research and Radiation Technology, Nasr City, Cairo 0002, Egypt

*Keywords:* X-ray diffraction, X-ray absorption, XANES, lithium silicate

\*) e-mail: paszk@ifpan.edu.pl

Lithium-based conducting glasses are promising candidates for electrolyte materials of thin-film batteries because they exhibit isotropic ionic conductivity. However, at room temperature most of such conducting glasses exhibit relatively low ionic conductivity values, in the range  $10^7$  to  $10^8$  S/m. In order to increase the conductivity, some specific additives have been used, one of them being vanadium. In a recent work on borate glasses, vanadium dopant at a level of several percent was used for this purpose [1-3]. It has been noticed that annealing of vanadium doped borate glass results in a change of physical properties [1]. This may suggest that vanadium ions occupy specific crystallographic sites.

In this work, a related material, vanadium-doped lithium silicate glass is studied. The glass was prepared by heating a mixture of quartz ( $\text{SiO}_2$ ), lithium carbonate ( $\text{Li}_2\text{CO}_3$ ) and vanadium pentoxide ( $\text{V}_2\text{O}_5$ ) at a level of up to 5.5 weight percent at 1400 for 3 h and then cooled. As prepared glass was annealed for 4 h at 550°C. The X-ray diffraction experiments were performed at a conventional diffractometer.

The described synthesis procedure gives a virtually pure  $\text{Li}_2\text{Si}_2\text{O}_5$  phase of orthorhombic  $Ccc2$  space group [4] with vanadium present in the lattice and with traces of impurity phases. We noticed that the observed crystallisation is faster than that reported in literature for phosphate glasses [5]. Rietveld refinements were performed using various models assuming a partial occupation at Li or Si sites. The results indicate that location of vanadium at Si sites is more likely. The lattice parameters are found to vary isotropically with increasing vanadium content.

The X-ray absorption experiment was conducted at the Cemo beamline (Hasylab, Hamburg). XANES spectra at the vanadium K edge were measured at room temperature using fluorescence and transmission detection mode. In all cases, a very pronounced pre-pik was observed. According to Ref. [6], this feature indicates that vanadium atoms are in the +5 ionic state.

## References

- [1] N.A. El-Alaily, R.M. Mohamed, "Effect of irradiation on differential thermal properties and crystallization behavior of some lithium borate glasses", *Nucl. Instrum. Meth. Phys. Res. B* **179** (2001) 230-242.
- [2] Y.-I. Lee, J.-H. Lee, S.-H. Hong, Y. Park, "Li-ion conductivity in  $\text{Li}_2\text{O}-\text{B}_2\text{O}_3-\text{V}_2\text{O}_5$  glass system", *Solid State Ionics* **175** (2004) 687-690.
- [3] S.Y. Marzouk, N.A. Elalaily, F.M. Ezz-Eldin, W.M. Abd-Allah, "Optical absorption of gamma-irradiated lithium-borate glasses doped with different transition metal oxides", *Physica B* **382** (2006) 340-351.
- [4] B.H.W.S. de Jong, H.T.J. Supér, A.L. Spek, N. Veldman, G. Nachtegaal, J.C. Fischer, "Mixed alkali systems: Structure and  $^{29}\text{Si}$  MASNMR of  $\text{Li}_2\text{Si}_2\text{O}_5$  and  $\text{K}_2\text{Si}_2\text{O}_5$ ", *Acta Crystallogr. B* **54** (1998) 568-577.
- [5] Y. Iqbal, W.E. Lee, D. Holland, P.F. James, "Crystal nucleation in  $\text{P}_2\text{O}_5$ -doped lithium disilicate glasses", *J. Mater. Sci.* **34** (1999) 4399-4411.
- [6] P. Chaurand, J. Rose, V.Briois, M. Salome, O. Proux, V. Nassif, L. Olivi, J. Susini, J.-L. Hazemann, J.-Y. Bottero "New methodological approach for the vanadium K-edge X-ray absorption near-edge structure interpretation: Application to the speciation of vanadium in oxide phases from steel slag", *J. Phys. Chem. B* **111** (2007) 5101-5110.

## LATTICE PARAMETER OF POLYCRYSTALLINE DIAMOND IN THE LOW-TEMPERATURE RANGE

**W. Paszkowicz**<sup>1</sup>, **P. Piszora**<sup>2</sup>, **W. Łasocha**<sup>3,4</sup>, **I. Margiolaki**<sup>5</sup>, **M. Brunelli**<sup>5</sup>, and **A. Fitch**<sup>5</sup>

<sup>1</sup> Institute of Physics PAS, al. Lotników 32/46, 02-668 Warszawa, Poland

<sup>2</sup> Adam Mickiewicz University, Faculty of Chemistry,  
ul. Grunwaldzka 6, Poznań 60-780, Poland

<sup>3</sup> Jagellonian University, Faculty of Chemistry, ul. Ingardena 3, 30-060 Kraków, Poland

<sup>4</sup> Institute of Catalysis and Surface Chemistry PAS,  
ul. Niezapominajek 8, 30-239 Kraków, Poland

<sup>5</sup> European Synchrotron Radiation Facility (ESRF), ID31, Materials Science Group, Inorganic Chemistry I,  
6 rue Jules Horowitz, BP 220, 38043 Grenoble, France

*Keywords:* thermal expansion, X-ray diffraction, diamond

\*) e-mail: paszk@ifpan.edu.pl

Diamond exhibits, due to strong covalent bonding, a very weak thermal expansion at low temperatures. Below room temperature, the total variation of the unit-cell dimension is less than  $10^{-3}$  Å, being comparable to the precision of lattice-parameter determination at a typical instrument. Experimental studies have been published for diamond single crystals [1, 2], whereas detailed experimental studies for polycrystalline diamond have been reported mainly above the room temperature.

In the present study, the results of measurement of lattice parameters of commercial polycrystalline diamond will be presented. The measurements were performed using Debye-Scherrer geometry at ID31 beamline (ESRF) equipped with a bank of nine detectors preceded by Si 111 analyser crystals. Lattice parameters were calculated using the Rietveld refinement. The obtained

experimental lattice parameter and thermal expansion temperature dependence will be discussed on the basis of available literature data.

### References

- [1] T. Saotome, K. Ohashi, T. Sato, H. Maeta, K. Haruna, F. Ono, "Thermal expansion of a boron-doped diamond single crystal at low temperatures", *J. Phys.: Condens. Matt.* **10** (1998) 1267–1272.
- [2] T. Sato, K. Ohashi, T. Sudoh, K. Haruna, H. Maeta, "Thermal expansion of a high purity synthetic diamond single crystal at low temperatures", *Phys. Rev. B* **65** (2002) 092102.
- [3] C. Giles, C. Adriano, A. Freire Lubambo, C. Cusatis, I. Mazzaro, M. Goncalves Hönnicke, "Diamond thermal expansion measurement using transmitted X-ray back-diffraction", *J. Synchrotron Radiat.* **12** (2005) 349–353.

# A COMPARISON OF THE VALENCE BAND STRUCTURE OF BULK AND EPITAXIAL GeTe-BASED DILUTED MAGNETIC SEMICONDUCTORS

**M.A. Pietrzyk<sup>1\*</sup>, B.J. Kowalski<sup>1</sup>, B.A. Orlowski<sup>1</sup>, W. Knoff<sup>1</sup>, T. Story<sup>1</sup>, W. Dobrowolski<sup>1</sup>,  
V.E. Slyko<sup>2</sup>, E.I. Slyko<sup>2</sup>, and R.L. Johnson<sup>3</sup>**

<sup>1</sup> Institute of Physics, Polish Academy of Sciences, Al. Lotników 32/46, 02-668 Warsaw, Poland

<sup>2</sup> Chernivtsi Branch of the Institute for Materials Science Problems, National Academy of Sciences of Ukraine,  
5 Vilde Str., 58001 Chernivtsi, Ukraine

<sup>3</sup> Institute of Experimental Physics, University of Hamburg, Luruper Chaussee 149, D-22761 Hamburg, Germany

*Keywords:* photoemission spectroscopy, diluted magnetic semiconductors

\*) e-mail: pietrzyk@ifpan.edu.pl

In this work we present a comparison of the experimental results, which have been obtained in the resonant photoemission study of electronic structure of epitaxial layers and bulk crystals of GeTe doped with Mn and/or Eu. Narrow-gap IV–VI semiconductors are known to form solid solutions not only with magnetic ions with partially filled 3d shell (e.g. Mn, Fe), but also with the elements with partially filled 4f shell (e.g. Eu, Gd). Such diluted magnetic semiconductors (DMS) exhibit transport, optical and magnetic properties attracting large interest from the point of view of basic research as well as of applications in infrared radiation sources, detectors, thermoelectric generators and, recently, spintronic devices.

The ferromagnetic ordering in IV-VI –based diluted magnetic semiconductors (DMS) is governed by the Ruderman–Kittel–Yoshida–Kasuya interaction mediated by free holes related to native defects.  $\text{Ge}_{1-x}\text{Mn}_x\text{Te}$  exhibits ferromagnetic properties with the Curie temperature which is relatively high and strongly dependent on Mn concentration ( $T_C \approx 190$  K) [1]. However, the introduction of Eu ions to the system leads to a similar Curie temperature but for markedly lower Mn contents [2]. Therefore, this study was performed in order to reveal Mn 3d and Eu 4f contributions to the valence band of several GeTe-based DMSs prepared by two different techniques.

The bulk polycrystals of  $\text{Ge}_{0.86}\text{Mn}_{0.14}\text{Te}$  and  $\text{Ge}_{0.4}\text{Mn}_{0.5}\text{Eu}_{0.1}\text{Te}$  were grown by the Bridgman method in the Institute for Problems of Materials Science, National Academy of Sciences of Ukraine. The  $\text{Ge}_{0.9}\text{Mn}_{0.1}\text{Te}$ ,  $\text{Ge}_{0.98}\text{Eu}_{0.02}\text{Te}$  and GeTe epitayers were grown on  $\text{BaF}_2$  (111) substrates by an MBE method with use of GeTe, Eu,  $\text{Te}_2$  and Mn solid sources in the Institute of Physics of the Polish Academy of Sciences (Warsaw, Poland). The substrate temperature was 400–450°C. The chemical composition of the samples was assessed by energy dispersive X-ray fluorescence analysis. Their crystalline structure was determined by X-ray diffraction. Clean sample surfaces for photoemission measurements were prepared *in situ* by

scraping the sample with a diamond file under UHV conditions (for polycrystals) or by  $\text{Ar}^+$  ion sputtering and annealing (for epitayers). The  $\text{Ge}_{1-x-y}\text{Mn}_x\text{Eu}_y\text{Te}$  surface alloy (for comparison with the  $\text{Ge}_{0.4}\text{Mn}_{0.5}\text{Eu}_{0.1}\text{Te}$  polycrystal) on a  $\text{Ge}_{1-x}\text{Eu}_x\text{Te}$  epitayer was fabricated *in situ* by Mn deposition and annealing under UHV conditions.

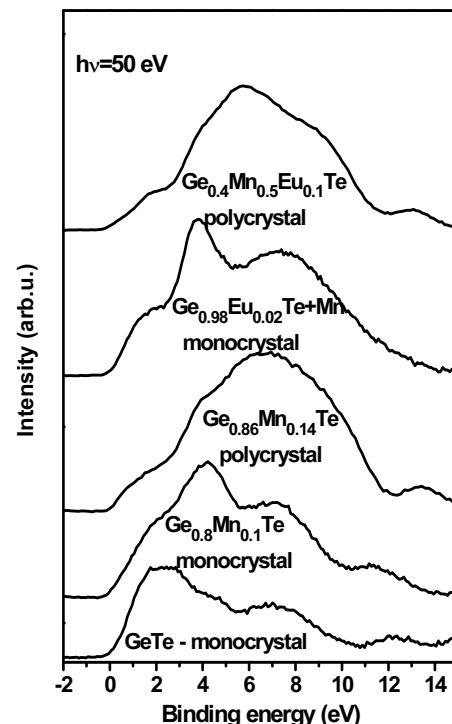


Figure 1. The comparison of the valence band photoemission spectra of GeTe,  $\text{Ge}_{0.9}\text{Mn}_{0.1}\text{Te}$ ,  $\text{Ge}_{0.98}\text{Eu}_{0.02}\text{Te}$  + Mn MBE layers and  $\text{Ge}_{0.4}\text{Mn}_{0.5}\text{Eu}_{0.1}\text{Te}$ ,  $\text{Ge}_{0.86}\text{Mn}_{0.14}\text{Te}$  bulk crystals for photon energy 50 eV.

The photoemission measurements were performed and photoelectron energy distribution curves were collected in the regime of resonant photoemission after

each stage of the system preparation procedure. All photoemission measurements were made at room temperature with fixed energy resolution of 250 meV. The secondary electron background has been subtracted by means of the Shirley method.

The valence bands of these samples were studied by means of resonant photoemission spectroscopy (RPES). In this technique the radiation energy  $h\nu$  is tuned to the intra-ion electron transition *e.g.*  $3p$ - $3d$  for transition metal atoms or  $4d$ - $4f$  for rare earth atoms. Then, the regular photoemission process

$$3p^63d^n + h\nu = 3p^63d^{n-1} + e^- \text{ (for TM atoms)}$$

is accompanied by excitation of the ion:

$$3p^63d^n + h\nu = [3p^53d^{n+1}]^*.$$

The quantum interference between these two processes leads to autoionization:

$$[3p^53d^{n+1}]^* \rightarrow 3p^63d^{n-1} + e^-$$

and resonant photoemission described by the Fano formula:

$$I(h\nu) = I_0 \frac{(q + \varepsilon)^2}{\varepsilon^2 + 1}$$

where  $q$  is the symmetry parameter (Fano factor),  $\varepsilon$  is the reduced energy variable which corresponds to the photon energy in photoemission experiments [3]. RPES is particularly useful for studying the contribution of partially filled shells ( $d$  or  $f$ ) of transition metals or rare earth elements to the electronic structure of DMSs.

This technique is based on the Fano-type  $p$ - $d$  or  $d$ - $f$  resonances which lead to strong increase of emission from  $d(f)$  shell and help to reveal related spectral features. The photoemission measurements were performed at the FLIPPER II system in HASYLAB (Hamburg, Germany). The spectra of GeTe,  $Ge_{1-x}Mn_xTe$ ,  $Ge_{1-x}Eu_xTe$ ,  $Ge_{1-x}Mn_xEu_yTe$  were measured for the photon energy range of 130 - 160 eV (corresponding to Eu  $4d$ - $4f$  resonance for both  $Eu^{2+}$  and  $Eu^{3+}$ ) and 30-60 eV (Mn  $3p$ - $3d$ ).

The spectra (photoelectron energy distribution curves) covered the range of electron binding energy starting from the valence band edge down to the Mn  $3p$  level. Figure 1 shows a typical set of energy distribution curves taken at photon energy of 50 eV (near the Mn  $3p$ - $3d$  resonance) for  $Ge_{0.96}Mn_{0.14}Te$ ,  $Ge_{0.4}Mn_{0.5}Eu_{0.1}Te$  polycrystal samples, GeTe,  $Ge_{0.9}Mn_{0.1}Te$ , mocrystalline epilayers and  $Ge_{0.98}Eu_{0.02}Te$  surface alloy ( $Ge_{0.98}Eu_{0.02}Te + Mn$ ). In order to estimate the destiny of state of Mn  $3d$  we have to subtract the antiresonance from resonance. The difference spectra of MBE layer we can compare with the difference spectra of bulk samples  $Ge_{0.96}Mn_{0.14}Te$  and  $Ge_{0.4}Mn_{0.5}Eu_{0.1}Te$ . The shape is similar to that reported for  $Ge_{1-x}Mn_xTe$  [4].

The valence band density of states distribution of  $Ge_{1-x}Mn_xEu_yTe$  was determined for the first time, to our knowledge. The change of the Eu  $4f$  position induced by introduction of Mn ions, indicating an Mn-Eu interaction, was detected.

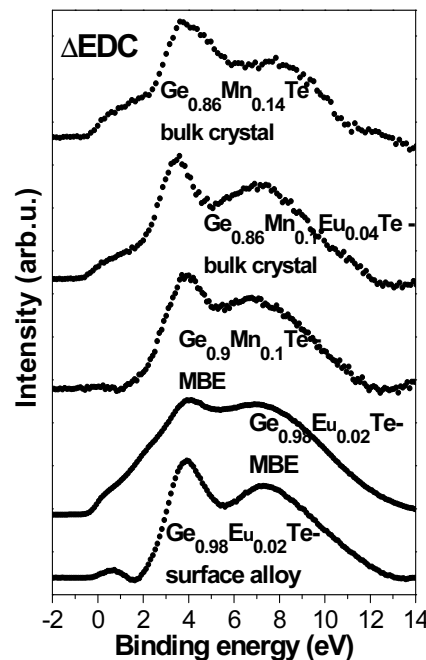


Figure 2. The difference EDCs spectra measured for bulk crystal and MBE layers.

For all investigated systems, the Mn  $3d$  states contribution occurred in the upper part of the valence band, with a maximum at the binding energy of about 3.8 eV. Its shape corresponded to that expected for  $Mn^{2+}$  ions surrounded by six Te ions in the octahedral coordination.

It was proved that strong, additional feature occurring for polycrystals is non-resonant, and most probably not related to presence of Mn ions. Thus, it is not related to the ferromagnetic behaviour of the bulk crystals.

**Acknowledgements:** The authors acknowledge support by MSHE (Poland) grants N202 101 31/0749 and DESY/68/2007 as well as by the European Community via the Research Infrastructure Action under the FP6 Structuring the European Research Area" Programme (through the Integrated Infrastructure Initiative "Integrating Activity on Synchrotron and Free Electron Laser Science") at DESY.

## References

- [1] Y. Fukuma, H. Asada, S. Miyawaki, T. Koyanagi, S. Senba, K. Goto, H. Sato, "Carrier-induced ferromagnetism in  $Ge_{0.92}Mn_{0.08}Te$  epilayers with a Curie temperature up to 190 K," *Appl. Phys. Lett.* **93** (2008) 252502.
- [2] W. Dobrowolski, M. Arciszewska, B. Brodowska, V. Domukhovski, V.K. Dugaev, A. Grzeda, I. Kuryliszyn-Kudelska, M. Wójcik, E.I. Slyanko, "IV–VI ferromagnetic semiconductors recent studies," *Sci. Sintering* **38** (2006) 109-116.
- [3] U. Fano, "Effects of configuration interaction on intensities and phase shifts", *Phys. Rev.* **124** (1961) 1866.
- [4] S. Senba, K. Fujimoto, H. Sato, Y. Fukuma, M. Nakatake, M. Arita, K. Tsuji, H. Asada, T. Koyanagi, H. Namatame, M. Taniguchi, "Mn  $3p$ - $3d$  resonant photoemission spectroscopy of ferromagnetic semiconductor  $Ge_{1-x}Mn_xTe$ ," *J. Electron Spectrosc. Relat. Phenom.* **629** (2005) 144–147.

## THRESHOLD PHOTOELECTRON SPECTRA OF ISOXAZOLE OVER THE PHOTON ENERGY RANGE 9-30 eV

**M. Dampc<sup>1</sup>, B. Mielewska<sup>1</sup>, M.R.F. Siggel-King<sup>2</sup>, G.C. King<sup>3</sup>, B. Sivaraman<sup>4</sup>,  
S. Ptasińska<sup>4</sup>, N. Mason<sup>4</sup>, and M. Zubek<sup>1\*</sup>**

<sup>1</sup> Department of Physics of Electronic Phenomena, Gdańsk University of Technology, 80-233 Gdańsk, Poland

<sup>2</sup> Daresbury Laboratory, Daresbury, Warrington, WA4 4AD, UK

<sup>3</sup> School of Physics and Astronomy, Manchester University, Manchester M13 9PL, UK

<sup>4</sup> Department of Physics and Astronomy, The Open University, Milton Keynes, UK

*Keywords:* threshold photoionization, isoxazole

\*) e-mail: mazub@mif.pg.gda.pl

Isoxazole C<sub>3</sub>H<sub>3</sub>NO is a five-member heterocycle molecule containing carbon ring in which two neighbouring carbon atoms are replaced by oxygen and nitrogen. It is used for synthesis of antibiotic, antitumour and anti-HIV agents *e.g.* [1] and is also considered as an analogue for biological molecules which are fragments of sugar-phosphate backbone of DNA.

We report results of threshold photoionization studies which used penetrating field technique (Fig. 1) [2]. The threshold photoelectron spectrometer [3] was used to collect spectra over the photon energy range from 9.9 eV to 30 eV beyond the previous He I measurements [4, 5]. The overall energy resolution was estimated to be better than 15 meV. This work was carried out at Synchrotron Radiation Source in Daresbury, UK using the five meter McPherson high resolution monochromator providing radiation in the 5–35 eV range with the highest resolution of 2 meV.

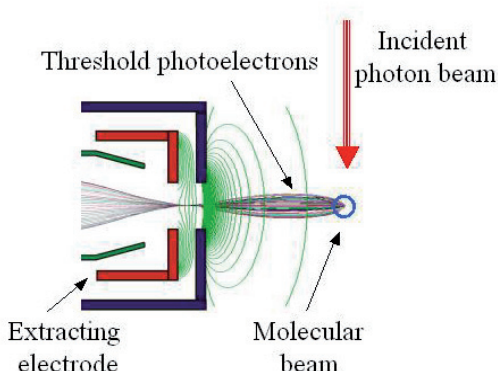


Figure 1. Penetrating field technique.

The complete threshold photoelectron spectrum of isoxazole is presented in Fig. 2. It consists of several bands with the first ionization threshold at 9.977 eV. The first band with resolved fine vibrational structures originates from ionization from the highest occupied molecular orbital 3a''( $\pi_3$ ). The next band in the 11–13 eV range, can be associated with the 2a''( $\pi_2$ ) and the 15a'( $LP_n$ ) (nitrogen lone pair) orbitals. At higher energy, apart from clearly visible bands, fitting procedure revealed few further underlying bands.

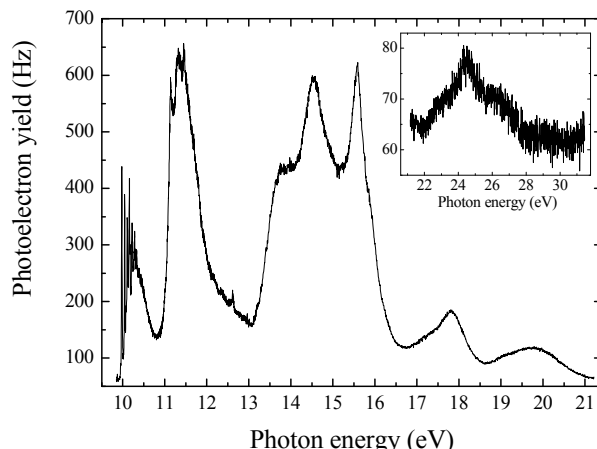


Figure 2. Threshold photoelectron spectrum of isoxazole measured in the energy range 9.9–30 eV.

### References

- [1] B.-L. Deng, M.D. Cullen, Z. Zhou, T.L. Hartman, R.W. Buckheit, Jr., Ch. Panneccouque, E. De Clercq, P.E. Fanwick, M. Cushman, "Synthesis and anti-HIV activity of new alkenyldiarylmethane (ADAM) non-nucleoside reverse transcriptase inhibitors (NNRTIs) incorporating benzoxazolone and benzisoxazole rings", *Bioorg. Med. Chem.* **14** (2006) 2366–2374.
- [2] S. Cvejanović, F.H. Read, "A new technique for threshold excitation spectroscopy", *J. Phys. B: Atom. Mol. Phys.* **7** (1974) 1180–1193.
- [3] R.I. Hall, A. McConkey, K. Ellis, G. Dawber, L. Avaldi, M.A. MacDonald, G.C. King, "A penetrating field electron-ion coincidence spectrometer for use in photoionization studies", *Meas. Sci. Technol.* **3** (1992) 316–324.
- [4] I.C. Walker, M.H. Palmer, J. Delwiche, S.V. Hoffmann, P. Limão Vieira, N.J. Mason, M.F. Guest, M.-J. Hubin-Francquin, J. Heinesch, A. Giuliani, "The electronic states of isoxazole studied by VUV absorption, electron energy-loss spectroscopies and ab initio multi-reference configuration interaction calculations", *Chem. Phys.* **297** (2004) 289–306.
- [5] T. Kobayashi, T. Kubota, K. Ezumi, C. Utsunomiya, "Photoelectron angular distribution study of some isoxazoles combined with perturbation theoretic approach", *Bull. Chem. Soc. Jpn.* **55** (1982) 3915–3919.

## NANOMETER PATTERNING AND HOLOGRAPHIC IMAGING USING TABLE-TOP EUV LASER

**P.W. Wachulak<sup>1\*</sup>, A. Bartnik<sup>1</sup>, C.S. Menoni<sup>2</sup>, J.J. Rocca<sup>2</sup>,**  
**H. Fiedorowicz<sup>1</sup>, and M.C. Marconi<sup>2</sup>**

<sup>1</sup> Military University of Technology, Institute of Optoelectronics, ul. Kaliskiego 2, 00-908, Warsaw, Poland

<sup>2</sup> Colorado State University, Electrical and Computer Engineering, 1320 Campus Delivery,  
Engineering Res. Center Fort Collins, CO 80523, USA

*Keywords:* holography, interferometric lithography, EUV laser

\*) e-mail: wachulak@gmail.com

Manipulation in the scales comparable to the sizes of molecules and even atoms is currently a very attractive. Nanopatterning and nano-meter resolution imaging are very important to control the matter on these small scales. Nanopatterning allows for surface modifications while nano-meter resolution imaging acts as a feedback mechanism used to evaluate the results.

A nanometer scale periodic patterns obtain with Interference Lithography (IL) were realized in commercial photoresists (PMMA and HSQ) with typical size below 100 nm using a compact nanopatterning tool based on a Lloyd's mirror interferometer. The EUV source used was a table top capillary discharge laser  $\lambda = 46.9$  nm producing pulses with an energy of approximately 0.4 mJ and duration of 1.2 ns FWHM. High spatial coherence radius – 570  $\mu\text{m}$  at 1.7 m from the laser output and temporal coherence, for  $\Delta\lambda/\lambda \approx 1 \times 10^{-4}$  equal to 470  $\mu\text{m}$ , allowed for parallel imprint of the dense arrays of holes and nano-pillars with feature size as small as 58 nm, shown in Fig. 1a) for PMMA resist, imprinted over the large area of  $0.5 \times 0.5 \text{ mm}^2$  [1].

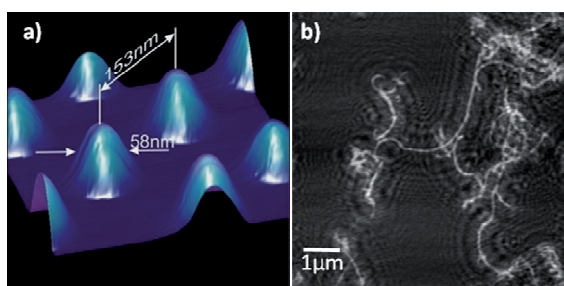


Figure 1. Example of the nanopattern in PMMA obtained using EUV light and IL technique (a) and reconstructed hologram of carbon nanotubes with resolution of 46 nm (b).

Using the EUV laser a high resolution holographic imaging was performed in a Gabor in-line scheme with a wavelength resolution. Low numerical aperture holograms of an AFM tips were imaged with a resolution of  $\sim 160$  nm [2, 3], while high NA hologram of carbon nanotubes, used as an object, was numerically reconstructed with a spatial resolution of  $45.8 \pm 1.9$  nm based on a knife-edge technique and independently

assessed by a Gaussian filtering and correlation method [4]. The result of the reconstruction is shown in Fig. 1b). These experiments were performed at Colorado State University.

Next step in high resolution imaging will be designing and prototyping the EUV microscope based on an incoherent plasma source with gas puff target built at Military University of Technology [5]. The microscope will utilize the diffraction optics, namely Fresnel zone plates, for imaging the object with high magnification and sub-100 nm resolution.

The results show that EUV lasers combined with IL schemes have potential to become a useful compact alternative for printing nanometer features in a university laboratory environment. Short wavelength of the EUV laser opens a possibility for sub-50 nm holographic imaging and may become a photon based, high resolution imaging method complimentary to scanning electron microscopy and atomic force microscopy especially with further development of even shorter wavelength EUV sources in “water window” region. New existing and future sources at MUT may also substantially contribute to the high resolution EUV imaging in the near future.

**Acknowledgements:** This work was supported by the National Science Foundation ERC for Extreme Ultraviolet Science and Technology, Award Number EEC-0310717.

<sup>#</sup>) This work was done during the Ph.D. studies at Colorado State University, Fort Collins, USA, under the supervision of Prof. Mario C. Marconi.

### References:

- [1] P.W. Wachulak, M.G. Capeluto , C. S. Menoni, J.J. Rocca, M.C. Marconi, *Opto-electr. Rev.* **16** (4) (2008) 444–450.
- [2] P.W. Wachulak, M.C. Marconi, R.A. Bartels, C.S. Menoni, J.J. Rocca. *Optics Express* **15** (2007) 10622-10628.
- [3] P.W. Wachulak, R.A. Bartels, M.C. Marconi, C.S. Menoni, J.J. Rocca, Y. Lu, B. Parkinson. *Optics Express* **14** (2006) 9636.
- [4] P.W. Wachulak, M.C. Marconi, R.A. Bartels, C.S. Menoni, J.J. Rocca, *J. Opt. Soc. Am. B* **25** (11) (2008) 1811.
- [5] H. Fiedorowicz, A. Bartnik, R. Jarocki, R. Rakowski, M. Szczurek, H. Daido, N. Sakaya, M. Suzuki, H. Nagatomo, H. Tang, Ch.I. Woo, Y. Tohayam, S. Yamagami, T. Nakayama, *Proc. SPIE*, vol. 3767(1999) 10–20 .

# THE DETERMINATION OF MOLECULAR STRUCTURE OF 2-METHYLCYCLOHEXANONE

**H. Drozdowski \*** and **K. Nowakowski**

*Faculty of Physics, Adam Mickiewicz University, ul. Umultowska 85, PL 61-614 Poznań, Poland*

*Keywords: molecular structure function, X-ray diffraction*

\*) e-mail: riemann@amu.edu.pl

The atomic and molecular structure of 2-methylcyclohexanone at 293 K was investigated using the X-ray diffraction method [1]. Monochromatic radiation MoK $\alpha$  enabled determination of the scattered radiation intensity between  $S_{min} = 0.430 \text{ \AA}^{-1}$  and  $S_{max} = 14.311 \text{ \AA}^{-1}$ . The curves of reduced radiation intensity were analysed by the reduction method of Blum and Narten [2].

The aim of the study was to establish the role of the cyclohexane ring and the functional groups ( $-CH_3$ ,  $=O$ ) attached to it of the molecule of the liquid studied. The numbering scheme is defined in Fig. 1.

The bond distances used were: C(1)–O = 1.22 Å; C(1)–C(2) = C(2)–C(3) = C(3)–C(4) = 1.53 Å; C(2)–H = C(3)–H = 1.09 Å. The mean least inter- and intramolecular distances were determined with the following accuracy: for  $1.0 < r \leq 2.0 \text{ \AA}$ :  $\Delta r = \pm 0.01 \text{ \AA}$ , for  $2.0 \leq r \leq 3.0 \text{ \AA}$ :  $\Delta r = \pm 0.02 \text{ \AA}$ , for  $3.0 \leq r \leq 4.0 \text{ \AA}$ :  $\Delta r = \pm 0.05 \text{ \AA}$  [3].

The results permitted the determination of the intermolecular and intramolecular distances, the coordination numbers and the packing coefficient [1].

The packing coefficient of molecules in liquid 2-methylcyclohexanone is approximately 58%.

In the liquid 2-methylcyclohexanone the neighbouring molecules assume the arrangement in which their dipole moments are antiparallel [1]. The methyl group  $-CH_3$  shows the  $C_{3v}$  symmetry (Fig. 1).

Because of the supposed role of the cyclohexyl ring and the functional groups:  $=O$  and  $-CH_3$  attached to it at the equatorial position, for mutual configurations of molecules in liquid 2-methylcyclohexanone, it seems very probable that the proposed model of local arrangement can also hold for other derivatives of cyclohexane in the liquid phase.

## References

- [1] H. Drozdowski, K. Nowakowski, Z. Błaszczałk, "The WAXS studies of cyclohexane derivatives", *Pol. Crystallogr. Meet.* **50** (2008) 79–80.
- [2] H. Drozdowski, "X-ray scattering in liquid  $\beta$ -naphthalene derivatives", *J. Mol. Struct.* **595** (1–3) (2001) 83–92.
- [3] H. Drozdowski, *Badania struktury i korelacji molekularnych ciekłych pochodnych naftalenu metodą dyfrakcji rentgenowskiej* Seria Fizyka Nr 75, (Wydawnictwo Naukowe UAM, Poznań 2001), pp. 43–47.

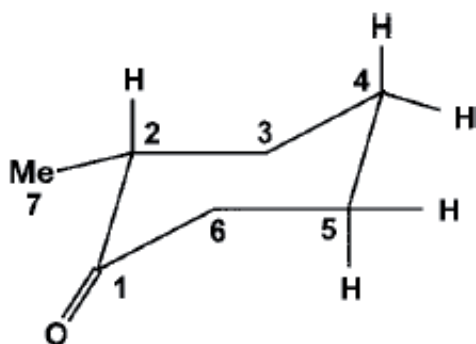


Figure 1. Definition of structural parameters for 2-methylcyclohexanone.

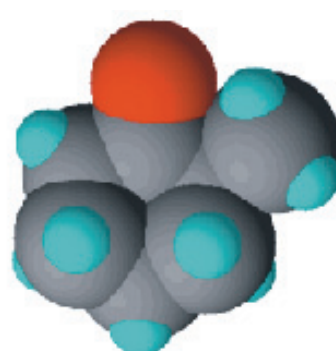


Figure 2. A model of 2-methylcyclohexanone molecule structure.

# STUDY OF THE STRUCTURE AND OF THE INTERNAL ORDERING DEGREE IN LIQUID CYCLOHEXYLAMINE $C_6H_{11}-NH_2$

**H. Drozdowski \* and K. Nowakowski**

Faculty of Physics, Adam Mickiewicz University,  
ul. Umultowska 85, PL 61-614 Poznań, Poland

*Keywords:* angular-distribution function, intermolecular ordering

\*) e-mail: riemann@amu.edu.pl

The study of the structure and molecular correlations of cyclohexylamine is a continuation of earlier works on methylcyclohexane in the liquid phase [1].

The structure of cyclohexylamine (Fig. 1) at 293 K was investigated using the X-ray diffraction method. The scattered intensity distribution was measured for the angles  $6^\circ \leq 2\theta \leq 120^\circ$  at every  $0.2^\circ$ , where  $2\theta$  is the scattering angle. An angular distribution of X-ray radiation scattered in liquid cyclohexylamine was measured (Fig. 2).

The use of short-wave radiation  $MoK_\alpha$  enabled determination of the shortest interatomic distances within cyclohexane ring. The bond distances and bond angles used were:  $C-C = 1.53 \text{ \AA}$ ;  $C-NH_2 = 1.36 \text{ \AA}$ ;  $C-H = 1.09 \text{ \AA}$ ;  $\angle CCC = \angle CCH = \text{regular tetrahedral}$ .

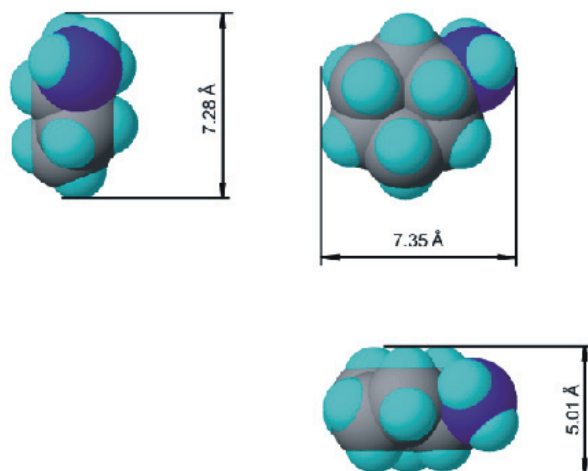


Figure 1. A model of liquid cyclohexylamine structure projected onto three orthogonal planes ( $d = 0.867 \text{ g/cm}^3$ ;  $M = 99.18 \text{ g/mol}$ ;  $V_0 = 190 \text{ \AA}^3$ ).

A simple model of short-range arrangement of the molecules was proposed [2]. In liquid cyclohexylamine only in the aniparallel conformation the distance between the centres of the amine groups is  $NH_2(1)\dots NH_2(2) = 6.70 \text{ \AA}$  [2].

The interpretation of the results was carried out using the reduction method of Blum and Narten [3].

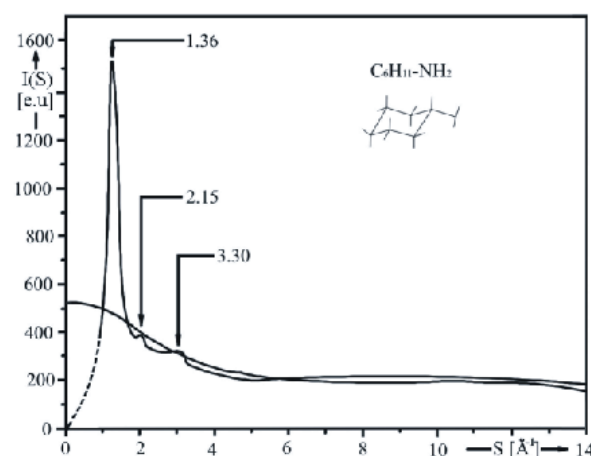


Figure 2. Normalized, experimental curve of angular distribution of X-ray scattered intensity, and total independent scattering curve in liquid cyclohexylamine.

These results are also consistent with the values presumed in the conformational structure investigation of the liquids studied performed by empirical and semi-empirical MOLCAO calculations [4].

## References

- [1] H. Drozdowski, K. Nowakowski, "X-ray diffraction studies of liquid methylcyclohexane  $C_6H_{11}-CH_3$  structure at 293 K", *Acta Phys. Polon. A* **114** (2) (2008) 383–389.
- [2] H. Drozdowski, K. Nowakowski, Z. Błaszczyk, "A relation between X-ray diffraction based liquid cyclohexylamine  $C_6H_{11}-NH_2$  structure and packing coefficient", *Pol. Crystallogr. Meet.* **51** (2009) 268–269.
- [3] H. Drozdowski, K. Nowakowski, "X-ray scattering in liquid cyclohexane derivatives at 293 K", *J. Mol. Struct.* (2009) in press.
- [4] J.M. Haile, *Molecular Dynamics. Elementary Methods* (John Wiley & Sons, New York, 1992).

# INTERACTIONS OF CATIONIC GEMINI SURFACTANTS WITH DMPC

**Z. Pietralik, M. Chrabaśczewska, and M. Kozak\***

*Department of Macromolecular Physics, Faculty of Physics A. Mickiewicz University,  
ul. Umultowska 85, 61-614 Poznań, Poland*

*Keywords: phospholipids, DMPC, Gemini surfactants, small angle X-ray scattering*

\*) e-mail: mkozak@amu.edu.pl

In water solutions phospholipids exhibit tendency to aggregation and formation of different structural phases (lamellar, cubic, hexagonal *etc.*) [1]. In mixtures of phospholipids with short-chain phospholipids or surfactants the bicellar phase can be formed [2].

The study has been performed on the model systems of biological membranes obtained on the basis of 1,2-dimyristoyl-sn-glycero-3-phosphocholine (DMPC) and cationic gemini surfactants – derivatives of 1,1'-(1,4-butane)bis 3-alkyloxymethylimidazolium chlorides (with octyl, decyl and cyclododecyl chains).

A series of the SAXS measurements were performed at DESY, EMBL Beam Line X33, (Hamburg, Germany) [3] using the synchrotron radiation ( $\lambda = 0.15 \text{ nm}$ ) and the Mar 345 image plate detector. The measurements were performed at temperatures ranging from 6 to 30°C and for the scattering vector  $0.05 < s < 5.0 \text{ nm}^{-1}$  ( $s = 4\pi \sin \theta / \lambda$ ). Additional SAXS data set was collected in MaxLab, Beam Line 7-11 (Lund, Sweden) [4]. The data were collected at temperatures from 6 to 30°C for the scattering vector  $0.05 < s < 3.6 \text{ nm}^{-1}$  using the synchrotron radiation ( $\lambda = 0.1066 \text{ nm}$ ) and the MAR 165 CCD detector.

All data sets were normalized to the incident beam intensity, corrected for detector response and the scattering of the buffer was subtracted using the computer program PRIMUS [5].

The SAXS results implied a gradual disappearance of the lamellar phase typical of DMPC and a probable formation of the bicellar phase. Also the temperature range of the main phase transition in DMPC was shifted towards lower temperatures.

**Acknowledgements:** The research was supported in part by research grant (No. N N202 248935) from the Ministry of Science and Higher Education (Poland). The data collection was supported by EC - EMBL Hamburg Outstation, contract number: RII3-CT-2004-506008. The data collection in MAXLab were supported by the EC - Research Infrastructure Action under the FP6 "Structuring the European Research Area" Programme (through the Integrated Infrastructure Initiative "Integrating Activity on Synchrotron and Free Electron Laser Science").

## References

- [1] R. Koynova, M. Caffrey, "Phases and phase transitions of the phosphatidylcholines," *BBA-Rev Biomembranes* **1376** (1998) 91-145.
- [2] J. Katsaras, T.A. Harroun, J. Pencer, M.P. Nieh, "«Bicellar» lipid mixtures as used in biochemical and biophysical studies," *Naturwiss.* **92** (2005) 355–366.
- [3] M.W. Roessle, R. Klaering, U. Ristau, B. Robrahn, D. Jahn, T. Gehrmann, P. Konarev, A. Round, S. Fiedler, C. Hermes, D.I. Svergun, "Upgrade of the small-angle X-ray scattering beamline X33 at the European Molecular Biology Laboratory, Hamburg," *J. Appl. Crystallogr.* **40** (2007) 190–194.
- [4] M. Knaapila, C. Svensson, J. Barauskas, M. Zackrisson, S.S. Nielsen, K.N. Toft, B. Vestergaard, L. Arleth, U. Olsson, J.S. Pedersen, Y. Cerenius, "A new small-angle X-ray scattering set-up on the crystallography beamline I711 at MAX-lab," *J. Synchrotron Radiat.* **16** (2009) 498–504.
- [5] P.V. Konarev, V.V. Volkov, A.V. Sokolova, M.H.J. Koch, D.I. Svergun, "PRIMUS: a Windows PC-based system for small-angle scattering data analysis," *J. Appl. Crystallogr.* **36** (2003) 1277–1282.

# COMPOSITION AND STRUCTURE OF CZOCHRALSKI SILICON IMPLANTED WITH $H_2^+$ AND $Mn^+$ AND ANNEALED UNDER ENHANCED HYDROSTATIC PRESSURE

**M. Kulik**<sup>1</sup>, **A.P. Kobzew**<sup>2</sup>, **A. Misiuk**<sup>3</sup>, **W. Wierzchowski**<sup>4</sup>, **K. Wieteska**<sup>5</sup>,  
**J. Bak-Misiuk**<sup>6</sup>, **A. Wnuk**<sup>3</sup>, and **B. Surma**<sup>3</sup>

<sup>1</sup> Institute of Physics, Maria Curie-Skłodowska University, Lublin,  
Pl. Marii Curie-Skłodowskiej 1, 20-031 Lublin, Poland

<sup>2</sup> Joint Institute for Nuclear Research JINR, Joliot-Curie 6, 141980 Dubna, Moscow region, Russia

<sup>3</sup> Institute of Electron Technology, Al. Lotników 46, 02-668 Warsaw, Poland

<sup>4</sup> Institute of Electronic Materials Technology, 01-919 Warsaw, Poland

<sup>5</sup> Institute of Atomic Energy, 05-400 Otwock-Świerk, Poland

<sup>6</sup> Institute of Physics, PAS, Al. Lotników 32/46, 02-668 Warsaw, Poland

*Keywords:* Czochralski silicon, implantation, high pressure, diffraction

Depth distribution of implanted species and microstructure of oxygen-containing Czochralski grown silicon (Cz-Si) implanted with light (such as  $H^+$ ; Si:H is important for so called smart cut processing [1]) or heavy ions (such as  $Mn^+$ ; Si:Mn is considered as promising material for spintronics [2]) are strongly influenced by hydrostatic pressure (HP) applied during the post-implantation treatment.

Composition and structure of Si:H (prepared by implantation of Cz-Si with  $H_2^+$ ; dose,  $D = 1.7 \times 10^{17} \text{ cm}^{-2}$ , energy,  $E = 50 \text{ keV}$ , (projected range of  $H_2^+$ ,  $R_p(H) = 275 \text{ nm}$ ) and of Si:Mn (implantation with  $Mn^+$ ;  $D = 1 \times 10^{16} \text{ cm}^{-2}$ ,  $E = 160 \text{ keV}$ ,  $R_p(Mn) = 140 \text{ nm}$ ), processed at up to 923 K under Ar pressure up to 1.2 GPa for up to 10 h, were investigated by ERD, RBS, and photoluminescence methods.

The defect structure of Si:Mn was also investigated by synchrotron diffraction topography at HASYLAB (Germany). High sensitivity to strain associated with small inclusions and dislocation loops was provided by

monochromatic ( $\lambda = 0.1115 \text{ nm}$ ) beam topography. High resolution X-ray diffraction was also used.

As it follows from ERD measurements (Fig. 1), HP applied during annealing of Si:H at 723–923 K affects strongly the distribution of implanted hydrogen preventing in part its out-diffusion.

Processing of Si:Mn under HP at up to 920 K for up to 10 h did not produce resolved structure defects. On the other hand, just such processing results in magnetic ordering [3]. Synchrotron topography made it possible to detect strains and large defects related to Si:Mn sample bending and unhomogeneity.

## References

1. A. Misiuk, A. Shalimov, B. Surma, J. Bak-Misiuk, A. Wnuk, *J. Alloys Comp.* **401** (2005) 205.
2. A. Wolska, K. Lawniczak-Jablonska, M. Klepka, W.S. Walczak, A. Misiuk, *Phys. Rev. B* **75** (2007) 113201.
3. W. Osinniy, A. Misiuk, M. Szot, K. Swiatek, J. Bak-Misiuk, A. Barcz, W. Jung, *Mater. Sci. - Poland* **26** (2008) 751.

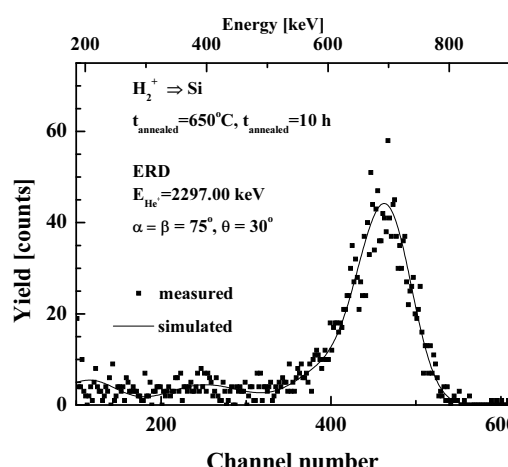


Figure 1. Typical spectrum of hydrogen measured by ERD methods.

# HIGH-TEMPERATURE STUDIES OF $\text{Pb}_{1-x}\text{Cd}_x\text{Te}$ SOLID SOLUTION: STRUCTURE STABILITY AND CdTe SOLUBILITY LIMIT

R. Minikayev<sup>1</sup>, E. Dynowska<sup>1</sup>, P. Dziawa<sup>1</sup>, E. Kamińska<sup>2</sup>,  
A. Szczerbakow<sup>1</sup>, D. Trots<sup>3</sup>, and W. Szuszkiewicz<sup>1\*</sup>

<sup>1</sup> Institute of Physics, Polish Academy of Sciences, Al. Lotników 32/46, 02-668 Warsaw, Poland

<sup>2</sup> Dept. of Mathematics and Natural Science, College of Science, Cardinal Stefan Wyszyński University,  
ul. Dewajtis 5, 01-815 Warsaw, Poland

<sup>3</sup> Institute for Materials Science, Darmstadt University of Technology,  
Petersenstr. 23, D-64287 Darmstadt, Germany

*Keywords:* X-ray powder diffraction, lattice parameter, solubility limit, precipitate

\*) e-mail: szusz@ifpan.edu.pl

## 1. Introduction

The solid solution of lead telluride with cadmium telluride constitutes an attractive system for developing of the mid-IR optoelectronic devices based on quantum dots. The thermo-electric properties of  $\text{Pb}_{1-x}\text{Cd}_x\text{Te}$  solution are also considered as a basis of other possible devices. These applications are powered by extremely low solubility of both materials [1] resulting from the difference in their crystal structure - rock-salt (RS) for PbTe and zinc-blende (ZB) for CdTe. It was a reason that only polycrystalline ternary  $\text{Pb}_{1-x}\text{Cd}_x\text{Te}$  bulk samples obtained by Bridgman growth technique were so far available. Recently, the successful growth of  $\text{Pb}_{1-x}\text{Cd}_x\text{Te}$  single crystals of 1 ccm volume with (100) natural crystal facets, and Cd content up to 11 at.% by self-selecting vapour transport method (SSVG) [2] has been reported [3]. In the latter paper the X-ray diffraction revealed the single-phase RS crystal structure of obtained samples and their relatively high crystal quality confirmed by FWHM of 004 X-ray rocking curve of about 100 arcsec. The decrease of the lattice parameter with increasing Cd content  $x$  had linear character with  $da/dx \approx -0.43 \text{ \AA}$  for studied samples. The results of Hall effect and electrical conductivity measurements as well as the photoluminescence measurements were also obtained in the temperature range from 4.2 K to 300 K [3].

The goal of the present work was to study the structure properties of  $\text{Pb}_{1-x}\text{Cd}_x\text{Te}$  solid solution at high temperatures (HT) and to get new information about the phase diagram corresponding to the system above mentioned.

## 2. Experimental details

In this work the analysis of selected structure properties of  $\text{Pb}_{1-x}\text{Cd}_x\text{Te}$  (where  $x = 0; 0.013; 0.056; 0.096$ ) were studied by X-ray diffraction measurements performed at temperatures ranging from 301 K to 1073 K. First, good quality single  $\text{Pb}_{1-x}\text{Cd}_x\text{Te}$  crystals grown by SSVG method were powdered and analysed at room temperature (RT) using X'Pert Philips diffractometer and Cu  $K_{\alpha 1}$  radiation. Later on, the HT measurements using a synchrotron radiation were carried out taking advantage of a powder diffractometer installed at the B2 beamline

at Hasylab/DESY. The instrumental parallel-beam set-up included a Ge(111) double monochromator, and a curved on-site readable imaging plate [4]. The samples were prepared as a mixture of powdered  $\text{Pb}_{1-x}\text{Cd}_x\text{Te}$  crystals and fine diamond powder. For sample mounting a thin-wall quartz capillary was applied. During all measurements the capillary rotates inside a graphite hitter. The radiation wavelength,  $\lambda = 0.5276 \text{ \AA}$ , was calibrated *in situ*, using the diamond standard (advantages of such calibration method have been described in Ref. [5]). For the analysis of the diffraction patterns Rietveld method using the Fullprof.2k (v. 2.70) program was applied [6].

## 3. Results and discussion

The results of preliminary X-ray diffraction measurements performed at RT confirmed a single-phase (RS) character of all investigated  $\text{Pb}_{1-x}\text{Cd}_x\text{Te}$  solid solutions. Figure 1 presents the composition dependence of the lattice parameter value determined in Ref. [3] (shown by the dashed line), values of the lattice parameters corresponding to the samples investigated in the present paper are marked by the open circles in this figure.

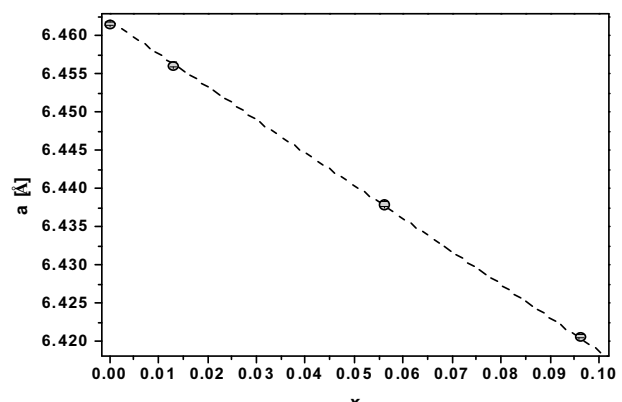


Figure 1. The initial lattice parameter value (determined by X-ray diffraction) versus the chemical composition of  $\text{Pb}_{1-x}\text{Cd}_x\text{Te}$  solid solutions analysed in this paper. The dashed line was taken from Ref. [3].

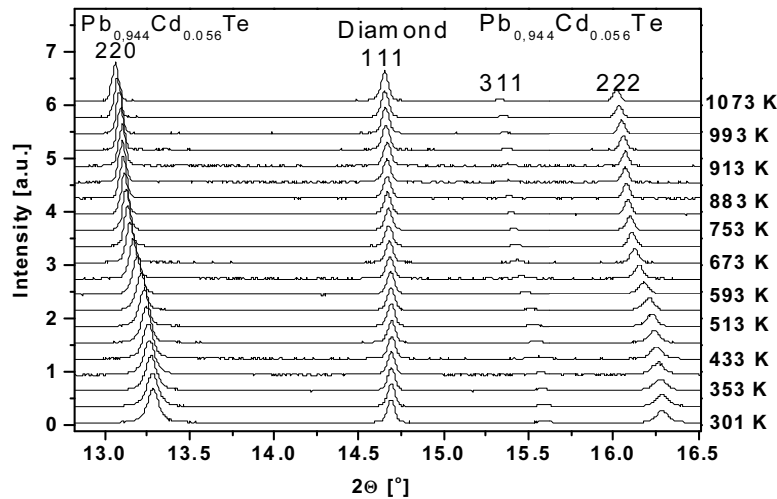


Figure 2. The temperature-dependent peak shift for the sample containing  $\text{Pb}_{0.944}\text{Cd}_{0.056}\text{Te}$  solid solution (the diffraction patterns at limited angular range are shown).

Figure 2 shows a part of the temperature evolution of X-ray diffraction pattern taken with the use of synchrotron radiation for  $\text{Pb}_{0.944}\text{Cd}_{0.056}\text{Te}$  sample. As one can see, the angular shift of Bragg peaks corresponding to the solid solution under studies is slightly different below and above the temperature of about 650 K. The 111 reflection from diamond powder being the internal standard in the analyzed sample is also seen in this figure. The similar data were obtained for other investigated samples.

The example of the result of Rietveld refinement, performed for the diffraction pattern collected at  $T = 301$  K is shown in Fig. 3. The high quality of the analysis taking into consideration the single phase character of  $\text{Pb}_{0.904}\text{Cd}_{0.096}\text{Te}$  solid solution and the diamond powder only excluded possible presence of other crystal phase in the investigated sample.

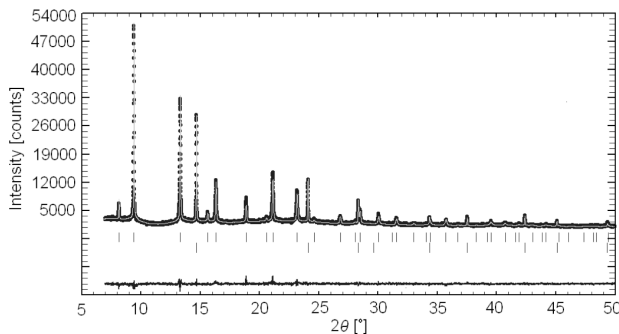


Figure 3. The Rietveld analysis of powder diffraction pattern obtained for the sample containing  $\text{Pb}_{0.904}\text{Cd}_{0.096}\text{Te}$  solid solution and the diamond powder. Points: the experimental data taken with the use of synchrotron radiation, solid line: theoretical curve. The first and the second set of vertical bars correspond to  $\text{Pb}_{0.904}\text{Cd}_{0.096}\text{Te}$  and diamond, respectively.

Due to the application of procedure above mentioned it was possible to demonstrate unexpected, non-monotonous temperature dependence of the lattice parameter value corresponding to every  $\text{Pb}_{1-x}\text{Cd}_x\text{Te}$  sample with the initial  $x$  value different from zero. The comparison of dependences found for all measured samples is given in Fig. 4.

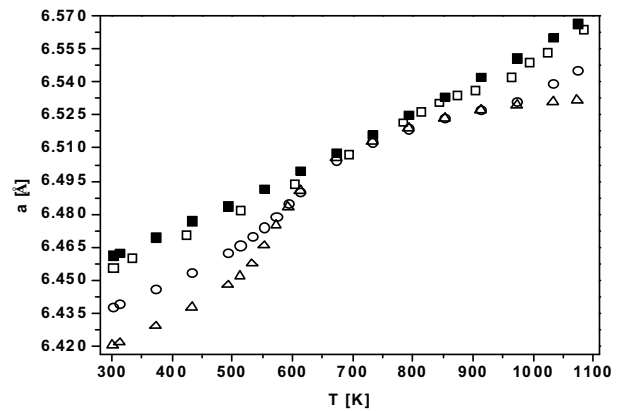


Figure 4. The lattice parameter value versus temperature for all  $\text{Pb}_{1-x}\text{Cd}_x\text{Te}$  solid solutions analysed in this paper. Full squares:  $x = 0$ ; open squares:  $x = 0.013$ ; circles:  $x = 0.056$ ; triangles:  $x = 0.096$ .

The scenario of the temperature evolution of sample structure, corresponding to  $\text{Pb}_{1-x}\text{Cd}_x\text{Te}$  samples with  $x > 0$  may be understood in the following manner. Due to a very rapid sample cooling from the growth temperature (being close to about 1100 K) to room temperature, applied in SSVG method [2, 3], a metastable solid solution was obtained. The exact chemical composition of this solution, determined prior to the accompanied by the HT studies with the use of synchrotron radiation, was far from that corresponding to the solubility limit. Thus, the ‘initial’ sample composition reflected the HT, ‘frozen’ equilibrium state of the solid solution. A partial decomposition of the sample was clearly observed as the

result of increasing sample temperature from about 500 K to 650 K. This effect was indicated by the increase of the lattice parameter significantly higher than the linear one expected on the basis of our data determined for pure PbTe (see Fig. 4). It means that some part of Cd present at the beginning in  $\text{Pb}_{1-x}\text{Cd}_x\text{Te}$  solid solution is missing at higher temperatures. The same time possible creation of the second crystal phase (like, e.g., Cd, Te, or ZB CdTe) was not observed. Due to the lack of new crystal phase at this temperature range one may suppose a creation of an amorphous CdTe precipitates or clusters in the sample. The minimal chemical composition of every solid solution, observed in the present studies, was close to  $x = 0.01$  and corresponded to the temperature of about 650 K. It should be stressed that this composition value does not depend on the ‘initial’ sample composition, as it was demonstrated in Fig. 4. This finding may be interpreted as the real CdTe solubility limit in PbTe for the temperature indicated above. Further increase of temperature resulted in a partial dissolution of CdTe in  $\text{Pb}_{1-x}\text{Cd}_x\text{Te}$  and finally at some, high temperature the final solid solution composition was about the same as that at the beginning of measurements. One may suppose that at this last temperature the second phase (not visible in the diffraction patterns) disappears and the solid solution under investigation starts to be once more one-phase and uniform material. The only exception was the sample initially determined as  $\text{Pb}_{0.904}\text{Cd}_{0.096}\text{Te}$  solid solution. After the measurements performed at high temperatures and cooling down this sample back to RT the ZB CdTe precipitates were observed and the chemical composition of the final solid solution was estimated as equal to  $x \approx 0.08$ .

The scenario described above is not new. The possible creation of temperature activated precipitates in systems composed of two substances characterized by a broad miscibility gap has been reported and discussed in the literature for a few systems composed of selected II-VI and IV-VI semiconducting compounds exhibiting ZB (or wurtzite) structure and RS structure, respectively [7-10]. The new results presented in this paper completed published previously phase diagram for PbTe-CdTe system [8, 11] limited in the past to temperatures above 870 K and solid solution compositions exceeding the value  $x = 0.05$ .

#### 4. Conclusions

Due to the access to bulk  $\text{Pb}_{1-x}\text{Cd}_x\text{Te}$  solid solution it was possible to contribute to the phase diagram of this system for  $x < 0.1$  and  $T < 1100$  K. In particular, new

information concerning the CdTe solubility limit in PbTe was obtained. Such findings may have important influence on the optimization of material devoted to possible future applications.

**Acknowledgements:** The research leading to these results has received funding from the European Community's Seventh Framework Programme (FP7/2007-2013) under grant agreement n° 226716. Partial financial support of RM, ED, and WSz by the Ministry of Sciences and Higher Education (Poland) through grant DESY/68/2007 is also acknowledged.

#### References

- [1] T. Schwarzl, E. Kaufmann, G. Springholz, K. Koike, T. Hotei, M. Yano, W. Heiss, "Temperature-dependent midinfrared photoluminescence of epitaxial PbTe/CdTe quantum dots and calculation of the corresponding transition energy", *Phys. Rev. B* **78** (2008) 165320.
- [2] A. Szczerbakow, K. Durose, "Self-selecting vapour growth of bulk crystals – principles and applicability ", *Prog. Cryst. Growth Charact. Mater.* **51** (2005) 81.
- [3] M. Szot, A. Szczerbakow, K. Dybko, L. Kowalczyk, E. Smajek, M. Bukała, M. Galicka, P. Sankowski, R. Buczko, P. Kacman, V. Domukhovski, E. Łusakowska, P. Dziawa, A. Mycielski, T. Story, "Experimental and theoretical analysis of PbTe-CdTe solid solution grown by physical vapour transport method", *Acta Phys. Pol. A* (in press).
- [4] M. Knapp, C. Baehtz, H. Ehrenberg, H. Fuess, "The synchrotron powder diffractometer at beamline B2 at HASYLAB/DESY: status and capabilities", *J. Synchr. Radiation* **11** (2004) 328.
- [5] W. Paszkowicz, M. Knapp, C. Bähtz, R. Minikayev, P. Piszora, J.Z. Jiang, R. Bacewicz, "Synchrotron X-ray wavelength calibration using a diamond internal standard: application to low-temperature thermal-expansion studies ", *J. Alloys Compds* **382** (2004) 107.
- [6] J. Rodriguez-Carvajal, "Line Broadening analysis using FullProf\*: determination of microstructural properties", *Newslett. IUCr Commission Powd. Diff.* **26** (2001) 12.
- [7] V. Leute, N.J. Haarmann, H.M. Schmidtke, "Solid state reactions in the quasaternary system (Cd, Pb)(S, Te)", *Z. Phys. Chem.* **190** (1995) 253.
- [8] V. Leute, R. Schmidt, "The quasaternary system  $(\text{Cd}_k\text{Pb}_{1-k})(\text{S}/\text{Te}_{1-l})$ ", *Z. Phys. Chem.* **172** (1991) 81.
- [9] V. Leute, A. Jamour, "Double conversions between PbS-single crystals and polycrystalline CdTe in solid state", *J. Phys. Chem. Solids* **32** (1971) 1435.
- [10] H.M. Schmidtke, V. Leute, "Investigation of the reaction between a CdSe-crystal and a Pb and S containing reactive gas phase", *J. Phys. Chem. Solids* **45** (1984) 547.
- [11] N.Kh. Abrikosov, *Semiconducting II-VI, IV-VI, and V-VI Compounds* (Plenum Press, New York, 1969).

## XRD STUDIES OF NB/SAPPHIRE(001) THIN FILMS DEPOSITED WITH THE ULTRA-HIGH-VACUUM CATHODIC ARC TECHNIQUE

**R. Nietubyc<sup>1\*</sup>, W. Caliebe<sup>2</sup>, E. Dynowska<sup>3</sup>, K. Nowakowska-Langier<sup>1</sup>, J. Pełka<sup>3</sup>, and P. Romanowski<sup>3</sup>**

<sup>1</sup> The Andrzej Soltan Institute for Nuclear Studies, Świerk, Poland

<sup>2</sup> Hasylab at DESY, Notkestr. 85, D-22603 Hamburg, Germany

<sup>3</sup> Institute of Physics PAS, Warsaw, Poland

*Keywords:* thin metallic films, x-ray diffraction

\*) e-mail: r.nietubyc@ipj.gov.pl

Niobium films on the single crystal substrate have been studied. The films of thicknesses less than 5 nm, 5 nm, 15 nm and 400 nm were deposited onto sapphire (001) surface by mean of the cathodic arc in UHV conditions [1-3]. Energy of incoming Nb<sup>3+</sup>ions in the range of tens electronvolts and substrate temperature about 200°C are distinctive characteristics of that deposition method. The aim of performed XRD studies was to recognize the structural forms of Nb film formed in the early stages of growth. The measurements were preformed at the wiggler beamline W1 using the photon energy 8048 eV corresponding to the wavelength  $\lambda = 0.15406$  nm (Cu K<sub>α1</sub> characteristic line).

According to our studies, the growth of Nb layer is realized in three stages: the first one is the growth of very

thin and preferably (110)-oriented layer. In the next stage an increasing of the layer thickness lead to the almost single crystal layer with (110) lattice planes parallel to the substrate surface. In the last stage, observed for the thickest layer, the appearance of thin polycrystalline Nb layer, probably on the surface, have been observed.

### References

- [1] R. Nietubyc, J. Pelka, M.J. Sadowski, P. Strzyżewski, *AIP Conf. Proc.* **993** (2008) 415.
- [2] P. Strzyżewski, M.J. Sadowski, R. Nietubyc, K. Rogacki, W. Paszkowski, T. Paryjczak, J. Rogowski, *Mater. Sci.–Poland* **26** (2008) 213.
- [3] J. Langner, R. Mirowski, M.J. Sadowski, P. Strzyżewski, J. Witkowski, S.Tazzari, L. Catani, A. Cianchi, J. Lorkiewicz, R. Russo, *Vacuum* **80** (2006) 1288.

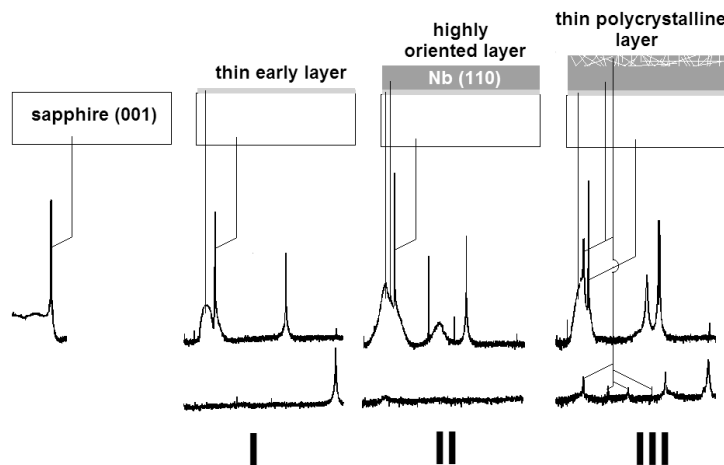


Figure 1. The growth of Nb film as seen with the x-ray eye.

# COLLOIDAL ZnO AND ZnO/MgO CORE/SHELL NANOCRYSTALS - SYNTHESIS AND PROPERTIES

**B. Sikora, A. Baranowska-Korczyk, W. Zaleszczyk, A. Nowicka, K. Fronc, W. Knoff,  
K. Gas, W. Paszkowicz, W. Szuszkiwicz, K. Świątek, Ł. Kłopotowski, K. Sobczak,  
P. Dlużewski, G. Karczewski, T. Wojtowicz, I. Fijalkowska, and D. Elbaum**

*Institute of Physics, Polish Academy of Sciences, Al. Lotników 32/46 02-668 Warsaw, Poland*

*Keywords:* zinc oxide, , nanoparticles, nanocrystals, quantum dots

\*) e-mail: sikorab@ifpan.edu.pl

ZnO nanocrystals nad ZnO/MgO core/shell nanocrystals have interesting biological properties (antibacterial, antifungal). ZnO nanocrystals have recently attracted a lot of attention as promising candidates for novel devices, due to a possibility of continuous tuning of optical and electronic properties by varying the particle sizes. They are also of interest for pharmaceutical industry, medicine and/or biology. Obtained nanocrystals were characterized structurally by Atomic Force Microscopy (AFM), Transmission Electron Microscopy (TEM) (Fig 1), X-ray diffraction (Fig. 2) and optically by absorption and emission.

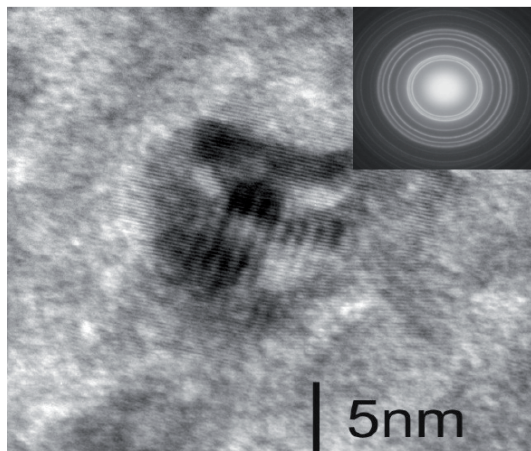


Figure 1. Transmission Electron Microscopy of the ZnO nanocrystals proved a wurtzite crystalline structure.

We prepared ZnO nanocrystals in colloidal suspensions using a sol-gel method. The growth was carried out in various solvents, different incubation times, and temperatures. By measuring the absorbance, and emission of the nanocrystals solution, we monitored the growth. We observed a decrease of the reaction activation energy with an increase in the polarity of the applied solvent. Therefore, the growth rate was higher in a solvent with greater dielectric constant. With increasing nanocrystal sizes the absorption onset was red-shifted. An effective mass approximation model [1] was used to determine the nanocrystal radii. The results were compared with sizes obtained from AFM analysis and a good correlation was found. Depending on conditions and reaction time, we obtained nanocrystals with radii ranging from 2 to 5 nm. Photoluminescence spectra

revealed two emission bands. One (narrow 10 nm line width), observed around 375 nm, due to a band-to-band recombination. This PL line behaved analogously to the absorption onset, red-shifted with increasing nanocrystal size. The other emission band was a broad (100 nm line width), centered around 530 nm, probably related to oxygen vacancies.

Addition of MgO shell resulting in a more intense and stable visible emission that is characteristic of nanocrystalline ZnO. MgO prevents aggregation of ZnO nanoparticles.

XRD patterns of powdered ZnO/MgO nanocrystals and TEM data proved wurtzite crystalline structure.

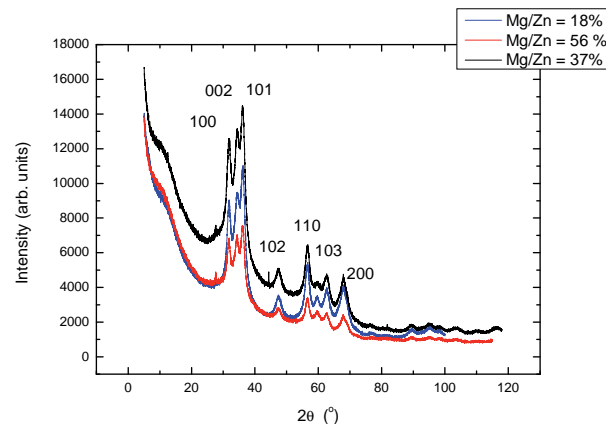


Figure 2. X-ray diffraction pattern (wavelength 1.54060 Å) for ZnO/MgO core/shell powder as a function of thickness shell. The Zn:Mg ratio was: 18%, 37% and 56%. The results proved the wurtzite crystalline structure.

**Acknowledgements:** The research was partially supported by the European Union within European Regional Development Fund, through grant Innovative Economy (POIG.01.01.02-00-008/08) and was partially supported by the Ministry of Science and Higher Education (Poland) through Grant No. N515 015 32/0997 and No. N N518 424036.

## References

- [1] S. Monticone, R. Tufeu, A.V. Kanaev, "Complex nature of the UV and visible fluorescence of colloidal ZnO Nanoparticles", *J. Phys. Chem. B.* **102** (1998), 2854–2862.

## ZnO NANOFIBERS PREPARED BY ELECTROSPINNING – CHARACTERIZATION AND DOPING

**A. Baranowska-Korczyc\***, **B. Sikora**, **W. Zaleszczyk**, **A. Nowicka**, **K. Fronc**, **W. Knoff**,  
**P. Dziawa**, **K. Gas**, **W. Paszkowicz**, **R. Minikayev**, **W. Szuszakiewicz**, **K. Świątek**,  
**T. Wojciechowski**, **A. Reszka**, **Ł. Kłopotowski**, **K. Sobczak**, **P. Dłużewski**,  
**G. Karczewski**, **T. Wojtowicz**, **J. Bujak**, and **D. Elbaum**

*Institute of Physics, Polish Academy of Sciences, Al. Lotników 32/46, 02-668 Warsaw, Poland*

*Keywords:* zinc oxide, nanowire

\*) e-mail: akorczyc@ifpan.edu.pl

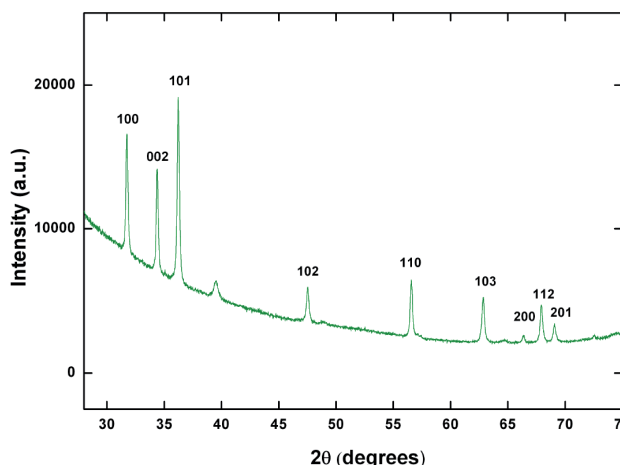


Figure 1. XRD result of ZnO nanofibers (calcination temperature: 500°C).

Electrospinning is a method capable to produce fibers with diameters ranging from tens of nanometer to microns. Electrospun nanofibrous scaffolds have great potential in several biomedical applications, such as wound dressing, enzyme immobilization, drug delivery, tissue engineering, and they can serve as materials for biosensors. Semiconductor nanofibers are also candidates for applications in electronics and optoelectronics.

We synthesized zinc oxide (ZnO) nanofibers by sol-gel processing. The first step was to form the nanofibres by electrospinning technique using a suspension of zinc acetate in poly(vinyl alcohol) (PVA) or poly(ethylene oxide) (PEO) as precursors. Then, the nanofibres were calcined in air at 500°, 600°, 700°C [1] for 4 h to obtain ZnO nanofibers [2, 3]. By adding acetates of other metals, we obtained nanofibers doped with Co, Fe, Al, Mn, Mg.

Structural characterization was performed by Atomic Force Microscopy (AFM), Scanning Electron Microscopy (SEM), and X-ray diffraction (XRD). Additionally, optical characterization was done by cathodoluminescence (CL) and photoluminescence (PL) measurements at room temperature.

XRD investigations proved that the nanofiber material is a wurtzite ZnO (Fig. 1, Fig. 2). AFM and

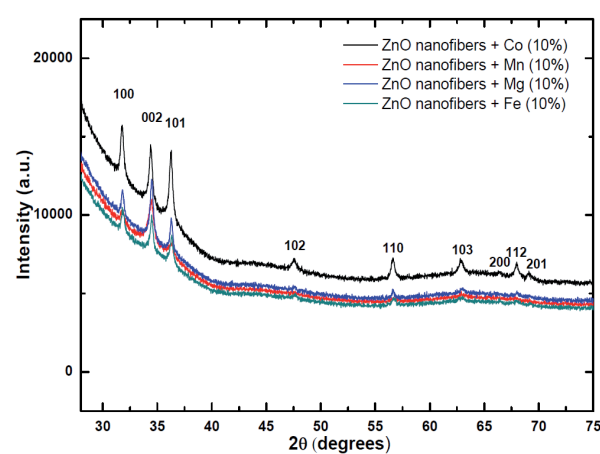


Figure 2. XRD result of Co, Mn, Mg and Fe doped ZnO nanofibers (calcination temperature: 500°C).

SEM studies both revealed nanofiber diameters ranging from 100 to 300 nm. Moreover, SEM images of undoped ZnO show that the nanofibers consist of nanocrystallites which diameters from 10 to 50 nm as jointly determined by XRD and SEM (Fig. 3). However, metal-doped nanofibers contain significantly smaller nanocrystallites.

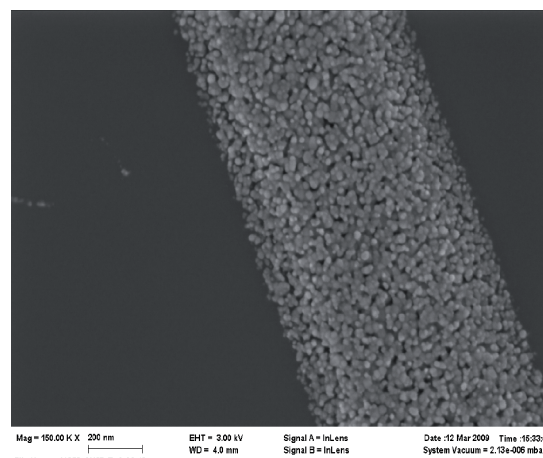


Figure 3. SEM image of ZnO nanofibers (calcination temperature: 500°C).

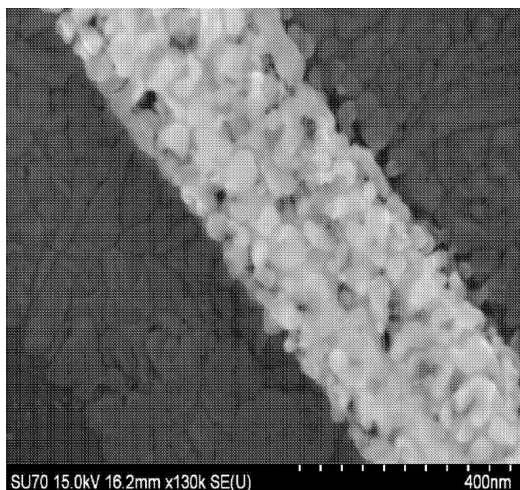


Figure 4. SEM image of ZnO nanofibers (calcination temperature: 700°C).

PL spectra of undoped nanofibers consist of two emission bands. One, centered around 390 nm, is due to ZnO band-to-band recombination. The other one, a defect band 200 nm wide centered around 550 nm most probably originates from oxygen vacancies. These emission lines are absent in PL spectra of Co-doped

nanofibers. In this case, the emission is dominated by an intra-Co transition at 689 nm, proving that Co ions are incorporated into ZnO lattice. Moreover, preliminary PL studies of single nanofibers were performed.

The effect of ZnO nanofibers calcination temperature was investigated by SEM. We observed increased crystal size (*cf.* Fig. 4) and investigated the evolution of CL spectra with growing calcination temperatures.

**Acknowledgements:** The research was partially supported by the European Union within European Regional Development Fund, through grant Innovative Economy (POIG.01.01.02-00-008/08) and was partially supported by the Ministry of Science and Higher Education (Poland) through Grant No. N515 015 32/0997.

## References

- [1] J.Y. Park, S.S. Kim, "Growth of nanograins in electrospun ZnO nanofibers," *J. Am. Ceram. Soc.* **92** (2009) 1691–1694.
- [2] H. Wu, D. Lin, R. Zhang, W. Pan, "ZnO nanofiber field-effect transistor assembled by electrospinning," *J. Am. Ceram. Soc.* **2** (2008) 656–659.
- [3] H.R. Siddheswaran, R. Sankar, M. Ramesh Babu, M. Rathnakumari, R. Jayavel, P. Murugakoothan, P. Sureshkumar, "Preparation and characterization of ZnO nanofibers by electrospinning," *Cryst. Res. Technol.* **41** (2006) 446–449.

## SOLUTION STRUCTURE OF RAR1-GST-TAG FUSION PROTEIN

**M. Kozak<sup>1\*</sup>, M. Taube<sup>1</sup>, E. Banachowicz<sup>2</sup>, and A. Jarmołowski<sup>3</sup>**

<sup>1</sup> Department of Macromolecular Physics, Faculty of Physics, A. Mickiewicz University,  
ul. Umultowska 85, 61-614 Poznań, Poland

<sup>3</sup> Department of Gene Expression, Institute of Molecular Biology and Biotechnology, Faculty of Biology,  
A. Mickiewicz University, Umultowska 89, 61-614 Poznań, Poland

<sup>2</sup> Molecular Biophysics Division, Faculty of Physics, A. Mickiewicz University,  
ul. Umultowska 85, 61-614 Poznań, Poland

*Keywords:* small angle X-ray scattering, solution structure, Rar1

\*) e-mail: mkozak@amu.edu.pl

Plants are able to recognize pathogen attack and respond to them by R gene triggered resistance and cell death [1, 2]. Rar1 protein is a common element of signaling pathways in those processes.

Rar1 is a small, monomeric protein (for example Rar1 from *Hordeum vulgare* is characterized by molecular mass of 25.5 kDa and polypeptide chain is build of 232 amino acid residues). Sequence consist of two 60-amino acid zinc binding domains (CHORDs), located on the C- and N-terminus of the protein [1]. In plants a highly conserved motif between those two regions can be found. It is also a zinc binding motif, containing three invariant cysteine and a histidine residues.

At molecular level Rar1 interacts with two important proteins - suppressor of the G2 allele of Skp1 (SGT1) and heat-shock protein 90 (HSP90) via respectively CHORDI and CHORDII domains [2].

The low-resolution structure and conformation of Rar1-Glutathione S-transferase-tag fusion protein from barley in solution has been studied by small angle scattering of synchrotron radiation (SAXS).

SAXS measurements were preformed on the X-33 EMBL beamline at DESY, Hamburg (Germany) using the Pilatus photon counting detector. Protein samples (4.7, 7.5, 15.3 mg/ml) were measured in 50 mM Tris/HCl pH 7.6 using synchrotron radiation (wavelength  $\lambda=0.15$  nm) at temperature 283 K. The sample-to-detector distance was 1.7 m, corresponding to the scattering vector range form 0.057 to 5.178 nm<sup>-1</sup> ( $s = 4\pi\sin\theta/\lambda$  where  $2\theta$  is the scattering angle).

The overall structural parameters characterizing molecule, such as maximum diameter  $D_{\max}$  and radius of gyration were computed using GNOM. The Rar1-GST fusion protein forms in solution dimers characterized by  $R_G=6.19$  nm and  $D_{\max}=23$  nm.

Using experimental SAXS curve also the 3D model has been reconstructed using *ab initio* methods and program DAMMIN [3]. The exemplary low resolution model in solution is presented in Fig. 1.

We also compared the low resolution model of particle with structure predicted by homology-modelling using SWISS-MODEL ([www.expasy.ch](http://www.expasy.ch)).

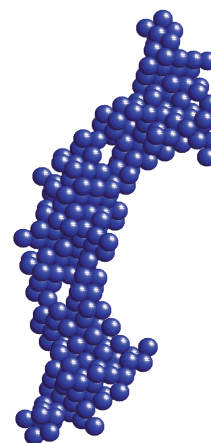


Figure 1. Low-resolution model of Rar1-Glutathione S-transferase-tag fusion protein in solution reproduced by DAMMIN.

**Acknowledgements:** The data collection was supported by European Community - EMBL Hamburg Outstation, contract number: RII3-CT-2004-506008.

### References

- [1] K. Shirasu, T. Lahaye, M.W. Tan, F. Zhou, C. Azevedo, "A novel class of eukaryotic zinc-binding proteins is required for disease resistance signaling in barley and development in *C. elegans*," *Cell* **99** (1999) 355–366.
- [2] C.T. Heise, C.S. Le Duff, M. Boter, C. Casais, J.E. Airey, A.P. Leech, B. Amigues, R. Guerois, G.R. Moore, K. Shirasu, C. Kleanthous, "Biochemical characterization of Rar1 cysteine- and histidine-rich domains (CHORDs): A novel class of zinc-dependent protein–protein interaction modules," *Biochem.* **46** (2007) 1612–1623.
- [3] D.I. Svergun, "Restoring low resolution structure of biological macromolecules from solution scattering using simulated annealing," *Biophys. J.* **76** (1999) 2879–2886.

## Membership of Poland in ESRF

Starting from year 2004, Poland is an Associated Member of the European Synchrotron Radiation Facility (ESRF) in Grenoble, France. Nevertheless, one should remember that this is not given us for ever. In July 2006, a three-years project for financing the participation of Poland at the level of 1% of ESRF budget was approved by Ministry of Science and Poland joined 25 European countries (including Israel) belonging to ESRF. Since that date, for the scientists from Polish academic and scientific institutions applications for beamtime at the ESRF experimental stations became possible. Prof. K. Jablonska was the leader of the project which was allocated at the Institute of Physics Polish Academy of Science in Warsaw. This project ended in June 2009. The web page of the Polish membership in ESRF can be found at [http://info.ifpan.edu.pl/esrf/Local\\_Publish/](http://info.ifpan.edu.pl/esrf/Local_Publish/), where all useful information about the project are collected.

In order to get financing of Polish contribution to ESRF for next two years, it was necessary to apply for funds to Ministry of Science and High Education in the beginning of 2009. In the application, a report from the project presenting the scientific output from the experiments performed at ESRF had to be prepared. In the Table 1 and histogram (see Fig. 1) the readers can find information about the interest of Polish scientists to the use of ESRF in number of shifts applied from all countries and from Poland and number of shifts available at ESRF and allocated for Polish scientists. As one can see, there is an interest in Polish scientific community in use of this source of radiation and we are quite successful in getting access to ESRF.

Table 1. Shifts allocated for Poland.

Year	All applications		Applications from Poland		Available in ESRF		Allocated for Poland	
	shifts	shifts	percent	shifts	shifts	percent	shifts	shifts
2006/II	15 570	364	2.3%	6 852	180	2.6 %		
2007	29 959	598	2.0%	13 681	240	1.75%		
2008	31 105	661	2.1%	13 836	204	1.5 %		

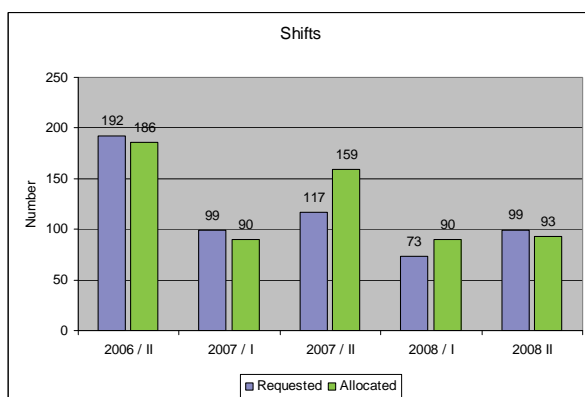


Figure 1. Time evolution of shifts requested (left) and allocated (right) for Poland.

Moreover, the Ministry has asked for various details concerning the use of ESRF; we provided them with the list of institutions contributing in the projects and the corresponding numbers of used shifts. 40 institutions participated in the applications but the final number of beneficent was lower as not all projects have been accepted. In many cases in one project several institutions participated.

We have been asked also to present a list of publications resulting from performed experiments together with the corresponding journal impact factors as well as a list of conference presentations, doctoral theses etc. Unfortunately, the lack of answers from project participants (despite several reminders sent by e-mail) led to a risk of failure of the continuation of financing. I would like to thank Wojciech Paszkowicz for his extensive searching of internet and databases and collecting information about 84 papers published from experiments performed at ESRF. Only due to reporting of so successful output from the ESRF project the approval was received and we are happy to inform that the Ministry has decided to extend the project for next two years. In 2011 it will be necessary to apply again and to again prove that the funds spent for Polish contribution give reasonable scientific profit. Therefore, I would like to ask all of ESRF users to remember about regular visiting the web page of the project and to systematically inform us about all papers, doctoral theses and conference presentations with contribution of data collected at ESRF. In all published information the grant ESRF/73/2006 must be explicitly acknowledged. Following this way and providing the data on publications is crucial for the further access to ESRF. The access to ESRF, although limited and concerning a light source of specific characteristics, is even more important considering fact that policy of the European Union is directed towards strong limitation of the open access to large facilities. So both, the national light sources and the experimentalists using them are expected to lose the financing which helped them in the first decade of 21st century. Moreover, one of machines, DORIS III synchrotron in Hamburg, will be closed in 2012. Unfortunately, the number of beamlines at the replacing Petra ring will be much smaller.

It is a pleasure for me to inform you that Poland being the associated member, for the first time has a representation in the Scientific and Advisory Committee of ESRF. For the three years turn Prof. Mariusz Jaskólski (Poznań) was elected in May 2009 as a representative of all associated members. Moreover, at the 51th ESRF Council meeting in June 2009, it was approved that an associated country can be owner of a national beamlines at ESRF (so called CRG stations). Therefore, new possibilities are in front of us. All is in our hands!!!

K. Jablonska

**10<sup>th</sup> International School and Symposium on  
Synchrotron Radiation in Natural Sciences  
ISSRNS 2010**



**Szklarska Poręba 2010**



Conference site: Hotel LAS

fot. Hotel „LAS”

The 10<sup>th</sup> jubilee International School and Symposium on Synchrotron Radiation in Natural Science (ISSRNS'2008) will be organized by Polish Synchrotron Radiation Society (PTPS) ([www.synchrotron.org.pl](http://www.synchrotron.org.pl)) in cooperation with Adam Mickiewicz University (Poznań, Poland) ([www.amu.edu.pl](http://www.amu.edu.pl)) in hotel “LAS” in Szklarska Poreba (Poland) on 6-12 June 2010.

ISSRNS is a traditional forum for discussing fundamental issues of application of the synchrotron radiation and related methods in natural sciences. The aim of this interdisciplinary meeting is to bring together scientists working with synchrotron radiation. The Symposium will focus on novel applications of synchrotron radiation in physics, chemistry, material and life sciences.

The meeting will be held in the comfortable hotel “LAS” ([www.hotel-las.pl](http://www.hotel-las.pl)) located in Szklarska Poreba (the town near Jelenia Góra, Lower Silesian Voivodeship). Szklarska Poreba is situated in the south-western part of Poland in Karkonosze and Izery mountain range, in the vicinity of large central European cities with international airports (Prague 139 km, Wrocław 140 km away, Dresden 180 km).

Szklarska Poreba region is place known of occurrence of precious ores. There have been classified over 50 minerals, which commonly occur in Karkonosze and Izery mountains. Many of them present properties of such gemstone as: amethyst,

aventurine, topaz, olivine, tourmaline, aquamarine, hyacinth, beryl, moonstone, agate, mountain crystal and smoky quartz. Therefore this beautiful town is known as the Mineralogical Capital of Poland.

Szklarska Poreba is also an important regional and national centre for mountain hiking, cycling and skiing.

The topics of the meeting will cover main areas of applications of synchrotron radiation:

- macromolecular crystallography,
- scattering techniques in structural analysis of condensed matter,
- x-ray absorption, fluorescence and photoelectron spectroscopies,
- x-ray magnetic dichroism,
- x-ray diffraction
- applications of synchrotron radiation in soft matter physics,
- synchrotron radiation in nanosciences,
- synchrotrons, free electron lasers and alternative radiation sources - design and development.

The programme of the Symposium will comprise invited lectures, oral communications (20 minutes) and poster presentations. The abstracts of all presentations presented on ISSRNS will be published in a volume of *Synchrotron Radiation in Natural Science*, and the proceedings in a reputable international journal. The official language of the meeting is English.

### **International Advisory Board**

Francesco d'Acapito - *European Synchrotron Radiation Facility, Grenoble, France*  
Edward Goerlich - *Jagellonian University, Kraków, Poland*  
Jürgen Härtwig - *European Synchrotron Radiation Facility, Grenoble, France*  
Mariusz Jaskólski - *Center for Biocrystallographic Research, Polish Academy of Sciences, Poznań, Poland*  
Andrzej Kisiel - *Jagellonian University, Kraków, Poland*  
Peter Laggner - *Institute of Biophysics and Nanosystems Research, Graz, Austria*  
Andrea Lausi - *Sincrotrone Trieste, Trieste, Italy*  
Jarosław Majewski - *Los Alamos National Laboratory, USA*  
Giorgio Margaritondo - *Ecole Polytechnique Federale de Lausanne, Switzerland*  
Gerhard Materlik - *Diamond Light Source, Didcot, United Kingdom*  
Bronisław Orłowski - *Institute of Physics, Polish Academy of Sciences Warszawa; Polish Synchrotron Radiation Society, Poland*  
Adam Patkowski - *A. Mickiewicz University, Poznań, Poland*  
Christian Riekel - *European Synchrotron Radiation Facility, Grenoble, France*  
Leonid Rivkin - *LPAP Swiss Federal Institute of Technology Lausanne, Paul Scherrer Institute Villigen, Switzerland*  
Masaki Taniguchi - *Hiroshima Synchrotron Radiation Center, Hiroshima University, Japan*  
Ernst Weihreter - *Helmholtz-Zentrum Berlin, Elektronenspeicherring BESSY II, Germany*  
Alexander Wlodawer - *Macromolecular Crystallography Laboratory NCI-Frederick, Frederick, USA*

### **Organizing Committee**

Maciej Kozak (Chairman) - *A. Mickiewicz University, Poznań, Poland*  
Wojciech Kwiatek - *Institute of Nuclear Physics, Polish Academy of Sciences, Kraków, Poland*  
Wojciech Paszkowicz - *Institute of Physics, Polish Academy of Sciences, Warsaw, Poland*  
Paweł Piszora - *A. Mickiewicz University, Poznań, Poland*  
Krystyna Jabłonska - *Institute of Physics, Polish Academy of Sciences, Warsaw, Poland*  
Kamil Szpotkowski - *A. Mickiewicz University, Poznań, Poland*  
Michał Taube - *A. Mickiewicz University, Poznań, Poland*  
Zuzanna Pietralik - *A. Mickiewicz University, Poznań, Poland*

### **For further information, post or e-mail to:**

Maciej Kozak

ISSRNS 2010  
Department of Macromolecular Physics  
Faculty of Physics  
A. Mickiewicz University  
Umultowska 85  
61-614 Poznań  
Poland

Phone. 0048-61-8295266  
Fax: 0048-61-8295245

e-mail : 10issrns@amu.edu.pl  
website: www.10issrns.amu.edu.pl

## **Wspomnienie**

### **Prof. nzw. U.W. dr hab. Jerzy Gronkowski (1949 – 2009)**



Z wielkim bólem i żalem żegnamy Jerzego Gronkowskiego, zmarłego 6 lutego 2009 r., po przegranej walce z bardzo ciężką chorobą. Był naszym serdecznym, bardzo życzliwym kolegą, a od 1997 r. – naszym przełożonym.

Prof. Jerzy Gronkowski, wychowanek VI Liceum im. Jana Kochanowskiego w Radomiu, podjął po maturze studia na Wydziale Fizyki Uniwersytetu Warszawskiego, które ukończył w roku 1971. Pracę magisterską wykonywał w Pracowni Rentgenowskiej Zakładu Ciała Stałego Instytutu Fizyki Doświadczalnej, kierowanego przez prof. Leonarda Sosnowskiego. W październiku 1971 r. został zatrudniony w Instytucie Fizyki Doświadczalnej Wydziału Fizyki U.W. na stanowisku asystenta.

Całe swoje życie naukowe związał z naszym Zakładem Badań Strukturalnych, który w 1974 r. został utworzony z Pracowni Rentgenowskiej Zakładu Fizyki Ciała Stałego. Poświęcił się tematyce dyfrakcji promieni X w monokryształach i badaniom defektów sieci krystalicznej. Stopień doktora uzyskał w 1979 r. na Wydziale Fizyki Uniwersytetu Warszawskiego. Tematyką jego pracy doktorskiej, wykonywanej pod kierunkiem prof. Juliana Auleytnera, było badanie kontrastu dyfrakcyjnego dyslokacji w monokrysztale Si w przypadku Bragga dla fali padającej płaskiej. Struktura subtelna kontrastu dyfrakcyjnego dyslokacji w monokryształach Si była przedmiotem kolejnych jego prac.

W roku akademickim 1981/1982 odbył staż naukowy w Laboratorium Mineralogii Krystalografii Uniwersytetu im. Marii i Piotra Curie, Paris VI, kierowanym przez prof. A. Authiera. Współpracował wtedy z prof. Cecile

Malgrange, rozwijając teorię dyfrakcji promieni X w kryształach zdeformowanych, dla przypadku Bragga. Przebywał potem na kilkumiesięcznych stażach w tym samym Laboratorium w latach 1989 – 1999.

Na podstawie uzyskanych wyników, dotyczących rozwijanej w ramach tej współpracy tematyki, otrzymał stopień doktora habilitowanego na Wydziale Fizyki Uniwersytetu Warszawskiego w roku 1992.

Po uzyskaniu stopnia doktora habilitowanego prowadził badania mikrodefektów rozłożonych statystycznie w monokryształach oraz w układach wielowarstwowych, stosując metody wysokorozdzielczej dyfraktometrii rentgenowskiej oraz topografii rentgenowskiej. Rozwijał aparat teoretyczny i numeryczny niezbędny do ścisłego opisu tych zjawisk i stosowanych metod pomiarowych. W toku tych prac rozpoczął badania wpływu stopnia spójności wiązki padającej na obserwowane wyniki (np. na obraz otrzymywany w topografii przekrojowej) i rozważał zmiany tego stopnia wywołane przez mikrodefekty rozłożone statystycznie w kryształach.

Jego działalność naukowa zaowocowała publikacją około 80-ciu prac. Dla celów dydaktyczno-popularyzatorskich opublikował artykuł w *Postępach Fizyki* w 1986 r. „Promieniowanie Synchrotronowe – nowe perspektywy rozwoju metod rentgenowskich”, który stał się bardzo przydatny dla studentów, dając podstawy wiedzy o tym cennym narzędziu badawczym.

Prof. Jerzy Gronkowski był bardzo dobrym dydaktykiem. Prowadził zajęcia na Pracowni Fizycznej I, gdzie przejawiał dużo inwencji, ustawiając nowe ćwiczenia.

Za Jego duży wkład w rozwój Pracowni Fizycznej I otrzymał w r.1981 nagrodę dydaktyczną wraz z M. Bardadin-Otwinowską, K. Pniewską i M. Izyckim.

Przez wiele lat prowadził ćwiczenia z dyfrakcji promieni X na Pracowni Fizycznej dla Zaawansowanych (tzw. Pracowni II). Kształcił także studentów wyższych lat w ramach studiów specjalistycznych w dziedzinie fizyki promieni X.

Prowadzony przez Niego wykład „Podstawy dyfrakcji promieni X i neutronów” cieszył się dużym uznaniem i powodzeniem wśród studentów. Także wykłady: monograficzny i specjalistyczny z dziedziny dyfrakcji promieni X dla studentów ostatnich lat studiów (powiadzone wymiennie z prof. M. Lefeld-Sosnowską), były przez studentów cenione.

Wychował wielu magistrów i dwóch doktorów.

Na zaproszenie pełnił także zajęcia dydaktyczne na Uniwersytecie D. Diderota (Paris VII) oraz na 23-cim Międzynarodowym Kursie Krystalografii w Erice.

Za swoją pracę naukową i dydaktyczną otrzymał wiele nagród, między innymi nagrody indywidualne Rektora UW, Nagrodę Sekretarza III Wydziału PAN oraz nagrodę zespołową Polskiego Towarzystwa Fizycznego dla Redakcji *Postępów Fizyki*.

W roku 1997 prof. Jerzy Gronkowski przejął kierownictwo Zakładu Badań Strukturalnych Instytutu Fizyki Doświadczalnej Wydziału Fizyki. Był bardzo przez pracowników Zakładu i studentów ceniony dzięki Jego wiedzy, kulturze osobistej, dużej umiejętności spokojnego rozwiązywania spornych problemów oraz autorytetowi, jakim cieszył się wśród nas. Funkcję tę

pełnił do końca życia – dopóki choroba nie uniemożliwiła mu pracy.

Jako członek Polskiego Towarzystwa Promieniowania Synchrotronowego udzielał się w pracy organizacyjnej Towarzystwa. Był członkiem Komitetów organizacyjnych Konferencji „Promieniowanie Synchrotronowe w Naukach Przyrodniczych” (ISSRNS), międzynarodowych oraz krajowych. W szczególności bardzo duży był wkład Jego pracy w organizację krajowej 5-ej Konferencji Użytkowników Promieniowania Synchrotronowego (5 KSUPS) w Warszawie w 1999 r. Był także głównym organizatorem Międzynarodowej Konferencji dotyczącej Wysokorozdzielczej Dyfraktometrii i Topografii (X-TOP) w 2002 r.

Bardzo dużo czasu i wysiłku włożył w pracę komitetu redakcyjnego *Postępów Fizyki*, którego członkiem był od roku 1997, a Redaktorem Naczelnym od roku 2003. Jego zaangażowanie w pracę komitetu i jej rezultaty jego koledzy z redakcji cenili bardzo wysoko, o czym świadczy artykuł pożegnalny, jaki ukazał się w pierwszym zeszycie Postępów Fizyki w 2009 roku.

Jego ogromne zaangażowanie w pracę, pomoc chętnie udzielana współpracownikom, a przede wszystkim Jego życzliwość sprawiły, że będzie Go nam zawsze bardzo brakowało.

Zostanie na zawsze w naszych sercach i wdzięcznej pamięci.

*Maria Lefeld-Sosnowska  
i cały Zespół Zakładu Badań Strukturalnych  
Instytutu Fizyki Doświadczalnej  
Wydziału Fizyki Uniwersytetu Warszawskiego*



Prof. Jerzy Gronkowski w gronie współpracowników i studentów z Zakładu Badań Strukturalnych w grudniu 2005 r.

## Z ŻYCIA PTPS



Fot. 1. Uczestnicy IX Międzynarodowej Szkoły i Sympozjum *Promieniowanie Synchrotronowe w Naukach Przyrodniczych (ISSRNS-2008)* w Mąchocicach Kapitułnych w 2008 r.

fot. J. Pelka

W pięknej scenerii Górz Świętokrzyskich odbyła się w Mąchocicach Kapitułnych koło Kielc w hotelu „Ameliówka” w dniach od 15 do 20 czerwca 2008 r. IX Międzynarodowa Szkoła i Sympozjum na temat *Promieniowanie Synchrotronowe w Naukach Przyrodniczych (9<sup>th</sup> International School and Symposium on Synchrotron Radiation in Natural Science) (ISSRNS-2008)* (Fot. 1) współorganizowane przez Polskie Towarzystwo Promieniowania Synchrotronowego i Instytut Fizyki PAN w Warszawie. Uczestnicy Szkoły mieli okazję podziwiać piękno okolicy podczas wycieczki na Święty Krzyż (Fot. 2).

Na konferencję przyjechało wielu zagranicznych naukowców reprezentujących synchrotronowe ośrodki badawcze, m.in. J. Baruchel (Fot. 3), A.N. Fitch i P. Glatzel z ESRF w Grenoble, H.A. Dürr z BESSY w Berlinie, R. Belkhou z SOLEIL we Francji, C. Bressler ze Szwajcarii, Th. Tschentscher i E. Welter z DESY w Hamburgu oraz kilku polskich specjalistów pracujących za granicą - T. Tyliszczak z ALS w Berkely i P. Grochulski z CLS w Kanadzie, a także J.H. Je z Korei Południowej, D.L. Nagy z Węgier i C.M. Schneider z Niemiec. Dzięki ich interesującym wykładom uczestnicy konferencji mogli poznać najnowsze trendy badawcze, nowe techniki pomiarowe oraz możliwości źródeł promieniowania synchrotronowego.

Materiały konferencyjne, zawierające wybrane wykłady, referaty i prezentacje plakatowe, ukazały się w roku 2009 w tomie 78 międzynarodowego czasopisma „*Radiation Physics and Chemistry*”.

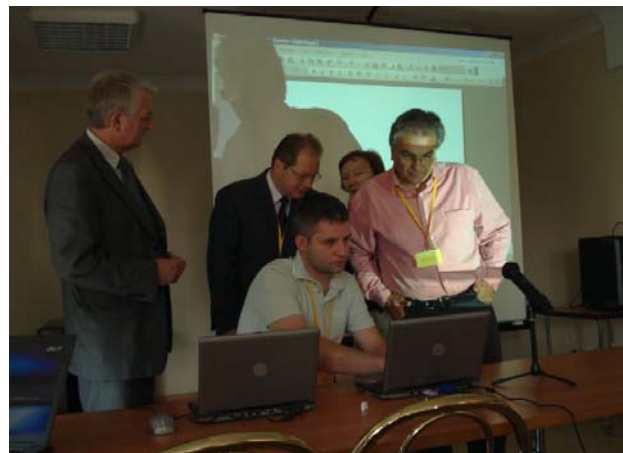
Bezpośrednio po zakończeniu Sympozjum w tym samym miejscu w dniach 20 i 21 czerwca 2008 roku odbyła się II Krajowa Konferencja "Polski Synchrotron – Linie Eksperymentalne" współorganizowana, podobnie jak ISSRNS, przez nasze Towarzystwo. Głównym organizatorem tego spotkania było Narodowe Centrum Promieniowania Synchrotronowego (NCPS) w Krakowie.

W trakcie Międzynarodowego Sympozjum, w dniu 19 czerwca 2008 roku odbyło się Walne Zebranie Polskiego



Fot. 2. Uczestnicy ISSRNS-2008 na platformie widokowej na Łysej Górze.

fot. J. Dąbrowski



Fot. 3. Profesor José Baruchel z ESRF (pierwszy z prawej) przygotowuje się do wygłoszenia wykładu inauguracyjnego ISSRNS-2008.

fot. W. Paszkowicz

Towarzystwa Promieniowania Synchrotronowego, na którym przedstawione zostały merytoryczne i finansowe sprawozdania z działalności Zarządu za okres 2005 – 2008. Po kilku wyjaśnieniach Skarbnika, Wojciecha Kwiatka, Walne Zebranie udzieliło absolutorium ustępującemu Zarządowi.

Bardzo ważnym punktem porządku Walnego Zebrania było przedstawienie przez Krzysztofa Krółasa (Fot. 4), kierującego projektem *Narodowe Centrum Promieniowania Synchrotronowego*, stanu prac związanych z budową polskiego synchrotronu w czerwcu 2008 roku.



Fot. 4. Wystąpienie Krzysztofa Krółasa na Walnym Zebraniu Członków PTPS w Mąchocicach Kapitułnych.

fot. W. Paszkowicz

Na początku wystąpienia podziękował on Prezes i Zarządowi PTPS za wystosowanie w maju 2008 r. do Minister Nauki i Szkolnictwa Wyższego listu podkreślającego konieczność przyspieszenia prac nad przyjęciem do realizacji projektu narodowego źródła synchrotronowego i jego znaczenie dla przyszłości nauki w Polsce i możliwości jej prawidłowego rozwoju. W dalszym ciągu wypowiedzi zostały przedstawione starania o budowę polskiego synchrotronu wspierane przez konsorcjum składające się z 21 uczelni wyższych i 12 instytutów naukowych. Ważne było także uruchomienie strony internetowej NCPS, dzięki której około dwudziestu polskich uczonych pracujących aktualnie za granicą wyraziło poparcie dla tej idei, deklarując swoją pomoc przy projektowaniu i realizacji, a część nawet gotowa jest wrócić, aby pracować w kraju. Aktualna sytuacja we wrześniu 2009 roku jest przedstawiona w artykule Edwarda A. Görlicha w tym numerze *Biuletynu*. Znaczne ograniczenie finansowania synchrotronu do poziomu 40 mln euro powoduje zasadnicze zmiany projektu z dużego synchrotronu o energii 3 GeV do małego o maksymalnej energii 1.5 GeV. Istnieje szansa, że umowa na budowę synchrotronu i pierwszej linii eksperymentalnej będzie podpisana w końcu 2009 roku i dopiero jej podpisanie gwarantuje finanse na

przedsięwzięcie, a po podpisaniu tej umowy będzie można starać się o finansowanie następnych linii pomiarowych. Koszt następnych linii może być finansowany przez MNiSW w ramach oddzielnych projektów badawczych.

Długą i dosyć burzliwą dyskusję wywołała propozycja Zarządu, który uprzednio podjął odpowiednią uchwałę na podstawie p. 27 *Statutu PTPS*, przeprowadzenia drogą elektroniczną wyboru nowych władz Towarzystwa na kadencję 2008–2011. Walne Zebranie ostatecznie wypracowało na podstawie *Statutu PTPS* tekst trzech uchwał, w których zadecydowało, że wybory odbędą się drogą elektroniczną (uchwała 1), przyjęto tryb i terminarz wyborów (uchwała 2) oraz określiły kroki w przypadku gdyby wybory okazały się nieprawomocne lub nieskuteczne (uchwała 3) oraz powołało Komisję do głosowania elektronicznego. Po Walnym Zebraniu odbyło się ognisko (Fot. 5), przy którym nadal rozmawialiśmy o sprawach Towarzystwa.



Fot. 5. Kontynuacja dyskusji przy ognisku.

fot. J. Dąbrowski

Wybory przeprowadzone jesienią 2008 roku dostarczyły trochę emocji, ponieważ w pierwszym głosowaniu (wybory Prezesa) w wakacyjnym terminie w dniach 2 – 3 września 2008 roku wzięły udział tylko 53 osoby na 117 uprawnionych do głosowania i Komisja była zmuszona uznać głosowanie za nieważne, gdyż wymagane kworum wynosiło 59 osób. W drugim podejściu było znacznie lepiej. W wyborze Prezesa PTPS w dniach 6 – 7 października 2008 roku wzięło udział 86 osób, z czego 76 opowiedziało się za powtórną elekcją Krystyny Jabłońskiej, z która zresztą nikt nie konkurował. Następnie w dniach 13 – 14 października 2008 roku 81 osób wzięło udział w wyborze członków nowego Zarządu i 79 osób w wyborze Komisji Rewizyjnej. Do Zarządu kandydovalo 13 osób, z czego 10 osób mogło być wybrane. Używając nomenklatury sportowej złoty medal (68 głosów) zdobył Wojciech Kwiatek, srebrny (65 głosów) – Wojciech Paszkowicz i brązowy (57 głosów) – Danuta Żymierska, miejsca punktowane zajęli: w kolejności zdobytych głosów: Andrzej Burian (52), Edward A. Görlich (48) i Bronisław Orłowski (45), a do finału jeszcze zakwalifikowali się: Bogdan Kowalski (44), Anna Wolska

Szuszkiewicz – 65 głosów, Elżbieta Dynowska – 63, Maria Lefeld-Sosnowska – 59 i Wojciech Wierzchowski – 55, i zostali wybrani powtórnie.

Od wyborów ub. roku Zarząd PTPS zebrał się pięć razy. Na pierwszym posiedzeniu w Warszawie w dniu 5 listopada 2008 roku nowo wybrany Zarząd ukonstytuował się. Ponownie powierzono funkcje wiceprezesów Andrzejowi Burianowi i Maciejowi Kozakowi, sekretarza – Danucie Żymierskiej, skarbnika – Wojciechowi Kwiatkowi i wydawcy – Wojciechowi Paszkowiczowi. Odpowiedzialną za sprawy internetu została Anna Wolska.

Zarząd przyjął następujący plan działalności na kadencję 2008-2011:

- kontynuacja realizacji celów statutowych o charakterze edukacyjnym (organizacja 8 KSUPS w r. 2009 i X ISSRNS w r. 2010),
- wspieranie działalności Narodowego Centrum Promieniowania Synchrotronowego na rzecz budowy polskiego źródła promieniowania synchrotronowego,
- wspieranie inicjatyw na rzecz udziału polskiego środowiska naukowego w budowie, a w przyszłości w eksploatacji Europejskiego Rentgenowskiego Lasera na Swobodnych Elektronach (EXFEL) w Hamburgu (przewidywany udział Polski na poziomie 2%),
- wspieranie inicjatyw na rzecz budowy lasera w zakresie miękkiego promieniowania rentgenowskiego (POLFEL) w Świeku,
- działania na rzecz ułatwienia polskim użytkownikom dostępu do źródeł promieniowania synchrotronowego.

Towarzystwo będzie wspierało udział Polski w budowie i eksploatacji dużych instalacji badawczych.

W ramach oszczędności finansowych następne cztery zebrania Zarządu w dniach 11 marca 2009 roku, 22 kwietnia 2009 roku, 29 czerwca 2009 roku oraz 3 września 2009 roku były konferencjami internetowymi. W dniu 24 września 2009 roku w Podlesicach odbędzie się zebranie Zarządu przygotowujące Walne Zebranie.

Prezes Towarzystwa skoncentrowała swoją aktywność na uczestnictwie Polski w ESRF i projekcie EXFEL. Prof. Krystyna Jabłońska wystąpiła o specjalny projekt badawczy

na kontynuację polskiego udziału w ESRF. MNiSW przyznało fundusze na ten cel na kolejne dwa lata. Projekt ten jest koordynowany w Instytucie Fizyki PAN w Warszawie. Dotąd polscy naukowcy wykorzystywali łącznie w polskich i międzynarodowych projektach ok. 3% dostępnego czasu, czyli więcej niż wynosi wkład Polski do budżetu ESRF (1%). Wiceprezes PTPS, Maciej Kozak, prowadził w ESRF rozmowy w sprawie ewentualnego wykupienia przez Polskę jednej z dwóch linii narodowych, brytyjskiej lub hiszpańskiej.

Polskim przedstawicielem w Zarządzie spółki ESRF jest Krystyna Jabłońska, Prezes PTPS. Polskim przedstawicielem w Komitecie ds. ekonomicznych i finansowych jest Bogdan Kowalski, członek Zarządu PTPS. Drogą wyboru Mariusz Jaskólski, długoletni członek PTPS, został przedstawicielem krajów mających status członków stowarzyszonych w Naukowym Komitecie Doradczym (SAC) w ESRF. Kontynuowano negocjacje z pozostałymi krajami będącymi członkami stowarzyszonymi, które wnoszą wkład 1% do budżetu ESRF (Izrael, Austria i Portugalia) oraz z powstałym w 2009 roku konsorcjum CENTRALSYNC, składającym się z Czech, Węgier i Słowacji i mającym wkład 1,1 %, w celu utworzenia struktury z wkładem powyżej 5% mającej prawa udziałowca spółki ESRF.

Prezes PTPS brała aktywny udział (jako członek) w pracach zespołu negocjującego udział Polski w projekcie EXFEL.

Miło mi zakomunikować, że liczba członków naszego Towarzystwa systematycznie rośnie i aktualnie wynosi 141 osób, w tym 120 uprawnionych do głosowania (1 członek honorowy i 119 członków zwyczajnych) oraz 21 członków sympatyków z Polski i z zagranicy.

Więcej szczegółów i zdjęć mogą Państwo znaleźć na stronie internetowej PTPS

<http://www.synchrotron.org.pl>

do odwiedzania której serdecznie zapraszam.

*Danuta Żymierska  
Sekretarz PTPS*

## **The Future of European Transnational Access for Synchrotrons and FELs**

Dear colleague:

We believe that you will be as concerned as we are about the future of the European Commission support of transnational access. It is our duty to inform you about recent events that, unfortunately, enhance our concerns.

For many years, first with bilateral contracts with facilities and then with the Integrated Infrastructure Initiative IA-SFS, European Commission funding made it possible for thousands of scientists to access synchrotrons and FELs based on merit, eliminating both national barriers and practical financial problems. This transformed the network of European facilities into a formidable, world-leading integrated system. The impact is particularly positive for colleagues based in countries with no synchrotrons and FELs: they can, in practice as well as in principle, use top-level instruments without being forced to permanent emigration.

It is important to note that the IA-SFS has been selected as one of the 40 “success stories” of the 6th Framework Programme to be included in a publication, edited by the European Commission, that will be distributed to the general public, National and Regional authorities, European Parliament, Delegations and Representations of the European Union all over the world.

Unfortunately, recent events are threatening the very future of this successful strategy. ELISA, the proposal that continues IA-SFS, is likely to be funded at a sharply reduced level with real cuts exceeding 60%. Similar problems affect other types of facilities: so there is increasing concern that European transnational access itself will be in jeopardy in the near future.

We believe that this is a strategic mistake that will undermine decades of efforts towards the integration of large facilities in Europe and penalize tens of thousands of European scientists. The concerned users should be made aware of the situation and make an informed decision on how to react.

Concerted actions in that sense have already started but a broader grass-root approach might be needed. We would be personally grateful if you could visit the Web page <http://www.elettra.eu/ELISA/questionnaire/> and use it to communicate with us in that sense. Whereas no immediate action is planned, we would like to know that you are indeed concerned about this issue and its impact on European science.

With many thanks for your attention and our best regards

Giorgio Margaritondo,  
*President of the IA-SFS Council*

Freddy C. Adams, Odile Dutuit, Andrea E. Russell  
*User representatives in the IA-SFS Council*

## Manifesto: European Synchrotron User Organisation (ESUO)

The availability of synchrotron radiation has a strong impact on the developments of many scientific disciplines. Multidisciplinary research activities in structural biology, material sciences or earth and environmental sciences, for example, are strongly dependent on its use. Due to continuous growth in user demand for synchrotron radiation, the number of large facilities in Europe is increasing significantly. Besides the world-leading facility ESRF, national sources like SOLEIL and DIAMOND have been finished recently and further sources, like PETRA III, ALBA, MAX IV and Polish national source are under construction or in the planning phase. Altogether they will give the European users the opportunity to find the most suitable facility and optimal beamline for their research.

However, access to these facilities does strongly depend on funding issues. With the exception of ESRF, access for non-national users to the nationally financed sources has been usually supported by European funds through the so-called Integrated Infrastructure Initiative (I3) provided via FP6 and FP7 programme calls. Unfortunately, the actual budget provided by the EU for these activities has been reduced. Moreover, there is discussion of further reductions and the transfer of funding responsibility completely to national programmes.

Distribution of the EU money provided by I3 and discussion on new activities to raise the EU funding is guided by the ELISA – European Light Source Activities- steered by a council representing the majority of the European synchrotron radiation facilities. In order to respond better to user needs the ELISA management is going to expand the council by facility-independent user representatives. This process has already been initiated by inviting some user representatives as observers to their council meeting in München in June 8, 2009.

These first ELISA user representatives have agreed to form an *ad-hoc* committee for the establishment of a European Synchrotron User Organisation (ESUO), *i.e.* a council of users working with synchrotron radiation. This initiative is guided by the conviction that access to European Synchrotron Radiation Facilities must be a genuine European mission. It cannot only depend on national interest but also must promote trans-national activities to stimulate science in Europe. EU funding for European projects must also support access to these large facilities by European users.

For several countries these access programmes are the only way to perform synchrotron radiation experiments.

At present we propose to form the European Synchrotron User Organization (ESUO) based on "One Country – One Vote" principle as is common in many European organizations. This body is planned to comprise representatives of each User Organization associated with the various European synchrotron radiation facilities. The aim of the ESUO is to coordinate the synchrotron radiation user activities and to facilitate access to the most appropriate beamline within Europe. The members of the *ad-hoc* committee are convinced that trans-European access to large facilities is a genuine mission for the European Union. Therefore ESUO will prepare documents supporting a new future European Access programme. As an umbrella organization ESUO can support the activities and formation of national and facility-related user organizations and stimulate discussions on unified beamline and beamtime application standards. The ESUO has great potential to be a beneficial influence for all synchrotron radiation users at all facilities in Europe. Therefore we ask each European country to propose one delegate to ESUO who can either be appointed by the respective national user organization or if such an organization does not exist, by a group of synchrotron users of the country.

Considering the time table of European Commission for new calls, the first meeting of ESUO is planned for the end of November 2009 in order to discuss a first draft of a memorandum of understanding and a letter of intent to European Commission. The names of the national delegates should be sent to the coordinator of the initiative, Ullrich Pietsch, as soon as possible.

*Ad-doc* committee for formation of European User Organization:

Ullrich Pietsch

(University of Siegen, Germany),  
spokesperson for the ESUO initiative

Maria Arménia Carrondo

(Universidade Nova de Lisboa, Portugal),

Keijo Hämäläinen

(University of Helsinki, Finland),

Krystyna Lawniczak-Jablonska

(Polish Academy of Science, Poland)

**AUTHOR'S INDEX**

S. abd el All	73	J.C. Dore	70	
D. Adamek	45	V. Drozd	60	E. Kamińska
F.C. Adams	99	H. Drozdowski	38, 79, 80	Cz. Kapusta
J. Antonowicz	60	M. Duda	46	G. Karczewski
D. Arvanitis	34, 50	T. Durakiewicz	23	Z. Kąkol
R. Bacewicz	60	O. Dutuit	99	A.R. Khorsand
J. Bak-Misiuk	25, 54, 55, 62, 82	E. Dynowska	47, 54, 62, 63, 83, 86	N.-T.H. Kim-Ngan
E. Banachowicz	90	P. Dziawa	83	G.C. King
A. Baranowska- Korczyk	87, 88	D. Elbaum	87, 88	M.T. Klepka
T. Balcer	65	F.M. Ezz-Eldin	73	D. Klinger
A. Barcz	34, 50, 62	H. Fiedorowicz	78	Ł. Kłopotowski
A. Bartnik	78	L. Fijałkowska	88	W. Knoff
M.J. Bellemare	67	S. Filipek	71	A.P. Kobzew
W. Białyk	37	A. Fitch	74	T. Kołodziej
F. Bijkerk	31	K. Fronc	87, 88	A. Kołodziejczyk
Z. Błaszczyk	38	M. Gajda	24	A. Kosar
A. Boczkowska	48	K. Gas	87, 88	K. Kościewicz
D.S. Bohle	67	J. Geurts	47	M. Kowalik
A. Brodka	70	A.J. Gleeson	56	B.J. Kowalski
S. Bruijn	31	E.A. Görlich	41, 42	M. Kozak
M. Brunelli	74	W. Graeff	28, 39, 44, 54, 55	B. Kozakowski
M. Bućko	63, 64	M.A. Green	32	A. Kozłowski
J. Bujak	87	H. Grigoriew	48	K. Królas
M. Burghammer	69	D. Grolimund	24	I. Kruk
A. Burian	22, 70	E.M. Gullikson	31	S. Krzywda
T. Burian	56	J. Hajdu	56	J. Krzywiński
W. Caliebe	47, 54, 62, 69, 86	V. Hajkova	31, 56	P. Kuczera
M.A. Carrondo	100	A. Hallen	34, 50	A. Kuczumow
J. Chalupsky	31, 56, 69	K. Hämäläinen	100	M. Kulik
R. Chałas	58	S. Hau-Riege	56, 69	J. Kusz
H. Chapman	69	L. Hawelek	70	W.M. Kwiatek
L. Chow	25	W. Hofman	39	T. Kyotani
M. Chrabaszczewska	81	V. Honkimäki	70	M. Lankosz
J. Cihelka	31, 56, 69	P.-Y. Hsieh	32	C. Lathe
M. Dampc	77	J. Jagielski	3, 29	K.awniczak- Jablonska
J. Darul	59, 61	R. Jakiela	54, 62	28, 44, 94
R. Davies	69	A. Jarmołowski	90	M. Lefeld- Sosnowska
H. Dąbkowska	68, 72	M. Jaskólski	37	M. Lekka
P. Dłużewski	87, 88	U. Jastrow	69	J. Lekki
W. Dobrowolski	75	R.L. Johnson	75	D.C. Ling
J.Z. Domagała	26, 47, 54	L. Juha	31, 56, 69	R. London
		M. Jurek	31, 56, 69	C.A. Londos

D. Lübbert	26	C. Riekel	69	M. Taube	90
W. Łasocha	74	J.J. Rocca	78	K. Tiedtke	31, 56, 69
T. Łukasiewicz	28, 44	A. Romaniuk	38	S. Toleikis	31, 56, 69
A. Malinowska	28, 44	P. Romanowski	47, 54, 62, 86	K. Tomala	41, 42
M.C. Marconi	78	C. Ronning	47	D. Trots	59, 83
G. Margaritondo	99	A.E. Russell	99	T. Tschentscher	56
I. Margiolaki	74	J. Sadowski	34, 52, 54, 62	S. Turczyński	28
N. Mason	77	R. Sato	71	K.R. Tybor	30
K. Mazur	39	K. Schneider	64	W. van Beek	32
C.S. Menoni	78	J. Sekutowicz	3, 29	E.D. van Hattum	31
K. Michałów	64	P. Seremak-Peczkis	63	R. van de Kruijs	31
B. Mielewska	77	U. Shymanovich	31	L. Vyšín	56
R. Minikayev	68, 72, 83, 88	A. Sienkiewicz	67	H. Wabnitz	31, 56, 69
A. Misiuk	25, 55, 82	M.R.F. Siggel-King	77	P.W. Wachulak	78
M. Młynarczyk	41	B. Sikora	87, 88	M.S. Walczak	67
S. Müller	47	M. Sikora	33, 63, 67	A. Wawro	69
R. Nietubyć	3, 29, 30, 86	B. Sivaraman	77	E. Werner-Malento	68, 72
J. Nowak	58	E.I. Slyntko	75	L. Wiegert	48
K. Nowakowska-Langier	86	V.E. Slyntko	75	A. Wierzbicka	26
K. Nowakowski	79, 80	A. Smykla	45	E. Wierzbicka	44
A. Nowicka	87, 88	K. Sobczak	87, 88	W. Wierzchowski	28, 39, 44, 54, 55, 65, 82
W. Nowicki	61, 69	R. Sobierajski	3, 29, 31, 56, 69	K. Wieteska	28, 39, 44, 54, 55, 82
B.A. Orlowski	42, 75	K. Sokolowski-Tinten	31, 56, 69	A. Wnuk	55, 82
C. Palusziewicz	24	Z. Stachura	24	T. Wojciechowski	54, 62
C.W. Pao	25	M.J. Stankiewicz	15, 41	T. Wojtowicz	87, 88
P. Pasierb	63	P. Starowicz	42	J. Wolny	46, 57
W. Paszkowicz	68, 69, 72, 73, 74, 87, 88	J. Stępień	64	A. Wolska	34, 49, 50, 52, 67, 71, 73
D. Pawlak	28	N. Stojanovic	31, 56, 69	G. Wrochna	3, 29, 30
J.B. Pełka	3, 29, 30, 56, 69, 86	T. Story	75	D. Yang	55
M. Pękała	60	W. Strupiński	39	D.A. Zając	63, 64
M. Piccinini	24	R. Strzałka	57	W. Zajączkowski	63
A. Pietnoczka	60	L. Suárez	67	P. Zajdel	32
Z. Pietralik	81	B. Surma	55, 82	R. Zalecki	43
M.A. Pietrzyk	75	J. Szade	22, 42	W. Zaleszczyk	87, 88
U. Pietsch	100	A. Szczepaniak	37	W. Zalewski	60
P. Piszora	59, 61, 74	A. Szczerbakow	83	C. Ziereis	47
E. Pławski	3, 29	M. Szczerbowska-Boruchowska	45	F. Zontone	66
M. Podgórczyk	24	J. Szewiński	3, 29	M. Zubek	77
D. Pomykalska	64	W. Szuszkiewicz	47, 83, 87, 88	D. Żymierska	56, 69, 96
W.F. Pong	25	J. Śliwińska	64	Z.R. Żytkiewicz	26
R. Przeniosło	40	K. Świątek	87, 88		
J. Przewoźnik	63, 64	M. Świrkowicz	44		
S. Ptasińska	77	W. Tabiś	66		
M. Rękas	63, 64	Z. Tarnawski	66		

---

## Polskie Towarzystwo Promieniowania Synchrotronowego (PTPS)

**Siedziba:**  
ul. Radzikowskiego 152  
31-342 Kraków  
tel. (0) 12 662 82 35

Nr konta bankowego:  
Bank PeKaO SA I Oddział w Krakowie  
80 1240 1431 1111 0000 1045 5083

**Adres do korespondencji:**  
Dr Danuta Żymierska  
Instytut Fizyki PAN  
al. Lotników 32/46  
02-668 Warszawa  
tel/fax: (0) 22 843 60 34  
[e-mail: zarzad@synchrotron.org.pl](mailto:zarzad@synchrotron.org.pl)  
<http://www.synchrotron.org.pl>

**Składki członkowskie dla członków zwyczajnych:**  
Wysokość składek członkowskich (od 1 stycznia 2009 r.):  
Samodzielni pracownicy naukowi – 50 zł  
Doktorzy – 40 zł  
Pozostali – 30 zł

---

## Zarząd Polskiego Towarzystwa Promieniowania Synchrotronowego (Kadencja: 2008 – 2011)

**Prezes:**  
Prof. dr hab. Krystyna Jabłońska  
Instytut Fizyki PAN  
al. Lotników 32/46  
02-668 Warszawa  
e-mail: jablo@ifpan.edu.pl

**Wiceprezes:**  
Prof. dr hab. Andrzej Burian  
Instytut Fizyki  
Uniwersytet Śląski  
ul. Uniwersytecka 4  
40-007 Katowice  
e-mail: burian@us.edu.pl

**Wiceprezes:**  
Dr hab. Maciej Kozak  
Wydział Fizyki  
Uniwersytet im. A. Mickiewicza  
ul. Umultowska 85  
61-614 Poznań  
e-mail: mkozak@amu.edu.pl

**Sekretarz:**  
Dr Danuta Żymierska  
Instytut Fizyki PAN  
al. Lotników 32/46  
02-668 Warszawa  
e-mail: zymier@ifpan.edu.pl

**Skarbnik:**  
Doc. dr hab. Wojciech Kwiatek  
Instytut Fizyki Jądrowej PAN  
ul. Radzikowskiego 152  
31-142 Kraków  
e-mail:  
wojciech.kwiatek@ifj.edu.pl

**Wydawca:**  
Doc. dr hab. Wojciech Paszkowicz  
Instytut Fizyki PAN  
al. Lotników 32/46  
02-668 Warszawa  
e-mail: paszk@ifpan.edu.pl

**Członek Zarządu ds. Strony Internetowej:**  
Dr inż. Anna Wolska  
Instytut Fizyki PAN  
al. Lotników 32/46  
02-668 Warszawa  
e-mail: wolska@ifpan.edu.pl

### Członkowie:

Dr hab. Edward A. Görlich  
Instytut Fizyki  
Uniwersytet Jagielloński  
ul. Reymonta 4  
30-059 Kraków  
e-mail: ufgoerli@cyf-kr.edu.pl

Doc. dr hab. Bogdan Kowalski  
Instytut Fizyki PAN  
al. Lotników 32/46  
02-668 Warszawa  
e-mail: kowab@ifpan.edu.pl

Prof. dr hab. Bronisław Orłowski  
Instytut Fizyki PAN  
al. Lotników 32/46  
02-668 Warszawa  
e-mail: orbro@ifpan.edu.pl

Dr Paweł Piszora  
Wydział Chemii  
Uniwersytet im. A. Mickiewicza  
ul. Grunwaldzka 6  
60-780 Poznań  
e-mail: pawel@amu.edu.pl

---

## Zawiadomienie Walne Zebranie Polskiego Towarzystwa Promieniowania Synchrotronowego

Zapraszamy na Walne Zebranie PTPS, które odbędzie się w trakcie 8. Krajowego Sympozjum Użytkowników Promieniowania Synchrotronowego w Podlesicach w hotelu "Ostaniec" w piątek, 25. września 2009 roku o godz. 18.00 z podanym poniżej porządkiem obrad.

Sekretarz PTPS  
D. Żymierska

Prezes PTPS  
K. Jabłońska

### Porządek obrad:

1. Powitanie uczestników i przyjęcie porządku obrad.
2. Sprawy członkowskie.
3. Sprawozdanie merytoryczne z działalności Zarządu PTPS za okres od 19.06. 2008 r. do 24.09. 2009 r.
4. Sprawozdanie finansowe Zarządu.
5. Sprawozdanie Komisji Rewizyjnej.
6. Dyskusja nad sprawozdaniami.

7. Głosowanie nad przyjęciem sprawozdań.
8. Organizacja w Polsce Międzynarodowej Konferencji XAFS16 w roku 2015.
9. Plany działalności PTPS.
10. Sprawy bieżące.
11. Wolne wnioski.



## TECHNIKA PRECYZYJNA I PRÓZNIOWA

PREVAC sp. z o.o. powstała w 1996 roku w Rogowie na Górnym Śląsku.

Działalność firmy skoncentrowana jest na projektowaniu i produkcji specjalistycznych systemów oraz komponentów pracujących w warunkach wysokiej (HV) lub ultra wysokiej (UHV) próżni, przeznaczonych do badania właściwości fizyko-chemicznych ciał stałych i cienkich warstw.

Wiedza zespołu pozwala na dostarczanie różnorodnych systemów próżniowych całkowicie dostosowanych do indywidualnych potrzeb klienta.

Największym potencjałem firmy jest wieloletnie doświadczenie w technologii próżniowej zdobyte podczas 13-letniej obecności na rynku oraz wiedza młodych, ambitnych i kreatywnych specjalistów tworzących zespół pracowników.

Podstawą sukcesu firmy PREVAC sp. z o.o. jest dbałość o bardzo wysoką jakość oferowanych produktów i usług oraz dążenie do ciągłego udoskonalania procesów w firmie. Ukoronowaniem dbałości o jakość jest uzyskanie Certyfikatu TÜV Rheinland InterCert Kft. za zgodność systemu zarządzania jakością z wymogami normy ISO 9001:2000. Ponadto potwierdzeniem innowacyjności firmy są liczne nagrody a wśród nich główna nagroda w XI edycji konkursu „Polski Produkt Przyszłości” w kategorii „Wyrób Przyszłości”.

Firma PREVAC sp. z o.o. działa aktywnie na rzecz upowszechniania zastosowań próżni w nauce i technice będąc Członkiem Wspierającym Polskiego Towarzystwa Próżniowego.

Dzięki współpracy z firmami wiodącymi w technologii próżniowej, takimi jak: Leybold Vacuum, Physical Electronics, Gammadata Scienta, Gamma Vacuum, Standford Research System itp., budowana przez firmę aparatura wyposażona jest w najwyższej jakości komponenty.

Produkty firmy znajdują swoich odbiorców na terenie Anglii, Szwecji, Norwegii, Włoch, Niemiec, Francji, Hiszpanii, Czech, Japonii, Chin, Rosji, Indii, Australii, RPA, USA, Kanady itd.



Prevac sp. z o.o.  
44-362 Rogów, ul. Raciborska 61  
Tel. +48 (032) 459 20 00  
Fax +48 (032) 459 20 01  
e-mail: [prevac@prevac.pl](mailto:prevac@prevac.pl)